8-2014

Mechanistic insights and functionalization of alkynes in homogeneous gold catalysis.

Manish Kumar
University of Louisville

MECHANISTIC INSIGHTS AND FUNCTIONALIZATION OF ALKYNES IN HOMOGENEOUS GOLD CATALYSIS

By

Manish Kumar
B.S., Himachal Pradesh University, Shimla, India, 2005
M.S., Panjab University, Chandigarh, India, 2007

A Dissertation
Submitted to the Faculty of the
College of Arts and Sciences of the University of Louisville
in Partial Fulfillment of the Requirements
for the Degree of

Doctor of Philosophy

Department of Chemistry
University of Louisville
Louisville, Kentucky

August, 2014

MECHANISTIC INSIGHTS AND FUNCTIONALIZATION OF ALKYNES IN HOMOGENEOUS GOLD CATALYSIS

By

Manish Kumar

A Dissertation Approved on

2nd June, 2014

by the following Dissertation Committee:

_____

Dr. Gerald B. Hammond

Dissertation Director

_____

Dr. Christopher T. Burns

_____

Dr. Richard P. Baldwin

_____

Dr. Francis P. Zamborini

_____

Dr. Humberto R. Gutierrez

DEDICATION

This dissertation is dedicated to my respected & beloved guru ‘Saint Shri Asharam Ji Bapu’, beautiful & great country ‘Mother India’, and my family members especially Grandparents, Parents, & brave Sister.

ACKNOWLEDGEMENTS

Let me convey my 'vote of thanks' to all those who helped me to materialize this dissertation. I am extremely obliged to my research advisor, Dr. Gerald B. Hammond, for being an excellent and supportive mentor during my Ph.D. studies. I would like to thank him for his motivation and encouragement on science and lessons on life, which I will remember forever. I have hugely benefited from the 'freedom of thought' and independence that he conveys to his co-workers. I also want to express my deep gratitude towards the incredibly humble and intelligent Dr. Bo Xu, for guiding me throughout my doctoral work.

I would also like to thank the faculty members at the University of Louisville, Dr. Francis P. Zamborini, Dr. Christopher T. Burns, and Dr. Richard P. Baldwin of the Department of Chemistry, and Dr. Humberto R. Gutierrez of the Physics Department for their precious input, and for serving in my Ph.D. thesis defense committee. I am also thankful to Dr. Michael H. Nantz, Dr. Craig A. Grapperhaus, and Dr. Mark E. Noble for their valuable suggestions and serving in my ORP and research committee. I would also like to acknowledge Dr. Craig A. Grapperhaus to help and allow me to do voltammetry studies in his lab. Also, I am thankful to Dr. Neal Stolowich who has been tremendously helpful in running NMR experiments. I would like to acknowledge the XPS studies support provided by Dr. Jacek Jasinski (Conn Centre, University of Louisville), and the important input provided

by Dr. Martin Scobie (Karolinska Institutet, Swedon), described at length in Chapter 2 and 5 of this thesis, respectively. Also, I am grateful to Dr. Mark S. Mashuta for crystallographic support and Dr. William N. Richmond for technical help. I am also very thankful to Tracy's and Steve's help for their stockroom chemical supplies and other many technical problems.

I am thankful to various funding agencies; the National Science Foundation, the National Institute of Health, the University of Louisville for teaching support, and the Institute of Molecular Diversity and Drug Design of the University of Louisville (IMD-3) for a travel award.

During the course of my doctoral work, I was fortunate to be part of a dedicated research group: Dr. Bo Xu, Dr. LePing Liu, Dr. Weibo Wang, Dr. Zhuang Jin, Dr. Jose C. Aponte, Dr. Junbin Han, Dr. Deepika Malhotra, Shengzong Liang, Elisa Otome, Zhichao Lu, Mallory Durham, Ebule Rene and Andrew Flach. I believe our bond of friendship will always remain intact even after I leave the lab. Last but not the least, I would like to thank the office staff in the Chemistry Department; Dr. Wittebort, Sherry Nalley, Syble Bullock, Aaron Howell, and Sabrina Haug, for being so supportive and helpful. I am thankful to all my friends at the University of Louisville: Manoj, Neeraj, Deepika, Davinder, Gori, Rahul, and Rajat. It is a true blessing to have you all in my life.

I have a deep appreciation and sincere regards for my motivating grandparents (Sh. Goverdhan Singh, Smt. Shalo Devi), and parents (Sh. Kuldip Singh, Smt. Surendra Devi), without their prayers and blessing I would not have made it this far. I am also highly obliged to my brave young sister, Mamta, for her unconditional love

and being so supportive throughout, even to the point of sacrificing her education to take care of our family.

I would like to acknowledge my beloved Guru ji, Saint Shri Asharam ji Bapu (Diamond of my life) for his blessing and motivation on how to live a real life with happiness and pride. Finally, thanks to my great country, Mother India (country of spirtuality), who inspired me to pursue my higher degree education from another great country, the United States of America (country of opportunity).

ABSTRACT

MECHANISTIC INSIGHTS AND FUNCTIONALIZATION OF ALKYNES IN HOMOGENEOUS GOLD CATALYSIS

Manish Kumar

2nd June, 2014

The focus of my dissertation work was to study the basic mechanistic insights of gold-catalyzed reactions. Although the various mechanistic pathways of gold catalysis are better understood nowadays, numerous questions still remain unanswered concerning the nature of deactivation of the catalyst's active species, high resistance towards protodeauration, and how we can solve these problems to improve the efficiency of gold catalysis. To address these challenges in gold catalysis we conducted first a detailed experimental study to understand the mechanism of deactivation of gold active species. Based on the combination of experimental data, we proposed that gold disproportionation is preferred as compared to reduction of the active gold catalyst. To address the high resistance toward protodeauration, we explored a new strategy to enhance the efficacy of gold-catalyzed reactions through hydrogen-bonding assisted protodeauration using additives chosen for their pK_{BHX} (hydrogen-bond basicity). To address the threshold phenomenon, we observed that high gold affinity impurities (halides,

bases) in solvents, starting materials, filtration or drying agents could affect the reactivity of the gold catalyst adversely, which, in turn, may significantly reduce the TON of cationic gold. Use of a suitable acid activator (e.g. HOTf, $In(OTf)_3$) re-activates the gold catalyst and makes the reaction proceed smoothly at low gold catalyst loading. To explore the reactivity of Au catalysts towards oxygen-atom transfer reactions, we investigated the gold-catalyzed addition of *O*-nucleophiles to alkynes and found that this reaction can produce synthetically important vinyl ether products in excellent yields and regioselectivities at room temperature. At higher temperature, 3,3-sigmatropic rearrangement of vinyl ether products gives access to highly functionalized benzotriazoles.

TABLE OF CONTENTS

LIST OF FIGURES

LIST OF TABLES

LIST OF SCHEMES

CHAPTER 1. OVERVIEW OF THIS DISSERTATION

1.1 Background of gold catalysis

Gold catalysis is considered one of the most important breakthroughs in organic synthesis for the synthesis of common core structures of various natural products, synthetic intermediates, and pharmaceuticals during the last decade.[1-8] The first breakthrough in gold catalysis occurred in 2000, when Hashmi and coworkers developed a new gold-catalyzed methodology for C-C bond formation.[9] Then onwards, cationic gold species were regarded as the most powerful catalysts for the electrophilic activation of alkynes/allenes/alkenes towards a variety of nucleophiles due to the relativistic effect of gold.[10-13] Gold catalysis is widely used in reactions like hydroamination, hydration, hydroalkoxylation of alkynes, cycloisomerization of enynes and isomerization of allenyl esters.[14-19] Unlike many transition metal catalyzed reactions, gold catalysis does not require anhydrous and air free conditions.

In the literature, it has been proposed that gold(I)-catalyzed nucleophilic addition reactions proceed through innersphere and outersphere mechanisms.[20-22] The most accepted catalytic cycle is shown in Scheme 1 (outersphere mechanism). First, a cationic gold complex (**Au**) acts as Lewis acid to activate C-C multiple bonds and form a η^2 complex **Au-S** (stage 1). At the same time, **Au** will also complex with

other components **I** (solvent, nucleophiles, products, additives) in the reaction system. Hoffmann and coworkers postulated that a symmetrical metal-olefin η^2-complex like **Au-S** does not have the right LUMO to interact with an incoming nucleophile.[23] Therefore, the transition state corresponding to the nucleophilic attack cannot resemble the equilibrium η^2-complex **Au-S**. But slippage of the metal creates a LUMO, which can interact with the HOMO of a nucleophile.[5] Thus, the slippage of **Au-S** will form a very reactive intermediate **B**, which is eventually attacked by the nucleophile to form **C**. Finally, **C** undergoes protodeauration (protodeauration means addition of proton to the place from where the removal of gold catalyst takes place to regenerate cationic gold) to give the final product. In this mechanism, a monomeric cationic gold(I) is proposed to be the catalytically active species.

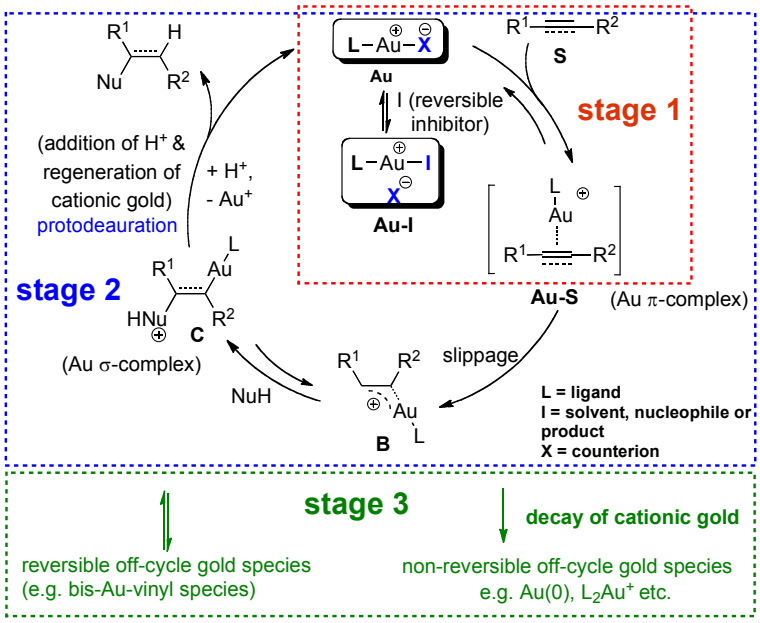

Scheme 1. Catalytic cycle of a typical gold-catalyzed reaction.

A parallel reaction--the decay of cationic gold(I) complexes--also takes place, leading to the formation of inactive species like Au(0), and L_2Au^+ (stage 3). Recently Widenhoefer and coworkers reported the formation of reversible off-cycle gold species (e.g. bis-Au-vinyl species, stage 3).[24]

1.2 Mechanistic insights in cationic gold catalysis

Although in general cationic gold species are regarded as the most powerful catalysts for the electrophilic activation of alkynes toward a variety of nucleophiles.[1-8,25], the following fundamental challenge has to be addressed before a wider adoption of gold catalysis in medicinal chemistry and material synthesis can take place, namely, catalyst loading (or turnover number) has to be improved. It is common to use 5% catalyst loading in gold catalysis; considering that gold is a precious metal and that it is difficult to recycle after each reaction, a 5% loading is often not practical in large-scale synthesis. Conversely, on many palladium-catalyzed coupling reactions (e.g., Suzuki reaction), the loading can be reduced to ppm levels.[26] To begin narrowing the gap with palladium, turnover numbers in gold catalysis have to be improved significantly. Despite their remarkable reactivity toward the electrophilic activation of alkynes, the challenge of cationic Au(I) complexes, such as the popular standard gold catalyst ($Ph_3PAu^+OTf^-$), is how to overcome their poor stability (which has led to the formation of a gold mirror and gold nanoparticles).[27] Although the basic mechanistic pathways are better understood nowadays, numerous questions still remain unanswered concerning the nature of deactivation of catalyst's active species, and how we can prevent the deactivation to improve the efficiency of gold catalysis.

In this regard, we conducted the first detailed experimental study of the deactivation of cationic gold, and examined the influence of each component in the reaction system (e.g. substrate, counterion, solvent) on the decay process (Scheme 2). We found that a substrate (alkyne/allene/alkene) that induced disproportionation of gold(I) might play a key role in the decay process. Our mechanism was supported by kinetic, XPS, voltammetry studies and high-resolution ESI-MS data. The detailed description of deactivation of the gold catalyst will be described in Chapter 2.

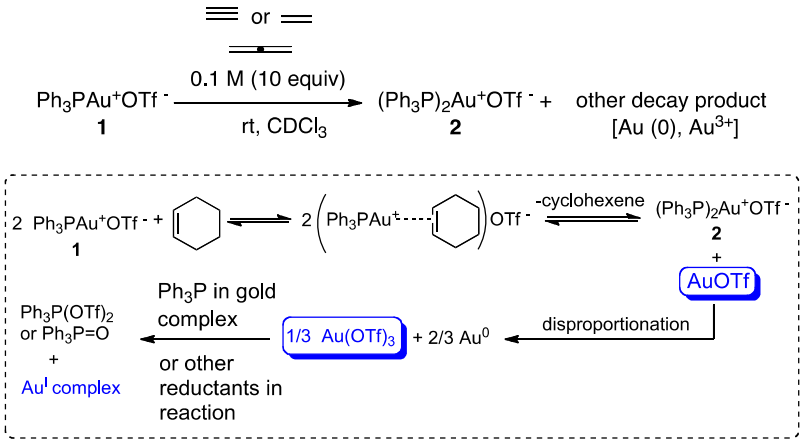

Deactivation mechanism of active gold catalyst in gold catalysis:
Kumar, M.; Jasinski, J.; Hammond, G. B.; Xu, B. *Chem. Eur. J.* **2014**, *20*, 3113-3139.

Scheme 2. Outline of deactivation mechanism of active gold catalyst.

It is well established that most gold-catalyzed reactions go through two major stages (Scheme 1).[28] In stage 1 (from L-Au^+ to **C**) a nucleophile attacks a gold activated alkyne/alkene η^2-complex to generate a charged *trans*-vinyl gold complex intermediate **C** (or an alkyl gold complex in the case of alkenes). In stage 2, **C** is converted to product with concomitant regeneration of the cationic gold species via protodeauration. The turnover limiting stage for a large percentage of

gold catalyzed reactions actually occurs in the protodeauration stage.[29] This circumstance is not surprising because a protonated vinyl gold intermediate **C** is reluctant to undergo protodeauration easily due to the fact that its positive charge will hinder interaction with another proton-containing molecule (acid). Keeping this fact in mind, we observed in our investigations that additives that are good hydrogen-bond acceptors increase the efficiency of gold-catalyzed reactions in those instances where protodeauration is the rate-determining step (Scheme 3). The efficiency of additives capable of hydrogen bonding-assisted protodeauration correlated with their standing in a scale of hydrogen bonding basicity (measured by pK_{BHX}). All additives used in our study were commercially available. The detailed description of additive effects through hydrogen bonding will be described in Chapter 3.

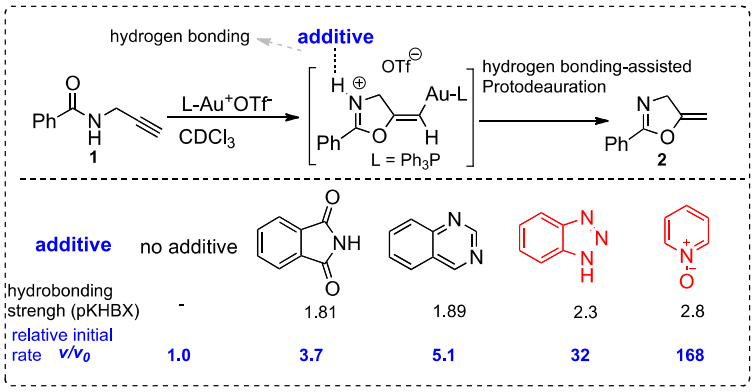

Enhanced reactivity in gold catalysis through hydrogen bonding:
Wang, W.; **Kumar, M.**; Hammond, G. B.; Xu. B. *Org. Lett.* **2014**, *16*, 636-639.

Scheme 3. Outline of enhanced reactivity in gold catalysis through hydrogen bonding.

In kinetic studies of catalyzed reactions it is customary to study the relationship between the rate of the reaction and the concentration of the catalyst to learn more about the mechanism of the reaction. Although a linear correlation between the

concentration of the catalyst and the initial rate data often exists when the rate is plotted against concentration, numerous studies have shown that the regression line does not intersect with the origin (eq 1, A≠0). If there is no background reaction, the rate should be zero when the catalyst concentration is zero, so A (intercept) should also be zero, but this is not the case in many reactions (A is usually less than zero),[30-32] indicating that a threshold catalyst concentration is required. Beyond vaguely implying some sort of catalyst poisoning, literature reports have not addressed the causes of this type of threshold. Although this phenomenon is ubiquitous in catalysis, relatively little effort has been spent on the investigation of this anomaly and the possible implications of this threshold phenomenon in catalysis.[30-32] During our research to improve the efficiency of gold catalysis,[29,33-36] we found that this threshold phenomenon is common in gold-catalyzed reactions.

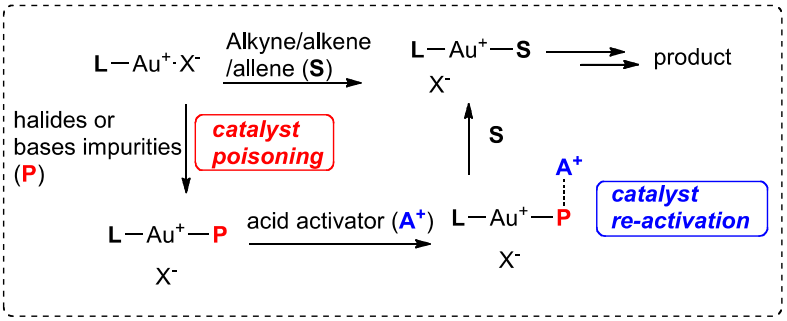

Cationic gold catalyst poisoning and re-activation
Kumar, M.; Hammond, G. B.; Xu. B. *Org. Lett.* **2014**, (*DOI: 10.1021/ol501663f*).

Scheme 4. Outline of cationic gold catalyst poisoning and re-activation.

We observed during our investigations that high gold affinity impurities (halides, bases) in solvents, starting materials, filtration or drying agents could affect the reactivity of the gold catalyst adversely (Scheme 4), which may significantly reduce the TON of cationic gold catalyzed reactions. Use of a suitable acid

activator (e.g. HOTf, $In(OTf)_3$) re-activates the gold catalyst and makes the reaction proceed smoothly at low gold catalyst loading. The detailed description of the threshold phenomenon will be described in Chapter 4.

1.3 Functionalization of alkynes through addition of *N*-hydroxy heterocycles

N-heterocycles such as benzotriazoles and indoles are among the most important structural classes in medicinal chemistry.[37-47] For example, 4-functionalized benzotriazoles are important precursors for the synthesis of pyrimidine- or pyridine-based compounds used in the treatment of GSK3 mediated disorders because they inhibit glycogen synthase kinase (GSK3).[48] Many functionalized benzotriazoles and indoles are also important synthetic intermediates.[49,50] Gold complexes are well known for their ability to catalyze a wide variety of synthetically interesting reactions of alkynes/allenes/alkenes.[4,7,28,51-58] In particular, the gold-catalyzed oxygen transfer of a nucleophilic oxygen atom to an alkyne group is synthetically useful.[59-65]

To further explore the reactivity of Au catalysts towards oxygen-atom transfer reactions, we investigated the gold-catalyzed addition of *O*-nucleophiles to alkynes to produce synthetically important vinyl ether products in excellent yields and regioselectivities at room temperature. Although these vinyl ethers are generally not stable enough to be isolated with standard silica gel chromatography, they were stable in our hands. At higher temperatures, the subsequent 3,3-sigmatropic rearrangement of vinyl ether products gave access to the pharmaceutically important functionalized *N*-heterocycles.

This two-step sequence represents an efficient oxygen transfer protocol of a nucleophilic oxygen atom to an alkyne group (Scheme 5). Furthermore, the reaction of a vinyl ether with electrophiles, such as the electrophilic fluorinating

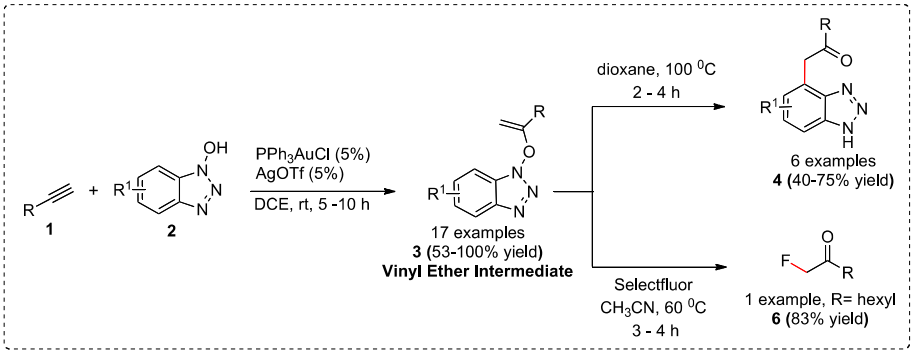

Gold-catalyzed addition of *N*-hydroxy heterocycles to alkynes
Kumar, M.; Scobie, M.; Mashuta, M. S.; Hammond, G. B.; Xu, B. *Org. Lett.* **2013**, *15*, 724-727.

Scheme 5. Outline of fuctionalization of alkynes through nucleophilic addition.

reagent Selectfluor, gives a fluorinated ketone in good yield and exclusive regioselectivity. The detailed syntheses will be described in Chapter 5.

CHAPTER 2. ALKYNE/ALKENE/ALLENE INDUCED DISPROPORTIONATION OF CATIONIC GOLD(I) CATALYST

2.1 Background

During the last six years both our group and others have been working rigorously for the development of new gold methodologies for the synthesis of interesting compounds. However gold catalysis, a landmark addition to the field of organic synthesis,[1,3,4,6,66,67] is not without shortcomings, the main one being the relatively low turnover numbers observed in the majority of gold-catalyzed reactions. Indeed, high turnover numbers (or low catalyst loadings) (10^6 TON) are observed only for a few types of gold catalyzed reactions (e.g., hydration of alkynes).[68-74] In most gold catalyzed reactions, catalyst loadings in the 1-5% range are the norm.[14-18] One reason for the low turnover numbers (TON) is the relatively fast decay of cationic gold and its conversion into non-reactive species (e.g., Au^0 - gold mirror and/or gold particles and $[L_2Au^I]^+$.[75-79] Despite this drawback, there has been no comprehensive systematic investigations on the decay of homogeneous gold catalysis, a stark contrast with the extensive work reported on catalyst deactivation in heterogeneous catalysis.[80] In this chapter, we answer some fundamental and intriguing questions on gold(I) decay, such as the effects of starting material,

nucleophile, solvent, counterion and additives, and we offer a probable pathway for gold(I) decay.

2.2 Results and discussion

A simplified gold catalytic cycle is shown in Scheme 6. The cationic gold complex (**L-Au**$^+$) acts as carbophilic Lewis acid,[81] activating an unsaturated C-C bond to form a π-complex [**L-Au**$^+$**-S**]. The interaction of [**L-Au**$^+$**-S**] with a nucleophile (**Nu**) yields a gold σ-complex ([**L-Au-S-Nu**]) that eventually undergoes protodeauration and the regeneration of cationic gold.

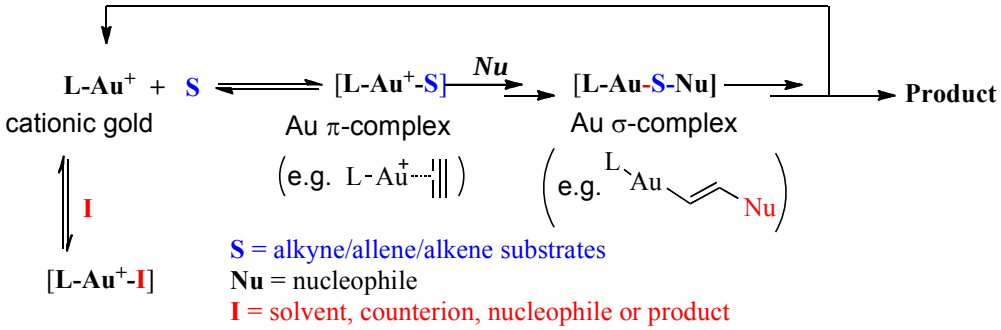

Scheme 6. Simplified representation of the gold catalytic cycle.

The complex [L-Au^I]$^+$X$^-$ (X = weakly coordinating counterion such as OTf $^-$) is relatively stable by itself, but in many reactions it decays at a fast rate (from a few minutes to a few hours). This behavior suggests that a cationic gold catalyst may decay rather rapidly in the presence of certain components in a reaction system. Because $Ph_3PAu^+OTf^-$ (**2-1**) is one of the most commonly used cationic gold catalysts,[15,16,18] we chose it as our model catalyst to study the deactivation process. **2-1** in $CDCl_3$ is relatively stable (^{31}P NMR peak at 27.4 ppm is the only peak)[82] and also catalytically active for 24 h at room temperature (Figure 1).

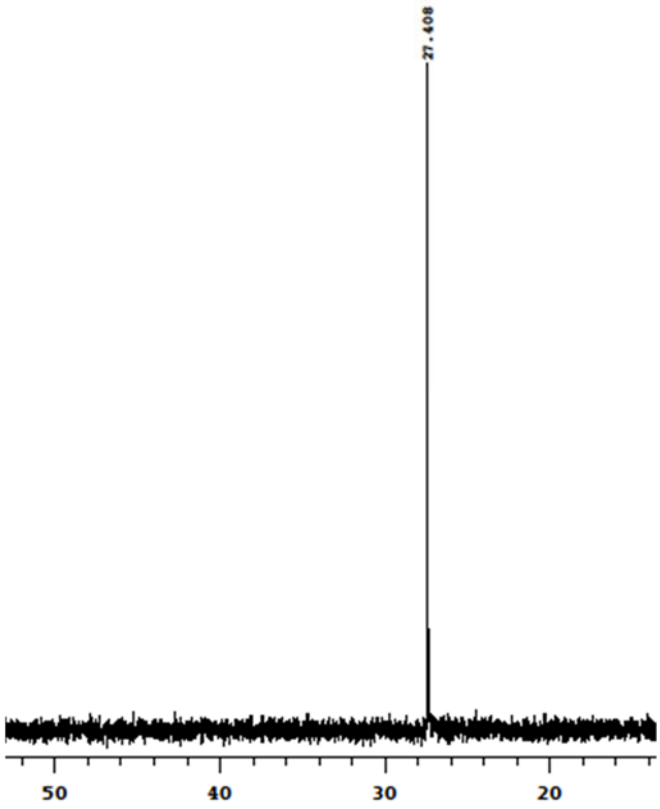

Figure 1. ^{31}P NMR signal for $Ph_3PAu^+OTf^-$ (2-1).

First, we investigated the kinetic stability of [L-Au^+-S] (Scheme 4, S = alkyne/allene/alkene). After adding cyclohexene (10 equiv vs. **2-1**) at room temperature, we noticed significant amounts of gold mirror/black particles (Au^0) in the NMR tube, a telltale indication that **2-1** (0.01 M in $CDCl_3$) had undergone significant decay. In the beginning, only a single ^{31}P NMR peak at 29.5 ppm was recorded, consistent with a gold-alkene π-complex or a fast equilibrium between free $Ph_3PAu^+OTf^-$ and [Ph_3PAu-alkene]$^+OTf^-$ (Figure 2). The signal at 29.5 ppm [gold(I)-alkene complex] decreased over time, and a new signal at 45.0 ppm increased over the same time period. We assigned this new signal the structure $(Ph_3P)_2Au^+OTf^-$ (**2-2**). This assignment is in agreement with the ^{31}P NMR shift

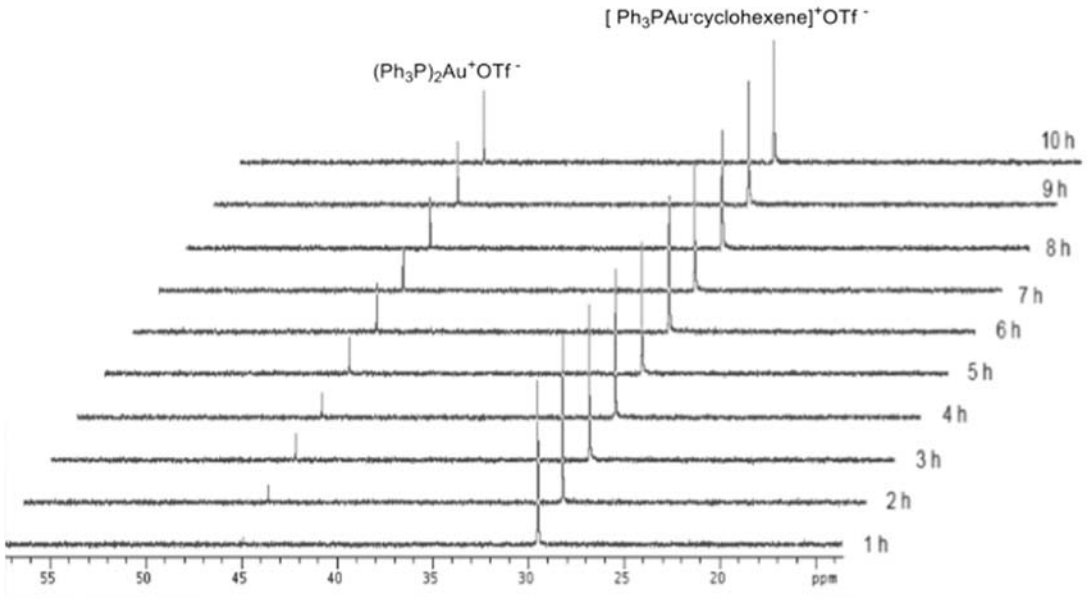

Figure 2. Decay of 2-1 in the presence of cyclohexene monitored by ^{31}P NMR spectroscopy.

value of **2-2** reported in the literature[83-86] and also with the chemical shift recorded for our independently synthesized **2-2** (Figure 3).

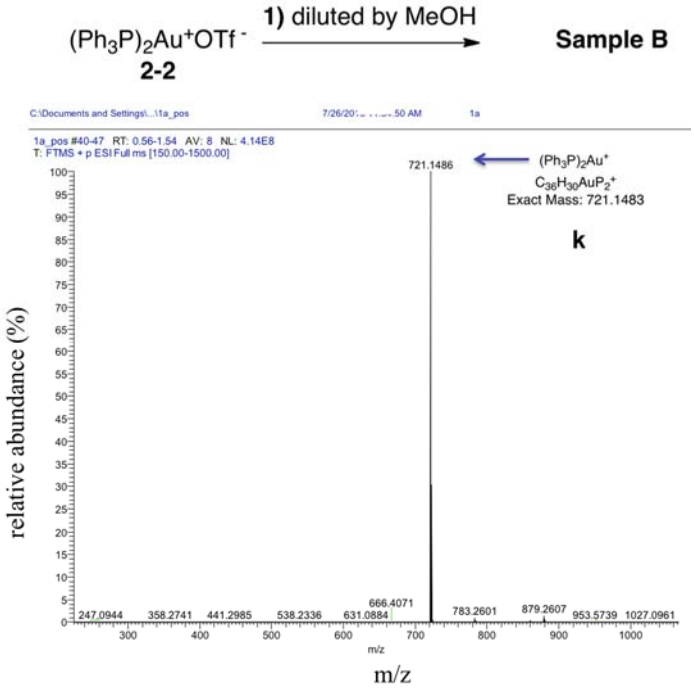

Figure 3. ESI-MS of sample B (Scheme 10).

This assignment was further confirmed by high resolution ESI mass spectroscopy ($[M\text{-}OTf]^+$ at m/z = 721.1483) (Figure 3). We also recorded the ^1H NMR of the reaction mixture, and found that cyclohexene itself had remained unchanged during the decay process. Moreover, we also observed cationic gold deactivation with different concentrations of cyclohexene, in which we found that increase in concentration of cyclohexene sped up the decay (Figure 4a). Furthermore, We also conducted NMR experiments to compare gold decay with diferrent unsaturated compounds like alkene/alkyne/allene (10 equiv vs. **2-1**). We observed that significant deactivation of the cationic gold catalyst **2-1** took place in all cases (Figure 4b).

Next, we investigated the influence of other common components (e.g. solvent, counterion, and additives) on the kinetics of gold catalyst decay. We found that solvent also affects the stability of the gold catalyst 1. Gold catalyst (**2-1)** was stable against deactivation for 24 h at room temperature in the solvents that we tested. However when cyclohexene (10 equiv vs. gold) was added, the decay process began in earnest. Highly coordinating solvents (CH_3CN, dioxane) have shown good aptitude in preventing the deactivation of the gold catalyst due to their high binding affinity with the gold catalyst, even higer than alkyne/alkene/allene (Figure 4c).

As mentioned above, $Ph_3PAu^+X^-$ alone is relatively stable, but when cyclohexene was added, different degrees of decay were observed in all cases (Figure 4d). Moreover, compared to the commonly used OTf^- counterion, NTf_2^- has great ability to stabilize the cationic gold catalyst. As described (Figure 4d), a more

coordinating counterion (NTf_2^-, $OPOF_2^-$) made a significant increase in the stability of our model gold catalyst **2-1**, rather than a non-coordinating counter ion (BF_4^-).[87] Just as it was the case with solvents and counterions, most of the additives we screened did not induce the decay of cationic gold, but when we tested how they influenced the decay kinetics in the presence of cyclohexene, we found that the decay of cationic gold slowed down differently depending on the type of additives used (Figure 4e). Many *N*-heterocycles and HMPA stabilized the gold catalyst significantly; similarly, other additives ($LiNTf_2$, pyridine *N*-oxide, sodium sufinimide, $KCTf_3$, DMPU) slowed down the decay of gold catalyst **2-1** to different extents.

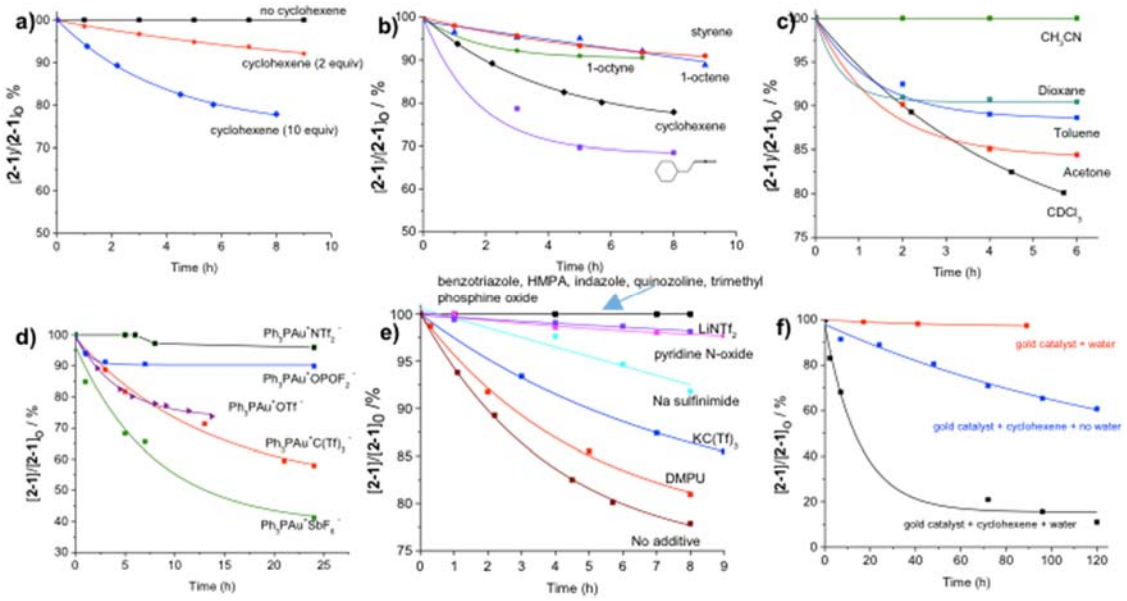

Figure 4. a) Decay of [$Ph_3PAu^+OTf^-$] (2-1) in the presence of cyclohexene; b) decay of 2-1 in the presence of alkene/alkyne/allene; c) decay of 2-1 in various solvents in the presence of cyclohexene; d) decay of [$Ph_3PAu^+X^-$] in the presence of cyclohexene; e) decay of 2-1 in the presence of cyclohexene and additives; and f) water effect on decay of 2-1.

Because trace water is ubiquitous in the reaction system, we investigated the effect of water on catalyst deactivation. We found that water alone has little effect on the

decay (Scheme 4f). Nevertheless, we observed a significantly faster deactivation of gold catalyst **2-1**, when **2-1** (0.01 M) was mixed with both cyclohexene (10 equiv) and water (1 equiv) at room temperature.

We postulated two possible pathways to explain the decay behavior (generation of Au^0 from Au^I). One pathway is disproportionation, and the other is reduction of gold(I) by certain reductants in the reaction system. Ceroni and coworkers[88] reported that gold nanoparticles (Au^0) can be produced by disproportionation of Au^+ ions. Some research groups have also speculated that the deactivation of the gold catalyst is due to disproportionation.[76,77] However, no direct experimental evidence has been reported to support these statements. We decided to investigate the actual gold valence change in the decay process experimentally. The redox potential of cationic gold should provide us with quantitative information to determine the ease of reduction of Au^I in a reaction system. Laguna and coworkers have studied the redox chemistry of Au^I and Au^{III} complexes using cyclic voltammetry in CH_2Cl_2 and also in acetonitrile.[89] In this work, they observed reduction of Au(III) to Au(I) for Au(III) complexes (eg., $PPN[AuCl_4]$) and reduction of Au(I) to Au(0) for most of the Au(I) complexes (eg., Ph_3PAuCl). They observed that peak potentials of -0.1 and -0.7 V vs. SCE for the successive reduction of $PPN[AuCl_4]$ [Au(III) complexes] in contrast to the reduction peaks at -2 V vs. SCE for Ph_3PAuCl [Au(I) complexes].

Initially we thought that cationic gold **2-1** ($Ph_3PAu^+OTf^-$, active gold species in catalysis) would have a different half potential as compared to covalent complex Ph_3PAuCl, inactive gold species in catalysis (-2 V vs. SCE). But we also observed

the same behaviour for a single irreversible redox event at very high negative half potential for our cationic gold **2-1** species as discussed next.

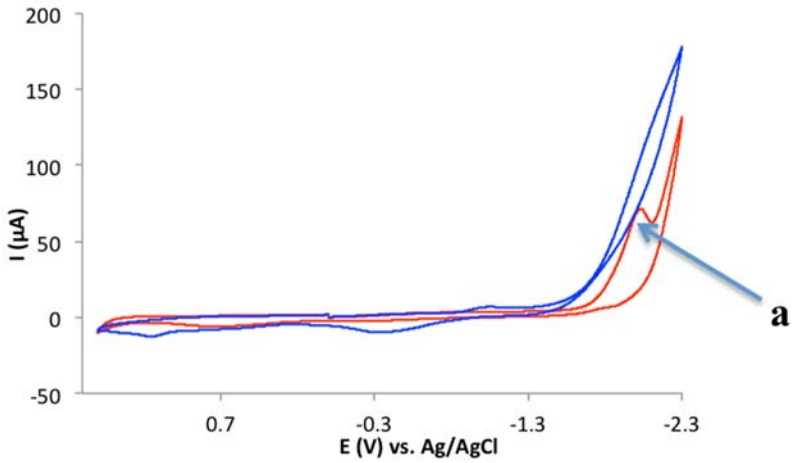

Figure 5. Cyclic voltammogram (red line) of 2-1 (2 mM in CH_2Cl_2 with 0.1 M tetrabutylammonium hexafluorophosphate (TBAHFP)). Blue line is background CV of supporting electrolyte in CH_2Cl_2.

We also chose CH_2Cl_2 as solvent to have a frame of reference to measure the reduction potential of cationic Au^I. The cyclic voltammogram of **2-1** revealed a single irreversible redox event (Figure 5) at a very negative formal potential (-2.5 V vs. ferrocenium/ferrocene). Data were collected at 100, 200, 400, 600, 800, and 1000 mV/s (Figure 6). Compared with the formal potential of Au^+ ($AuCl_2^-$/Au pair) in aqueous media (+1.11 V vs. SHE),[90,91] the highly negative potential of **2-1** in CH_2Cl_2 denotes that a direct reduction of catalyst **2-1** could be very difficult. This observation was further confirmed by adding a strong reductant to **2-1**. When [$CoCp^*_2$] (reduction potential in CH_2Cl_2 is -1.94 V vs. ferrocenium/ferrocene)[90] was added to a solution of **2-1**, no reduction took place. [$CoCp^*_2$] is already a very strong reductant, and most compounds in the reaction system are far less reducing.

Also, in our decay kinetic studies, we did not observe any change in the ^{1}H NMR of cyclohexene in the solution.

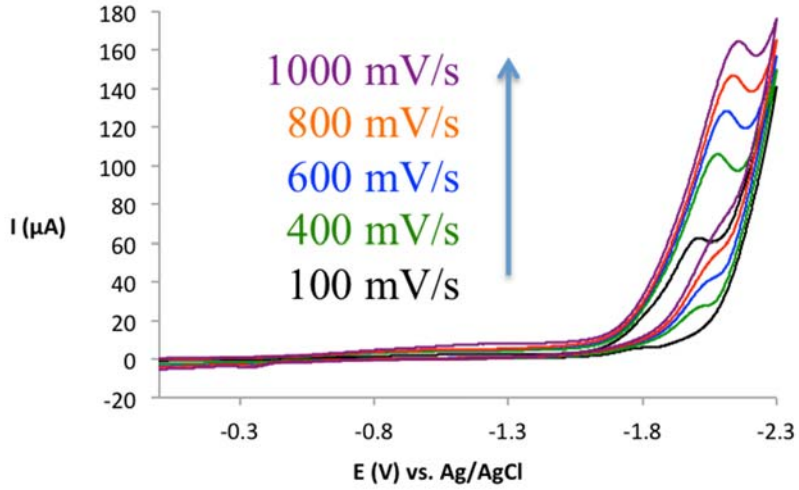

Figure 6. CV of gold catalyst 2-1 at different scan rate.

Because ^{31}P NMR, ^{1}H NMR or voltammetry do not reflect the change in the chemical state of gold itself, we used other more direct techniques to investigate the change in the chemical state of gold. XPS (X-ray photoelectron spectroscopy) is a quantitative spectroscopic technique that measures the elemental composition, chemical state, and electronic state of the elements that exist within a material.[92] We[93] and others[94,95] have used XPS in the determination of the chemical state of gold catalysts. The Au $4f_{7/2}$ peaks can be resolved into a doublet (spin-orbit splitting) and the binding energy of Au $4f_{7/2}$ electrons in each gold oxidation state are usually sufficiently wide apart to be differentiated using this technology.

First, we tested our gold standard samples ($ClAu^{I}PPh_3$ and $NaAu^{III}Cl_4$) and found that the Au $4f_{7/2}$ photoelectron peak was located at a BE value at 85.7 and 87.5 eV respectively, which is quite consistent with literature reports (Figure 7).

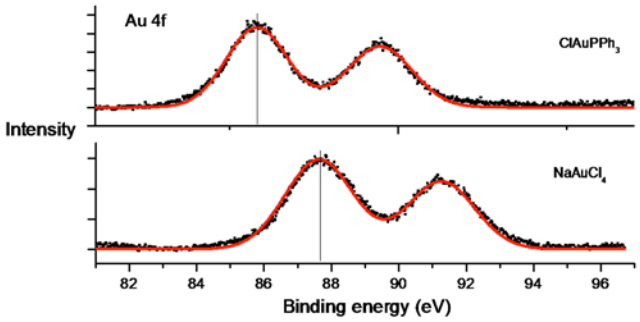

Figure 7. XPS spectra of standard samples ($Al_{K\alpha}$ = 1486.6 eV) corresponding to the Au $4f_{7/2}$ photoelectron peaks.

Then, we tested our cationic gold catalyst with various counterions. We prepared these cationic gold samples in chloroform; 24h later these solutions were dried in high vacuum and were subjected to XPS analysis (Figure 8, a-c). As expected, the gold valence in these three samples is still Au(I). We treated **2-1** (0.01 M in $CDCl_3$) with cyclohexene (10 equiv), after 48 h we filtered the mixture and collected the liquid portion (**sample 1**, Figure 8d) and solid precipitate (**sample-2**, Figure 8e). We conducted XPS analyses of both samples.

The majority of the solid sample (**sample 2**) was Au^0 (Figure 8e), and the liquid fraction was Au^I (Figure 8d). Because we detected none or very little of an Au^{III} component, it is highly possible that a reductive agent like the phosphine ligand reduced Au^{III} (because of the high oxidation power of cationic Au^{III} itself). Next, we investigated the disproportionation of gold(I) in the absence of a phosphine ligand. First, we tested a commercial Au^ICl sample; although the majority of it corresponded to Au^I, there was also a small amount of Au^{III} present (Figure 8f). We wanted to investigate the behavior of cationic gold(I) (Au^IOTf) under these conditions. Au^ICl and Ag^IOTf (1 equiv) were mixed (to prepare Au^1OTf) in dry dichloromethane with, and without, cyclohexene; after stirring for 30 min under

dark and anhydrous conditions, we observed the formation of black particles. We collected the black particles (**sample-3**) and conducted a XPS analysis of **sample 3** (Figure 8g), which denoted the presence of Au^0, Au^I and Au^{III}. We conducted the same experiment but in the company of cyclohexene, and observed a similar result.

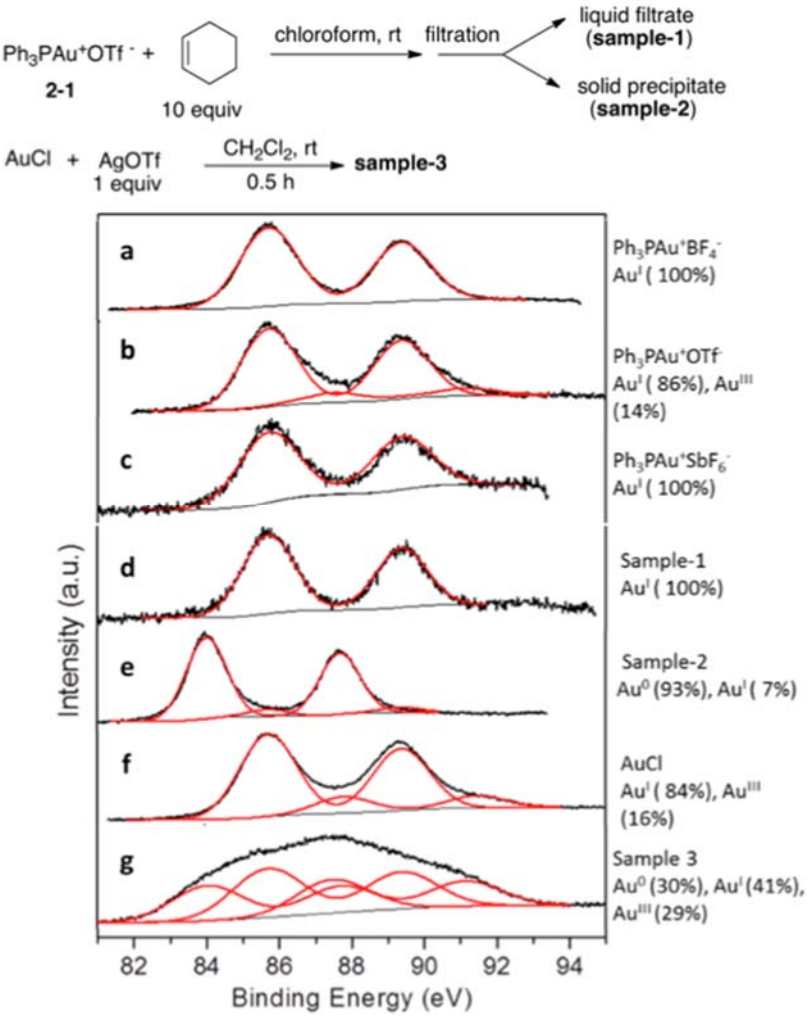

Figure 8. XPS spectra ($Al_{K\alpha}$ = 1486.6 eV) corresponding to the Au $4f_{7/2}$ photoelectron peaks.

^{1}H NMR analysis indicated no change in the structure of cyclohexene in the decay solution. This result suggested that cyclohexene did not play a role as reductant. All together, the experimental data supported the disproportionation of cationic gold(I) in the absence of a phosphine ligand.

Because XPS is conducted under high vacuum and the samples are tested in the solid state there was some concern that the gold catalyst might have changed under these conditions. We wanted to further confirm the existence of gold(III) by investigating the gold species directly in solution phase. Electrospray ionization mass spectroscopy (ESI-MS) is a soft ionization technique[96,97] and is an especially suitable technique because cationic gold intermediates are charged species. In a previous work we succeeded in detecting the existence of gold(III) species using high resolution-ESI-MS.[98] In this work first, we checked the high-resolution ESI-MS spectra of **sample 1** (Figure 9). We only detected the presence of various Au^{I} species (e.g. $[(Ph_3P)Au^{I}]^{+}$ (m/z 459.0571), $[(Ph_3P)Au^{I}.H_2O]^{+}$ (m/z 477.0677), $[(Ph_3P)_2Au^{I}]^{+}$ (m/z 721.1483)). This observation is consistent with our previous XPS analysis (Figure 8d).

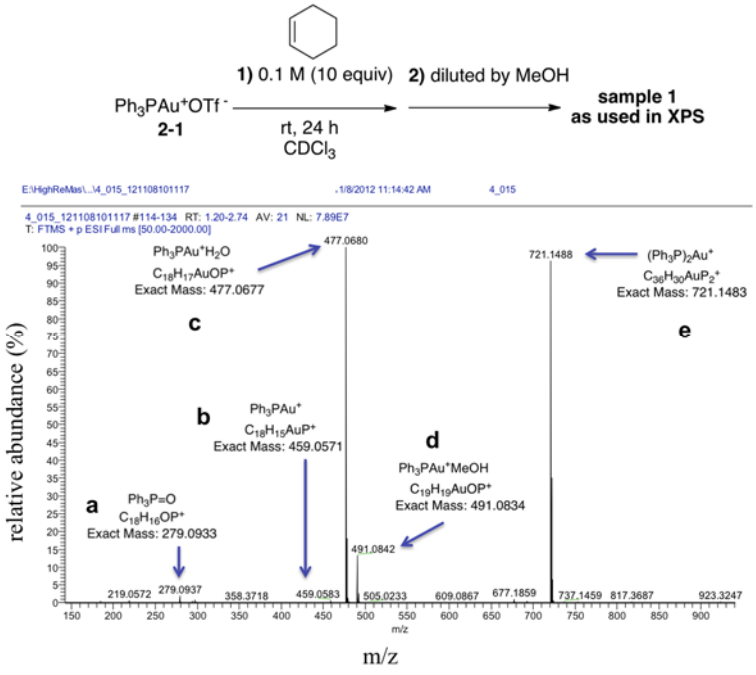

Figure 9. ESI-MS of Sample 1.

According to our previous studies of gold valence using ESI-MS,[93] Au^{III} species are difficult to detect under standard condition, but we have been able to detect Au^{III} species by adding a bidentate ligand and a halide (bipyridine and chloride).[93] Because Au^{III} complexes have square-planar geometry, a bidentate ligand should greatly stabilize the Au^{III} cation during the ionization process and chloride will

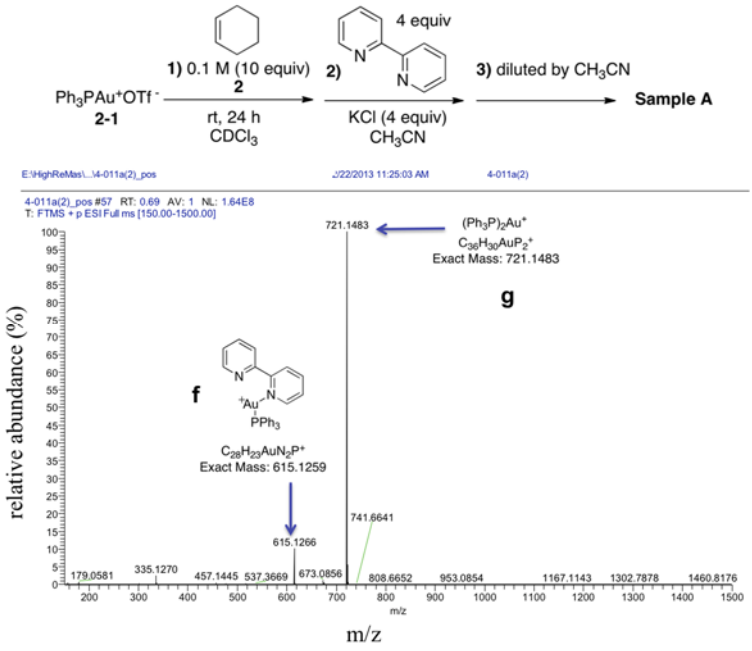

Figure 10. ESI-MS of Sample A (Scheme 10).

further stabilize cationic Au^{III}.[93] Therefore, we added bipyridine and chloride in **sample 1**. Again, only Au^{I} species (e.g. $[(Ph_3P)Au^{I}.bypridine]^+$ (m/z 615.1266), $[(Ph_3P)_2Au^{I}]^+$ (m/z 721.1483)) were detected (Figure 10). This result indicates there is no Au^{III} in the presence of a phosphine ligand (PPh_3). We used the same method to investigate the ESI-MS of **sample 3**. Various Au^{III} species were detected (Figure 11). Our high resolution-ESI-MS studies are consistent with our previous XPS studies, that is, there was no Au^{III} species (only Au^{I} species) in **sample-1,** but various Au^{III} species were detected in **sample-3**.

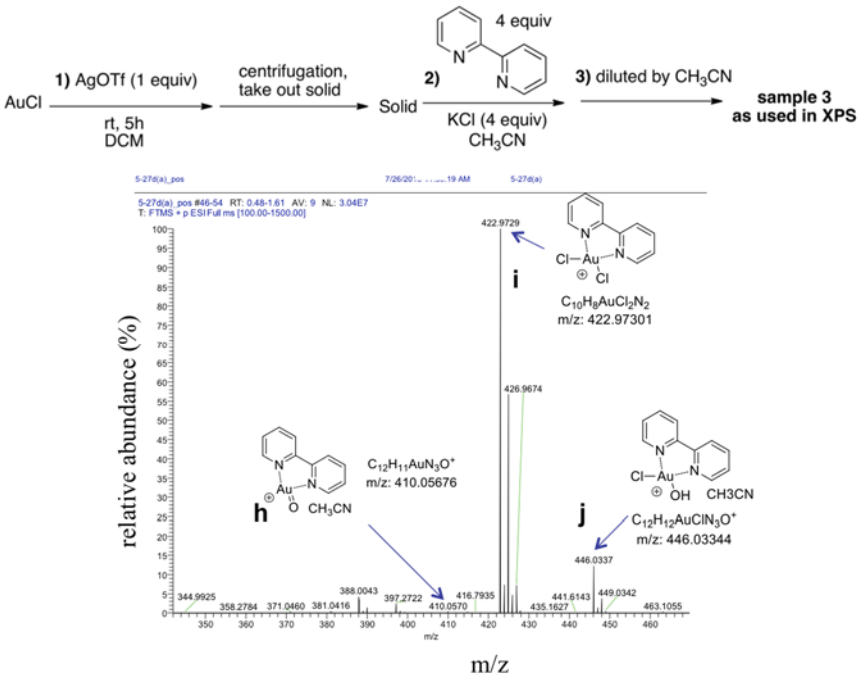

Figure 11. ESI-MS spectrum of sample 3.

Based on the combination of all the above experimental data, we are now in a good position to understand the decay mechanism, which can be summed up as follows:

1) Cationic Au^{I} without a suitable ligand (e.g. $Au^{I}OTf$) disproportionates readily compared to the non-cationic form (e.g. $Au^{I}Cl$) (see Figure 8, **sample 3**).

2) In the presence of a suitable ligand, cationic gold(I) decays (or disproportionates) at a much slower pace. $Ph_3PAu^{+}OTf^{-}$ is stable for at least 24h (Figure 8b) and $Au^{I}OTf$ disproportionates in less than 0.5 h (Figure 8g). This conclusion serves to explain why ligands are so ubiquitous in gold catalysis.

3) Cationic Au^{I}□π-complexes with π-donors (C-C unsaturated compounds like alkyne/allene/alkene) undergo relative fast decay, whereas cationic Au^{I}□complexes with most σ-donors (*N*-heterocycles, acetonitrile etc) are very stable.

The detailed role of substrates (alkyne/allene/alkene) in substrate-induced cationic gold decay is not very clear yet. Considering the great stabilization effect of the phosphine ligand (or NHC ligand) against disproportionation, our hypothesis is that an alkyne/allene/alkene may help to temporarily displace the phosphine ligand from the gold(I) center via a trans-effect. The trans-effect is the labilization (destabilization) of ligands that are *trans* to certain other ligands in a metal complex. Although most examples of trans-effect are observed in square planar complexes (e.g. Pd, Pt), we propose that it may also operate in linear metal complexes like gold(I) complexes.[99] And alkenes/alkynes are indeed the ligands that have shown the strongest trans-effect. Odell and coworkers demonstrated that alkenes and alkynes showed the highest trans effect of any other compounds in platinum complexes (trans effect: C_2H_4 ~ ^{i}PrCH=CHMe ~ $Me_2C(OH)C{\equiv}C$-$C(OH)Me_2$ >> Et_3Sb > Ph_3Sb > Me_3P > Et_3P > Ph_3P).[100]

Our proposed decay mechanism is shown in Scheme 7. First, cyclohexene will complex with cationic gold to form a gold-alkene π-complex, then, because of the trans-effect of the alkene, the phosphine ligand will be temporarily replaced to form complex **2-2** and free $Au^{I}OTf$. The disproportionation of $Au^{I}OTf$ generates Au^{0} and $Au^{III}(OTf)_3$. This disproportionation may be enhanced by the presence of trace water in the system. This statement is supported by a literature report that stated that a Au^{I} complex undergoes disproportionation in aqueous solution, while Au^{I} is stable in organic solvents.[101]

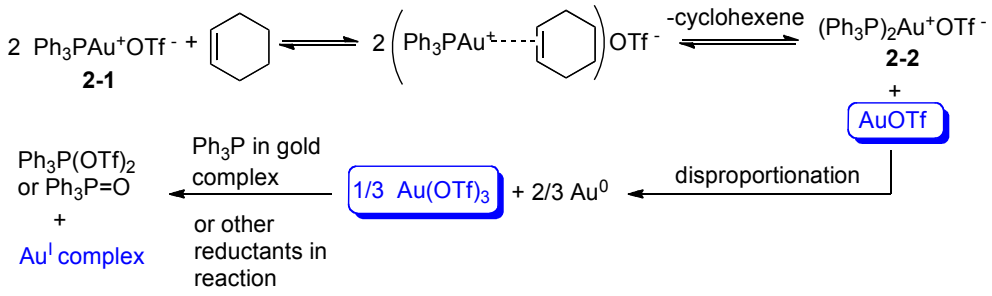

Scheme 7. Proposed mechanism for substrate-induced cationic gold decay.

The disproportionation of $Au^{I}OTf$ or its alkene/alkyne complex can be a relatively fast process (see Figure 8g, **sample 3**). This statement also has literature support: Dias and coworkers [102-105] reported that Au^{I} alkene or alkyne complexes without ligands are only stable at very low temperature, turning into black particles at room temperature. It is well known that Au^{III} will oxidize the phosphine ligand,[106] and it will be reduced to Au^{I} again.

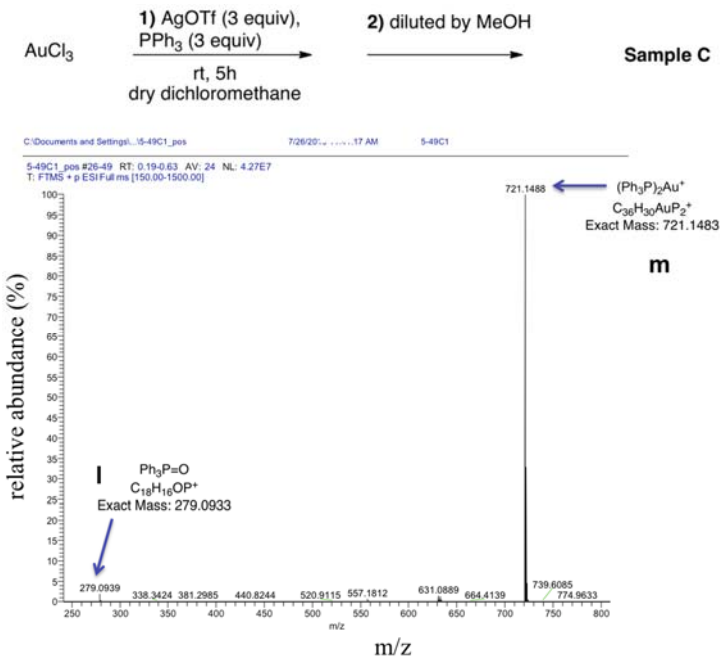

Figure 12. ESI-MS of Sample C (Scheme 10).

We propose that Ph_3P is oxidized to $Ph_3P(OTf)_2$,[107] which could then be hydrolyzed to give $Ph_3P{=}O$ in the presence of water. The presence of $Ph_3P{=}O$ has been confirmed by ESI-MS and TLC (by comparison with an authentic sample).

Furthermore, when we mixed $Au(OTf)_3$ (generated from $AuCl_3/Ag^{I}OTf$) with PPh_3 (**sample C**), we did obtain $(Ph_3P)_2Au^{+}OTf^{-}$ (**2-2**) and $Ph_3P{=}O$ (Figure 12). This behavior could explain why we were not able to detect Au^{III} in gold solutions using XPS and ESI-MS (**sample 1**).

We now can apply our decay mechanistic study to explain some unanswered questions:

i) What causes the decay of cationic gold? Induced cationic gold decay by unsaturated compounds (alkyne/allene/alkene) is the major reason for cationic gold decay. It should be noted that the starting material is not the only source of C-C unsaturated compounds; the products often contain C-C unsaturated compounds as well.

ii) Why is it that a high turnover can be achieved in some reactions but not in others? The decay process is highly dependent on the resting state of the gold catalyst. Based on our most recent study,[29] we have classified gold catalyzed reactions according to their turnover limiting stage: in type I, the formation of gold-σ-complex ([**L-Au-S-Nu**] in Scheme 6) is the turnover limiting stage; in type II, the regeneration of cationic gold catalyst (e.g. protodeauration) from [**L-Au-S-Nu**] is the turnover limiting stage. For type I reactions, the resting state is often [**L-Au^{+}-S**] (Scheme 6), thus, a relatively fast decay is to be expected, and so, turnover

numbers will be low in general. On the other hand, in type II reactions, the resting state is usually not [**L-Au$^+$-S**], so the decay is relatively slow and high TON are to be expected.

According to our recent study,[29] the hydroamination of an allene is a type I reaction (Scheme 8a). Toste and coworkers[32] have found that the gold resting state is the gold-allene complex **2-3A** in this reaction (Scheme 8a). Intermolecular hydroamination of an alkene [16] is a similar example (Scheme 8b). In these reactions, high loadings of gold catalyst (5% or higher) are typically used. And in these reactions, we did observe the formation of decay gold products **2-2** and Au^0 in the reaction mixture, especially when triflate was used as counterion.

A typical example of Type II reactions is the cyclization of propargyl amide (**2-7**) (Scheme 8c); its catalyst resting state is a [**L-Au-S-Nu**] type intermediate **2-7A**.[29,108] Thus, the decay of the active catalyst is expected to be slow. Indeed, low catalyst loadings (0.1%) have been achieved for this reaction.[109] Similarly, the alkyne hydration (Scheme 8d) reported by Nolan and coworkers,[70] and the intramolecular addition of a diol to an alkyne reported by Hashmi and coworkers[71,110,111] have been achieved with very high turnover numbers. In these reactions, the turnover limit determining stage is most likely the protodeauration of [**L-Au-S-Nu**] type complex (Scheme 6).[29]

We chose those reactions because acyclic and heterocyclic nitrogen-containing derivatives are common components of naturally occurring compounds agrochemicals, cosmetics, and pharmaceuticals; they are also useful intermediates in a number of industrial processes.

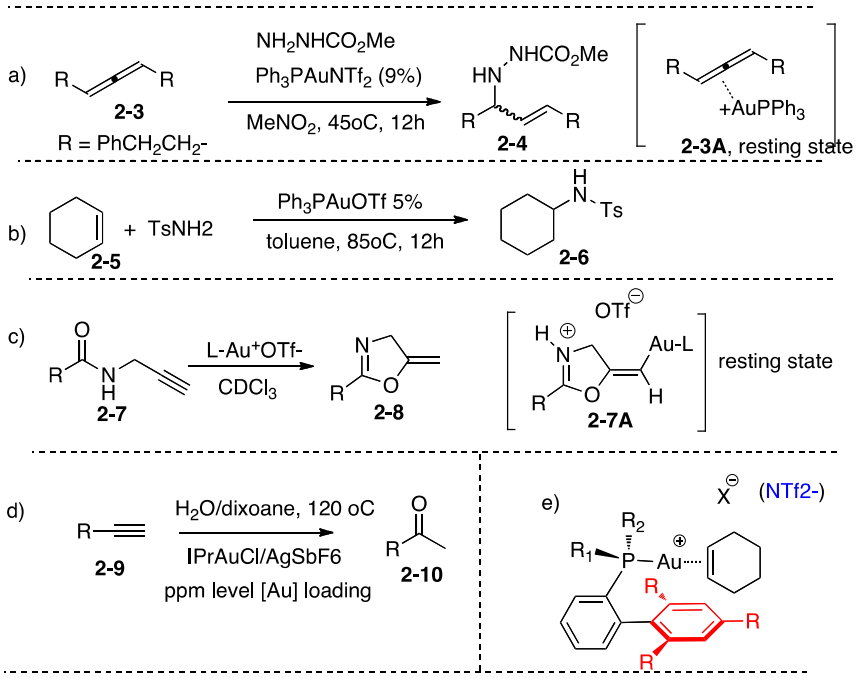

Scheme 8. Catalyst decay in different gold catalyzed reactions.

iii) What can we do to reduce the decay of an active gold catalyst? Our studies indicate that the use of σ-donors like *N*-heterocycles and CH_3CN will enhance the stability of the cationic gold,[9,112] but σ-donors also have significant detrimental effects on reactivity, so their use is usually not a good option. But it is still possible to disrupt the gold–alkyne/alkene interaction and therefore reduce the decay by using suitable ligands and counterions. We have reported recently that the use of a ligand containing a *o*-biphenyl steric handle can reduce the decay of cationic gold.[29,113] As shown in 8e, a *o*-biphenyl motif will clearly interrupt the bonding of the gold center with an alkene/alkyne, which may be the reason it slowed down its decay. A steric handle like *o*-biphenyl will not reduce the reactivity though; actually for many types of gold catalyzed reactions, ligands with biphenyl motif often give faster reactions.[4,114] In Figure 4d, we demonstrated that some counterions are more capable of stabilizing the cationic gold. NTf_2^- is a notable

example. The use of NTf_2^- won't reduce reactivity; in many reactions, NTf_2^- actually enables faster reactions compared with a commonly used counterion such as OTf^-.[87]

It should be noted that the alkyne/alkene/allene induced disproportionation of cationic gold(I) species may generate small gold clusters or gold nanoparticles under suitable conditions, which can exhibit high reactivity in certain gold catalyzed reactions.[72,115] Therefore, disproportionation may not be the end of the story for gold catalysts. We believe that if relatively large gold particles or a gold mirror are generated through disproportionation, the reactivity of the gold catalyst will be lost, but if we can control this disproportionation process so as to generate small gold clusters or gold nanoparticles, we may then be able to obtain new reactivity.

2.3 Summary

In summary, we have conducted the first detailed experimental studies to describe the possible mechanism of gold decay. There have been no reports with direct experimental details about the deactivation mechanism. In most gold-catalyzed reactions, catalyst loadings in the 1-5% range are the norm. One reason for the low turnover numbers (TON) is the relatively fast decay of cationic gold and its conversion into non-reactive species. We proposed two mechanisms i.e., reduction, and disproportionation. Our experimental studies support that disproportionation was the most preferable as compared to reduction, based on our individual studies of each step, and we proposed a mechanism. All our results, based on ^1H & ^{31}P

NMR, Cyclic Voltammetry, XPS, and High-Resolution ESI-MS spectroscopy, favor the disproportionation mechanism rather than reduction of gold catalyst. Our experimental studies support the substrate (alkyne/allene/alkene)-induced cationic gold decay (disproportionation) as the main reason behind cationic gold deactivation, but it should be noted that there could be other decay pathways. We also observed that decay depends on the resting state of the gold catalyst. We also found out that additive effects (neutral organic compound, counterion, solvent) could be useful to prevent the deactivation of the common gold catalyst. Our studies indicated that the use of σ-donors like *N*-heterocycles and CH_3CN enhance the stability of the cationic gold, but σ-donors also have a significant detrimental effect on reactivity, so their use is usually not a good option. But it is still possible to disrupt the gold–alkyne/alkene interaction and therefore reduce the decay by using suitable ligands and counterions that could be useful to lower gold catalyst loading, and could be useful to increase the turnover number in gold catalysis. In a future roadmap, and as a corollary of our finding that additives play a very important role in catalysis, we would like to expand the use of additives such as $LiNTf_2$ not only in other types of gold catalysis but also apply them to other metal catalyzed reactions. The work described in this chapter was published in *Chem. Eur. J.* **2014**, *20*, 3113-3119.

2.4 Experimental

General

^{1}H, ^{13}C, and ^{31}P NMR spectra were recorded with Varian spectrometers at 400, 100, 160MHz respectively, using $CDCl_3$, ^{d}acetone as a solvent. The chemical shifts are reported in δ (ppm) values relative to $CDCl_3$ (δ 7.26 ppm for ^{1}H NMR and (δ 77.0 ppm for ^{13}C NMR), relative to ^{d}acetone (δ 2.05 for ^{1}H NMR), multiplicities are indicated by s (singlet), d (doublet), t (triplet), q (quartet), m (multiplet), and br (broad). Coupling constants (*J*) are reported in Hertz. All deuterated solvents used in the reactions were used as received. All simple solvents (e.g. dichloromethane) were chemically dried using a commercial solvent purification system. All other reagents and solvents were employed without further purification. TLC was developed on Merck silica gel 60 F254 aluminum sheets. All the commercial reagents, and solvents were purchased from Aldrich or Strem or Fisher, and used without purification except cyclohexene (cyclohexene was redistilled). FT-ICR-MS - Fourier Transform-Ion Cyclotron Resonance-Mass Spectrometer was used for high resolution ESI-MS spectroscopy. Electrochemistry (Voltammetry) was performed with Potentiostat/Galvanostat Model 273.

Monitoring the reaction using *in situ* NMR spectroscopy

The model reaction was conducted in a NMR tube equipped with a screw cap and septa. All reactions were monitored using a Varian 400Mz NMR Spectrometer with the capacity to adjust the probe temperature with robotic sample changer at

room temperature. When ^{31}P NMR was used to monitor the progress of reaction, 85% H_3PO_4 (sealed in a capillary tube) was used as external standard for NMR integration. When ^{1}H NMR was used to monitor the progress of reaction, a solution of tetramethylsilane in $CDCl_3$ (sealed in a capillary tube) was used as external standard for NMR integration.

General procedure for preparation of Ph_3PAuCl and $Ph_3PAu^+X^-$ (X= OTf^-, NTf_2^-, $OPOF_2^-$, SbF_6^-, $C(Tf)_3^-$, BF_4^-)

Synthesis of gold complexes (L-AuCl).

Gold complexes (L-AuCl) were synthesized using a slightly modified version of a literature method.[116] These complexes were prepared via the following general procedure:

Sodium tetrachloroaurate(III) dihydrate (1 mmol) was dissolved in water, and the orange solution was cooled in ice. To this solution, 2,2'-thiodiethanol (3 mmol) was slowly added (ca. 30 min) with stirring. A solution of the phosphine ligand (1 mmol) in EtOH (if the ligand could not be dissolved, more EtOH was used) was added dropwise to yield a white solid. The solid was filtered, washed with water and then EtOH, and dried in vacuum.

Preparation of cationic gold (L-Au^+OTf^-) stock solution.

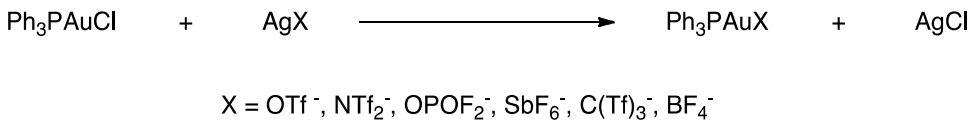

Standard stock solutions of cationic gold catalyst were made by weighing the L-Au(I)Cl (0.1 mmol) complex into a vial and adding corresponding deuterated

solvent, then 1.2 equiv of $Ag^{I}OTf$ (0.12 mmol) was added, the vial was sonicated for 3-5 min at room temperature, then the vial was centrifuged and the clear solutions was transferred to a clean glass vial. The solution was kept in freezer (-20^{o}C) until it was used.

Preparation of $((Ph_3P)_2Au^{+}OTf^{-})$ 2-2.

Cationic gold catalyst **2-1** was made by weighing the $Ph_3PAu(I)Cl$ (0.1 mmol) complex into a vial and adding corresponding dichloromethane solvent (2 mL), then 1.2 equiv of $Ag^{I}OTf$ (0.12 mmol) was added, the vial was stirred for 2-3 h at room temperature, then the vial was centrifuged and the clear solution was transferred to a clean glass vial and the solvent was removed at high vacuum to leave a white solid $Ph_3PAu^{+}OTf^{-}$ (**2-1**). Ph_3P (0.1 mmol) was added in a vial having **2-1** with dichloromethane (1 mL) and the solution was stirred at room temperature for 2-3 h. Solvent was removed at high vacuum to leave a white solid $(Ph_3P)_2Au^{+}OTf^{-}$ (**2-2**). **2-2** was characterized by ^{31}P NMR (45.0 ppm) and ESI-MS (Figure 3).

X-Ray photoelectron spectroscopy (XPS) studies

XPS is a quantitative spectroscopic technique that measures the elemental composition, chemical state and electronic state of the elements that exist within a material.[117] For example, it has been used in determination of chemical state of supported gold catalysts.[94] The binding energy of Au $4f_{7/2}$ electron of each gold oxidation state is usually wide enough apart to be differentiated by this technology (Table 1).

Table 1. The literature reports of binding energy of Au $4f_{7/2}$ electron.

Sample	Au^0	$ClAu^IPPh_3$	$ClAu^I(PPh_3)_2$	$Cl_3Au^{III}PPh_3$
Au $4f_{7/2}$ BE (eV)	84.0 ± 0.1	85.4	85.4	87.3

X-ray photoelectron spectroscopy (XPS) spectra were collected by a Thermo Fisher Scientific XPS spectrometer, equipped with standard Al Kα excitation source (1486.6 eV). Gold complex standards ($ClAu^IPPh_3$, $NaAu^{III}Cl_4$) were sampled as powders and pressed on a double-sided adhesive carbon tape. Gold catalyst aliquots were sampled as solution and solid (Scheme 9), dried in normal atmosphere on a double-sided adhesive carbon tape.

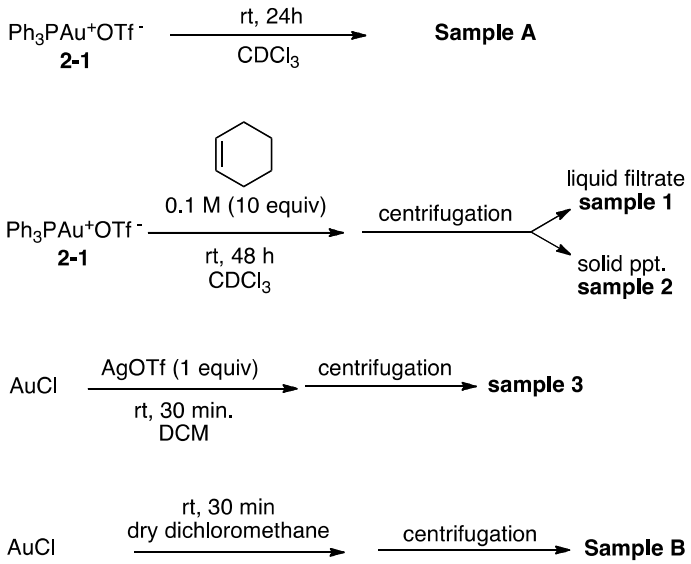

Scheme 9. Sample preparation for XPS studies.

The binding energy scale was calibrated by measuring C 1s peak (BE 284.6 eV) from the surface contamination and the accuracy of the measurement was 0.1-0.2 eV. A non-linear least square peak fitting routine was used for the analysis of XPS spectra, separating elemental species in different oxidation states. The curve fitting of the 4f core level spectrum was performed using two spin split Au $4f_{7/2}$ and Au

$4f_{5/2}$ components, separated by 3.67 eV, in a fixed intensity ratio (1.33). We tested our gold standard samples ($ClAu^{I}PPh_3$ and $NaAu^{III}Cl_4$), (Table 2, entries 1-2); the Au $4f_{7/2}$ photoelectron peak is located at a BE value at 85.7 and 87.5 eV respectively, which is quite consistent with literature reports (Table 1).

Table 2. Relative surface distribution of gold valence change based in XPS studies.

entry	Sample	Au $4f_{7/2}$ BE (eV)	Surface Au Species[a]
1	$ClAuPPh_3$	85.7	Au(I) 100%
2	$NaAuCl_4$	87.6	Au(III) 100%
3	**Sample A**	85.6 87.4	Au(I) 85.4% Au(III) 14.6%
4	**sample 1**	85.6	Au(I) 100%
5	**sample 2**	84.2 85.7	Au(0) 92.3% Au(I) 7.7%
6	**Sample B**	85.6 87.8	Au(I) 93.6% Au(III) 16.4%
7	**sample 3**	84.4 85.6 87.4	Au(0) 30.1% Au(I) 41.5% Au(III) 28.4%

[a]Ratio of gold complexes were estimated based on the area of the Au 4f peak

High resolution ESI-Mass spectroscopy studies

FT-ICR-MS analyses were done in a hybrid linear ion trap (LIT) FT-ICR mass spectrometer (LTQ-FT, Thermo Electron, Bremen, Germany) equipped with a TriVersa NanoMate ion source (Advion BioSciences, Ithaca, NY) with an "A" electrospray chip (nozzle inner diameter 5.5 μm) was used for mass spectral analysis. Applying 1.70 kV with 0.1psi head pressure operated the TriVersa NanoMate in positive ion mode. MS runs were recorded over an m/z range from 50 to 1,000 Da using optimized ion abundance targets enabled for the selected mass range. Initially, low-resolution LIT-MS scans were acquired for 0.50 min to track the stability of the ion spray, after which high mass

accuracy data were collected using the FTICR- MS analyzer where MS scans were acquired for 3 min at a target resolving power of m/Δm=200,000 at m/z=400 (10 % valley).

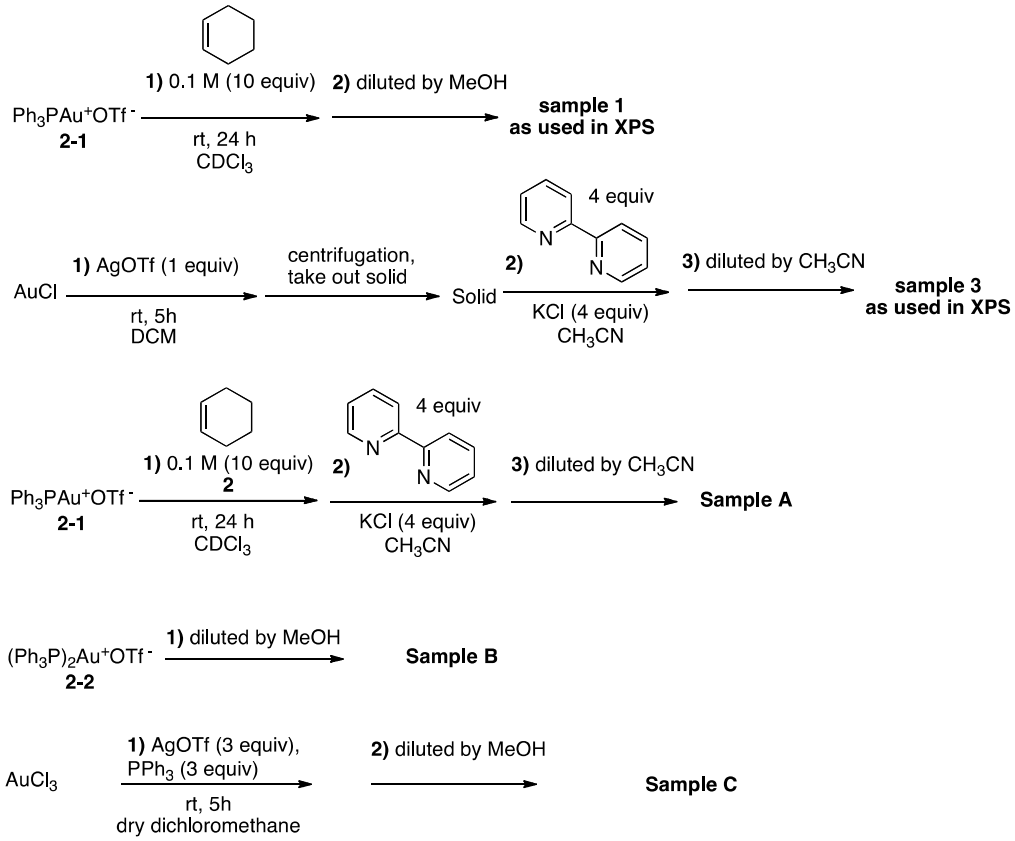

Scheme 10. Sample preparations for ESI-MS.

Five "microscans" (ICR-MS transients) were accumulated before Fourier transformation to produce each saved spectrum; thus the cycle time for each transformed, saved spectrum was about 5 s. The LTQ-FT was tuned and calibrated according to the manufacturer's default standard recommendations, which typically achieved better than 0.5 ppm mass accuracy at a resolving power of 200,000 at m/z=400. FT-ICR-MS mass spectra were centroided by Xcalibur and exported as exact mass lists into an Excel file using QualBrowser 2.0 SR2 (all software from Thermo Electron,"Bremen" version for

the LTQ-FT).

The mildness of ESI-MS allows direct sampling from the reaction mixture. Because cationic gold intermediates are charged species, they are especially suited for ESI-MS analysis. The samples were prepared (Scheme 10) for ESI-MS analysis.

Electrochemical (Voltammetry) studies

Electrochemical measurements were carried out in a 10 mL custom designed cell that was designed by E. Bothe of the Max-Planck Institute für Bioanorganische Chemie, Mülheim, Germany.[118] The cell is equipped with quartz windows with a 0.5 cm path length. The sample holder and cell were connected in a series to a circulating bath. To prevent condensation of the quartz cell during low-temperature measurements, the cell holder and the cell were placed in custom-built Plexiglas box fitted with Dynasil 4000 quartz windows (Pacific Quartz), through which nitrogen gas was purged. All measurements were recorded in dry, freshly distilled dichloromethane containing 0.1M tetrabutylammonium hexafluorophosphate (TBAHFP) as a supporting electrolyte. A platinum electrode-working electrode (area=0.071 cm^2) was used for cyclic voltammetry methods. In all cases, a Pt counterelectrode and an Ag/AgCl reference electrode was used. All data is scaled to ferrocenium/ferrocene. Cyclic voltammetry (CV) experiments were conducted on samples at room temperature with an analyte concentration of 2 mM. For each scan rate, a background voltammogram was collected on the solvent and supporting electrolyte prior to sample addition.

CHAPTER 3. ENHANCED REACTIVITY IN HOMOGENEOUS GOLD CATALYSIS THROUGH HYDROGEN BONDING

3.1 Background

It is well established that most gold-catalyzed reactions go through two major stages (Scheme 11).[28] In stage 1 (from L-Au^+ to **C**) a nucleophile attacks a gold alkyne/alkene η^2-complex **B** to generate a charged gold intermediate **C**. In stage 2, **C** is converted to product with concomitant regeneration of the cationic gold species via protodeauration (protodeauration means addition of proton to the place from where the removal of gold catalyst take place to regenerate cationic gold).[119] If **C** contains a relatively basic heteroatom (e.g. nitrogen) it may be reluctant to relinquish its proton.

A positively charged intermediate **C** is aversed to undergo protodeauration because its positive charge is a deterrent for an incoming proton. Indeed, many charged vinyl gold species have been isolated (e.g. **Au-2**) because they have shown high resistance towards protodeauration.[120-122] The turnover limiting stage for many gold catalyzed reactions actually occurs in the protodeauration stage (stage 2).[29] In this chapter, we investigated a new strategy to enhance the efficacy of gold catalyzed reactions through hydrogen-bonding assisted protodeauration, using

additives chosen by their pK_{BHX} (hydrogen-bond basicity)[123] rather than by their pK_a.

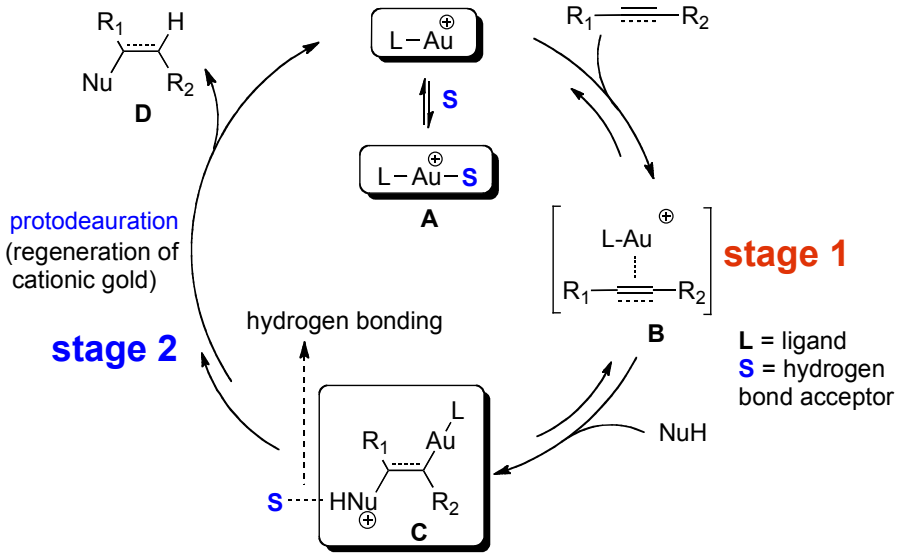

Scheme 11. Stages in the gold catalytic cycle.

The hydrogen bond is one of the fundamental noncovalent interactions between a drug molecule and its local environment in biological system. Despite its importance, scientists in the medicinal chemistry community have a poor understanding of the relative basicity (i.e., strength) of hydrogen-bond acceptors. In 2009, Laurence and co-workers reported a comprehensive database of hydrogen-bond basicity (measured by pK_{BHX}).[123]

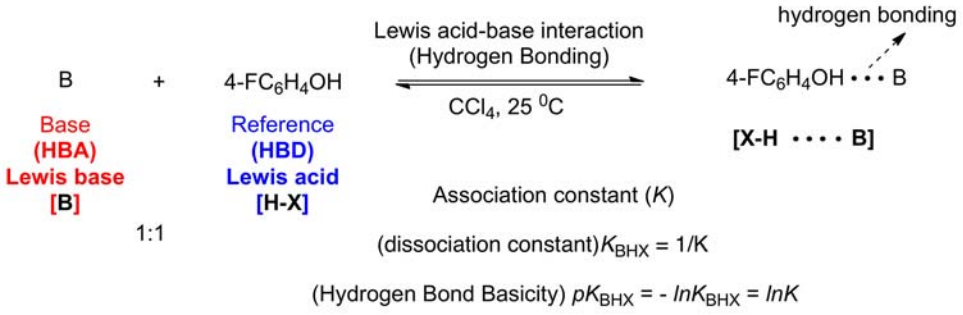

Scheme 12. Determination of hydrogen-bond basicity (pK_{BHX}).

The hydrogen bond is an attractive interaction between a hydrogen-bond donor (HBD; Lewis acid) XH and a hydrogen-bond acceptor (HBA; Lewis base). Comparative measures of pK_{BHX} are provided by the equilibrium constants K for [1:1 hydrogen-bonded complex] formation for a series of (HBAs) with a common reference (HBD). Laurence chose 4-fluorophenol as a common reference (HBA; Lewis acid) to obtain pK_{BHX} of different compounds. Thus, the hydrogen-bond basicity of a series of bases B is measured by the 1:1 complexation constant K of the equilibrium given in Scheme 12. The normal range of pK_{BHX} is from 1 – 5, a larger value indicates higher hydrogen-bond strength.

Addition of a relatively strong base has a deleterious effect in the protodeauration of **C** (Scheme 11). Although a base will remove the proton in **C**, it will also quench any acid in the system and by doing so it will inhibit protodeauration.

We asked ourselves if a hydrogen bond acceptor with low basicity could be a better alternative (**S** in Scheme 11). The nonbonding orbital of **S** will partially transfer its charge to the antibonding σ* orbital of **C**.[124,125] This effect will reduce the positive charge on **C** and cause the hydrogen bond acceptor to function as a proton shuttle, thus facilitating protodeauration. This concept is similar to general base catalysis,[126,127] with **S** acting as a general base. General base catalysis is a common occurrence in biological systems where strong bases are not tolerated and where deprotonation or proton transfer is mediated by weak bases through hydrogen-bonding interaction.[128-130]

In gold catalysis, the role of a hydrogen bond acceptor (**S** in Scheme 11) is more complex than that of a general base. Because **S** is aurophilic to some extent, it

competes with an alkyne/alkene starting material in their complexation with cationic gold (Scheme 11). Hence, with regards to stage 1, **S** could be considered a reversible inhibitor. Only if the acceleration effect of **S** outweighs its inhibitory effect, the effect of **S** in the overall reaction will be positive. Thus, **S** will be useful in gold catalysis only when protodeauration is the rate-determining step.

3.2 Results and discussion

To implement our proposed tactic we screened a diverse group of additives using a well-studied gold catalyzed reaction in which stage 2 (protodeauration) is known to be the slow step.[29] The reaction we chose was the gold-catalyzed cyclization of propargyl amide **3-1** to oxazole **3-2**[108,109,131,132] because its key vinyl gold intermediate (**Au-1**, L = IPr) had been identified by the Hashmi group in the case of gold(I),[132,133] and by Ahn[120] in the case of gold(III) (**Au-2**) (Figure 13). Based on those studies, we proposed that intermediate **Au-3** is equivalent to **C** in Scheme 11. We measured the initial reaction rate in the absence of an additive (v_0), and the initial reaction rate (v) in the presence of various additives, and then calculated the ratio v/v_0 for each additive. The data shown in Figure 13 indicated that basic additives completely inhibited the reaction [e.g. **A1** (Et_3N, pK_{aH} = 9.0), **A2** (imidazole, pK_{aH} = 7.1)]. These results are not surprising because stronger bases ought to inhibit the protodeauration step (stage 2 in Figure 13). Additives that were less basic than collidine (**A3**) did not inhibit the reaction, but most of them (e.g. **A4-A8**: alkene, phenol, sulfide, indole and acetyl imidazole) had no effect on the kinetics of the reaction ($v/v_0 = 1$). We were pleased though when *N*-heterocycles,

such as benzotriazole (**A16**, v/v_0 = 32), indazole (**A11**, v/v_0 = 10.3), and quinazoline (**A14**, v/v_0 = 5.1) showed dramatic acceleration effects and were astounded when pyridine *N*-oxide (**A18**) increased the reaction rate 168 times.

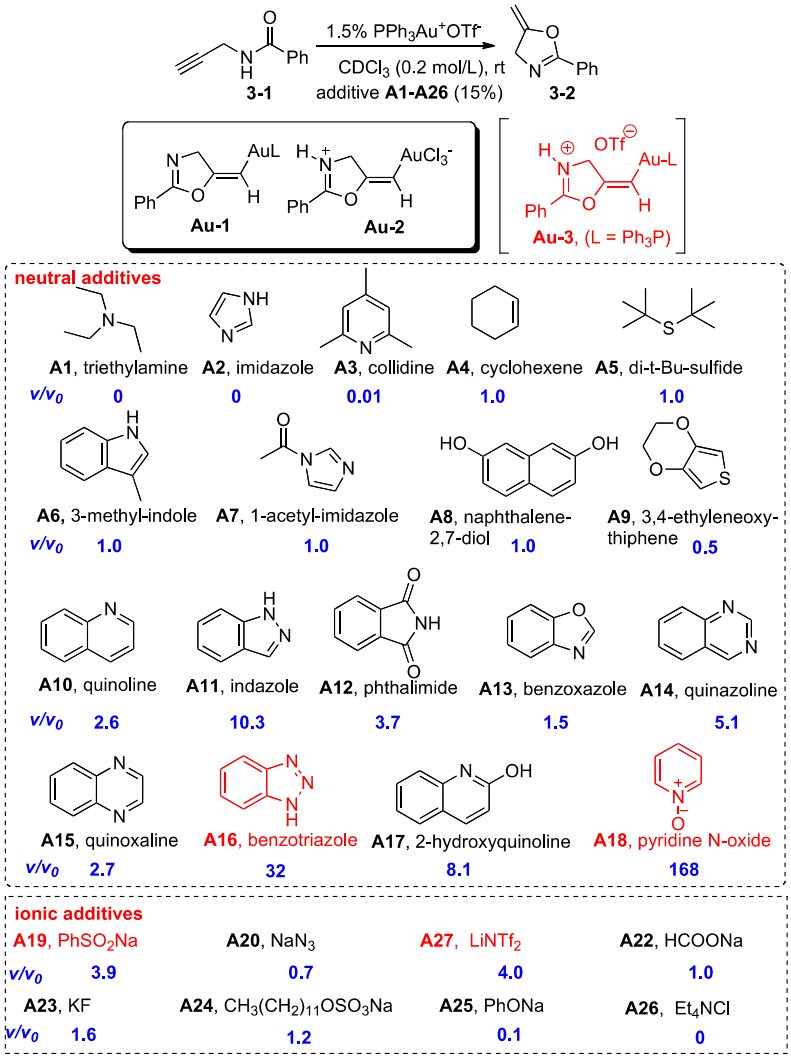

Figure 13. Survey of additive effects in the cyclization of 3-1.

The only way that benzotriazole (**A16**), a good hydrogen bond acceptor, could have accelerated the protodeauration of **Au-3** is through hydrogen bonding.

We tried to verify our hypothesis in Scheme 11 more directly (Figure 14). To be confident that we had generated the protonated vinyl gold complex **Au-3**, we

employed two different experimental conditions (Figure 14). In the first one, we mixed propargyl amide **3-1** with excess amounts of $Ph_3PAu^+OTf^-$; the purpose of the later was to consume all the starting material **3-1**, so there could be no proton acceptor left in the system (Figure 14b). For the second condition, we mixed propargyl amide **3-1** with catalytic amounts of $Ph_3PAu^+OTf^-$ and a strong acid, TfOH; the purpose of the strong acid was to make sure that the all the vinyl gold complex was protonated (Figure 14c). When monitored by ^{31}P NMR, both conditions ended up generating a single new peak at around 45 ppm (Figure 14b and Figure 14c).

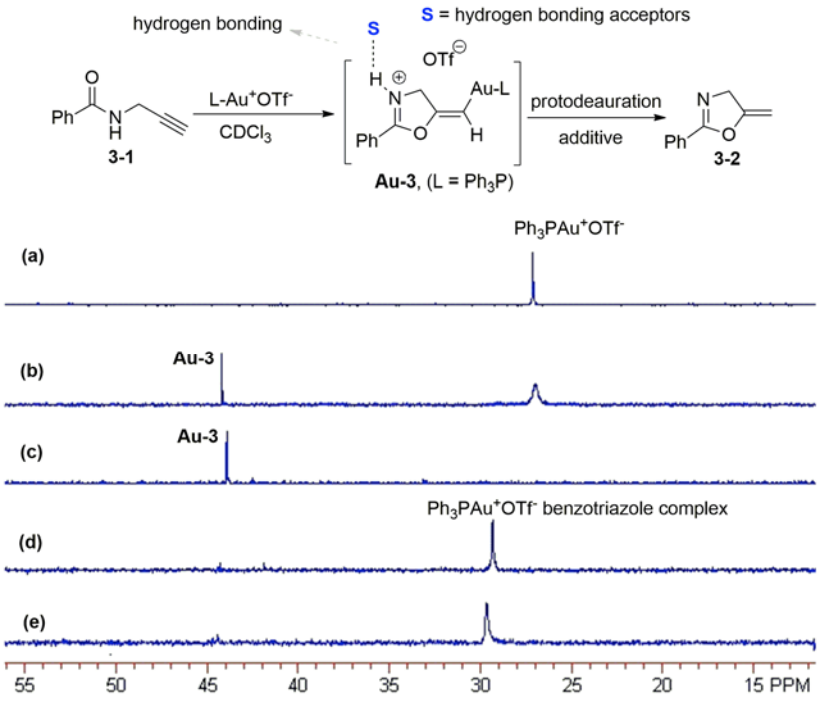

Figure 14. ^{31}P NMR study of protodeauration: a) $Ph_3PAu^+OTf^-$ in $CDCl_3$; b) 5 min after mixing of $Ph_3PAu^+OTf^-$ (2 equiv) with 3-1; c) 5 min after mixing of $Ph_3PAu^+OTf^-$ (0.05 equiv) with 3-1; d) 30 min after addition of benzotriazole (2 equiv towards gold) to b; e) 30 min after addition of benzotriazole (2 equiv towards gold) to c.

Because Hashmi and coworkers had isolated and identified the vinyl gold complex **Au-1** (L = IPr) in the presence of base (Et_3N)[132] and Ahn had identified the

corresponding vinyl gold (III) complex **Au-2**,[120] we thought reasonable to assign the new peak the structure **Au-3** (L = Ph_3P). Its characteristic vinyl proton at 5.2 ppm in ^{1}H-NMR confirmed this assignment.[134] **Au-3** is relatively stable in the two systems; both signal intensities didn't show significant change after 30 min. This behavior indicated that their protodeauration was a relatively slow process and allowed us the possibility of testing the effect of an additive on the protodeauration of **Au-3**. Thus, we added 2 equiv (vs. gold) of the additive benzotriazole to both systems, and after 30 min, the signals corresponding to **Au-3** had disappeared and were replaced by a new one that corresponded to a cationic gold benzotriazole complex (Figure 14d and Figure 14e).[135] In both cases, the starting material **3-1** converted to the expected product **3-2** after the additive was added, as indicated by its ^{1}H-NMR spectrum (quantitative yield). These experiments clearly indicated that the additive (benzotriazole) indeed accelerated the protodeauration of protonated vinyl gold complex **Au-3**. The pK_{aH} of a protonated vinyl gold intermediate (**Au-3**) should be around 4.4 (based on the pK_{aH} of 2-phenyl-oxazoline), but our most effective additives, pyridine N-oxide (pK_{aH} = 0.8) and benzotriazole (pK_{aH} < 0), both have much lower pK_{aH}. In other words, they are not basic enough to abstract the proton from a vinyl gold complex **Au-3**. But the hydrogen bond interaction between **Au-3** and additive will reduce the positive charge on **Au-3** and the hydrogen bond acceptor can act as proton shuttle and therefore facilitate protodeauration. This assumption is consistent with recent quantum mechanics calculations and experimental studies from various research groups. For example, Hashmi and co-workers proposed that in the hydration of alkynes, a cluster of

water molecules might act as proton shuttle to facilitate the protodeauration of a protonated vinyl gold intermediate.[130,136,137] Of course, in all these calculations, the assistance comes from the nucleophile, say, water or phenol; what we are proposing here is that a skillfully chosen additive may have a much greater influence.

Indeed, **A16** cannot accelerate the protodeauration of a neutral vinyl gold complex (Figure 15). According to Figure 13, an additive will act as a reversible inhibitor to slow down stage 1.

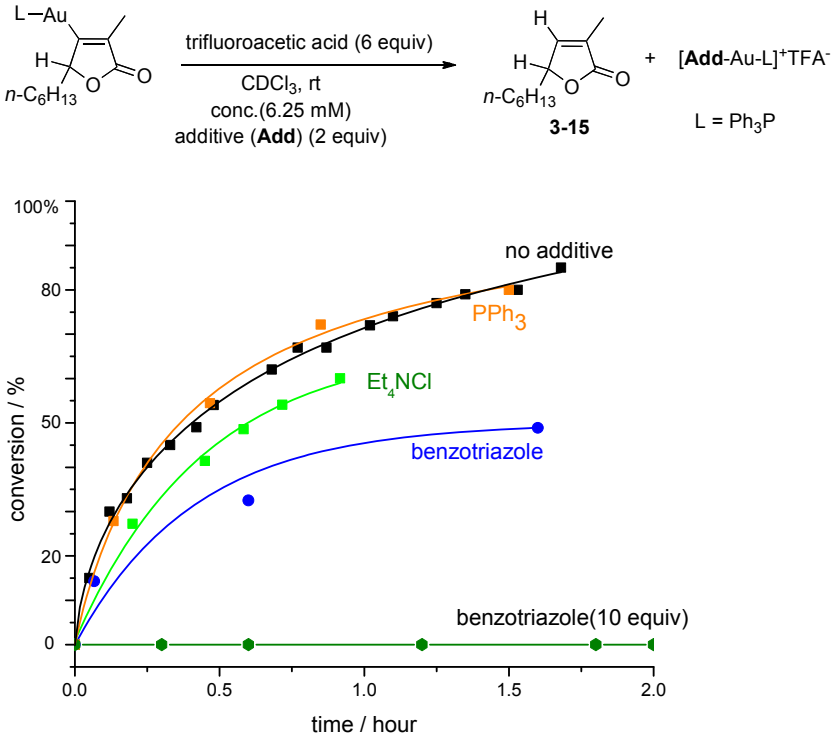

Figure 15. Additive effects on the protodeauration of Au-4

On the other hand, the cationic gold will coordinate with an additive to form a dynamic equilibrium, which will stabilize it against decay (stage 3). This was confirmed by our model reaction (Figure 15). Thus, the only reasonable

explanation is that the additive can accelerate stage 2 (protodeauration[119,138]). Because additives with gold affinity will naturally have a tendency to complex with cationic gold, an acceleration effect on the kinetics of protodeauration may be possible because these additives would rather form a more stable cationic gold additive complex after protodeauration (e.g., [**Add**-Au-L]$^+$ in). We selected protodeauration of **Au-4** as our model system because of our familiarity with this complex[139] and because its reaction with acid gives a clean protodeauration product.[29] We tested a number of additives, but all of them showed either similar or slower kinetic profile than the control. Even additives that are well known for their high affinity to cationic gold (e.g., Ph_3P, chloride) did not accelerate the protodeauration step. And when an excess amount (vs. acid) of an additive (e.g., benzotriazole) was used, the reaction was inhibited. This phenomenon can be rationalized by the competition of the additive for the proton (acid) in the reaction medium. These experimental results indicate that an additive may not be able to assist the protodeauration of neutral vinyl gold complexes based only on its affinity to cationic gold.

Although it is commonly assumed that the relative hydrogen-bond strength of an organic compound bears a simple correlation with its basicity (pK_{aH}), this assumption holds true only for structurally related compounds in a series.[124,125] As shown in Figure 16, the lack of a discernible pattern in the graph of $\ln(v/v_0)$ (from our survey in Figure 13) vs. pK_{aH} underscores the fact that the pK_{aH} of additives is not a good forecast of their usefulness.

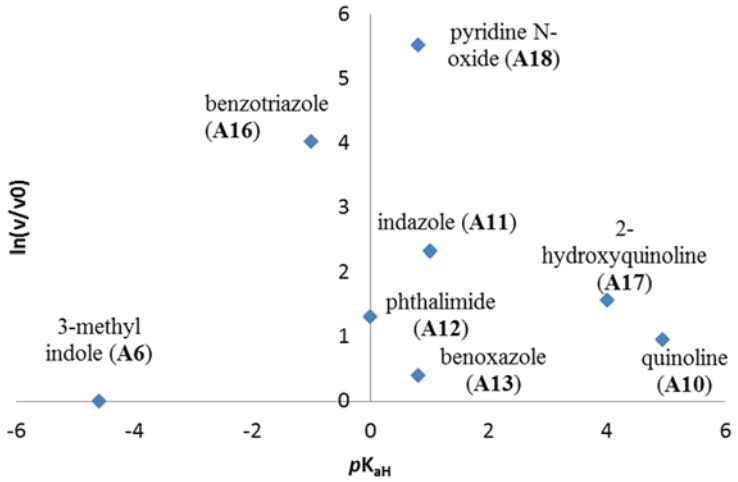

Figure 16. The activity of additives [measured by ln(v/v$_0$)] vs. their basicity (pK$_{aH}$).

Scheme 13 is showing how additives related to pK$_{BHX}$ in gold-catalyzed cyclization of propargyl amide. In our case, charged vinyl gold complex acts as HBD (Lewis acid) and an additive acts as HBA (Lewis base). Using Laurence's data we were able to establish a quantitative correlation between the efficiency of an additive and its hydrogen-bond basicity (Figure 17).

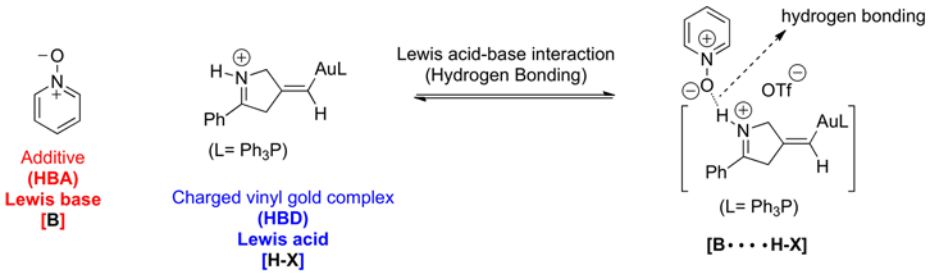

Scheme 13. Hydrogen-bonding in our reaction system (cyclization of propargyl amide).

The correlation in Figure 17 not only offers strong experimental support for the role of hydrogen bonding but it also serves as a practical guide for the selection of additives. Using Laurence's database as guide we selected other compounds that were good hydrogen bond acceptors (pK$_{BHX}$ > 2.6) and had low basicity (pK$_{aH}$ < 4), and found new hits such as DMPU, HMPA, and trimethylphosphine oxide

(v/v_0 = 18.7, 23.9, 30.2 respectively). All these were excellent accelerators for the cyclization of **3-1** even though their structures were quite different.

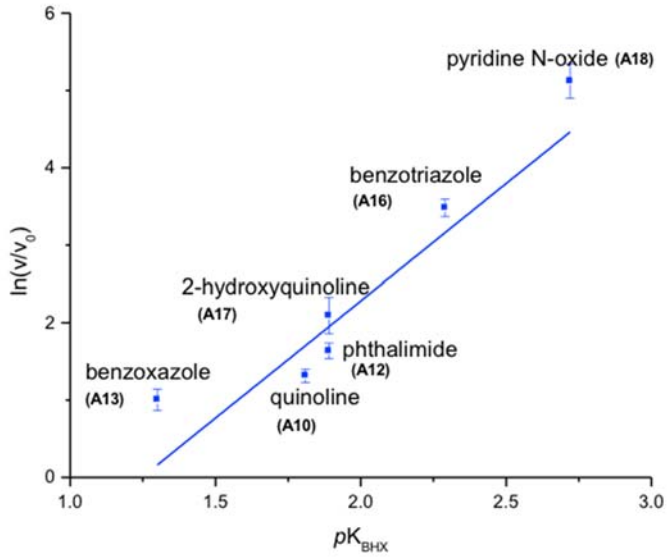

Figure 17. The activity of additives [measured by ln(v/v$_0$)] vs. their hydrogen-bond basicity (measured by pK$_{BHX}$).[140]

We also screened ionic additives (**A19-A26**) with different basicities and found that they too enhanced the kinetics of the reaction although their effects were moderate (Figure 13). Many ionic salts are also good hydrogen bonding acceptors[123] but because no comprehensive pK$_{BHX}$ data for ionic compounds is available, we could not correlate the reactivity of ionic additives with their pK$_{BHX}$.

To increase our understanding of hydrogen bond effects we explored other gold catalyzed reactions (Scheme 14). First we investigated the intermolecular hydroamination of alkynes.[29] As shown in Scheme 14a, a kinetic enhancement was observed in the presence of additives that had proven effective in the cyclization of **3-1** (e.g. pyridine *N*-oxide, benzotriazole), but the enhancement was less dramatic. We attributed this result to the fact that the starting material (amine) in the

hydroamination is in itself a relatively good proton acceptor and also a good hydrogen bond acceptor. We also investigated the intermolecular addition of methanol to alkyne (Scheme 14b). We found that hydrogen bond acceptors with relatively high gold affinity (pyridine *N*-oxide, benzotriazole) inhibited or slowed down the reaction.

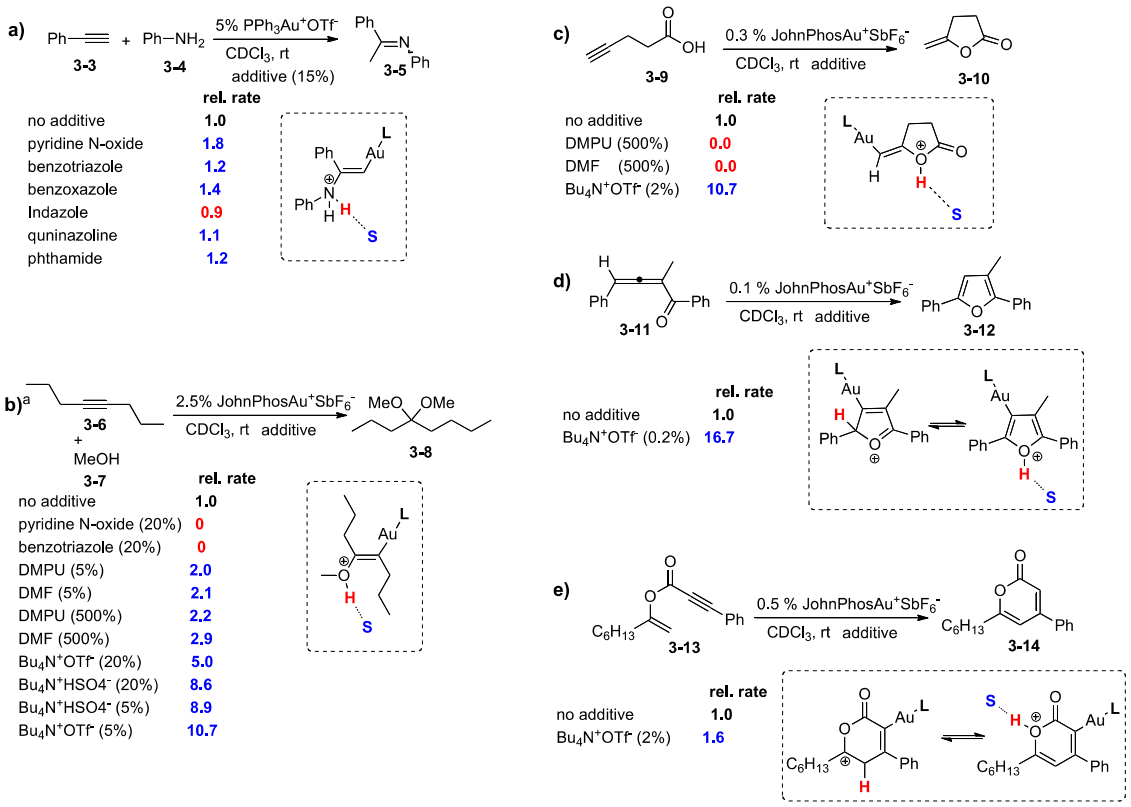

([a] part of **6** was hydrolyzed to ketone by trace water).

Scheme 14. Additive effects on various gold catalyzed reactions (S = hydrogen bond acceptor).

This result was not surprising because stage 1 is the slow or rate-determining step in this intermolecular reaction in which the nucleophile (MeOH) is weak compared to an amine. As expected, hydrogen bond acceptors with lower gold affinity (e.g., DMPU, DMF) [141-148] enhanced the rate of reaction (Scheme 14b), and ionic hydrogen bond acceptors (e.g., $Bu_4N^+OTf^-$) performed significantly better,

possibly because of their even lower affinity towards cationic gold. Although the pK_{BHX} of $Bu_4N^+OTf^-$ was not reported in Laurence's database, the pK_{BHX} values of related salts, such as $Bu_4N^+X^-$ (X = Cl, I) had been tabulated (pK_{BHX} = 2.8 and 4.2 respectively).[123] These values demonstrated their good hydrogen-bond acceptor properties. Given its similarities with $Bu_4N^+X^-$, $Bu_4N^+OTf^-$ should also be a good hydrogen bond acceptor, but the latter has the added advantage of its low basicity and low affinity towards gold. We found that $Bu_4N^+OTf^-$ enhanced the reaction rates of other reactions like cycloisomerization of allenone **3-11**,[149,150] cyclization of 4-pentynoic acid **3-9,**[151] and synthesis of α-pyrone[152] (Scheme 14c-e) substantially. In those reactions, neutral hydrogen bond acceptors were less effective, most likely because of their relatively high affinity towards cationic gold.

Other research groups reported that certain compounds improved the chemical yields in selected gold catalyzed reactions.[153,154] One notable example is the $Ph_3PAu^+OTf^-$ benzotriazole complex reported by Shi and coworkers;[135,155-158] this complex performed better than $Ph_3PAu^+OTf^-$ in a number of transformations, such as the Hashmi phenol synthesis or the rearrangement of propargyl esters. Our hydrogen bonding argument not only accounts for the $Ph_3PAu^+OTf^-$ benzotriazole complex success but also offers a guide for the selection of other suitable hydrogen bond acceptors.

3.3 Summary

In summary, the turnover limiting stage for many gold catalyzed reactions actually occurs in the protodeauration stage. The easiness of the protodeauration stage

depends on the stability of charged vinyl Au species in gold catalysis. Sometimes these compleses are so stable that they can be isolated and characterized by X-ray crystallography. The stability of a charged vinyl Au species limits the turnover number in catalysis because that makes protodeauration stage difficult to happen (positive charge is a deterrent for an incoming proton).

Our experimental studies support that although a strong base will remove the proton in **C**, it will also quench any acid in the system and by doing so it will inhibit protodeauration. Later on, we observed that additives having high hydrogen bond acceptor capability with low basicity toward cationic gold could be better alternatives as compared to strong bases. We observed that an ideal hydrogen bond acceptor additive should have: (i) high hydrogen bonding basicity (pK_{BHX}), (ii) low basicity (pK_a), and (iii) low affinity towards cationic gold. Additives with high hydrogen bonding basicity often show high affinity towards cationic gold. In general, if stage 1 of a given reaction is very fast (as in the cyclization of **3-1**), a good hydrogen bond acceptor with relatively high gold affinity (e.g., benzotriazole) will be useful because, even if it does slow down stage 1, its ability to speed up stage 2 will cause the overall reaction to be faster (because stage 1 is faster than stage 2). But if stage 1 in the target reaction is relatively slow, then the additive's high affinity towards cationic gold may slow down or inhibit the reaction. In this case, a hydrogen bond acceptor with a relatively low affinity towards cationic gold (e.g., DMPU, $Bu_4N^+OTf^-$) will be useful. Hence, the overall effectiveness of a hydrogen bond acceptor will depend on the balance between the two effects. All additives used in the study are commercially available compounds,

a clear advantage to synthetic chemists. In conclusion, we investigated a new strategy to enhance the efficacy of gold catalyzed reactions through hydrogen-bonding assisted protodeauration, using additives chosen by their pK_{BHX} (hydrogen-bond basicity) rather than by their pK_a. In the future, we would like to explore the application of the hydrogen bond basicity concept to other metal catalysis and organocatalysis. The work described in this chapter was published in *Org. Lett.* **2014**, *16*, 636-639.

3.4 Experimental

General

^{1}H, ^{13}C and ^{31}P NMR spectra were recorded at 400, 100 and 162 MHz respectively, using $CDCl_3$ as a solvent. The chemical shifts are reported in δ (ppm) values relative to $CHCl_3$ (δ 7.26 ppm for ^{1}H NMR and δ 77.0 ppm for ^{13}C NMR) and $CFCl_3$ (δ 0 ppm for ^{19}F NMR), multiplicities are indicated by s (singlet), d (doublet), t (triplet), q (quartet), p (pentet), h (hextet), m (multiplet) and br (broad). Coupling constants, *J*, are reported in Hertz. Coupling constants are reported in hertz (Hz). All air and/or moisture sensitive reactions were carried out under argon atmosphere. Solvents (tetrahydrofuran, ether, dichloromethane and DMF) were chemically dried using a commercial solvent purification system. All other reagents and solvents were employed without further purification. The products were purified using a CombiFlash system or a regular glass column. TLC was developed on Merck silica gel 60 F254 aluminum sheets. All the commercial phosphine ligands were purchased from Aldrich or Strem.

General procedure for kinetic experiments using *in situ* NMR spectroscopy

Standard stock solutions of catalyst were made by weighing the L-Au(I)Cl complex into a vial and adding corresponding deuterated solvent, then 1.2 equiv of $Ag^{I}OTf$ was added, the vial was sonicated for 3-5 min at room temperature, then the vial was centrifuged and filtered through a pad of Celite 545. The model reaction was conducted in a NMR tube equipped with a screw cap and septum. All reactions were monitored using a Varian 400MHz NMR Spectrometer with the capacity to adjust the probe temperature and with robotic sample changer.

When ^{31}P NMR was used to monitor the progress of reaction, 85% H_3PO_4 (sealed in a capillary tube) was used as external standard for NMR integration. When ^{1}H NMR was used to monitor the progress of a reaction, a solution of tetramethylsilane in $CDCl_3$ (sealed in a capillary tube) was used as external standard for NMR integration. In some cases, 1,3,5-tri-tert-butylbenzene (internal standard) was used. The reactions were monitored by single pulse ^{1}H NMR. The concentrations of substrate and product were determined by relative integration to the t-butyl peak in the standard (tetramethylsilane or 1,3,5-tri-tert-butylbenzene).

General synthesis of starting materials.

Gold complexes. All gold complexes (L-AuCl) were synthesized using a slightly modified version of a literature method.[116] These complexes were prepared via the following general procedure: Sodium tetrachloroaurate(III) dihydrate (1 mmol) was dissolved in water, and the orange solution was cooled in ice. To this solution,

2,2'-thiodiethanol (3 mmol) was slowly added (ca. 45 min) with stirring. A solution of the phosphine ligand (1 mmol) in EtOH (if the ligand could not be dissolved, more EtOH was used) was added dropwise to yield a white solid. The solid was filtered off, washed with water and then EtOH, and dried in vacuum.

Compound **3-1** was synthesized using literature methods [108,109,131,132] and ^{1}H-NMR of obtained product **3-2** is consistent with literature reports.[108,109,131,132] Compound **3-11** was synthesized using literature method [149,150,159] and ^{1}H-NMR of obtained product **3-12** is consistent with literature reports.[149,150,159] Compound **3-13** was synthesized using literature method[152] and ^{1}H-NMR of obtained product **3-14** is consistent with literature reports.[152] ^{1}H-NMR of obtained product **3-10** is consistent with literature report.[151]

All other starting materials are commercial available from Aldrich, Alfa Aecar and Acros.

Determination of the initial reaction rate for the cyclization of propargyl amide 3-1.

Determination of the initial reaction rate for the cyclization of propargyl amide **3-1** without additive: following the general procedure for kinetic experiments using *in situ* NMR spectroscopy, 0.15 mL of a standard cationic gold solution in $CDCl_3$ (0.01 M) and 0.35 mL $CDCl_3$ were introduced into a NMR tube, and then compound **3-1** (16 mg, 0.1 mmol) and the internal standard were introduced in its solid state. The reaction was kept at room temperature and was monitored for conversion up to 25% by single pulse ^{1}H NMR. A representative plot of [**3-2**] (mol/L) versus time (h) is shown in Figure 18. Because at the initial period of

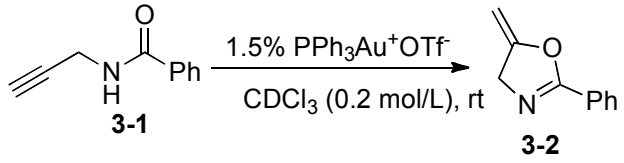

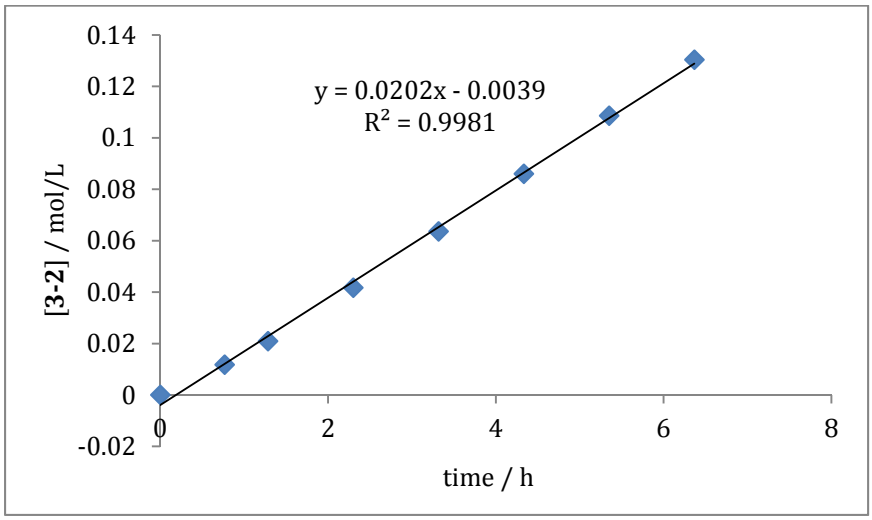

Figure 18. Determination of the initial reaction rate for the cyclization of propargyl amide 3-1.

Table 3. Initial reaction rate for the cyclization of propargyl amide 3-1 in the presence of additives.

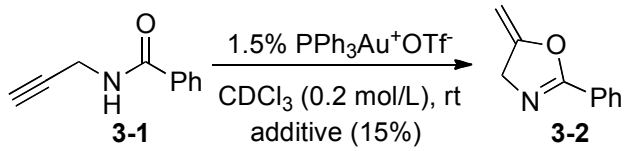

additive	pK_{HBX}	v (mol/L/h)	v (mol/L/h)	v (mol/L/h)	v/v0 average	ln(v/v0) average	standard deviation
		trial 1	trial 2	trial 3			
triazole	2.29	0.749	0.588	0.634	32.2	3.48	0.11
phthalimide	1.81	0.075	0.069	0.082	3.7	1.32	0.09
quinazoline	1.89	0.094	0.110	0.108	5.1	1.64	0.10
quinoxaline	1.3	0.052	0.064	0.050	2.7	1.00	0.14
2-hydroquinoline	1.89	0.126	0.186	0.187	8.1	2.09	0.24
pyridine oxide	2.72	3.867	3.800	2.600	167.8	5.12	0.22

reaction, the kinetic curve appeared to be linear, we used linear least squares to fit the data to determine the slope (reaction rate v_o). Determination of v in the

presence of an additive was conducted in a similar manner as above, except that the additive (15 mol%) was introduced into the NMR tube before the introduction of the starting material **3-1** and the standard (Table 3).

CHAPTER 4. CATIONIC GOLD CATALYST POISONING AND RE-ACTIVATION

4.1 Background

In kinetic studies of catalyzed reactions it is customary to study the relationship between the rate of reaction and the concentration of catalyst to learn more about the mechanism of the reaction. Although a linear correlation between the concentration of the catalyst and the initial rate data often exists when rate is plotted against concentration, numerous studies have shown that the regression line does not intersect with the origin (eq 1, A≠0; also, see Figure 19). If there is no background reaction, the rate should be zero when the catalyst concentration is zero, so A (intercept) should be zero, but this is not the case in many reactions (A is usually less than zero),[30-32] indicating that a threshold catalyst concentration is required. Beyond implying some sort of catalyst poisoning, literature reports have not addressed the causes of this type of threshold. Although this phenomenon is ubiquitous in catalysis, relatively little effort has been spent on the investigation of this anomaly and the possible implications of this threshold phenomenon.[30-32]

$$V = k[catalyst] + A \qquad (eq\ 1)$$

During our research to improve the efficiency of gold catalysis,[29,33-36] we found this threshold phenomenon is common in gold-catalysed reactions. We studied the correlation between rate and gold catalyst concentration in the cyclization of

propargyl amide **4-1** (Figure 19).[132,133] We found that there was a linear relationship between the rate of reaction and the concentration of gold catalyst with a negative intercept A (eq 1). If we extrapolate the data, the minimum gold concentration to start the reaction will be 0.9 mM, which represents a 0.9% gold loading. And indeed, the reaction didn't start at all when the catalyst loading is low (e.g. 0.3% loading). Other kinetic studies on gold catalyzed reactions showed similar trends. For example, Toste and coworkers have reported a linear relationship between rate and gold catalyst loading in the intermolecular hydroamination of allene (rate = 0.0423 [Au]-0.0355).[32] Their data suggested that the minimum catalyst concentration to start the reaction was 1.2 mM (0.81% loading).

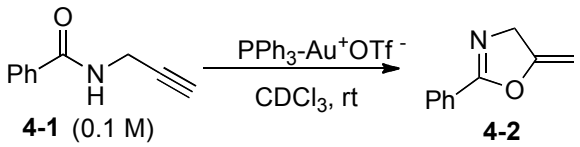

4-1 (0.1 M) **4-2**

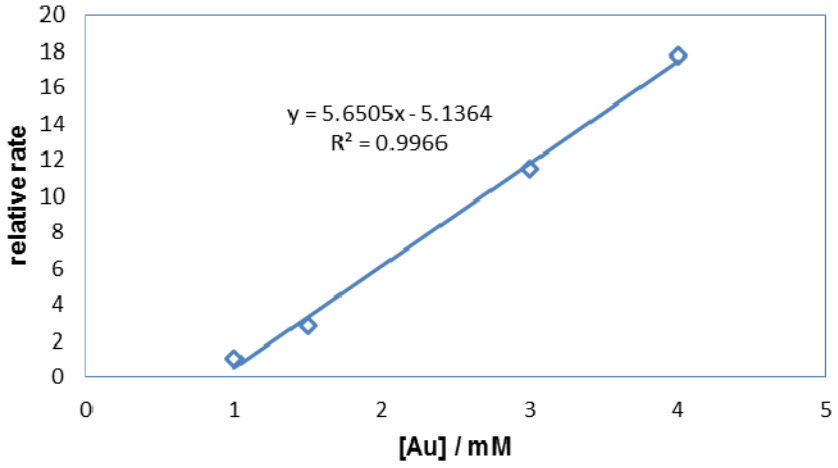

Figure 19. Correlation between rate and catalyst concentration.

We found that the threshold phenomena mentioned above is not limited to the examples above. When we lowered the loading of the gold catalyst below a certain level, the reaction simply would not start (rate was zero for a prolonged time). This occurrence lowers the turnover number (TON) in gold catalysis, and could be one of the main reasons why the TON in gold catalyzed reactions is generally low (1% or higher loading is usually required).

4.2 Results and discussion

A simple explanation for this threshold phenomenon is the poisoning of active catalyst. Impurities such as halides and basic alkali components are well known to contribute to catalyst poisoning in heterogeneous catalysis,[160-162] but there are comparatively few studies on deactivation of homogeneous catalysts.[163] Cationic gold catalyst is sought after because of its high tolerance towards moisture and oxygen (which means we can run reactions without special protection in most cases), but cationic gold has shown a very high affinity towards halides and basic components (e.g. OH^-).[147] A recent study by Maier and coworkers indicates that OH^- or Cl^- has approximately 10^6 times higher affinity towards cationic gold compared to an alkyne.[147]

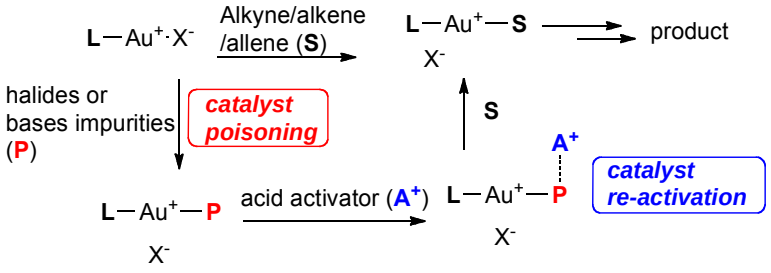

Scheme 15. Poisoning and re-activation of cationic gold catalyst.

This means that just trace amounts of these catalyst poisons like halides and basic components, present in the solvent or starting material, are enough to block the active site of the gold catalyst (Scheme 15) and may completely inhibit the reaction when relatively relative low gold catalyst loading is used. Of course, use of highly purified starting materials and solvents may solve this problem, but we would need time-consuming purification processes, and, often, it is not possible to remove all relevant impurities even after stringent purification protocols. Use of highly purified starting materials and solvents is especially impractical in larger scale synthesis. We propose here that it is not necessary to eradicate all the traces of possible catalyst poisons; instead, the problem can be solved by directly adding a suitable acid activator to the reaction (A^+ in Scheme 15). Acid activators that have high affinity towards **P** (catalyst **p**oison) may re-activate the gold catalyst (Scheme 15). In other words, an acid activator (A^+) acts as a sacrificial reagent to bind to possible catalyst poisons, so that the cationic gold is free to catalyze the reaction. Indeed, Nolan and coworkers had used Brønsted acids like HOTf to activate NHC-Au-OH complexes.[164,165]

We began our studies with the intramolecular hydroarylation of an alkyne[166] (Figure 20). We chose this reaction because direct transformations of aromatic C-H bonds represent a thriving field in organic chemistry, because it promotes efficient, atom economical construction of organic building blocks. We observed that when this reaction was carried at a higher gold catalyst loading (2% vs starting material), the reaction took place smoothly in $CDCl_3$ ($CDCl_3$ was used as received). But as we dropped down the catalyst loading to 0.2%, surprisingly, the reaction

didn't proceed at all (Figure 20). On the other hand, the reaction proceeded well at 0.2% loading using purified $CDCl_3$ as solvent (K_2CO_3-treated and freshly distilled). This result suggests that non-distilled $CDCl_3$ have certain impurities (most likely chlorine/chloride containing compounds)[167] that inhibit gold catalyst activity.

To make the influence of impurity in solvents more significant, we repeated the same reaction at a more diluted condition (changing [**4-3**] from 0.1 M to 0.02 M, keeping gold loading at 0.2%); the reaction still did not progress, even in freshly distilled $CDCl_3$. The reaction performed better in CD_2Cl_2 (probably because there are less halide impurities) at 0.1 M, but when the concentration was decreased to 0.02 M, the reaction became sluggish. Catalyst poisons that either could not be completely removed by simple distillation, or were present in the starting material **4-3** itself may have caused this change of behavior.

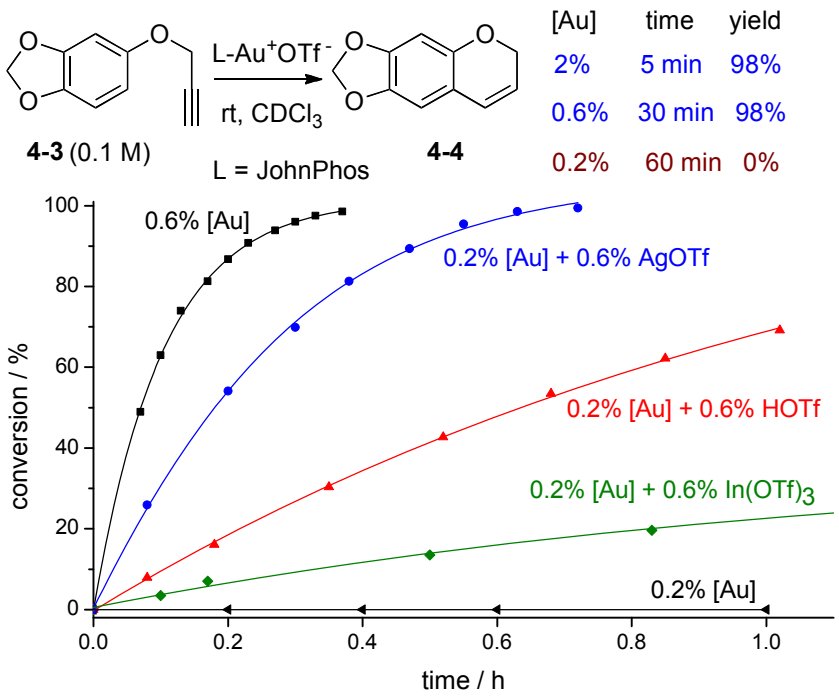

Figure 20. Influence of acid activators in alkyne hydroarylation reaction.

Next, we inspected the effect of common Brønsted acids or Lewis acids in the re-activation of the gold catalyst (Figure 20). We found that AgOTf and TfOH worked very well. Other Lewis acids like $Ga(OTf)_3$, $Eu(OTf)_3$, $Y(OTf)_3$, $Sn(OTf)_2$, $Zn(OTf)_2$, $(CuOTf)_2{\cdot}C_6H_6$ did not show any activity in the re-activation of the gold catalyst. Moreover, we observed that the reaction didn't occur in the presence of Lewis acid or Brønsted acid alone, without gold catalyst, under, otherwise, the same conditions.

We next examined an ester assisted hydration reaction (Figure 21).[168,169] We chose this reaction because it is a straightforward and atom-economical approach to the formation of carbonyl derivatives through alkyne hydration; it is not only environmentally benign, but also cost-effective.

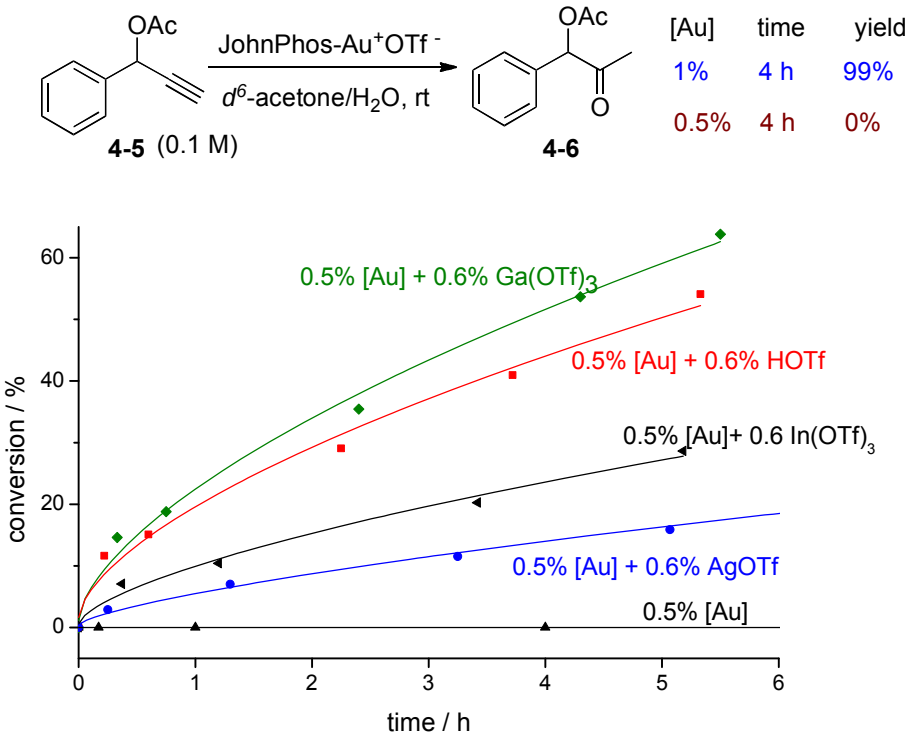

Figure 21. Influence of acid activators in hydration reaction of 4-5.

Again, the reaction proceeded well at 1% gold loading, but when the gold loading was reduced to 0.5%, the reaction did not proceed at all. Use of freshly distilled solvent (acetone) gave better results, but the reaction still did not ensue when the reaction was conducted at more diluted conditions. However, various acid activators re-started the reaction, among them, $Ga(OTf)_3$ provided the best result (Figure 21).

In the cycloisomerization of enyne (Figure 22),[170-172] we observed a similar effect as in previous reactions. We chose this reaction because cycloisomerizations of enynes have emerged as attractive tools for the synthesis of various types of cyclic compounds in an easy one-pot process in which a wide range of transition metal complexes can be used, either in a catalytic or stoichiometric manner.

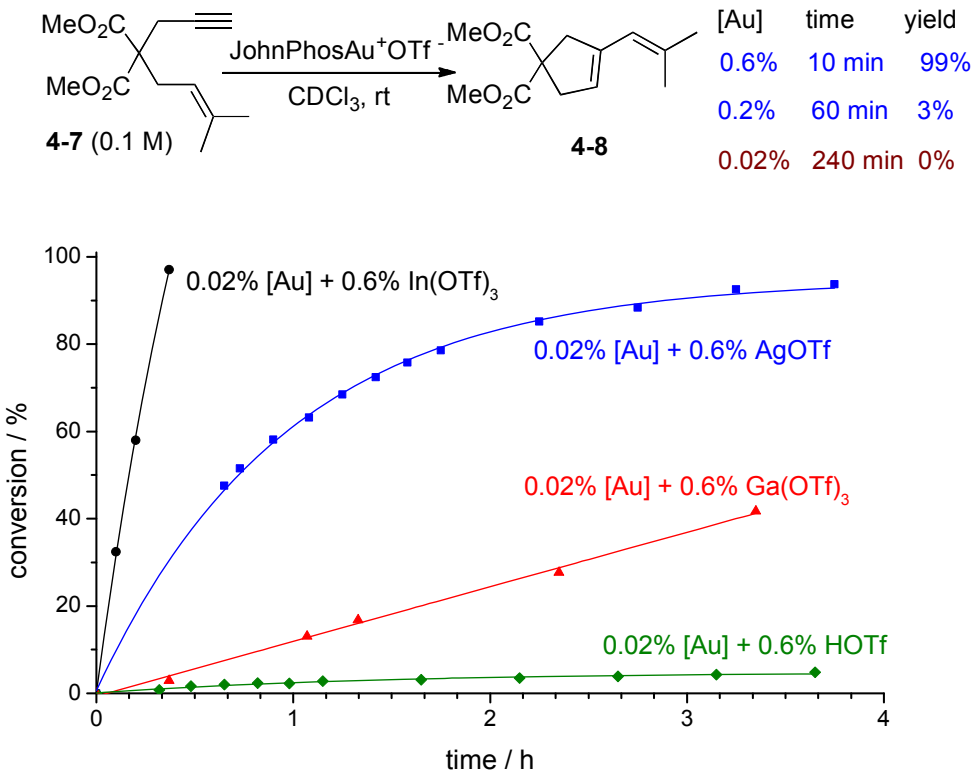

Figure 22. Influence of acid activators in cycloisomerization reaction.

Cycloisomerization of **4-7** took place very smoothly at 0.6% catalyst loading, but it became much slower at 0.2% gold catalyst loading, and its rate decreased to zero when catalyst loading was reduced to 0.02%. A Lewis acid activator, $In(OTf)_3$ caused the reaction to be completed in less than 1 h at very low gold catalyst loading (0.02%). $In(OTf)_3$ was very effective, but a Brønsted acid like HOTf was only marginally effective.

Then we focused our attention to the cyclization of hexynoic acid 4-9 (Figure 23).[151,173] We chose this reaction because it is a general, efficient, and convenient cyclization of alkynes bearing carboxylic acids to the corresponding lactones.

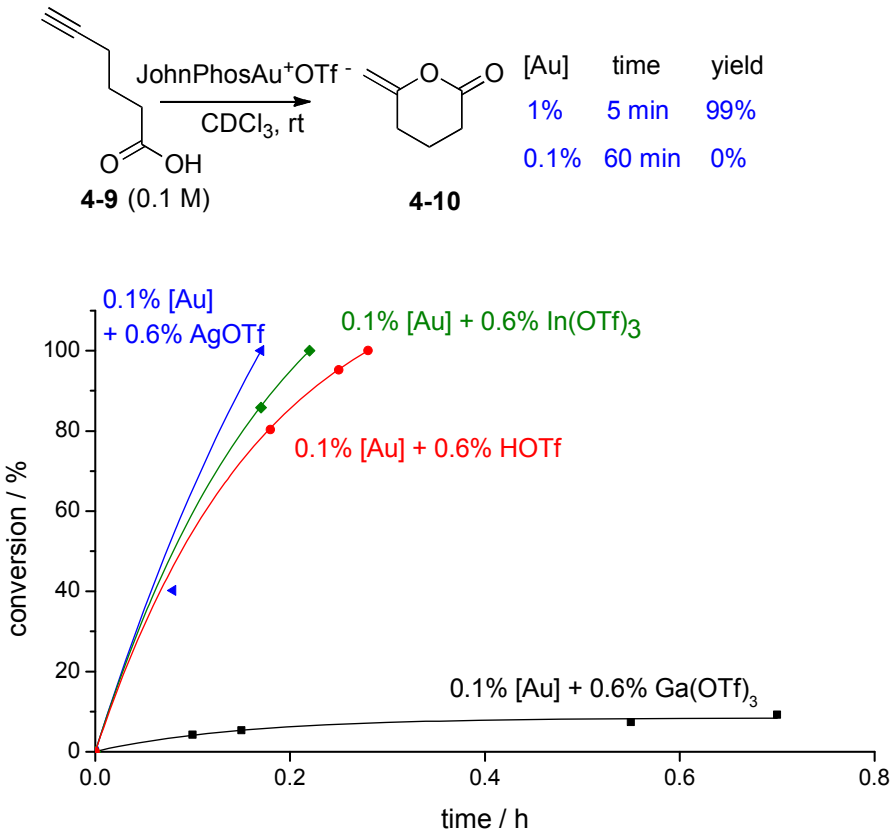

Figure 23. Influence of acid activators in cyclization of 4-9.

Again, we observed that cyclization took place quickly at 1% gold catalyst loading, but the reaction rate dropped down to zero at 0.1% gold catalyst loading. And again, acid activators (AgOTf, In(OTf)3, TfOH) could re-activate the gold catalyst (Figure 23).

Furan has found its widest application in the synthesis of many natural products and gold catalysis play very important role as catalyst for the synthesis of furan. In the cycloisomerization of allenone **4-11** (Figure 24),[149,159] the reaction with 0.2% gold catalyst loading was very fast. However, the same reaction with 0.04% catalyst loading was very sluggish.

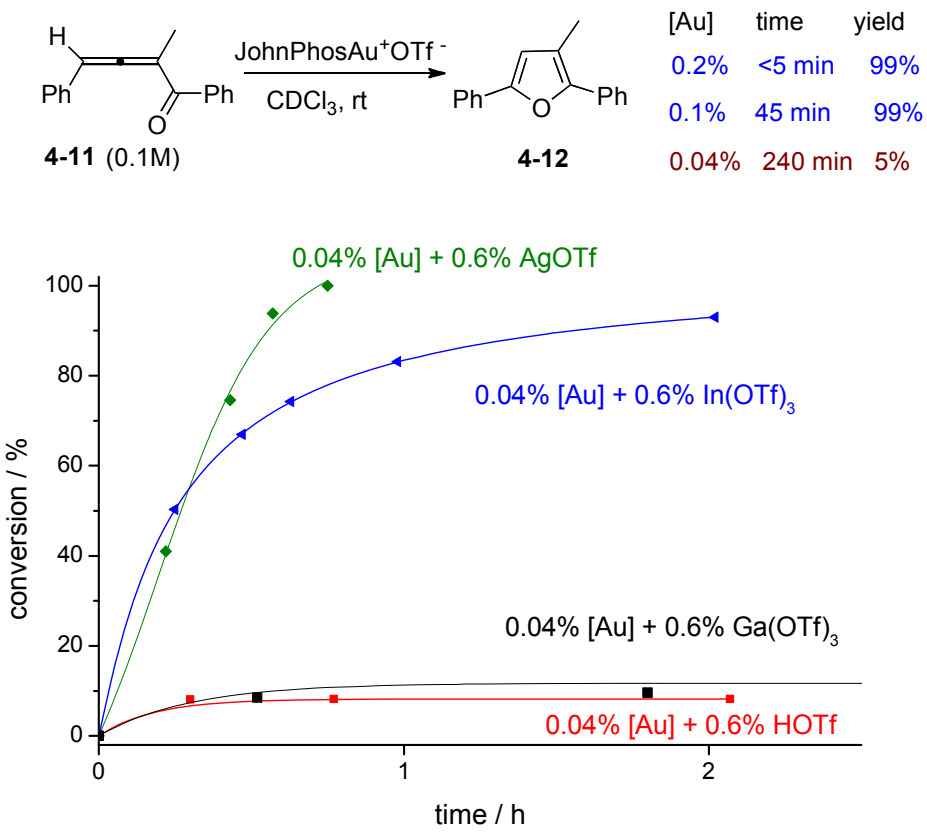

Figure 24. Influence of acid activators in cycloisomerization of 4-11.

Activators like AgOTf and $In(OTf)_3$ sped up the rate of reaction significantly; in contrast, TfOH and $Ga(OTf)_3$ did not have much effect on the reaction rate (Figure 24).

Contamination in solvents or starting materials is not the only source of gold catalyst poisons. External reagents, such as drying agents (e.g. molecular sieves) and filtration aids (e.g. Celite) are also commonly used in synthesis. They may also contain possible gold catalyst poisons (**P**) like halides and alkali bases. For example, a commonly used filtration aid, Celite 545, is prepared from diatomaceous earth treated with a base - sodium carbonate (flux calcined). Indeed, the hydration of **4-5** proceeded well with untreated gold catalyst (2%) loading (Table 4, entry 1) but when the gold catalyst (a solution in acetone) was pre-treated with molecular sieves 4Å, or filtered through Celite 545, the reaction did not proceed with the same catalyst loading (Table 4, entries 2, 3).

Table 4. Influence of molecular sieves and filtration agent.

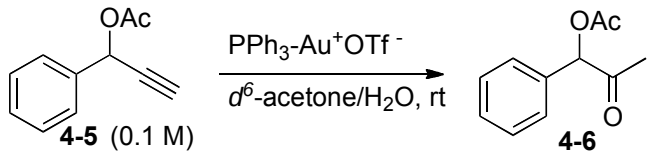

4-5 (0.1 M) **4-6**

entry	[Au]	cat. pre-treatment	time	yield
1	2%	none	3 h	99%
2	2%	filteration through Celite 545	3 h	0%
3	2%	dried over MS 4A	3 h	0%
4[a]	0.2%	$Ga(OTf)_3$ 0.6% added	3 h	25%
5[a]	0.2%	$Ga(OTf)_3$ 0.6% added	12 h	89%

[a] catalyst from entry 3 was used.

The inactive gold catalyst from entries 2 or 3 could be re-activated by the addition of an acid activator $Ga(OTf)_3$ (Table 4, entries 4-5). These results are consistent with literature reports: Yu and coworkers reported that treatment of $Ph_3PAu^+OTf^-$ with molecular sieves led to the formation of much less reactive trigold oxonium complex $[((Ph_3P)Au)_3O]^+OTf^-$ due to the presence of mild bases in molecular sieves.[174] The loss of reactivity of the gold catalyst by Celite filtration is also consistent with a previous report by Shi and coworkers.[169]

We propose that the possible gold catalyst poisons are the halides, bases or other high gold affinity impurities. A direct proof would be isolation and identification of these impurities, and then investigation of these impurities on the reactivity. It is difficult to do this at this time because routine analytic tools commonly used in organic synthesis (NMR, GC-MS, HPLC-MS) are not effective. In order to give an indirect proof, we investigated the effect of halide and bases on the reactivity and ability of acidic promoters to restore the reactivity (Table 5).

Table 5. Influence of halide and base on hydration of 4-5.

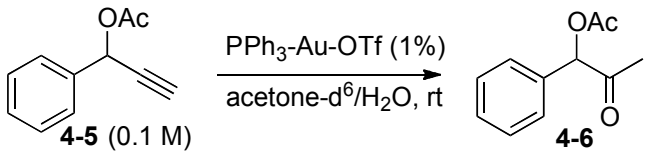

4-5 (0.1 M) **4-6**

entry	additive	time	yield
1	none	4 h	99%
2	$Bu_4N^+OH^-$ (1%)	24 h	2%
3	$Bu_4N^+Cl^-$ (1%)	24 h	8%
4	$Ga(OTf)_3$ (2%) added to entry 2	2 h	99%
5	$Ga(OTf)_3$ (2%) added to entry 3	2 h	99%

We still used hydration of **4-5** as our model reaction. Indeed, bases and halides like $Bu_4N^+Cl^-$ and $Bu_4N^+OH^-$ effectively inhibited the reaction (Table 5, entries 2 and 3). Similarly as Table 4, $Ga(OTf)_3$ effectively restored the reactivity (Table 5, entries 4 and 5).

It should be noted that the acid activators not only can re-activate the poisoned gold catalyst, but they can also positively influence the later stage in the gold catalytic cycle (e.g., protodeauration), acting as co-catalysts to speed-up the reactions.[175]

4.3 Summary

In summary, the threshold phenomenon is ubiquitous in gold catalysis; relatively little effort has been spent on the investigation of this anomaly and the possible implications of this threshold phenomenon. Threshold phenomenon means that a minimum concentration of catalyst is required to start the reaction. This occurrence lowers the turnover number (TON) in gold catalysis, and could be one of the main reasons why the TON in gold catalyzed reactions is generally low (1% or higher loading is usually required). A simple explanation for this threshold phenomenon is the poisoning of active catalyst due to the presence of impurities such as halides (Cl^-) and basic alkali components (OH^-) in solvent and starting materials that block the active site of the catalyst or inhibit the reaction if low catalyst loading was used in the reaction. We proposed that, the problem can be solved by directly adding a suitable acid activator to the reaction, which acts as a sacrificial reagent to bind to possible catalyst poisons.

Our experimental studies support that the reactions were carried smoothly at a higher gold catalyst loading. But as we dropped down the catalyst loading, surprisingly, the reactions did not proceed at all. This observation supports the catalyst poisoning that we described in the introduction. Later on, we observed that the common Brønsted acids or Lewis acids are helping in the re-activation of the gold catalyst even at low catalyst loading, which support the fact that acid activators reactivate the poisioned gold catalyst. Moreover, we also observed that contamination in solvents or starting materials is not the only source of gold catalyst poisons, but external reagents, such as drying agents (e.g. molecular sieves) and filtration aids (e.g. Celite) are also a source of poison in catalysis as described in the introduction. Furthermore, we observed that addition of impurities such as Cl^- & OH^- in the reaction system poisoned the gold catalyst, but as we added an acid activator to the poisoned system, it re-activated the gold catalyst and completed the reaction very easily. In conclusion, high gold affinity impurities (halides, bases) in solvents, starting materials, filtration or drying agents could affect the reactivity of gold catalysts adversely, which may significantly reduce the TON of cationic gold catalyzed reactions. The use of a suitable acid activator (e.g. HOTf, $In(OTf)_3$) re-activates the gold catalyst and contributes to making the reaction proceed smoothly at low gold catalyst loading. A similar protocol could benefit other cationic metal catalysis. In future, we would like to investigate whether acid activators only serve to re-activate a poisoned catalyst, or if they also can act as a cocatalyst in gold-catalyzed reactions. The work described in this chapter was accepted in *Org. Lett.* **2014,** *16*, 3452-3455.

4.4 Experimental

General

^{1}H, ^{13}C, and ^{31}P NMR spectra were recorded with Varian spectrometers at 400, 100, 160MHz respectively, using $CDCl_3$, ^{d}acetone as a solvent. The chemical shifts are reported in δ (ppm) values relative to $CDCl_3$ (δ 7.26 ppm for ^{1}H NMR and (δ 77.0 ppm for ^{13}C NMR), relative to ^{d}acetone (δ 2.05 for ^{1}H NMR), multiplicities are indicated by s (singlet), d (doublet), t (triplet), q (quartet), m (multiplet), and br (broad). Coupling constants (*J*) are reported in Hertz. All deuterated solvents used in the reactions were used as received. All simple solvents (e.g. dichloromethane) were chemically dried using a commercial solvent purification system. All other reagents and solvents were employed without further purification. TLC was developed on Merck silica gel 60 F254 aluminum sheets. All the commercial reagents, and solvents were purchased from Aldrich or Strem or Fisher, and used without purification except cyclohexene (cyclohexene was redistilled). FT-ICR-MS - Fourier Transform-Ion Cyclotron Resonance-Mass Spectrometer was used for high resolution ESI-MS spectroscopy.

Monitoring the reaction using *in situ* NMR spectroscopy

When ^{1}H NMR was used to monitor the progress of a reaction, a solution of tetramethylsilane in $CDCl_3$ (sealed in a capillary tube) was used as an external standard for NMR integration. In some cases, 1,3,5-tri-tert-butylbenzene (internal standard) was used. The reactions were monitored with ^{1}H NMR (single pulse or 1

scan for fast reactions, 8 scans for slow reactions). Some NMR measurements were conducted using a NMR experiment array (a series of spectra measured at predetermined time intervals over a period of time by adjusting the pre-acquisition delay). NMR experiment array gives better precision for both concentration (*via* integration) and reaction time, because each measurement is conducted at almost identical shimming and temperature conditions.

General procedure for preparation of starting materials

Synthesis of gold complexes (L-AuCl).

All gold complexes (L-AuCl) were synthesized using a slightly modified version of a literature method.[176] These complexes were prepared via either one of the following general procedures:

Method 1: Sodium tetrachloroaurate(III) dihydrate (1 mmol) was dissolved in water, and the orange solution was cooled in ice. To this solution, 2,2'-thiodiethanol (3 mmol) was slowly added (ca. 10 min) with stirring. After stirring at 0^{o}C for another 30 min, a solution of the phosphine ligand (1 mmol) in EtOH (if the ligand could not be dissolved, more EtOH was used) was added dropwise to yield a white solid. The solid was filtered off, washed with water followed by EtOH, and ultimately dried in vacuum.

Method 2: To a vial chloro(dimethylsulfide)gold(I) (1 mmol) was dissolved in dichloromethane and cooled in an ice bath. A solution of the phosphine ligand (1 mmol) in dichloromethane was added dropwise, and the resulting solution was allowed to warm to room temperature and stirred at room temperature for 3 h.

After TLC indicated complete consumption of the starting material, the reaction solution was concentrated to dryness under reduced pressure, and the gold complex product was further dried under high vacuum.

Synthesis of starting materials.

Compound **4-1** was synthesized using literature methods [108,109,131,132] and ^{1}H-NMR of obtained product **4-2** is consistent with literature reports.[108,109,131,132] Compound **4-3** was synthesized using literature methods[166] and ^{1}H-NMR of obtained product **4-4** is consistent with literature reports.[166] Compound **4-5** was synthesized using literature methods[168] and ^{1}H-NMR of obtained product **4-6** is consistent with literature reports.[168] Compound **4-7** was synthesized using literature methods[170] and ^{1}H-NMR of obtained product **4-8** is consistent with literature reports.[170] Compound **4-11** was synthesized using literature method[152] and ^{1}H-NMR of obtained product **4-12** is consistent with literature reports.[152] ^{1}H-NMR of obtained product **4-10** is consistent with literature reports.[149,150,159] All other starting materials are commercially available from Aldrich, Alfa Aecar and Acros.

Preparation of cationic gold (L-Au^{+}OTf $^{-}$) stock solution.

Standard stock solutions of cationic gold catalyst were made by weighing the L-Au(I)Cl (0.1 mmol) complex into a vial and adding corresponding deuterated solvent, then 1.2 equiv of Ag^{I}OTf (0.12 mmol) was added, the vial was sonicated for 3-5 min at room temperature, then the vial was centrifuged and the clear solution was transferred to a clean glass vial. The solution was kept in a freezer (-20 ^{o}C) until it was used.

Preparation of stock solutions of activator (TfOH, AgOTf, $In(OTf)_3$, and $Ga(OTf)_3$).

Stock solutions of activator (0.01 M) were prepared by weighing activator (0.02 mmol) in a glass vial and dissolved it in deuterated acetone (2 mL). The solution was kept in the freezer (-20 ^oC) until it was needed.

Kinetic study for cyclization of 4-1 using initial rate method

Determination of the initial reaction rate for the cyclization of propargyl amide **4-1**: following the general procedure for kinetic experiments using *in situ* NMR spectroscopy, a standard solution of $Ph_3PAu^+OTf^-$ (1 mM to 4 mM, per aliquot) in $CDCl_3$ (0.01 M) and different amount of $CDCl_3$ were introduced into a NMR tube at four different concentrations of standard gold solution, and then compound **4-1** (8 mg, 0.1 M) and the internal standard (1,3,5-tri-tert-butyl benzene) were introduced in their solid state. The reaction was kept at room temperature and was monitored for conversion up to 20% by single pulse ^1H NMR. Because at the initial period of reaction, the kinetic curve appeared to be linear, we used linear least squares fit of the data to determine the slope (reaction rate V_o).

General procedure for the hydroarylation of alkyne (4-3)

In the absence of acid activator: To a solution of alkyne **4-3** (6.3 μL, 0.05 mmol) in $CDCl_3$ (0.484 mL) inside the NMR tube, the stock solution of [P(*t*-Bu)$_2$*o*-biphenyl]Au^+OTf^- in $CDCl_3$ (10 μL, 0.01M, 0.2 mol%) was added to the reaction

mixture in the NMR tube. Reaction was analyzed by ^{1}H-NMR to monitor the progress of the reaction.

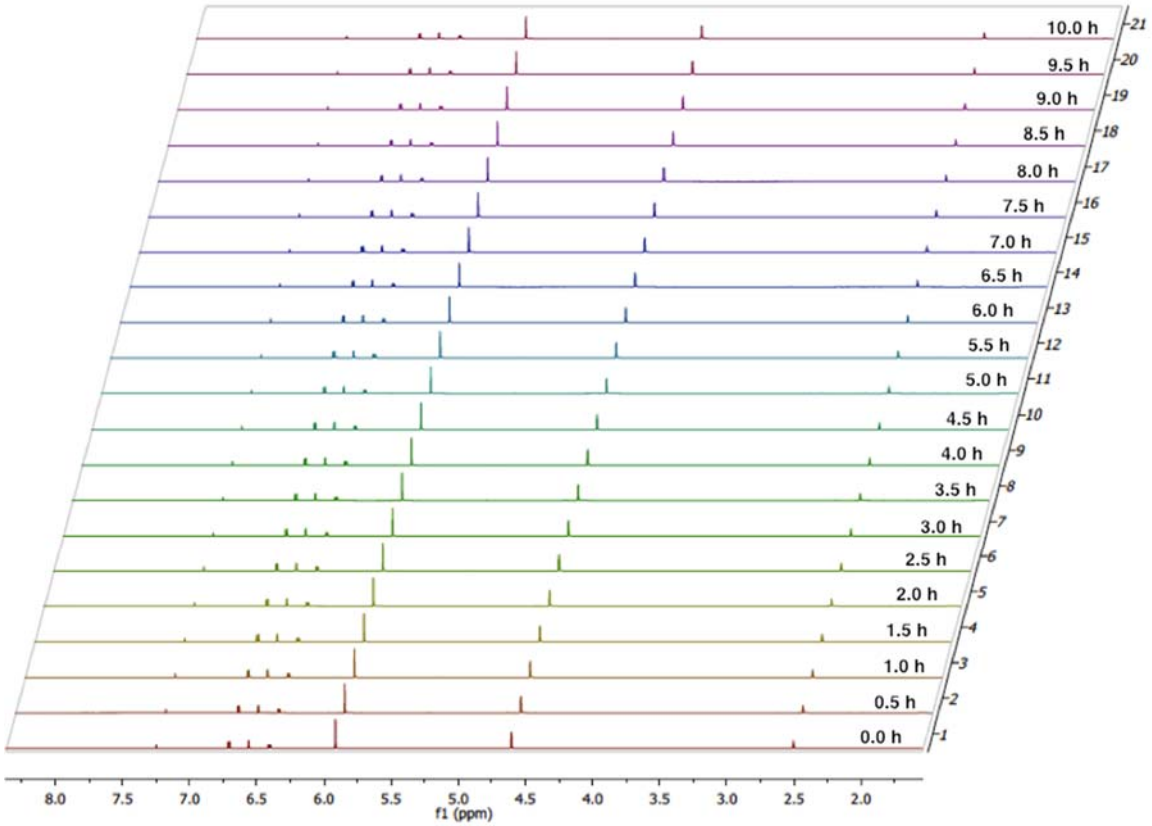

Figure 25. NMR array of hydroarylation 4-3 in the absence of acid activator.

In the presence of acid activator: To a solution of alkyne **4-3** (6.3 µL, 0.05 mmol) in $CDCl_3$ (0.454 mL) inside the NMR tube, the stock solution of [P(*t*-Bu)$_2$*o*-biphenyl]Au^{+}OTf $^{-}$ in $CDCl_3$ (10 µL, 0.01M, 0.2 mol%) was added to the reaction mixture in the NMR tube. Different activator stock solutions (30 µL, 0.01M, 0.6%) were introduced into corresponding NMR tubes. The progress of the reaction was monitored by ^{1}H-NMR.

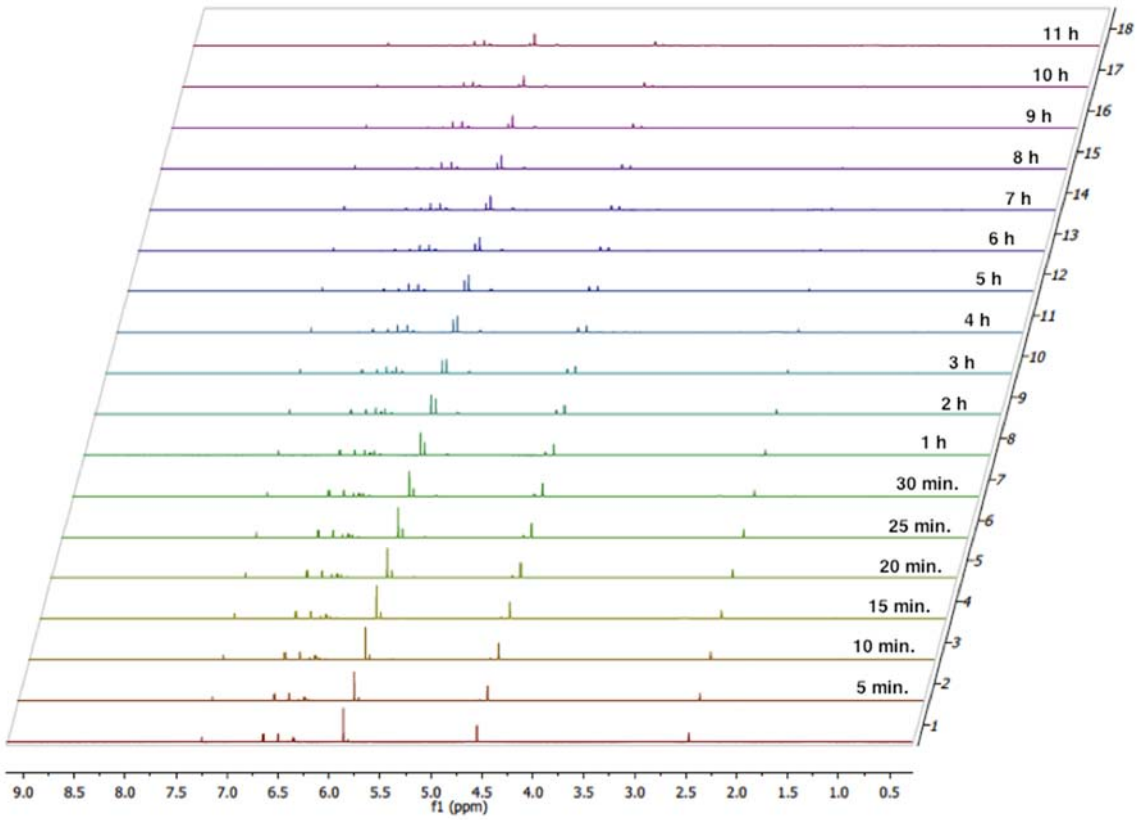

Figure 26. NMR array of hydroarylation of 4-3 in the presence of acid activators.

General procedure for the hydration of propargyl alkyne (4-5)

In the absence of acid activator: To a solution of propargyl ester **4-5** (8.71 μL, 0.05 mmol) in ^{d}acetone (0.466 mL) inside the NMR tube, the stock solution of [P(*t*-Bu)$_2$*o*-biphenyl]Au^{+}OTf^{-} in ^{d}acetone (25 μL, 0.01M, 0.5 mol%) was added to the reaction mixture in the NMR tube. The progress of the reaction was monitored by ^{1}H-NMR.

In the presence of acid activator: To a solution of propargyl ester **4-5** (8.71 μL, 0.05 mmol) in ^{d}acetone (0.437 mL) inside the NMR tube. The stock solution of [P(*t*-Bu)$_2$*o*-biphenyl]Au^{+}OTf^{-} in ^{d}acetone (25 μL, 0.01M, 0.5 mol%) was added to the reaction mixture in the NMR tube. Different activator stock solutions (30 μL,

0.01M, 0.6 mol%) were introduced into corresponding NMR tubes. The progress of reaction was monitored by ^{1}H-NMR.

General procedure for the cycloisomerization of 1,6-enyne (4-7)

In the absence of activator: To a solution of 1,6-enyne **4-7** (9.8 μL, 0.05 mmol) in $CDCl_3$ (0.488 mL) inside the NMR tube, the stock solution of [P(*t*-Bu)$_2$*o*-biphenyl]$Au^{+}OTf^{-}$ in $CDCl_3$ (2 μL, 0.01M, 0.04 mol%) was added to the reaction mixture in the NMR tube. The progress of the reaction was monitored by ^{1}H-NMR.

In the presence of acid activator: To a solution of 1,6-enyne **4-7** (9.8 μL, 0.05 mmol) in $CDCl_3$ (0.458 mL) inside the NMR tube, the stock solution of [P(*t*-Bu)$_2$*o*-biphenyl]$Au^{+}OTf^{-}$ in $CDCl_3$ (2 μL, 0.01M, 0.04 mol%) was added to the reaction mixture in the NMR tube. Different activator stock solutions (30 μL, 0.01M, 0.6 mol%) were introduced into corresponding NMR tubes. The progress of the reaction was monitored by ^{1}H-NMR.

General procedure for the cyclization of hexynoic acid (4-9)

In the absence of acid activator: To a solution of hexynoic acid **4-9** (6.25 μL, 0.05 mmol) in $CDCl_3$ (0.489 mL) inside the NMR tube, the stock solution of [P(*t*-Bu)$_2$*o*-biphenyl]$Au^{+}OTf^{-}$ in $CDCl_3$ (5 μL, 0.01M, 0.1 mol%) was added to the reaction mixture in the NMR tube. The progress of the reaction was monitored by ^{1}H-NMR.

In the presence of acid activator: To a solution of hexynoic acid **4-9** (6.25 μL, 0.05 mmol) in $CDCl_3$ (0.459 mL) inside the NMR tube, the stock solution of [P(*t*-

Bu)$_2$*o*-biphenyl]Au$^+$OTf $^-$ in $CDCl_3$ (5 μL, 0.01M, 0.04 mol%) was added to the reaction mixture in the NMR tube. Different activator stock solutions (30 μL, 0.01M, 0.6 mol%) were introduced into corresponding NMR tubes. The progress of the reaction was monitored by ^{1}H-NMR.

General procedure for the cycloisomerization of allenone (4-11)

In the absence of acid activator: To a solution of allenone **4-11** (12.4 mg, 0.05 mmol) in $CDCl_3$ (0.498 mL) inside the NMR tube, the stock solution of [P(*t*-Bu)$_2$*o*-biphenyl]Au$^+$OTf $^-$ in $CDCl_3$ (2 μL, 0.01M, 0.04 mol%) was added to the reaction mixture in the NMR tube. The progress of the reaction was monitored by ^{1}H-NMR.

In the presence of acid activator: To a solution of allenone **4-11** (12.4 mg, 0.05 mmol) in $CDCl_3$ (0.468 mL) inside the NMR tube, the stock solution of [P(*t*-Bu)$_2$*o*-biphenyl]Au$^+$OTf $^-$ in $CDCl_3$ (2 μL, 0.01M, 0.04 mol%) was added to the reaction mixture in the NMR tube. Different activator stock solutions (30 μL, 0.01M, 0.6 mol%) were introduced into corresponding NMR tubes. The progress of the reaction was monitored by ^{1}H-NMR.

CHAPTER 5. GOLD-CATALYZED ADDITION OF N-HYDROXY HETEROCYCLES TO ALKYNES AND SUBSEQUENT 3,3-SIGMATROPIC REARRANGEMENT

5.1 Background

Gold catalyzed addition of *O*-nucleophiles to alkynes will first give synthetically important vinyl ether products,[177] but these are usually not stable enough to be isolated by standard silica gel chromatography.[177] We found that a gold catalyzed addition of *N*-hydroxy heterocycles to alkynes gives an easily isolatable vinyl ether product **5-3**, and the subsequent 3,3-sigmatropic rearrangement of **5-3** (Scheme 16a) gives access to pharmaceutically important functionalized *N*-heterocycles.[37-39,42] Furthermore, reaction of **5-3** with an electrophile such as the electrophilic fluorinating reagent (Selectfluor), gives functionalized α-fluoroketones. Functionalized benzotriazoles are important precursors for the synthesis of pyrimidine- or pyridine-based compounds used in the treatment of GSK3 mediated disorders because they inhibit glycogen synthase kinase (GSK3).[48] Many functionalized benzotriazoles and indoles are also important synthetic intermediates.[49,50]

Gold-catalyzed oxygen transfers are synthetically useful and attract a lot of attention.[59-65,178-180] In 2009, Asensio and co-workers applied the oxygen transfer

concept in their intermolecular gold-catalyzed sulfoxide addition to alkynes that allowed the preparation of sulfur containing arenes (Scheme 16b).[181] A similar approach was employed by Zhang and co-workers in their synthesis of 2-alkylindoles from *N*-arylhydroxylamines and terminal alkynes (Scheme 16c).[182,183]

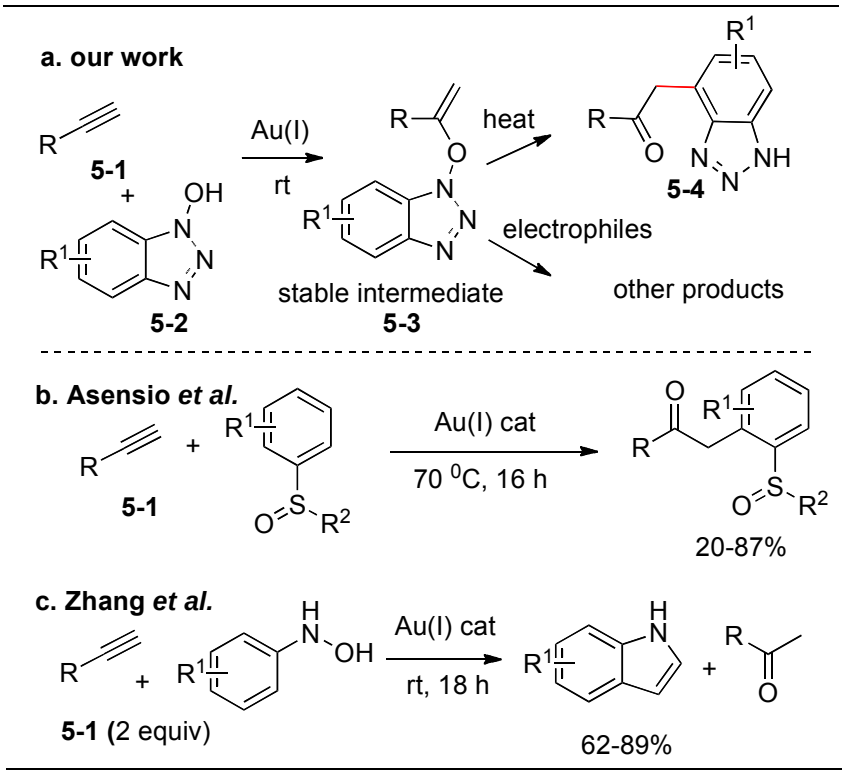

Scheme 16. Gold-catalyzed oxygen transfer reactions.

5.2 Results and discussions

We selected the reaction of 4-hydroxyhex-1-yne **5-1a** with *N*-hydroxybenzotriazole **5-2a** as our model reaction (Table 6). To our delight, when we treated **5-1a** (1 equiv) with **5-2a** (1.1 equiv) in the presence of a standard gold catalyst, i.e., Ph_3PAuCl (5%) with AgOTf (5%), we acquired a near quantitative isolated yield of the vinyl ether **5-3aa**, using DCE (dichloroethane) as solvent at room temperature (Table 6, entry 1). Reducing the loading of gold catalyst to 1%

did not reduce the yield, although it lengthened the reaction time (Table 6, entry 2). When we reduced the amount of **5-2a** from 1.5 equiv to 1.1 equiv, either in DCE or acetonitrile, the reaction yields were still excellent, although, the reaction was slower in acetonitrile (Table 6, entries 3-4). With optimized conditions in hand, we studied the scope for synthesis of other vinyl ethers **5-3** (Table 7).

Table 6. Reaction optimization for synthesis of vinyl ether 5-3.

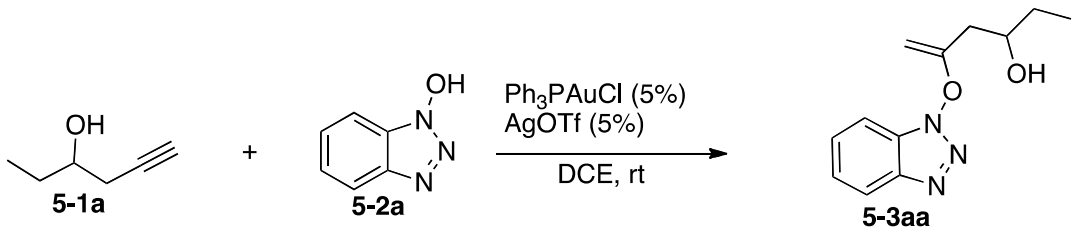

entry	equiv of **5-2a**	solvent	time	isolated yield (%)
1	1.5	DCE	6 h	quantitative
2[a]	1.5	DCE	24 h	quantitative
3	1.1	DCE	8 h	99%
4	1.1	CH_3CN	16 h	quantitative

[a] Ph_3PAuCl (1%), AgOTf (1%)

Terminal alkynes bearing aliphatic substituents (Table 7, entries 1, 3, 5, 7, 9) afforded good to excellent yields of the expected products. Functional groups like hydroxyl (Table 7, entries 1 and 7), methoxy (Table 7, entry 5) and alkenes (Table 7, entry 6) were well tolerated. In the case of aromatic alkynes, the reaction also gave high yields (Table 7, entries 2, 4). When we reacted 1,6-heptadiyne with 2.2 equiv of **5-2a**, an excellent yield of **5-3ha** was obtained (Table 7, entry 8). When substituted *N*-hydroxybenzotriazoles (Table 7, entries 10, 11, 12, 13) were screened, we found that *N*-hydroxybenzotriazoles substituted with electron

donating groups (Table 7, entries 12, 13) or with electron withdrawing groups (Table 7, entries 10, 11) gave excellent yields of product **5-3**. Moreover, when we used *N*-hydroxy-7-azabenzotriazole, we also isolated high yields of the expected 7-azabenzotriazole derivatives (Table 7, entries 14, 15, 16). We also investigated the use of an allene as a substrate (Table 7, entry 17). In this case, when allene **5-1k** was treated with *N*-hydroxybenzotriazole **5-2a**, we obtained **5-3qa** in lower yield (17%); the majority of unreacted allene **5-1k** was recovered, indicating that an allene is less reactive than the corresponding alkyne under these conditions. Interestingly, 1-hydroxyindazole (**5-2e**),[184] *N*-hydroxy-4-quinolone (**5-2f**),[185] and *N*-hydroxyquinazolinediones (**5-2g**)[186] didn't react with alkynes under the same conditions (Table 7, entries 18, 19, 20). The reasons for this are not clear to us at this point. Furthermore, we also examined few *N*-oxides such as benzo[c]cinnoline-*N*-oxide, and benzofuroxan, but they didn't show any reactivity with alkynes under the same conditions. Moreover, we also tested reaction of internal alkynes such as 2-decyne, and 5-decyne with *N*-hydroxybenzotriazole (**5-2a**), but their reactions were very sluggish.

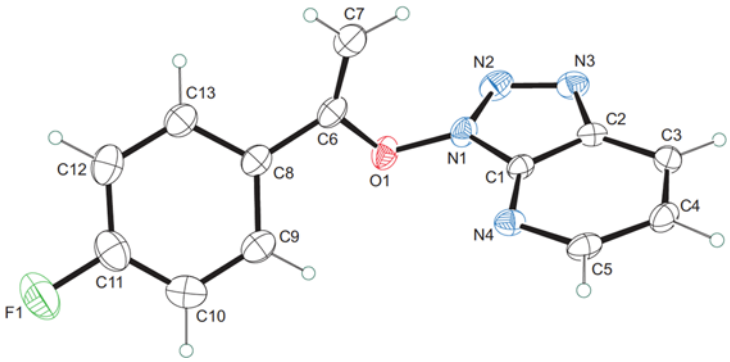

Figure 27. *ORTEP*-3 diagram of 5-3od showing 50% ellipsoids. Selected bond lengths (Å) O1-N1, 1.3697(18); O1-C6, 1.418(2); C6-C7, 1.313(3); N1-N2, 1.345(2); N2-N3, 1.309(2).

Table 7. Synthesis of vinyl ether intermediates.

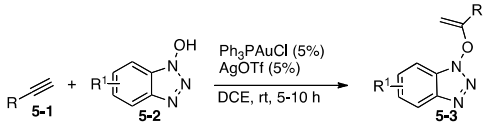

5-1 + 5-2 → 5-3

entry	5-1	5-2	5-3 (isolated yield %)
1.	5-1a	5-2a	5-3aa, 100%
2.	5-1b	5-2a	5-3ba, 80%
3.	5-1c	5-2a	5-3ca, 96%
4.	5-1d	5-2a	5-3da, 83%
5.	5-1e	5-2a	5-3ea, 89%
6.	5-1f	5-2a	5-3fa, 70%
7.	5-1g	5-2a	5-3ga, 53%; 5-3ga', 12%
8.	5-1h	5-2a	5-3ha, 95%[a]
9.	5-1i	5-2a	5-3ia, 100%
10.	5-1a	5-2b	5-3jb, 81%
11.	5-1c	5-2b	5-3kb, 87%
12.	5-1c	5-2c	5-3lc, 100%
13.	5-1a	5-2c	5-3mc, 92%
14.	5-1c	5-2d	5-3nd, 80%
15.	5-1d	5-2d	5-3od, 80%
16.	5-1j	5-2d	5-3pd, 70%
17.	5-1k	5-2a	5-3qa, 17%
18.	5-1c	5-2e	5-3re, 0%
19.	5-1c	5-2f	5-3sf, 0%
20.	5-1c	5-2g	5-3tg, 0%

[a] 2.2 equiv of **5-2a** was used

In nearly all cases, the reaction proceeds with exclusive regioselectivity. However, reaction of propargyl alcohol **5-1g** (Table 7, entry 7) also led to formation of a minor regioisomer **5-3ga'** (12% yield), possibly due to steric reasons. The structure of **5-3od** was confirmed by X-ray crystallography **(**Figure 27).

Next, we explored the use of vinyl ethers **5-3** as useful synthetic intermediates. We first investigated 3,3-sigmatropic rearrangements of **5-3**, which would lead to formation of new C-C bonds affording functionalized benzotriazoles. We investigated the effects of Lewis acids, bases, solvents, and temperature and found dioxane/100 ^{0}C was the optimal condition for rearrangement. We found that 3,3-sigmatropic rearrangement of vinyl ethers **5-3** gives the 7-substituted 1-H-benzotriazoles **5-4** as the major product, but we also isolated the *N*-sustituted ketones **5-5** as a side products. A detailed mechanism explaining formation of **5-5** is not clear yet.

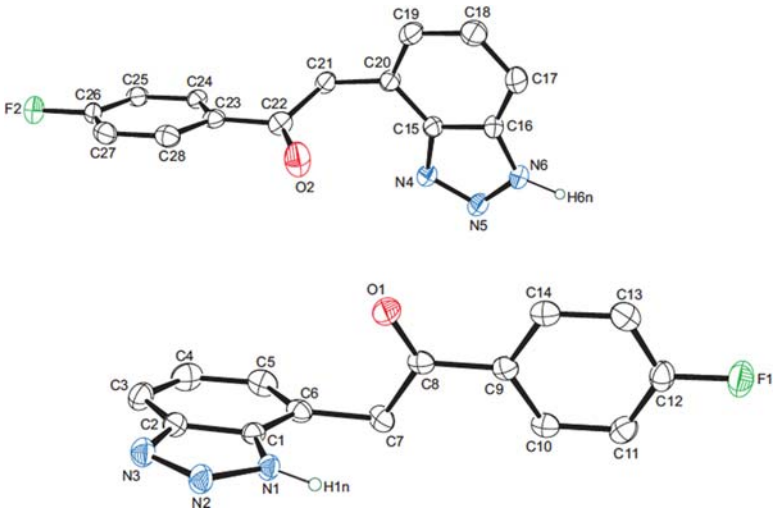

Figure 28. *ORTEP*-3 diagram of 5-4e illustrating two unique conformers present in the asymmetric unit shown at 50% ellipsoids. A third molecule identical to the top conformer in the asymmetric unit has been omitted for clarity. Additionally, only H atoms attached to N atoms are shown. Selected bond lengths (Å): O1-C8, 1.2238(19); C6-C7, 1.504(2); C7-C8, 1.516(2); N1-N2, 1.3497(17); N2-N3, 1.3130(19).

The structure of **5-4e** was confirmed unambiguously by X-ray crystallography (Figure 28). Depending on recrystallization conditions, either tautomer of **5-4e** could be obtained. In order to determine the scope of this transformation, we investigated several different vinyl ethers (Scheme 17) as substrates. Conversion into the expected 7-substituted benzotriazoles **5** proceeded with moderate to good yield (40 -75%).

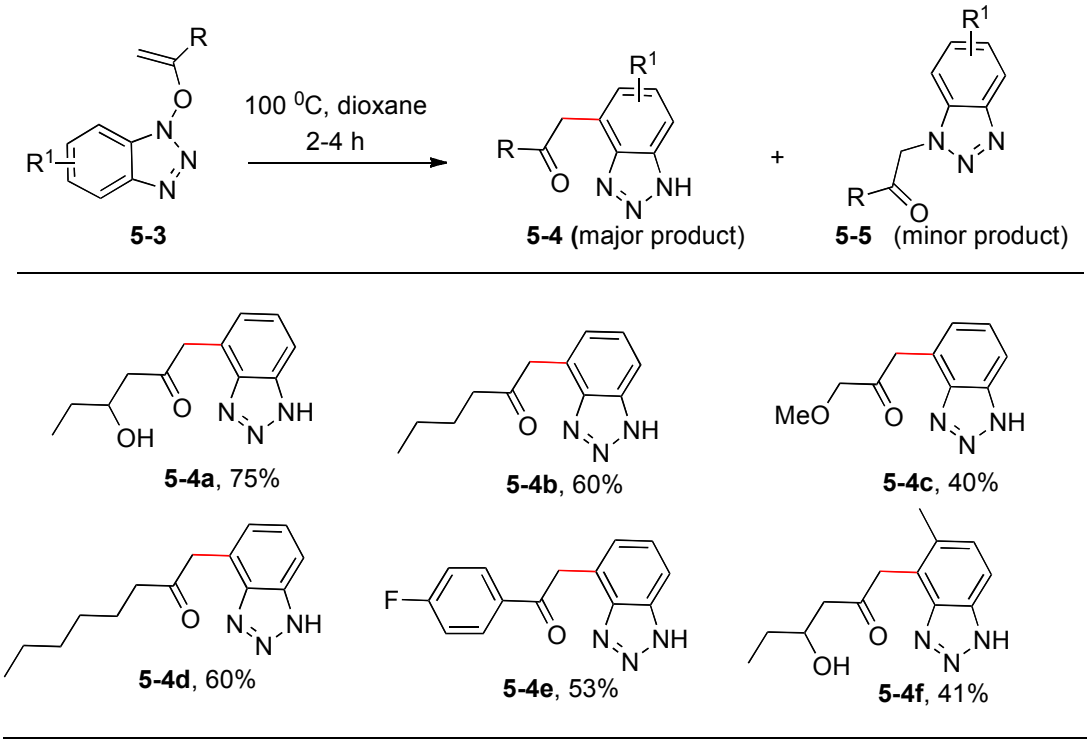

Scheme 17. Scope for 3,3-sigmatropic rearrangements of 5-3.

Encouraged by the utility of HOBt vinyl ethers in the synthesis of functionalised benzotriazoles, we explored their use in the synthesis of α-fluoroketones. Fluoroketones are known to be important intermediates and targets in medicinal chemistry.[93,187-189] However their regioselective synthesis is often non-trivial; we were pleased to discover that reaction of **5-3** with Selectfluor gave the functionalized fluoroketone **5-6** in 83% isolated yield and with high

regioselectivity (eq 1). By contrast, many similar literature fluorination methods are known to suffer from poor regioselectivity.[190]

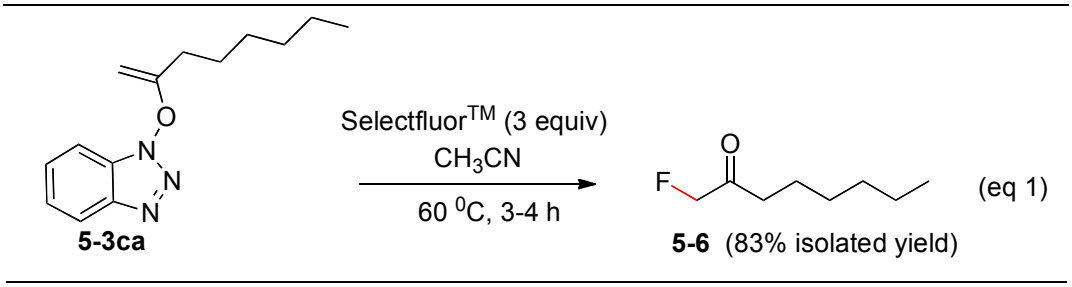

Equation 1. Electrophilic fluorination of vinyl ether products.

5.3 Summary

In summary, gold-catalyzed addition of *O*-nucleophiles to alkynes will give synthetically important vinyl ether products but these are usually not stable enough to be isolated by standard silica gel chromatography. In our case, vinyl ether products were very stable, easily isolated by standard silica gel chromatography. In this chapter, we developed a high yielding gold-catalyzed synthesis of HOBt derived vinyl ethers **5-3** from reaction of alkynes **5-1** with *N*-hydroxybenzotriazole **5-2a**, and briefly explored their synthetic utility. To improve the substrate scope, we found that *N*-hydroxy-7-azabenzotriazole works very well under the same condition. However, 1-Hydroxyindazole, *N*-hydroxy-4-quinolone, and *N*-hydroxyquinazolinediones didn't react with alkynes under the same conditions. Moreover, *N*-oxides such as cinnoline-*N*-oxide, and benzofuroxan also didn't show any reactivity with alkynes under the same conditions. We also tested reactions of internal alkynes such as 2-decyne, and 5-decyne with *N*-hydroxybenzotriazole **5-2a**, but these reactions were very sluggish, even after one week. Reaction of propargyl alcohol also led to the formation of a minor regioisomer, possibly due to

steric reasons. When allene **5-1k** was treated with *N*-hydroxybenzotriazole **5-2a**, we obtained **5-3qa** in lower yield (17%); the majority of unreacted allene **5-1k** was recovered, indicating that an allene is less reactive than the corresponding alkyne under these conditions.

In closing, 3,3-sigmatropic rearrangement of **5-3** gives access to functionalized *N*-heterocycles, while electrophilic fluorination of **5-3** gives high yielding regioselective access to a functionalized fluoroketone. Conversion into the expected 7-substituted benzotriazoles **5-4** proceeded with moderate to good yield (40 -75%). In some cases, we also observed low yield of **5-4**, because we also isolated the *N*-sustituted ketones **5-5** as a side products.The two-step sequence (nucleophilic addition / sigmatropic rearrangement) represents an efficient protocol for transfer of a nucleophilic oxygen atom to an alkyne group. The work described in this chapter was published in *Org. Lett.* **2013**, *15*, 724-727.

5.4 Experimental

General

^{1}H and ^{13}C NMR spectra were recorded at 500 and 126 (or 400 and 101) MHz respectively, using $CDCl_3$ as a solvent. The chemical shifts are reported in δ (ppm) values (^{1}H and ^{13}C NMR relative to $CHCl_3$, δ 7.26 ppm for ^{1}H NMR and δ 77.0 ppm for ^{13}C NMR and $CFCl_3$ (δ 0 ppm for ^{19}F NMR), multiplicities are indicated by s (singlet), d (doublet), t (triplet), q (quartet), p (pentet), h (hextet), m (multiplet) and br (broad). Coupling constants, *J*, are reported in Hertz (Hz). Solvents (tetrahydrofuran, ether, dichloromethane and DMF) were chemically

dried using a commercial solvent purification system. All other reagents and solvents were employed without further purification. The products were purified using a commercial flash chromatography system or a regular glass column. TLC was developed on silica gel 60 F254 aluminum sheets. Exact molecular weight of new compound was obtained by high-resolution electrospray ionization mass spectrometry (HREIMS).

Synthesis of *N*-hydroxybenzotriazole and *N*-hydroxyindole

Compound **5-2a**, **5-2b**, **5-2d** are available commercially. Compounds **5-2e, 5-2f, 5-2g** were synthesized following literature procedures.[184-186]

Procedure for preparation of 5-2c.

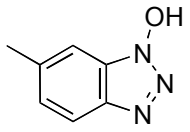

5-2c

A mixture of 4-chloro-3-nitrotoluene (2 g, 11.655 mmol) and hydrazine hydrate (3.3 mL, 116.6 mmol) in dry EtOH was heated under reflux for 20 h and then cooled to room temperature. From the reaction mixture, EtOH was evaporated under reduced pressure. This left a residue to which MeOH (20 mL) was added and the mixture was acidified with conc. HCl. This addition induced precipitation of a yellowish white solid, which was filtered. Evaporation of the solvent from the filtrate afforded additional amount of yellowish solid. The combined residues were taken up in $CHCl_3$. The chloroform solution was washed repeatedly with water and phases were separated. Then the organic layer was dried over anhyd. Na_2SO_4, and

the solvent was evaporated to afford a yellowish solid which was further purified by column chromatography over silica gel with using Hexane/EtOAc to give **5-2c** as a yellowish solid (2.7 g, 63 %); mp 177-179 °C; ^{1}H-NMR (Acetone-d_6, 400 MHz) 7.79 (d, 1H), 7.47 (s, 1H), 7.25 (d, 1H), 2.52 (s, 3H); ^{13}C-NMR (Acetone-d_6, 400 MHz) 141.8, 137.9, 128.7, 126.7, 118.6, 108.2, 20.8; High Res MS (ES^+) Calculated for $[C_7H_8N_3O]^+$ (MH^+): 150.0662; Found: 150.0663.

General procedure for the preparation for 5-3

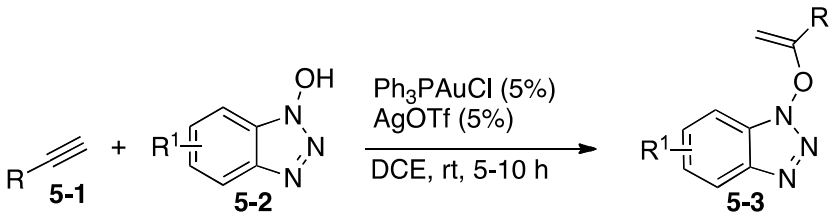

N-hydroxybenzotriazole **5-2** (45 mg, 0.336 mmol, 1.1 equiv) was added into a solution of the alkyne/allene **5-1** (30 mg, 0.306 mmol), Ph_3PAuCl (7.6 mg, 0.0153 mmol, 5 mol%) in 2 mL DCE (dichloroethane). The reaction was stirred at the room temperature for 8 h. The solvent was removed under reduced pressure to give crude product, the crude product was purified by flash silica gel chromatography to give the product **5-3** (53%-100%) yield.

5-((1H-benzo[d][1,2,3]triazol-1-yl)oxy)hex-5-en-3-ol (**5-3aa**)

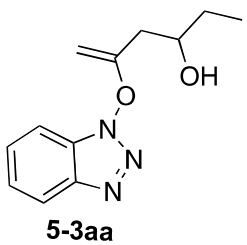

Compound **5-3aa** was prepared in 100% yield according to the general procedure (eluents: ethylacetate: hexane = 1:4). ^{1}H NMR (400 MHz, $CDCl_3$) δ 8.01 (d, 1H, *J* = 8.4 Hz), 7.46-7.54 (m, 2H), 7.35-7.39 (m, 1H), 4.34 (d, 1H, *J* = 4 Hz), 4.05 (m, 1H), 3.68 (d, 1H, *J* = 4 Hz), 2.95 (br, 1H), 2.64 (dd, 1H, *J* =16 Hz), 2.51 (dd, 1H, *J* = 16Hz), 1.55 (m, 2H), 1.02 (t, 3H, *J* = 4Hz); ^{13}C NMR (100 MHz, $CDCl_3$) δ 161.3, 143.2, 128.5, 127.6, 124.9, 120.2, 108.9, 89.3, 70.3, 39.2, 29.9, 9.9; High Res MS (ES^+) Calculated for $[C_{12}H_{16}N_3O_2]^+$ (MH^+): 234.1237; Found: 234.1238.

1-((1-phenylvinyl)oxy)-1H-benzo[d][1,2,3]triazole (**5-3ba**)

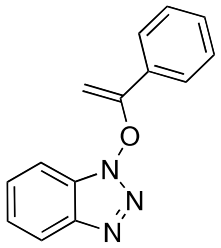

5-3ba

Compound **5-3ba** was prepared in 80% yield according to the general procedure (eluents: ethylacetate: hexane = 1:10). ^{1}H NMR (400 MHz, $CDCl_3$) δ 8.07 (d, 1H, *J* = 8 Hz), 7.77-7.79 (m, 2H), 7.46-7.55 (m, 2H), 7.42-7.45 (m, 4H), 4.94 (d, 1H, *J* = 4.4 Hz), 3.98 (d, 1H, *J* = 4.4 Hz); ^{13}C NMR (100 MHz, $CDCl_3$) δ 161.2, 143.4, 131.4, 130.0, 128.7, 128.6, 127.7, 125.8, 124.9, 120.4, 108.7, 88.4; High Res MS (ES^+) Calculated for $[C_{14}H_{12}N_3O]^+$ (MH^+): 238.0980; Found: 238.0980.

1-(oct-1-en-2-yloxy)-1H-benzo[d][1,2,3]triazole (**5-3ca**)

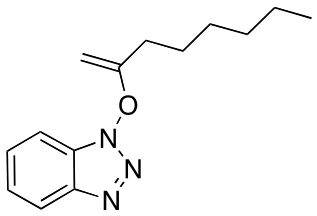

5-3ca

Compound **5-3ca** was prepared in 96% yield according to the general procedure (eluents: ethylacetate: hexane = 1:10). ^{1}H NMR (400 MHz, $CDCl_3$) δ 8.06 (d, 1H, *J* = 8.4 Hz), 7.47-7.56 (m, 2H), 7.40-7.44 (m, 1H), 4.24 (d, 1H, *J* = 4.0 Hz), 3.63 (d, 1H, *J* = 4 Hz), 2.45 (t, 2H, *J* = 8 Hz), 1.74 (p, 2H), 1.44-1.49 (m, 2H), 1.34-1.40 (m, 4H), 0.93 (t, 3H, *J* = 8 Hz); ^{13}C NMR (100 MHz, $CDCl_3$) δ 164.2, 143.3, 128.3, 127.7, 124.7, 120.4, 108.7, 86.8, 31.5, 31.3, 28.6, 26.9, 22.5, 14.1; High Res MS (ES^+) Calculated for $[C_{14}H_{20}N_3O]^+$ (MH^+):246.1601; Found: 246.1604.

1-((1-(4-fluorophenyl)vinyl)oxy)-1H-benzo[d][1,2,3]triazole (**5-3da**)

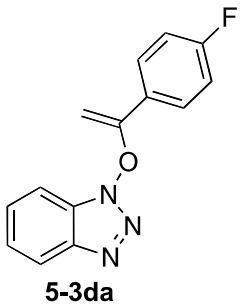

5-3da

Compound **5-3da** was prepared in 83% yield according to the general procedure (eluents: ethylacetate: hexane = 1:10). ^{1}H NMR (400 MHz, $CDCl_3$) δ 8.10 (d, 1H, *J* = 8 Hz), 7.77-7.81 (m, 2H), 7.56-7.57 (m, 2H), 7.44-7.47 (m, 1H), 7.17 (t, 2H, *J* = 8.8) 4.90 (d, 1H, *J* = 4.8 Hz), 3.98 (d, 1H, *J* = 4.0 Hz); ^{13}C NMR (100 MHz, $CDCl_3$) δ 164.9, 162.4, 160.3, 143.4, 128.6, 127.9, 126.4 (d, *J* = 290.4 Hz), 120.5,

115.9, 115.7, 108.6, 88.3; High Res MS (ES^+) Calculated for $[C_{14}H_{11}FN_3O]^+$ (MH^+): 255.0881; Found: 256.0883.

1-((3-methoxyprop-1-en-2-yl)oxy)-1H-benzo[d][1,2,3]triazole (**5-3ea**)

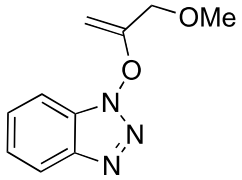

5-3ea

Compound **5-3ea** was prepared in 89% yield according to the general procedure (eluents: ethylacetate: hexane = 1:10). ^1H NMR (400 MHz, $CDCl_3$) δ 8.00 (d, 1H, J = 8.4 Hz), 7.49-7.50 (m, 2H), 7.37-7.38 (m, 1H), 4.57 (d, 1H, J = 3.6 Hz), 4.16 (s, 2H), 3.99 (d, 1H, J = 4.0 Hz), 3.44 (s, 3H); ^{13}C NMR (100 MHz, $CDCl_3$) δ 159.7, 143.3, 128.6, 127.5, 124.9, 120.3, 108.8, 91.6, 69.7, 58.4; High Res MS (ES^+) Calculated for $[C_{10}H_{12}N_3O_2]^+$: 206.0924; Found: 206.0926.

1-((1-(cyclohex-1-en-1-yl)vinyl)oxy)-1H-benzo[d][1,2,3]triazole (**5-3fa**)

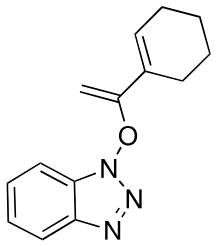

5-3fa

Compound **5-3fa** was prepared in 70% yield according to the general procedure (eluents: ethylacetate: hexane = 1:10). ^1H NMR (400 MHz, $CDCl_3$) δ 8.03 (d, 1H, J = 8.4 Hz), 7.50-7.51 (m, 2H), 7.37-7.41 (m, 1H), 6.64 (br, 1H), 4.43 (d, 1H, J = 4.4 Hz), 3.68 (d, 1H, J = 4.0 Hz), 2.22-2.23 (m, 4H), 1.73-1.78 (m, 2H), 1.62-1.68

(m, 2H); ^{13}C NMR (100 MHz, $CDCl_3$) δ 161.6, 143.4, 128.3, 128.2, 127.8, 124.8, 120.3, 108.9, 86.3, 25.4, 25.2, 22.3, 21.7; High Res MS (ES^+) Calculated for $[C_{14}H_{16}N_3O]^+$ (MH^+): 242.1288; Found: 242.1289.

2-((1H-benzo[d][1,2,3]triazol-1-yl)oxy)oct-1-en-3-ol (**5-3ga**)

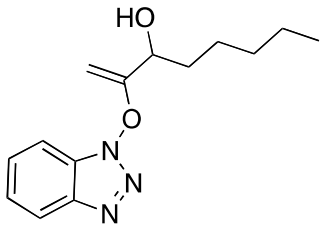

5-3ga

Compound **5-3ga** was prepared in 53% yield according to the general procedure (eluents: ethylacetate: hexane = 1:4). ^{1}H NMR (400 MHz, $CDCl_3$) δ 8.05 (d, 1H, *J* = 8.0 Hz), 7.50-7.53 (m, 2H), 7.39-7.43 (m, 1H), 4.58 (d, 1H, *J* = 4.0 Hz), 4.45 (m, 1H), 3.78 (d, 1H, *J* = 4.0 Hz), 2.53 (br, 1H), 1.87-2.53 (m, 2H), 1.51-1.61 (m, 2H), 1.37-1.41 (m, 2H), 0.92 (t, 3H, *J* = 7.2 Hz); ^{13}C NMR (100 MHz, $CDCl_3$) δ 165.1, 143.3, 128.6, 127.6, 124.9, 120.4, 108.8, 87.8, 70.5, 34.8, 31.6, 25.1, 22.6, 14.0; High Res MS (ES^+) Calculated for $[C_{14}H_{20}N_3O_2]^+$ (MH^+): 262.1550; Found: 262.1555.

1,1'-(hepta-1,6-diene-2,6-diylbis(oxy))bis(1H-benzo[d][1,2,3]triazole) (**5-3ha**)

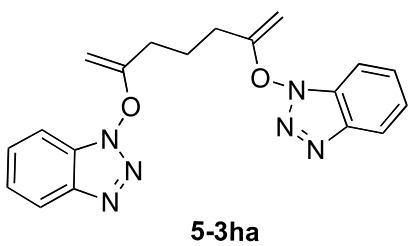

5-3ha

2.2 equiv of **5-2a** was used instead of 1.1 equiv in the reaction. Compound **5-3ha** was prepared in 95% yield according to the general procedure (eluents: ethylacetate: hexane = 1:10). ^{1}H NMR (400 MHz, $CDCl_3$) δ 8.75 (d, 1H, *J* = 8.8 Hz), 7.52-7.58 (m, 2H), 7.41-7.46 (m, 1H), 4.37 (d, 1H, *J* = 4.0 Hz), 3.76 (d, 1H, *J* = 3.6 Hz), 2.67 (t, 2H, *J* = 7.6 Hz), 2.21-2.29 (m, 1H); ^{13}C NMR (100 MHz, $CDCl_3$) δ 162.9, 143.4, 128.6, 127.7, 124.9, 120.5, 108.6, 88.1, 30.6, 24.3; High Res MS (ES^+) Calculated for $[C_{19}H_{19}N_6O_2]^+$: 363.1564; Found: 363.1567.

1-(hex-1-en-2-yloxy)-1H-benzo[d][1,2,3]triazole (**5-3ia**)

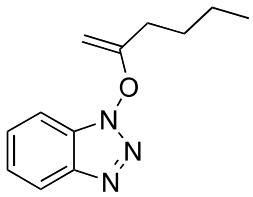

5-3ia

Compound **5-3ia** was prepared in 100% yield according to the general procedure (eluents: ethylacetate: hexane = 1:10). ^{1}H NMR (400 MHz, $CDCl_3$) δ 8.02 (d, 1H, *J* = 8.4 Hz), 7.44-7.52 (m, 2H), 7.36-7.40 (m, 1H), 4.21 (d, 1H, *J* = 3.6 Hz), 3.60 (d, 1H, *J* = 4.0 Hz), 2.42 (t, 2H, *J* = 7.6 Hz), 1.67-1.74 (p, 2H), 1.42-1.52 (m, 2H), 0.97 (t, 3H, *J* = 7.6 Hz); ^{13}C NMR (100 MHz, $CDCl_3$) δ 164.2, 143.3, 128.4, 127.7, 124.7, 120.3, 108.7, 86.8, 31.0, 29.0, 22.1, 13.8; High Res MS (ES^+) Calculated for $[C_{12}H_{16}N_3O]^+$ (MH^+): 218.1288; Found: 218.1289.

5-((6-(trifluoromethyl)-1H-benzo[d][1,2,3]triazol-1-yl)oxy)hex-5-en-3-ol (**5-3jb**)

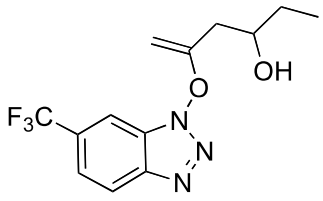

5-3jb

Compound **5-3jb** was prepared in 81% yield according to the general procedure (eluents: ethylacetate: hexane = 1:4). ^{1}H NMR (400 MHz, $CDCl_3$) δ 8.16 (d, 1H, *J* = 8.8 Hz), 7.91 (s, 1H), 7.63 (d, 1H, *J* = 8.8 Hz), 4.42 (d, 1H, *J* = 3.6 Hz), 4.04-4.10 (m, 1H), 3.72 (d, 1H, *J* = 4.0 Hz), 2.67-2.71 (dd, 1H, *J* = 14.8 Hz), 2.51-2.57 (dd, 1H, *J* = 15.2 Hz), 2.49 (br, 1H), 1.61-1.74 (m, 2H), 1.05 (t, 3H, *J* = 7.6 Hz); ^{13}C NMR (100 MHz, $CDCl_3$) δ 161.6, 144.4, 130.8 (q, *J* = 32.5 Hz), 127.1, 123.5 (q, *J* = 272.1 Hz), 121.6 (q, *J* = 3.1 Hz), 121.5, 107.5 (q, *J* = 4.6 Hz), 89.7, 70.4, 39.1, 30.1, 9.8; High Res MS (ES^+) Calculated for $[C_{13}H_{15}F_3N_3O_2]^+$ (MH^+): 302.1111; Found: 302.1113

1-(oct-1-en-2-yloxy)-6-(trifluoromethyl)-1H-benzo[d][1,2,3]triazole (**5-3kb**)

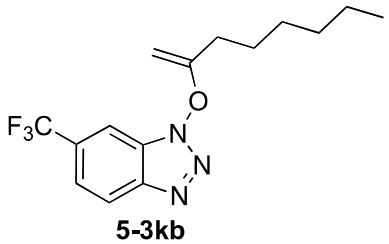

5-3kb

Compound **5-3kb** was prepared in 87% yield according to the general procedure (eluents: ethylacetate: hexane = 1:10). ^{1}H NMR (400 MHz, $CDCl_3$) δ 8.19 (d, 1H, *J* = 8.8 Hz), 7.81 (s, 1H), 7.65 (d, 1H, *J* = 8.8 Hz), 4.29 (d, 1H, *J* = 4.0 Hz), 3.63 (d, 1H, *J* = 4.4 Hz), 2.47 (t, 2H, *J* = 7.6 Hz), 1.71-1.79 (m, 2H), 1.46-1.49 (m, 2H), 1.34-1.39 (m, 4H), 0.93 (t, 3H, *J* = 7.2 Hz); ^{13}C NMR (100 MHz, $CDCl_3$) δ 164.5,

144.4, 130.7 (q, J = 32.5 Hz), 127.2, 123.6 (q, J = 271.9 Hz), 121.6 (q, J = 3.9 Hz), 121.5, 107.2 (q, J = 4.7 Hz), 87.2, 31.5, 31.3, 28.6, 26.8, 22.5, 14.0; High Res MS (ES^+) Calculated for $[C_{15}H_{19}F_3N_3O]^+$ (MH^+): 314.1475; Found: 314.1476

6-methyl-1-(oct-1-en-2-yloxy)-1H-benzo[d][1,2,3]triazole (**5-3lc**)

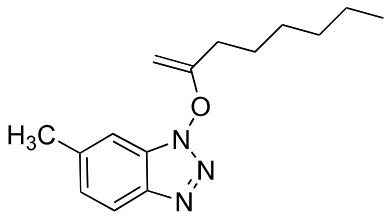

5-3lc

Compound **5-3lc** was prepared in 100% yield according to the general procedure (eluents: ethylacetate: hexane = 1:10). ^{1}H NMR (400 MHz, $CDCl_3$) δ 7.89 (d, 1H, J = 8.8 Hz), 7.20-7.22 (m, 2H), 4.21 (d, 1H, J = 4.0 Hz), 3.61 (d, 1H, J = 3.6 Hz), 2.51 (s, 3H), 2.42 (t, 2H, J = 7.6 Hz), 1.69-1.76 (p, 2H), 1.42-1.47 (m, 2H), 1.33-1.37 (m, 4H), 0.91 (t, 3H, J = 7.2 Hz); ^{13}C NMR (100 MHz, $CDCl_3$) δ 164.2, 142.1, 139.3, 128.1, 127.1, 119.8 107.7, 86.7, 31.5, 31.3, 28.7, 26.9, 22.6, 21.9, 14.1; High Res MS (ES^+) Calculated for $[C_{15}H_{22}N_3O]^+$ (MH^+): 260.1757; Found: 260.1760

5-((6-methyl-1H-benzo[d][1,2,3]triazol-1-yl)oxy)hex-5-en-3-ol (**5-3mc**)

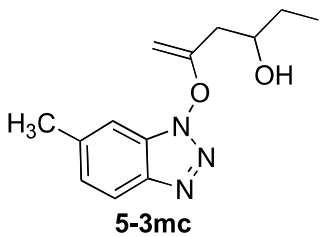

5-3mc

Compound **5-3mc** was prepared in 92% yield according to the general procedure (eluents: ethylacetate: hexane = 1:4). ^{1}H NMR (400 MHz, $CDCl_3$) δ 7.81 (d, 1H, *J* = 8.8 Hz), 7.20 (s, 1H), 7.13 (d, 1H, *J* = 8.4 Hz) 4.26 (d, 1H, *J* = 4.0 Hz), 3.95-4.02 (m, 1H), 3.62 (d, 1H, *J* = 4 Hz), 2.70 (bs, 1H), 2.56-2.61 (dd, 1H, *J* = 14.8 Hz), 2.45 (t, 1H, *J* = 8.4 Hz), 2.42 (s, 3H), 1.53-1.61 (m, 2H), 0.97 (t, 3H, *J* = 7.2 Hz); ^{13}C NMR (100 MHz, $CDCl_3$) δ 161.2, 141.9, 139.6, 128.0, 127.3, 119.7, 107.8, 89.3, 70.3, 39.3, 29.9, 21.9, 9.9; High Res MS (ES^+) Calculated for $[C_{13}H_{18}N_3O_2]^+$ (MH^+): 248.1394; Found: 248.1396

3-(oct-1-en-2-yloxy)-3H-[1,2,3]triazolo[4,5-b]pyridine (**5-3nd**)

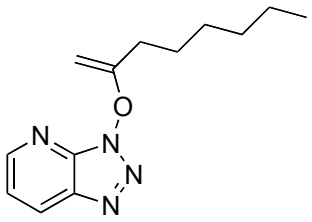

5-3nd

Compound **5-3nd** was prepared in 80% yield according to the general procedure (eluents: ethylacetate: hexane = 1:4). ^{1}H NMR (400 MHz, $CDCl_3$) δ 8.76 (d, 1H, *J* = 5.6 Hz), 8.42 (d, 1H, *J* = 10.0 Hz), 7.44 (dd, 1H, *J* = 13.2 Hz) 4.29 (d, 1H, *J* = 4.4 Hz), 3.69 (d, 1H, *J* = 4 Hz), 2.50 (t, 2H, *J* = 15.2), 1.80-1.73 (m, 2H), 1.52-1.45 (m, 2H), 1.40-1.34 (m, 4H), 0.92 (t, 3H, *J* = 6.8 Hz); ^{13}C NMR (100 MHz, $CDCl_3$) δ 164.9, 151.6, 139.9, 134.9, 129.3, 120.7, 86.9, 31.5, 31.3, 28.6, 26.7, 22.5, 14.9; High Res MS (ES^+) Calculated for $[C_{13}H_{18}N_3O_2]^+$ (MH^+): 247.1553; Found: 247.1555

3-((1-(4-fluorophenyl)vinyl)oxy)-3H-[1,2,3]triazolo[4,5-b]pyridine (**5-3od**)

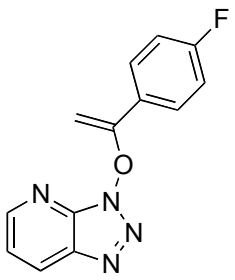

5-3od

Compound **5-3od** was prepared in 80% yield according to the general procedure (eluents: ethylacetate: hexane = 1:4). ^{1}H NMR (400 MHz, $CDCl_3$) δ 8.78 (d, 1H, *J* = 6 Hz), 8.45 (d, 1H, *J* = 10.0 Hz), 7.87-7.83 (m, 2H), 7.49-7.45 (m, 1H), 7.15 (m, 2H) 4.95 (d, 1H, *J* = 4.8 Hz), 4.15 (d, 1H, *J* = 4.8 Hz); ^{13}C NMR (100 MHz, $CDCl_3$) δ 164.9, 162.4, 160.9, 151.8, 139.9, 134.9, 129.4, 127.9 (d, *J* = 290.4 Hz), 120.9, 115.8, 115.6, 89.2; High Res MS (ES^+) Calculated for $[C_{13}H_{18}N_3O_2]^+$ (MH^+): 257.0833; Found: 257.0835

3-((1-(4-methoxyphenyl)vinyl)oxy)-3H-[1,2,3]triazolo[4,5-b]pyridine (**5-3pd**)

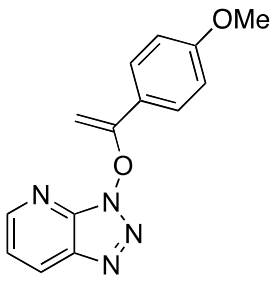

5-3pd

Compound **5-3pd** was prepared in 70% yield according to the general procedure (eluents: ethylacetate: hexane = 1:4). ^{1}H NMR (400 MHz, $CDCl_3$) δ 8.78 (d, 1H, *J* = 4.4 Hz), 8.44 (dd, 1H, *J* = 7.2 Hz), 7.79 (m, 2H), 7.47-7.44 (m, 2H), 6.97 (m, 2H) 4.88 (d, 1H, *J* = 4.4 Hz), 4.05 (d, 1H, *J* = 4.0 Hz), 3.87 (s, 3H); ^{13}C NMR (100 MHz, $CDCl_3$) δ 161.9, 160.9, 151.8, 140.0, 134.9, 129.4, 127.8, 124.0, 120.9,

113.9, 87.6, 55.4; High Res MS (ES^+) Calculated for $[C_{13}H_{18}N_3O_2]^+$ (MH^+): 269.1033; Found: 269.1035

1-(1H-benzo[d][1,2,3]triazol-4-yl)-4-cyclohexylbutan-2-one (**5-3qa**)

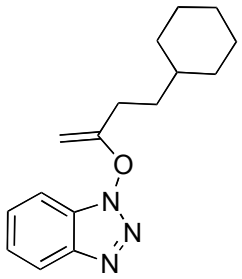

5-3qa

Compound **5-3qa** was prepared in 17% yield according to the general procedure (eluents: ethylacetate: hexane = 1:40). ^1H NMR (400 MHz, $CDCl_3$) δ 8.05 (d, 2H, J = 8.0 Hz), 7.47-7.55 (m, 2H), 7.39-7.43 (m, 1H), 4.23 (d, 1H, J = 3.6 Hz), 3.62 (d, 1H, J = 4.0 Hz), 2.45 (t, 2H, J = 8.0 Hz), 1.61-1.81 (m, 7H), 1.38-1.41 (m, 1H), 1.16-1.29 (m, 3H), 0.96-1.02 (m, 2H); ^{13}C NMR (100 MHz, $CDCl_3$) δ 164.7, 143.4, 128.3, 127.7, 124.7, 120.4, 108.8, 86.6, 37.1, 34.6, 33.1, 28.8, 26.6, 26.2; High Res MS (ES^+) Calculated for $[C_{16}H_{22}N_3O]^+$: 272.1757; Found: 272.1762.

General procedure for the preparation of 5-4

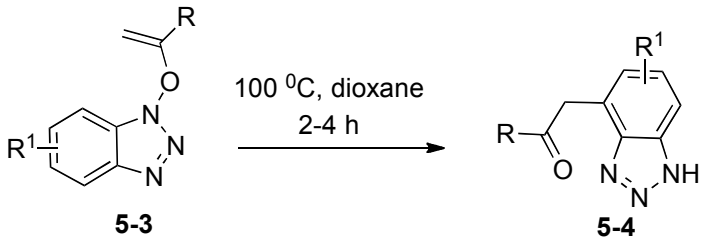

Vinyl ether intermediate **5-3** (50 mg) was dissolved in dioxane (2 mL). The mixture was stirred at 100 ^0C for 2-4 h. The solvent was removed under reduced

pressure to give crude product, the crude product was purified by flash silica gel chromatography to give the product **5-4** (40%-75%) yield.

1-(1H-benzo[d][1,2,3]triazol-4-yl)-4-hydroxyhexan-2-one (**5-4a**)

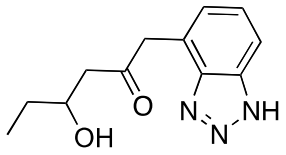

5-4a

Compound **5-4a** was prepared in 75% yield according to the general procedure (eluents: ethylacetate: hexane = 1:2). ^{1}H NMR (400 MHz, $CDCl_3$) δ 7.70 (d, 1H, *J* = 8.4 Hz), 7.31 (t, 1H, *J* = 8.4 Hz), 7.18 (d, 1H, *J* = 6.8 Hz), 4.25 (s, 2H), 4.11 (m, 1H), 2.79 (m, 2H), 1.55 (m, 2H), 0.93 (t, 3H, *J* = 7.2 Hz); ^{13}C NMR (100 MHz, $CDCl_3$) δ 208.7, 138.7, 126.8, 126.1, 121.8, 113.9, 69.8, 49.2, 46.6, 29.7, 9.8; High Res MS (ES^+) Calculated for $[C_{12}H_{16}N_3O_2]^+$ (MH^+): 234.1237; Found: 234.1239.

1-(1H-benzo[d][1,2,3]triazol-4-yl)hexan-2-one (**5-4b**)

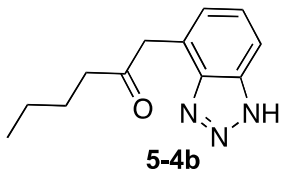

5-4b

Compound **5-4b** was prepared in 60% yield according to the general procedure (eluents: ethylacetate: hexane = 1:4). ^{1}H NMR (400 MHz, $CDCl_3$) δ 7.73 (d, 1H, *J* = 8.0 Hz), 7.34 (t, 1H, *J* = 8.4 Hz), 7.22 (d, 1H, *J* = 6.8 Hz), 4.16 (s, 2H), 2.59 (t, 2H, *J* = 7.6 Hz), 1.51 (m, 2H), 1.22 (m, 2H), 0.81 (t, 3H, *J* = 7.6Hz); ^{13}C NMR (100 MHz, $CDCl_3$) δ 208.8, 138.8, 138.6, 126.4, 126.2, 122.0, 113.8, 42.5, 25.6,

22.1, 13.7; High Res MS (ES^+) Calculated for $[C_{12}H_{16}N_3O]^+$ (MH^+): 218.1288; Found: 218.1291.

1-(1H-benzo[d][1,2,3]triazol-4-yl)-3-methoxypropan-2-one (**5-4c**)

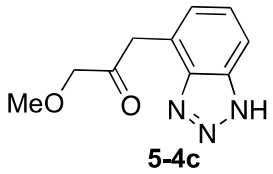

5-4c

Compound **5-4c** was prepared in 40% yield according to the general procedure (eluents: ethylacetate: hexane = 1:2). ^1H NMR (400 MHz, Acetone-d_6) δ 7.78 (d, 1H, *J* = 8.4 Hz), 7.42 (t, 1H, *J* = 7.6 Hz), 7.27 (d, 1H, *J* = 6.8 Hz), 4.29 (s, 2H), 4.25 (s, 2H), 3.39 (s, 3H); ^{13}C NMR (100 MHz, $CDCl_3$) δ 204.4, 125.9, 125.8, 112.6, 76.9, 58.4; High Res MS (ES^+) Calculated for $[C_{10}H_{12}N_3O_2]^+$: 206.0924; Found: 206.0927.

1-(1H-benzo[d][1,2,3]triazol-4-yl)octan-2-one (**5-4d**)

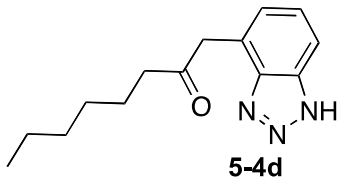

5-4d

Compound **5-4d** was prepared in 60% yield according to the general procedure (eluents: ethylacetate: hexane = 1:4). ^1H NMR (400 MHz, $CDCl_3$) δ 7.70 (d, 1H, *J* = 8.4 Hz), 7.34 (t, 1H, *J* = 7.6 Hz), 7.21 (d, 1H, *J* = 6.8 Hz), 4.23 (s, 2H), 2.58 (t, 2H, *J* = 7.2 Hz), 1.56 (m, 2H), 1.18 (m, 6H), 0.80 (t, 3H, *J* = 7.2 Hz); ^{13}C NMR (100 MHz, $CDCl_3$) δ 208.9, 139.6, 138.0, 126.3, 125.9, 122.6, 113.6, 45.6, 42.8,

31.4, 28.6, 23.5, 22.4, 13.9; High Res MS (ES^+) Calculated for $[C_{14}H_{20}N_3O]^+$ (MH^+):246.1601; Found: 246.1602.

2-(1H-benzo[d][1,2,3]triazol-4-yl)-1-(4-fluorophenyl)ethanone (**5-4e**)

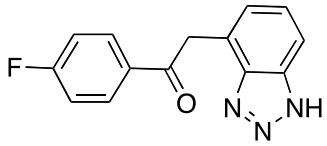

5-4e

Compound **5-4e** was prepared in 53% yield according to the general procedure (eluents: ethylacetate: hexane = 1:4). ^1H NMR (400 MHz, $CDCl_3$) δ 8.20 (m, 2H), 7.78 (d, 1H, *J* = 8.4 Hz), 7.42 (t, 1H, *J* = 7.6 Hz), 7.26 (m, 3H) 4.85 (s, 2H; ^{13}C NMR (100 MHz, $CDCl_3$) δ 195.5, 167.2, 164.7, 133.1, 131.0, 126.3, 125.9 (d, *J* = 290.4 Hz), 115.4, 115.2, 113.6, 40.7; High Res MS (ES^+) Calculated for $[C_{14}H_{11}FN_3O]^+$ (MH^+): 255.0881; Found: 256.0882.

4-hydroxy-1-(5-methyl-1H-benzo[d][1,2,3]triazol-4-yl)hexan-2-one (**5-4f**)

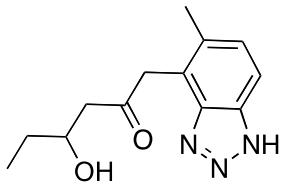

5-4f

Compound **5-4f** was prepared in 41% yield according to the general procedure (eluents: ethylacetate: hexane = 2:3). ^1H NMR (400 MHz, $CDCl_3$) δ 7.60 (d, 1H, *J* = 8.8 Hz), 7.22 (d, 1H, *J* = 8.4 Hz), 4.27 (s, 2H), 4.10 (m, 1H), 2.73 (m, 2H), 2.4 (s, 3H), 1.53 (m, 2H), 0.93 (t, 3H, *J* = 7.2 Hz); ^{13}C NMR (100 MHz, $CDCl_3$) δ 208.4,

139.6, 137.5, 134.6, 129.4, 119.1, 113.3, 70.0, 48.9, 43.7, 29.8, 18.9, 9.8; High Res MS (ES^+) Calculated for $[C_{13}H_{18}N_3O_2]^+$ (MH^+): 248.1394; Found: 248.1395

^{1}H and ^{13}C NMR spectra of compounds 5-3

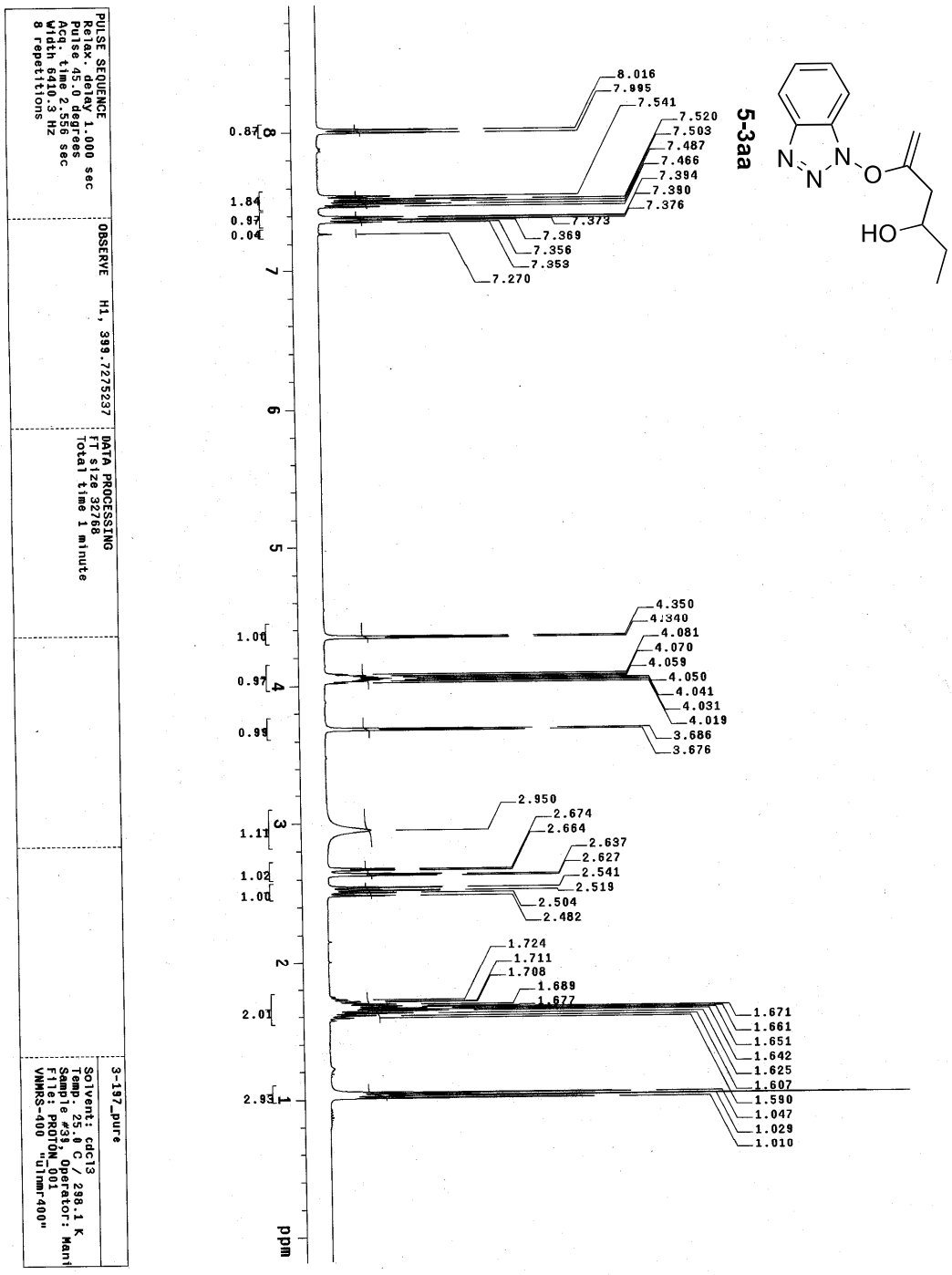
PULSE SEQUENCE
Relax. delay 1.000 sec
Pulse 45.0 degrees
Acq. time 2.556 sec
Width 6410.3 HZ
8 repetitions
OBSERVE H1, 399.7275237
DATA PROCESSING
FT size 32768
Total time 1 minute
3-197_pure
Solvent: cdcl3
Temp. 25.0 C / 298.1 K
Sample #31, Operator: Mani
File: PROTON_001
VNMRS-400 "ulmr400"
5-3aa
HO
8.016
7.995
7.541
7.520
7.503
7.487
7.466
7.394
7.390
7.376
7.373
7.369
7.356
7.353
7.270
4.350
4.340
4.081
4.070
4.059
4.050
4.041
4.031
4.019
3.686
3.676
2.950
2.674
2.664
2.637
2.627
2.541
2.519
2.504
2.482
1.724
1.711
1.708
1.689
1.677
1.671
1.661
1.651
1.642
1.625
1.607
1.590
1.047
1.029
1.010
0.87
1.84
0.97
0.04
1.00
0.97
0.99
1.11
1.02
1.01
2.01
2.93
ppm

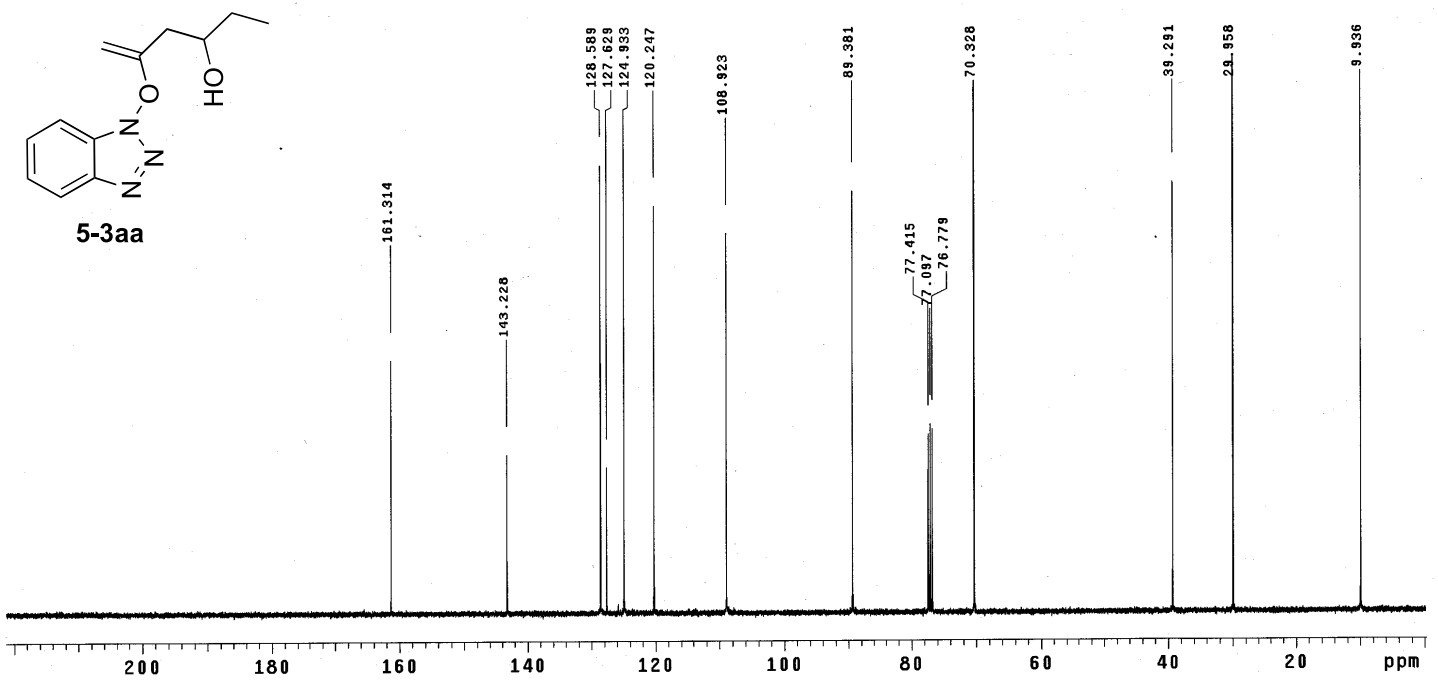

PULSE SEQUENCE Relax. delay 1.000 sec Pulse 45.0 degrees Acq. time 1.285 sec Width 25510.2 Hz 256 repetitions	OBSERVE C13, 100.5115675 DECOUPLE H1, 399.7295294 Power 42 dB continuously on WALTZ-16 modulated	DATA PROCESSING Line broadening 0.5 Hz FT size 65536 Total time 9 minutes			3-197_pure Solvent: cdcl3 Temp. 25.0 C / 298.1 K Sample #39, Operator: Mani File: CARBON_001 VNMRS-400 "ulnmr400"

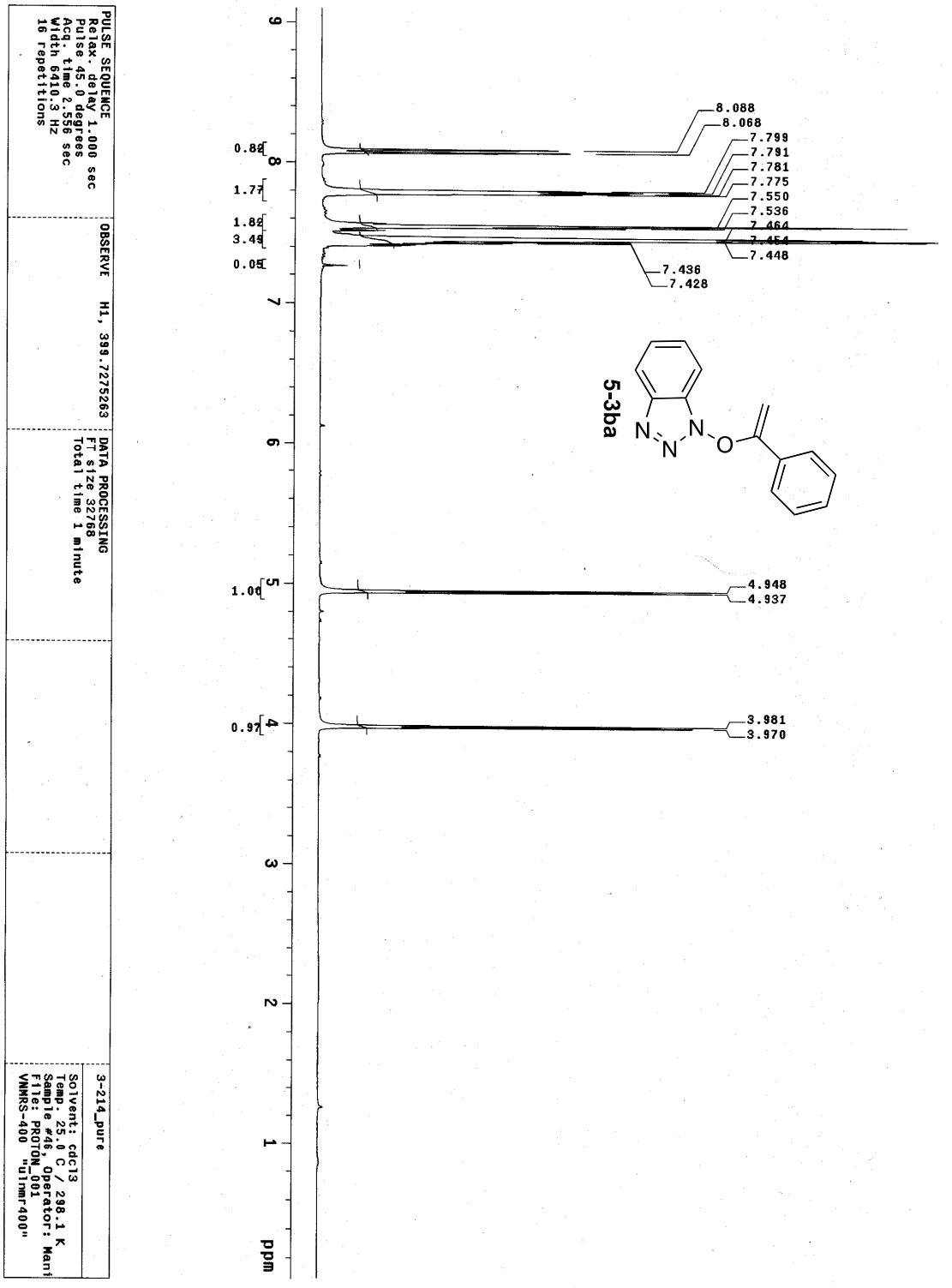
PULSE SEQUENCE
Relax. delay 1.000 sec
Pulse 45.0 degrees
Acq. time 2.556 sec
Width 6410.3 Hz
16 repetitions
OBSERVE H1, 399.7275263
DATA PROCESSING
FT size 32768
Total time 1 minute
3-214_pure
Solvent: cdcl3
Temp: 25.0 C / 298.1 K
Sample #46, Operator: Mani
File: PROTON_001
VNMRS-400 "ulnmr400"
8.088
8.068
7.799
7.791
7.781
7.775
7.550
7.536
7.464
7.454
7.448
7.436
7.428
4.948
4.937
3.981
3.970
0.88
1.77
1.82
3.48
0.05
1.00
0.97
5-3ba
ppm

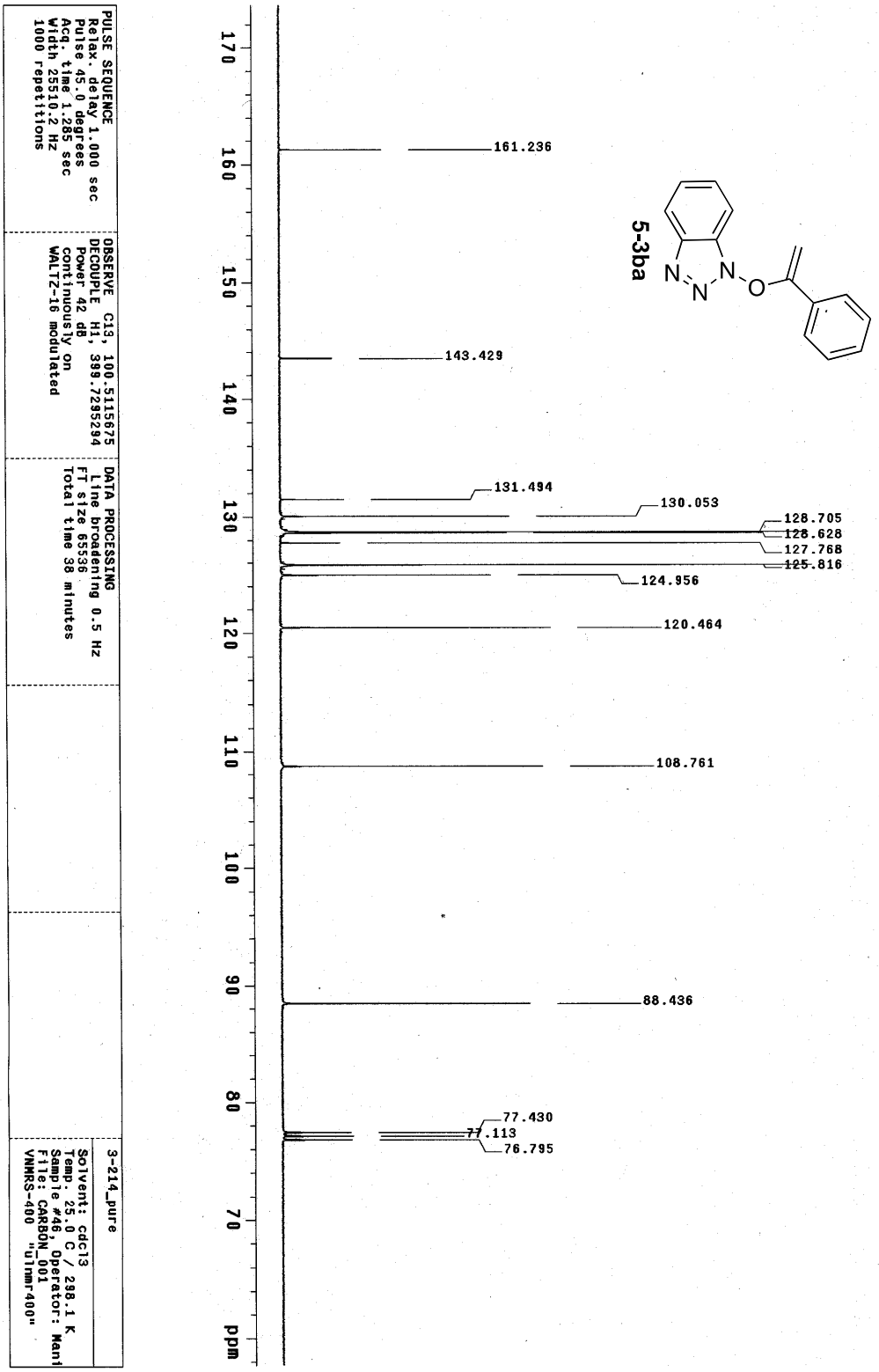
PULSE SEQUENCE
Relax. delay 1.000 sec
Pulse 45.0 degrees
Acq. time 1.285 sec
Width 25510.2 Hz
1000 repetitions
OBSERVE C13, 100.5115675
DECOUPLE H1, 399.7295294
Power 42 dB
continuously on
WALTZ-16 modulated
DATA PROCESSING
Line broadening 0.5 Hz
FT size 65536
Total time 38 minutes
3-214_pure
Solvent: cdcl3
Temp. 25.0 C / 298.1 K
Sample #46, Operator: Mani
File: CARBON_001
VNMRS-400 "Ulnmr400"
5-3ba
161.236
143.429
131.494
130.053
128.705
128.628
127.768
125.816
124.956
120.464
108.761
88.436
77.430
77.113
76.795
170
160
150
140
130
120
110
100
90
80
70
ppm

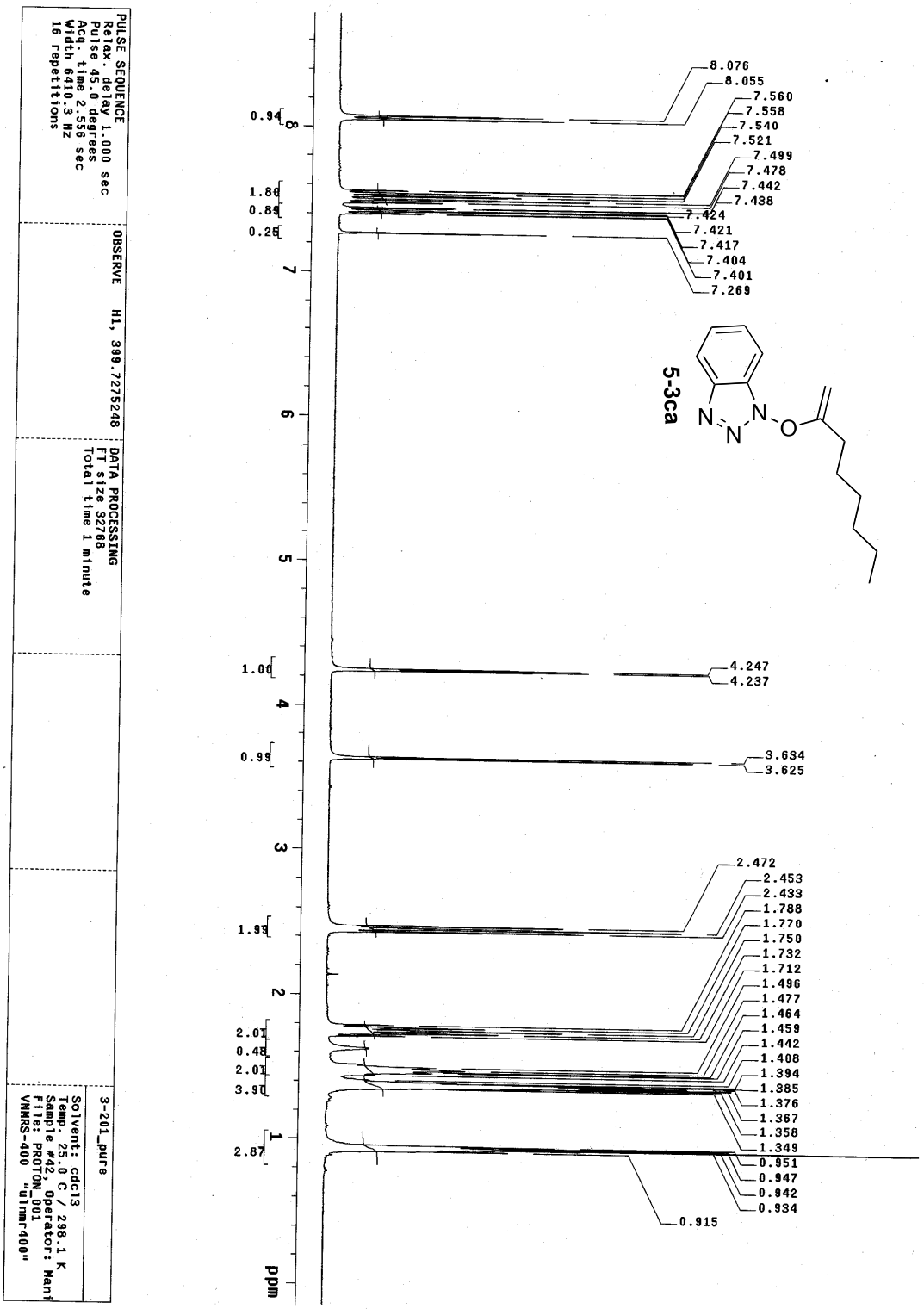
PULSE SEQUENCE
Relax. delay 1.000 sec
Pulse 45.0 degrees
Acq. time 2.556 sec
Width 6410.3 Hz
16 repetitions
OBSERVE H1, 399.7275248
DATA PROCESSING
FT size 32768
Total time 1 minute
3-201_pure
Solvent: cdcl3
Temp. 25.0 C / 298.1 K
Sample #42, Operator: Mani
File: PROTON_001
VNMRS-400 "uinmr400"
8.076
8.055
7.560
7.558
7.540
7.521
7.499
7.478
7.442
7.438
7.424
7.421
7.417
7.404
7.401
7.269
5-3ca
4.247
4.237
3.634
3.625
2.472
2.453
2.433
1.788
1.770
1.750
1.732
1.712
1.496
1.477
1.464
1.459
1.442
1.408
1.394
1.385
1.376
1.367
1.358
1.349
0.951
0.947
0.942
0.934
0.915
0.94
1.86
0.89
0.25
1.00
0.99
1.99
2.01
0.48
2.01
3.90
2.87
ppm

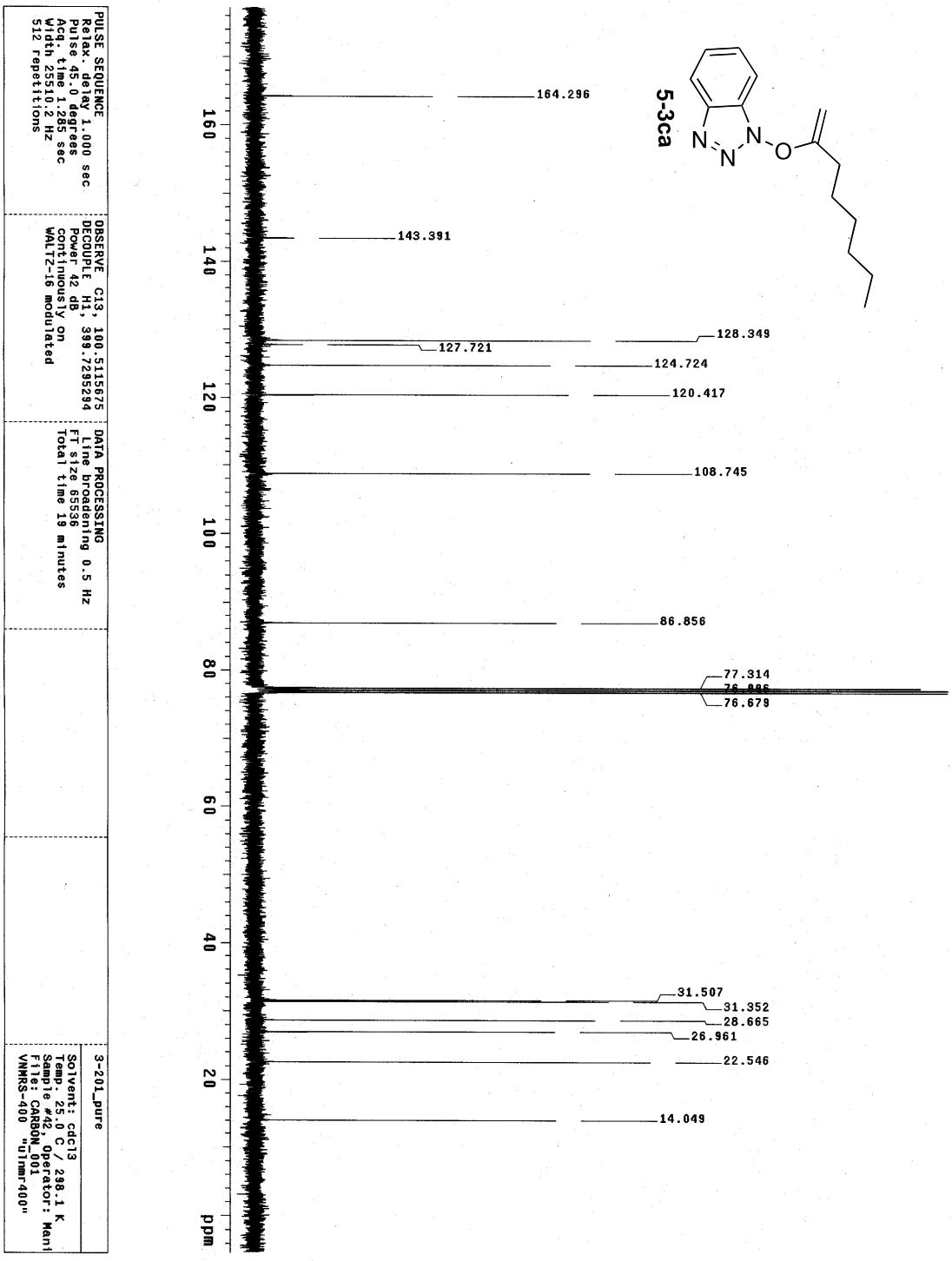
PULSE SEQUENCE
Relax. delay 1.000 sec
Pulse 45.0 degrees
Acq. time 1.285 sec
Width 25510.2 Hz
512 repetitions
OBSERVE C13, 100.5115675
DECOUPLE H1, 399.7295294
Power 42 dB
continuously on
WALTZ-16 modulated
DATA PROCESSING
Line broadening 0.5 Hz
FT size 65536
Total time 19 minutes
3-201_pure
Solvent: cdcl3
Temp. 25.0 C / 298.1 K
Sample #42, Operator: Manl
File: CARBON_001
VNMRS-400 "ulnmr400"
5-3ca
164.296
143.391
128.349
127.721
124.724
120.417
108.745
86.856
77.314
76.679
31.507
31.352
28.665
26.961
22.546
14.049
160
140
120
100
80
60
40
20
ppm

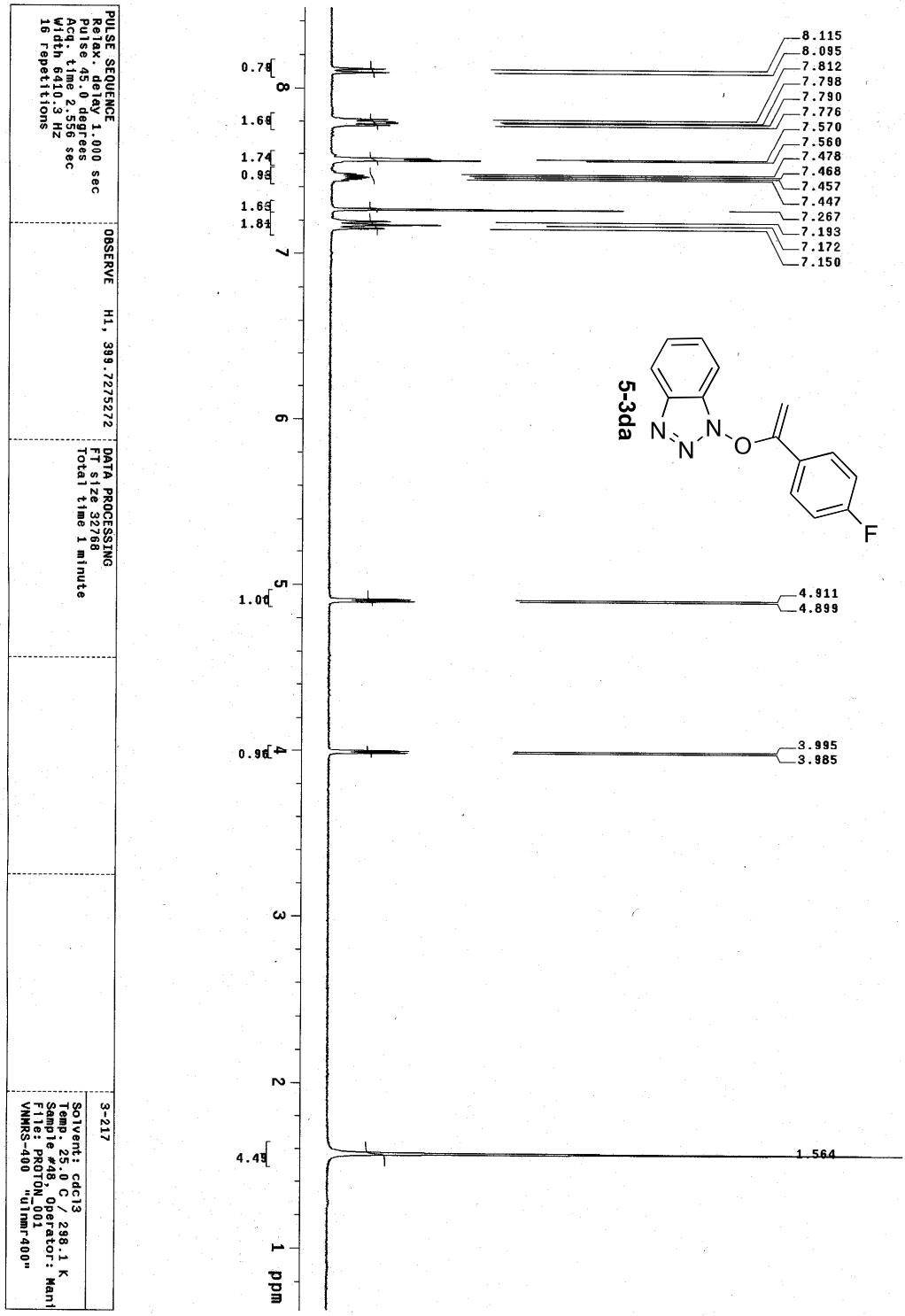
PULSE SEQUENCE
Relax. delay 1.000 sec
Pulse 45.0 degrees
Acq. time 2.556 sec
Width 6410.3 Hz
16 repetitions
OBSERVE H1, 399.7275272
DATA PROCESSING
FT size 32768
Total time 1 minute
3-217
Solvent: cdcl3
Temp. 25.0 C / 298.1 K
Sample #48, Operator: Manl
File: PROTON_001
VNMRS-400 "ulmr400"
8.115
8.095
7.812
7.798
7.790
7.776
7.570
7.560
7.478
7.468
7.457
7.447
7.267
7.193
7.172
7.150
4.911
4.899
3.995
3.985
1.564
0.78
1.68
1.74
0.98
1.65
1.81
1.00
0.96
4.45
5-3da
F
ppm

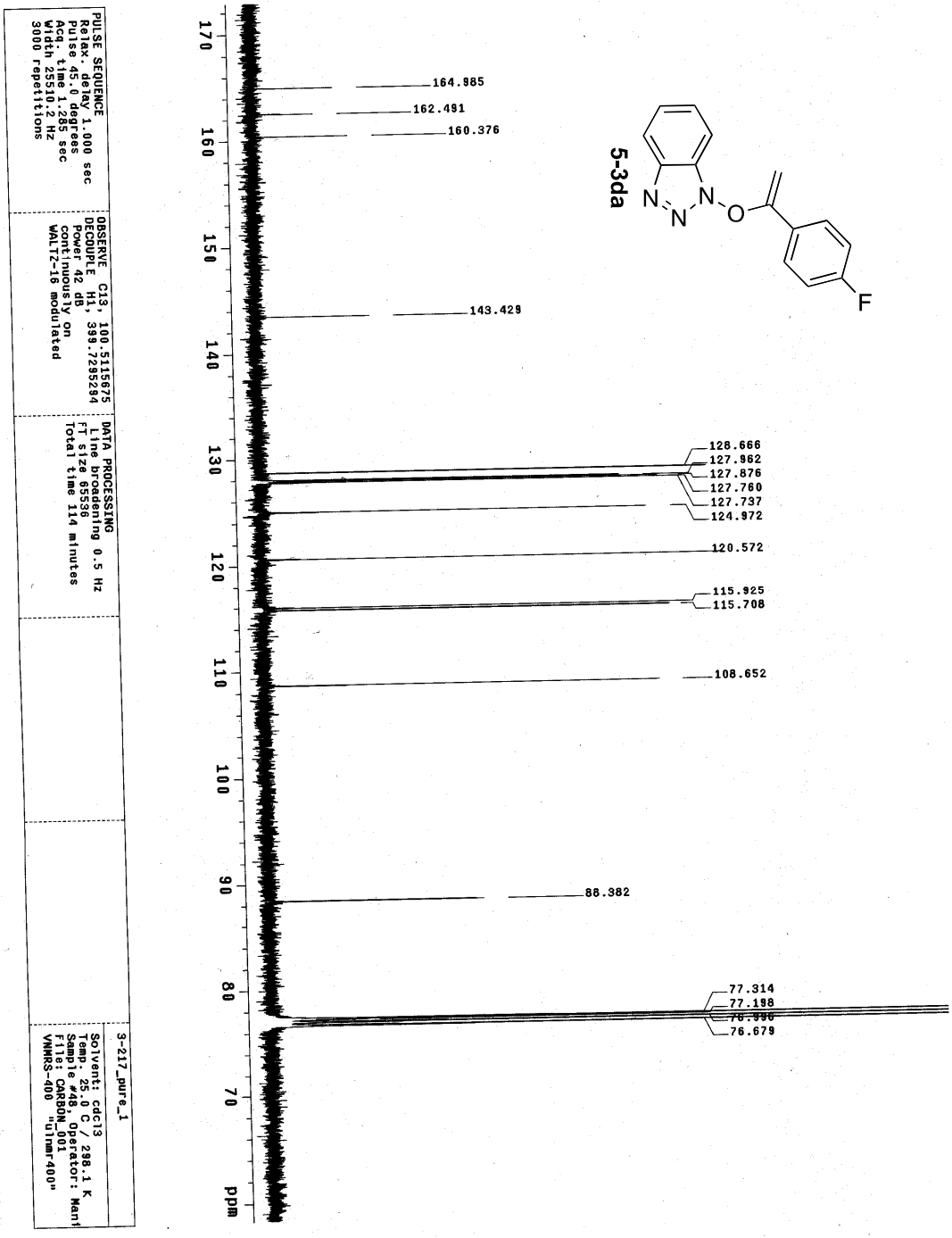
PULSE SEQUENCE
Relax. delay 1.000 sec
Pulse 45.0 degrees
Acq. time 1.285 sec
Width 25510.2 Hz
3000 repetitions
OBSERVE C13, 100.5115675
DECOUPLE H1, 399.7295294
Power 42 dB
continuously on
WALTZ-16 modulated
DATA PROCESSING
Line broadening 0.5 Hz
FT size 65536
Total time 114 minutes
3-217_pure_1
Solvent: cdcl3
Temp.: 25. 0 C / 298. 1 K
Sample #48 Operator: Manf
File: CARBON_001
VNMRS-400 "nimr400"
5-3da
164.985
162.491
160.376
143.429
128.666
127.962
127.876
127.760
127.737
124.972
120.572
115.925
115.708
108.652
88.382
77.314
77.198
76.679
ppm

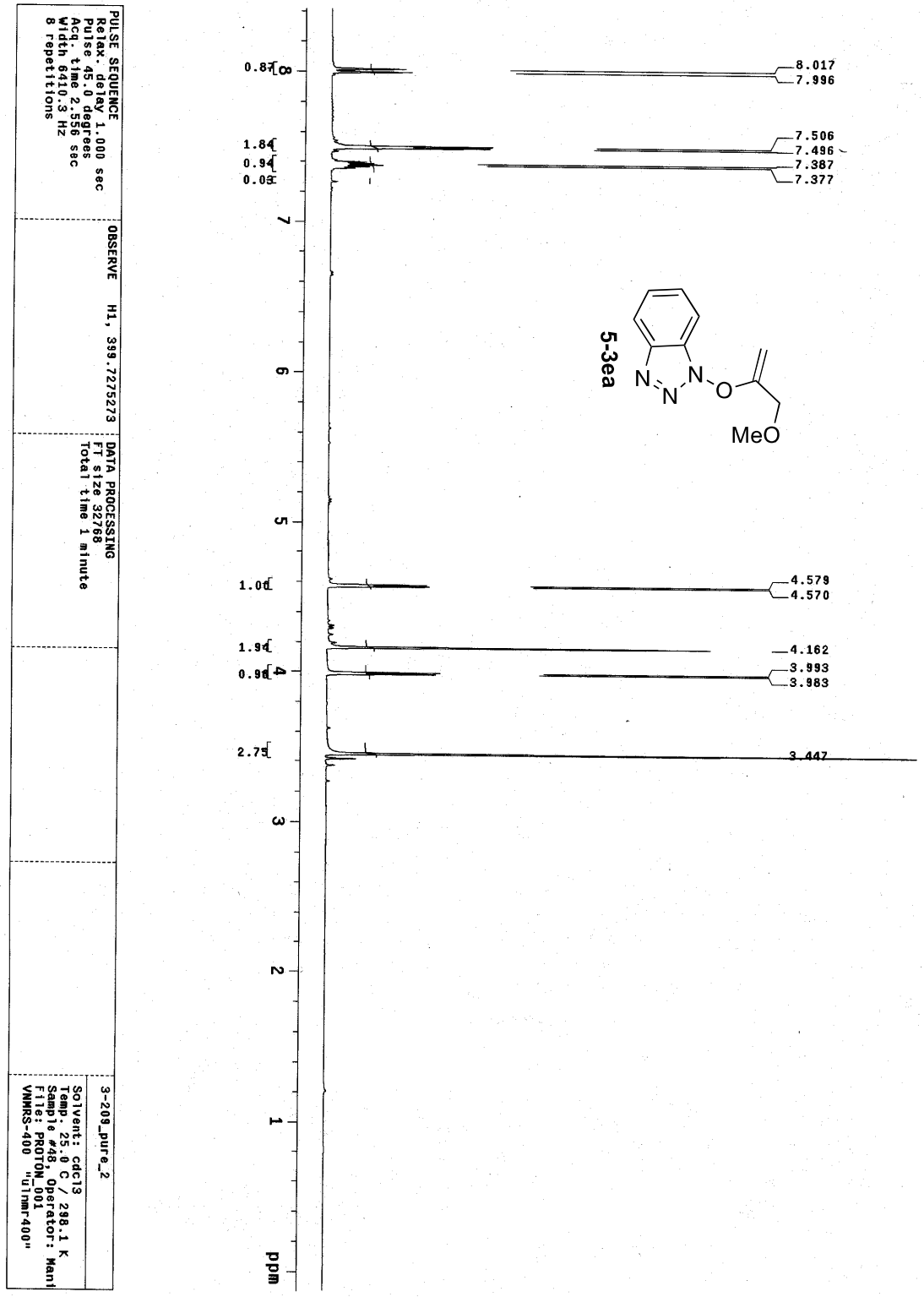
PULSE SEQUENCE
Relax. delay 1.000 sec
Pulse 45.0 degrees
Acq. time 2.556 sec
Width 8410.3 Hz
8 repetitions
OBSERVE H1, 399.7275273
DATA PROCESSING
FT size 32768
Total time 1 minute
3-209_pure_2
Solvent: cdcl3
Temp. 25.0 C / 298.1 K
Sample #48 Operator: Manl
File: PROTON_001
VNMRS-400 "uinmr400"
8.017
7.996
7.506
7.496
7.387
7.377
4.579
4.570
4.162
3.993
3.983
3.447
0.87
1.84
0.94
0.08
1.00
1.94
0.98
2.75
5-3ea
N
N
N
O
MeO
8
7
6
5
4
3
2
1
ppm

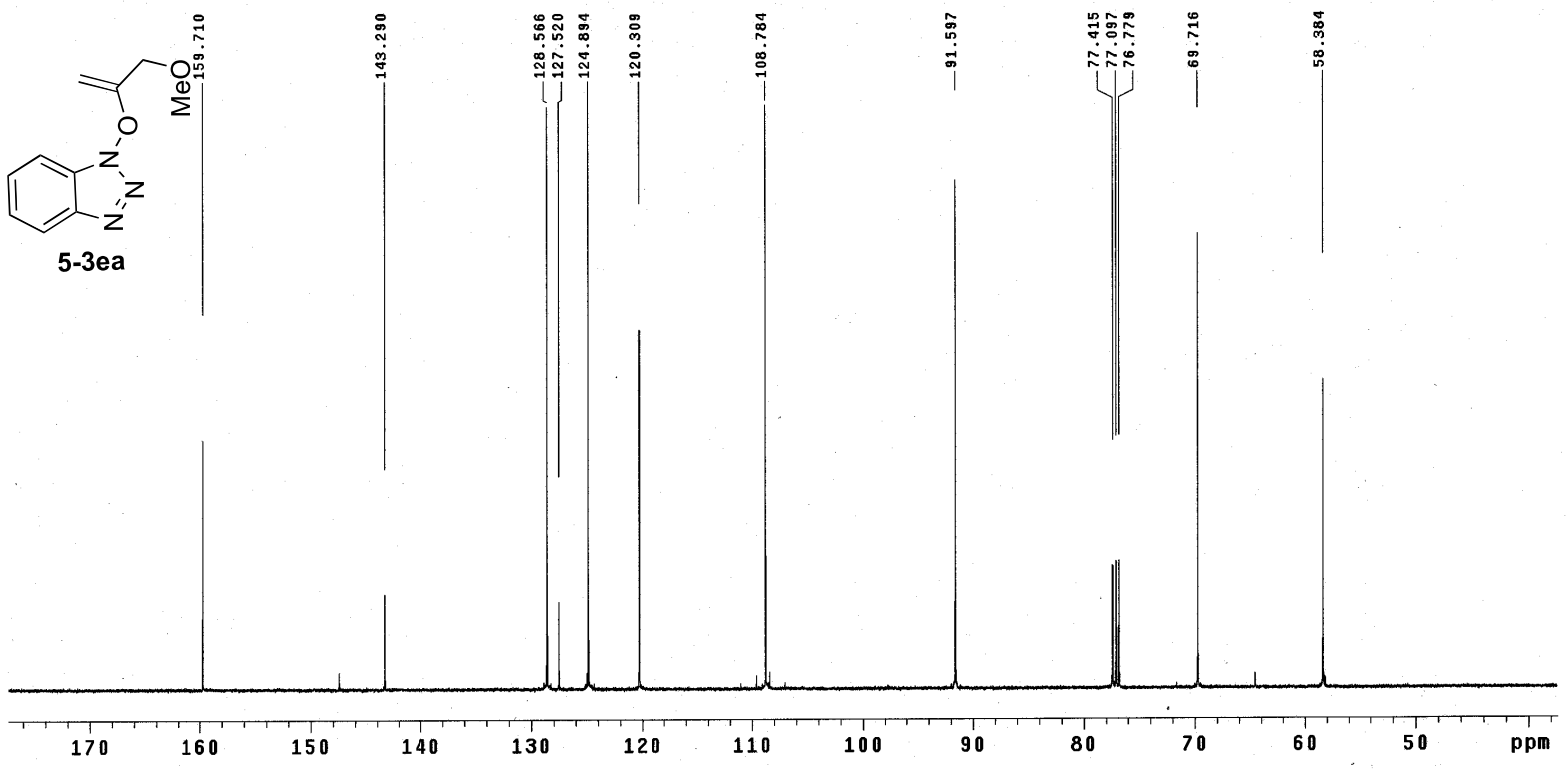

PULSE SEQUENCE Relax. delay 1.000 sec Pulse 45.0 degrees Acq. time 1.285 sec Width 25510.2 Hz 1000 repetitions	OBSERVE C13, 100.5115675 DECOUPLE H1, 399.7295294 Power 42 dB continuously on WALTZ-16 modulated	DATA PROCESSING Line broadening 0.5 Hz FT size 65536 Total time 38 minutes			3-209_pure_3 Solvent: cdcl3 Temp. 25.0 C / 298.1 K Sample #47, Operator: Mani File: CARBON_001 VNMRS-400 "ulnmr400"

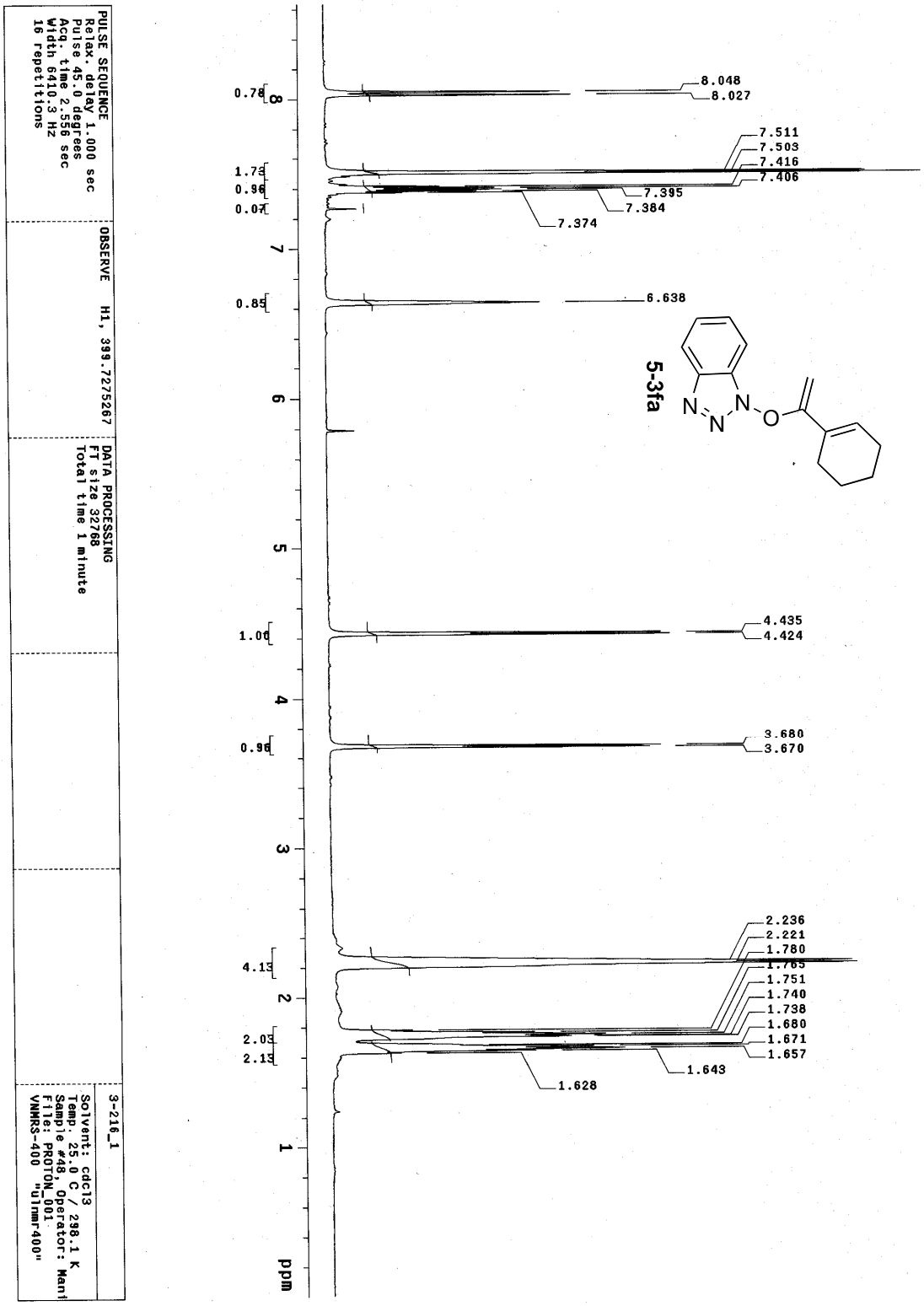
PULSE SEQUENCE
Relax. delay 1.000 sec
Pulse 45.0 degrees
Acq. time 2.556 sec
Width 6410.3 Hz
16 repetitions
OBSERVE H1, 399.7275267
DATA PROCESSING
FT size 32768
Total time 1 minute
3-218_1
Solvent: cdcl3
Temp. 25.0 C / 298.1 K
Sample #48, Operator: Mani
File: PROTON_001
VNMRS-400 "ilmr400"
8.048
8.027
7.511
7.503
7.416
7.406
7.395
7.384
7.374
6.638
4.435
4.424
3.680
3.670
2.236
2.221
1.780
1.765
1.751
1.740
1.738
1.680
1.671
1.657
1.643
1.628
0.78
1.73
0.96
0.07
0.85
1.00
0.96
4.13
2.03
2.13
ppm
5-3fa

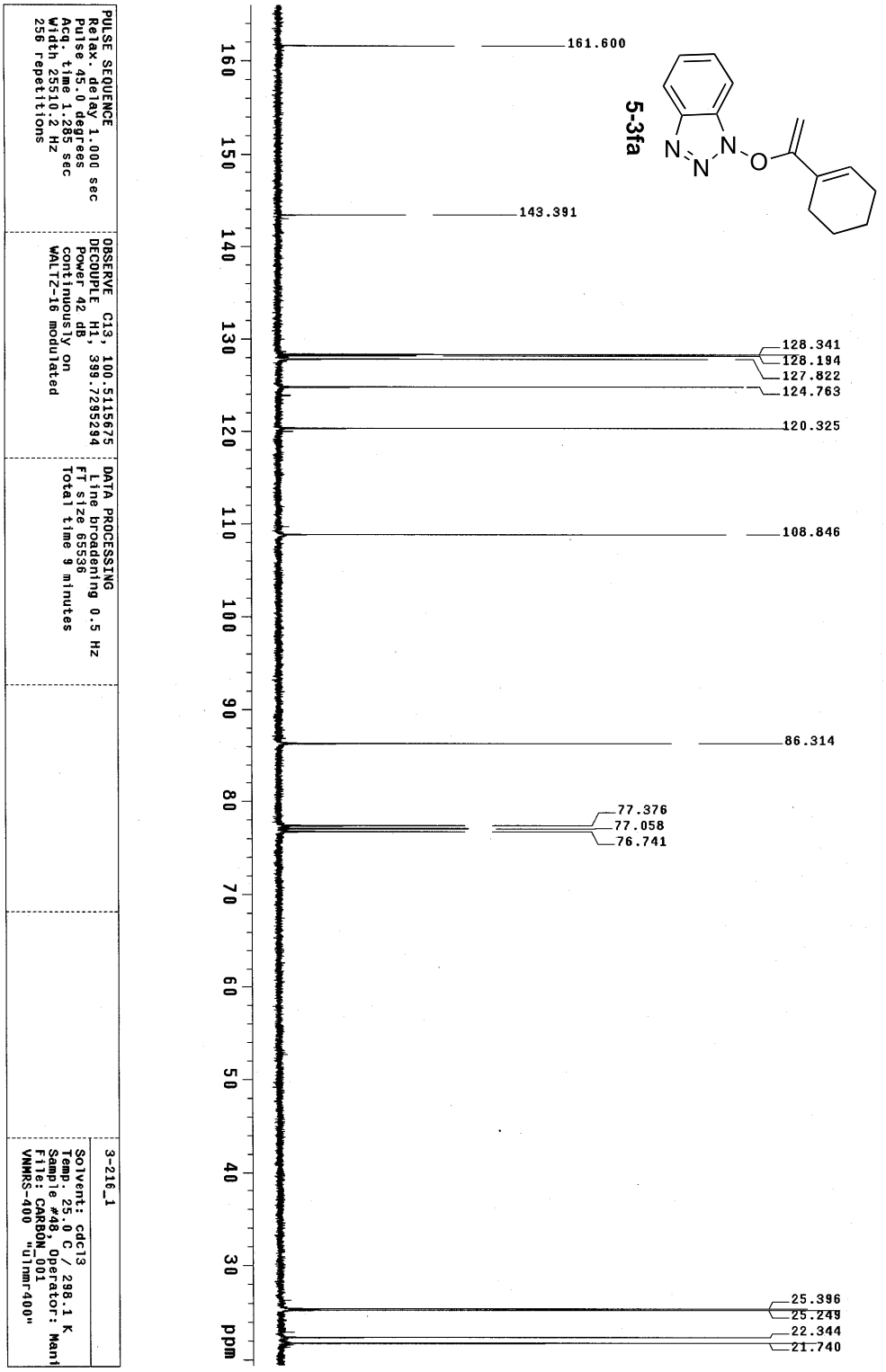
PULSE SEQUENCE
Relax. delay 1.000 sec
Pulse 45.0 degrees
Acq. time 1.285 sec
Width 25510.2 Hz
256 repetitions
OBSERVE C13, 100.5115675
DECOUPLE H1, 399.7295294
Power 42 dB
continuously on
WALTZ-16 modulated
DATA PROCESSING
Line broadening 0.5 Hz
FT size 65536
Total time 9 minutes
3-216_1
Solvent: cdcl3
Temp. 25.0 C / 298.1 K
Sample #48, Operator: Manl
File: CARBON_001
VNMRS-400 "ulnmr400"
5-3fa
161.600
143.391
128.341
128.194
127.822
124.763
120.325
108.846
86.314
77.376
77.058
76.741
25.396
25.249
22.344
21.740
160
150
140
130
120
110
100
90
80
70
60
50
40
30
ppm

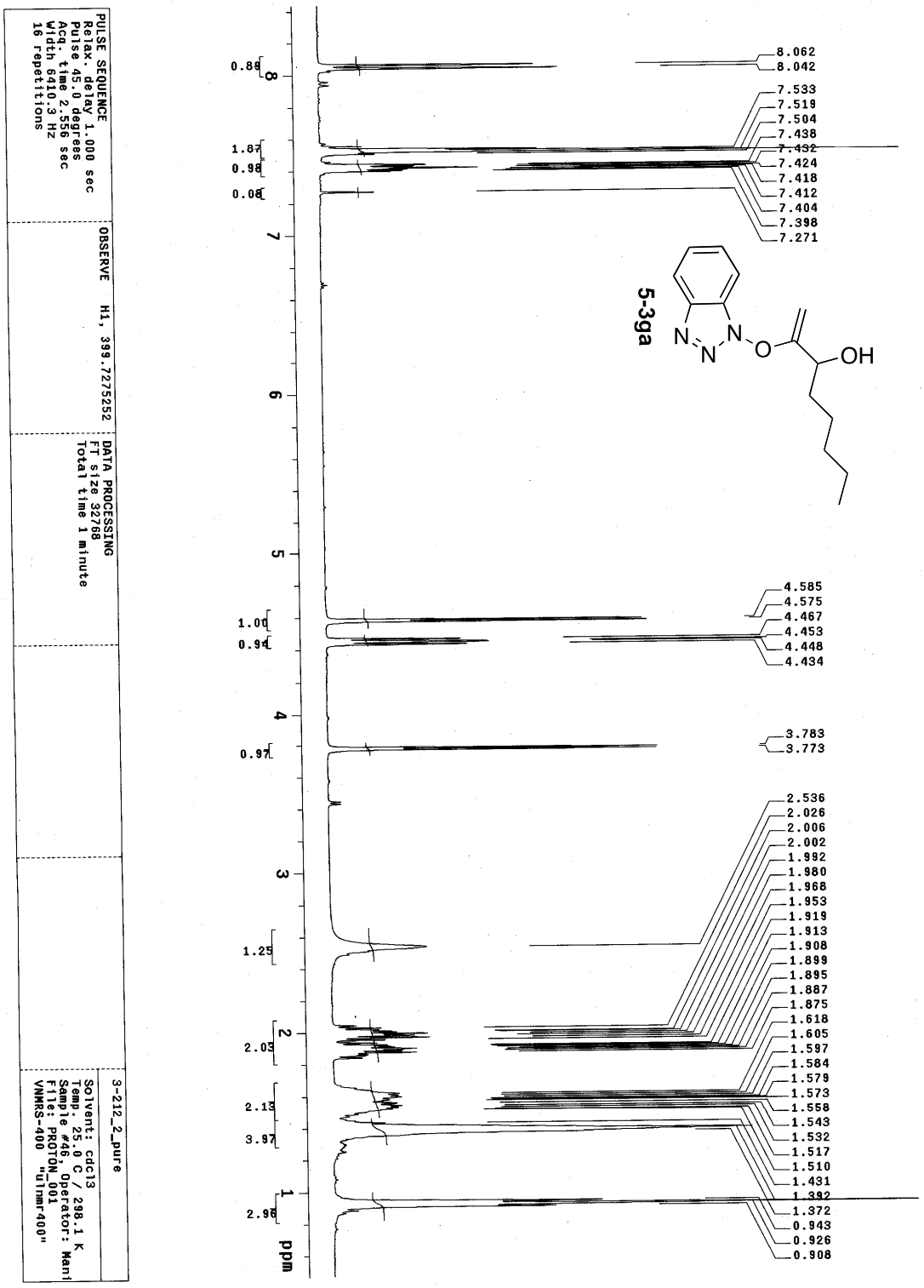
PULSE SEQUENCE
Relax. delay 1.000 sec
Pulse 45.0 degrees
Acq. time 2.556 sec
Width 6410.3 Hz
16 repetitions
OBSERVE H1, 399.7275252
DATA PROCESSING
FT size 32768
Total time 1 minute
3-212_2_pure
Solvent: cdcl3
Temp. 25.0 C / 298.1 K
Sample #40, Operator: Mani
File: PROTON_001
VNMRS-400 "ulnmr400"
5-3ga
8.062
8.042
7.533
7.519
7.504
7.438
7.432
7.424
7.418
7.412
7.404
7.398
7.271
4.585
4.575
4.467
4.453
4.448
4.434
3.783
3.773
2.536
2.026
2.006
2.002
1.992
1.980
1.968
1.953
1.919
1.913
1.908
1.899
1.895
1.887
1.875
1.618
1.605
1.597
1.584
1.579
1.573
1.558
1.543
1.532
1.517
1.510
1.431
1.392
1.372
0.943
0.926
0.908
0.88
1.87
0.98
0.08
1.00
0.94
0.97
1.25
2.03
2.13
3.97
2.96
ppm

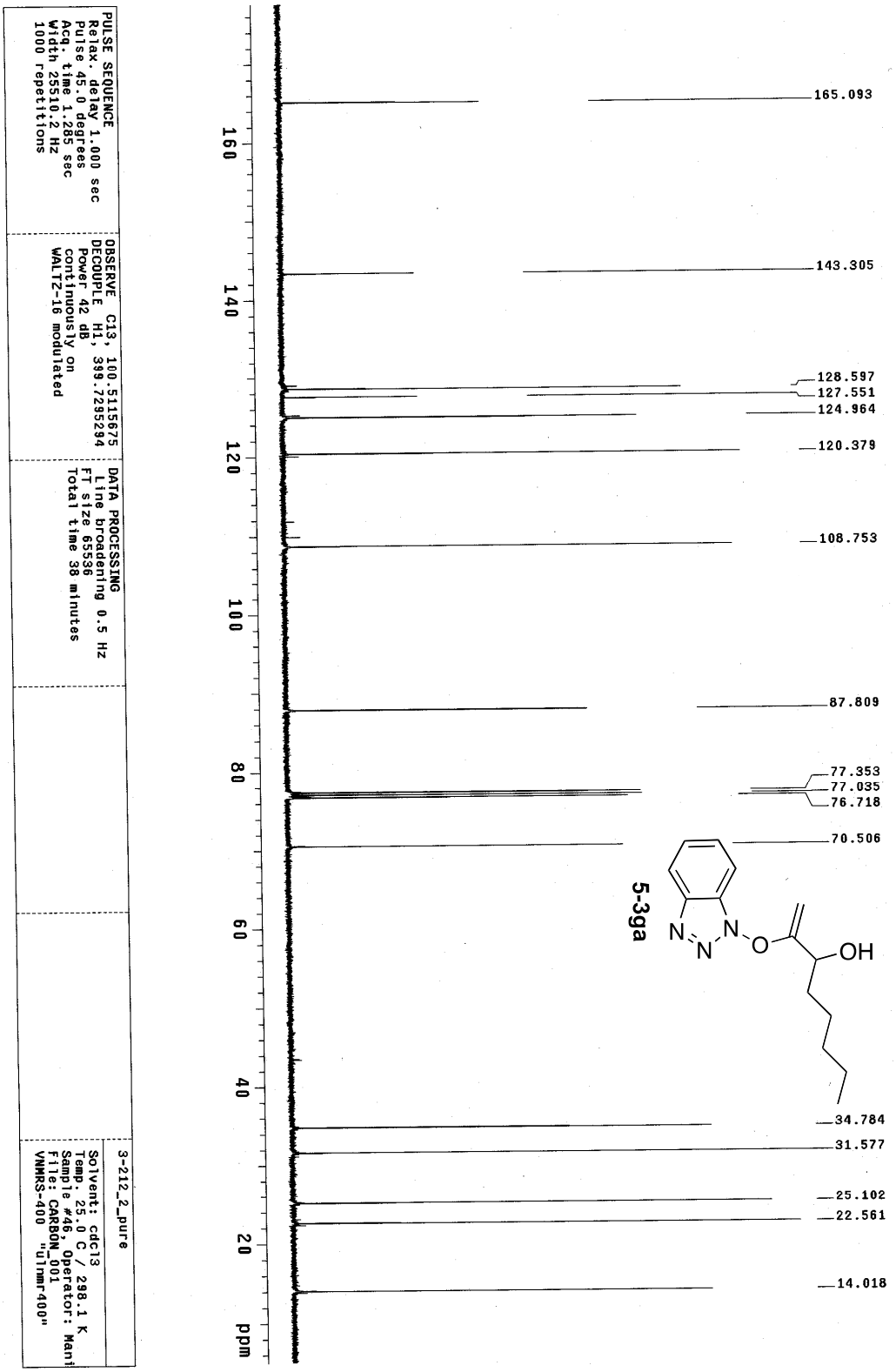
PULSE SEQUENCE
Relax. delay 1.000 sec
Pulse 45.0 degrees
Acq. time 1.285 sec
Width 25510.2 Hz
1000 repetitions
OBSERVE C13, 100.5115675
DECOUPLE H1, 399.7295294
Power 42 dB
continuously on
WALTZ-16 modulated
DATA PROCESSING
Line broadening 0.5 Hz
FT size 65536
Total time 38 minutes
3-212_2_pure
Solvent: cdcl3
Temp. 25.0 C / 298.1 K
Sample #46, Operator: Mani
File: CARBON_001
VNMRS-400 "ulnmr400"
165.093
143.305
128.597
127.551
124.964
120.379
108.753
87.809
77.353
77.035
76.718
70.506
34.784
31.577
25.102
22.561
14.018
5-3ga
OH
160
140
120
100
80
60
40
20
ppm

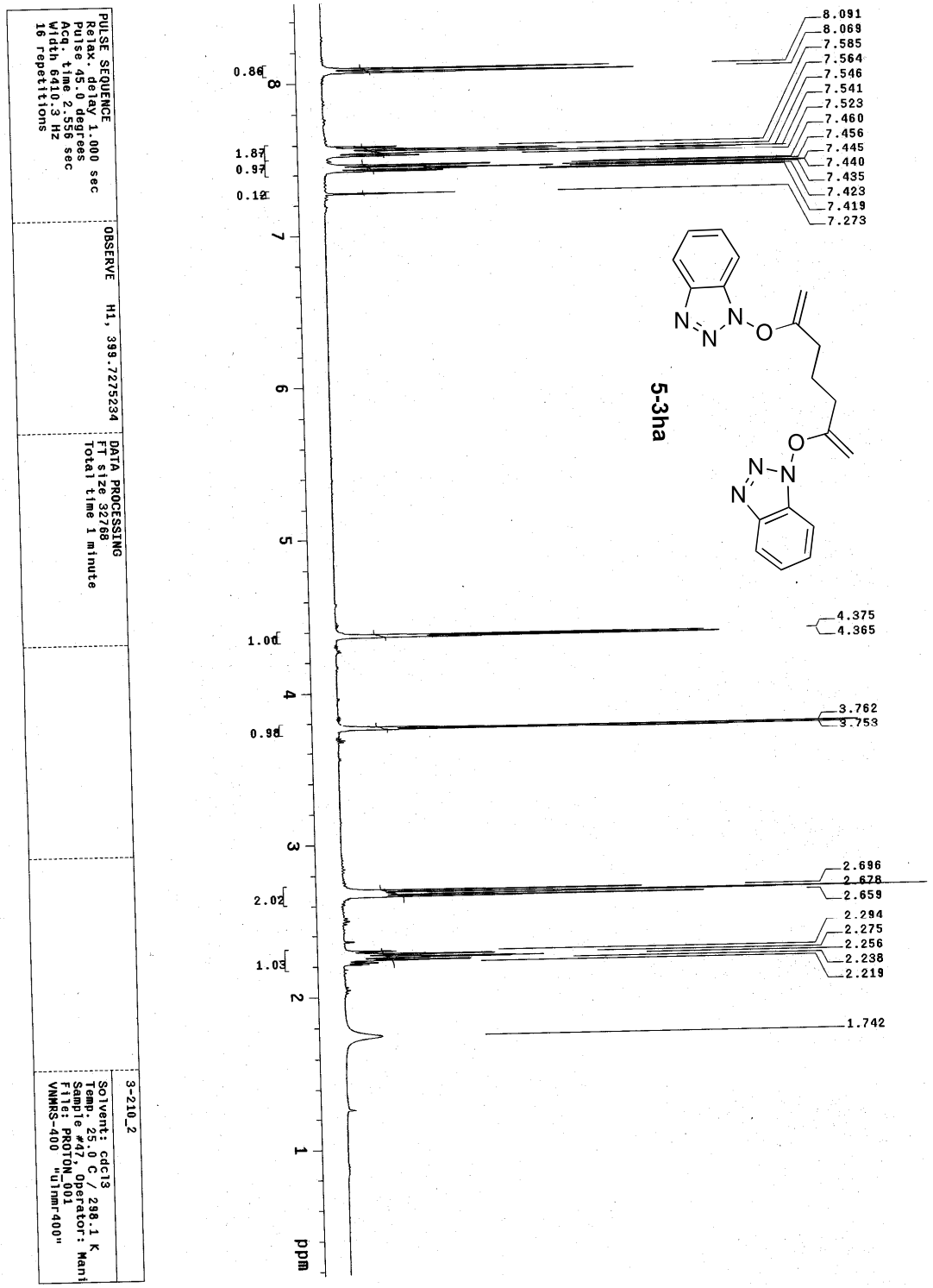
PULSE SEQUENCE
Relax. delay 1.000 sec
Pulse 45.0 degrees
Acq. time 2.556 sec
Width 6410.3 Hz
16 repetitions
OBSERVE H1, 399.7275234
DATA PROCESSING
FT size 32768
Total time 1 minute
3-210_2
Solvent: cdcl3
Temp. 25.0 C / 298.1 K
Sample #47, Operator: Mani
File: PROTON_001
VNMRS-400 "Ujnmr400"
8.091
8.069
7.585
7.564
7.546
7.541
7.523
7.460
7.456
7.445
7.440
7.435
7.423
7.419
7.273
4.375
4.365
3.762
3.753
2.696
2.678
2.659
2.294
2.275
2.256
2.238
2.219
1.742
0.86
1.87
0.97
0.12
1.00
0.98
2.02
1.03
5-3ha
ppm

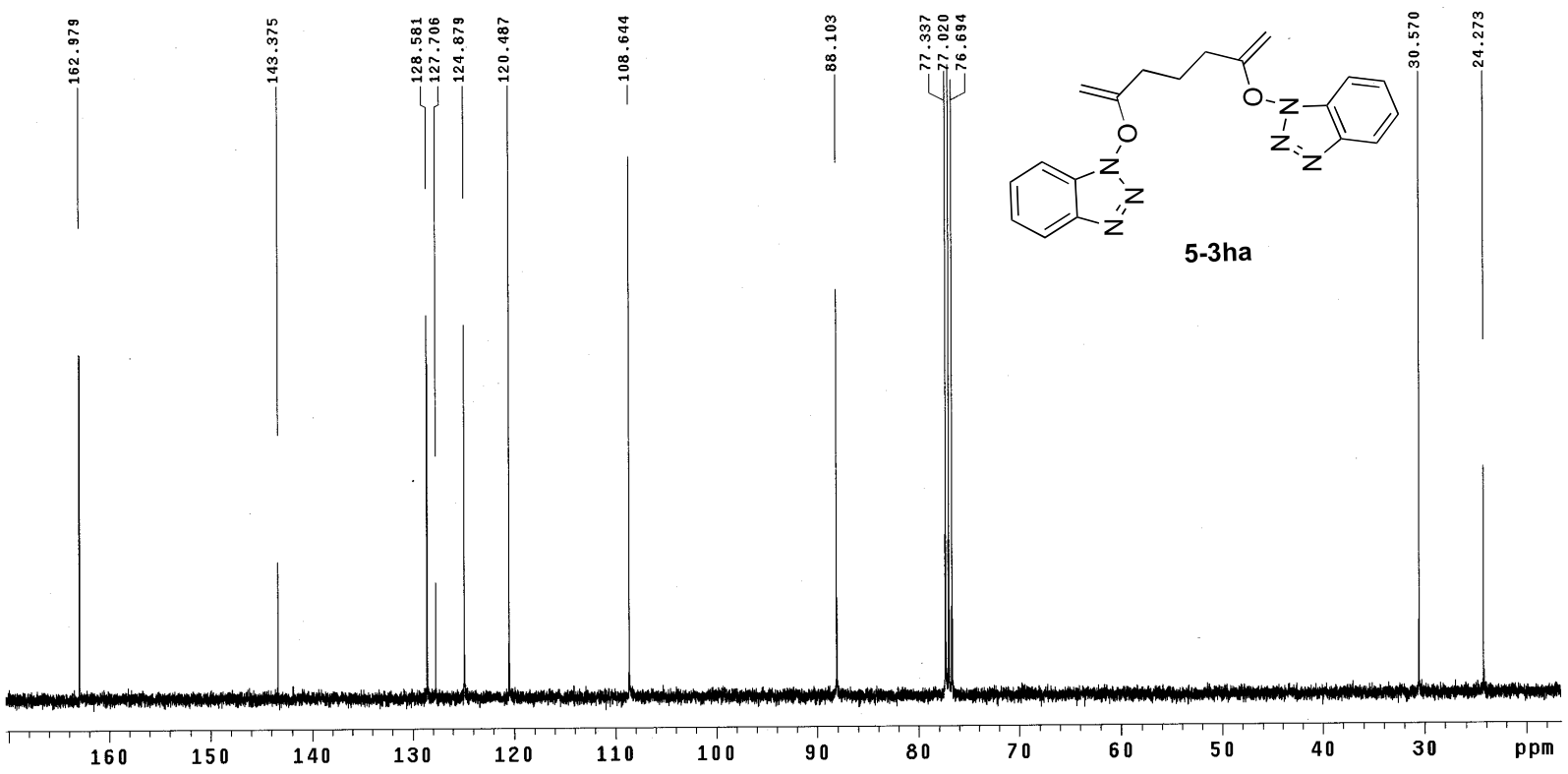

PULSE SEQUENCE Relax. delay 1.000 sec Pulse 45.0 degrees Acq. time 1.285 sec Width 25510.2 Hz 512 repetitions	OBSERVE C13, 100.5115675 DECOUPLE H1, 399.7295294 Power 42 dB continuously on WALTZ-16 modulated	DATA PROCESSING Line broadening 0.5 Hz FT size 65536 Total time 19 minutes			3-210_2 Solvent: cdcl3 Temp. 25.0 C / 298.1 K Sample #47, Operator: Mani File: CARBON_001 VNMRS-400 "ulnmr400"

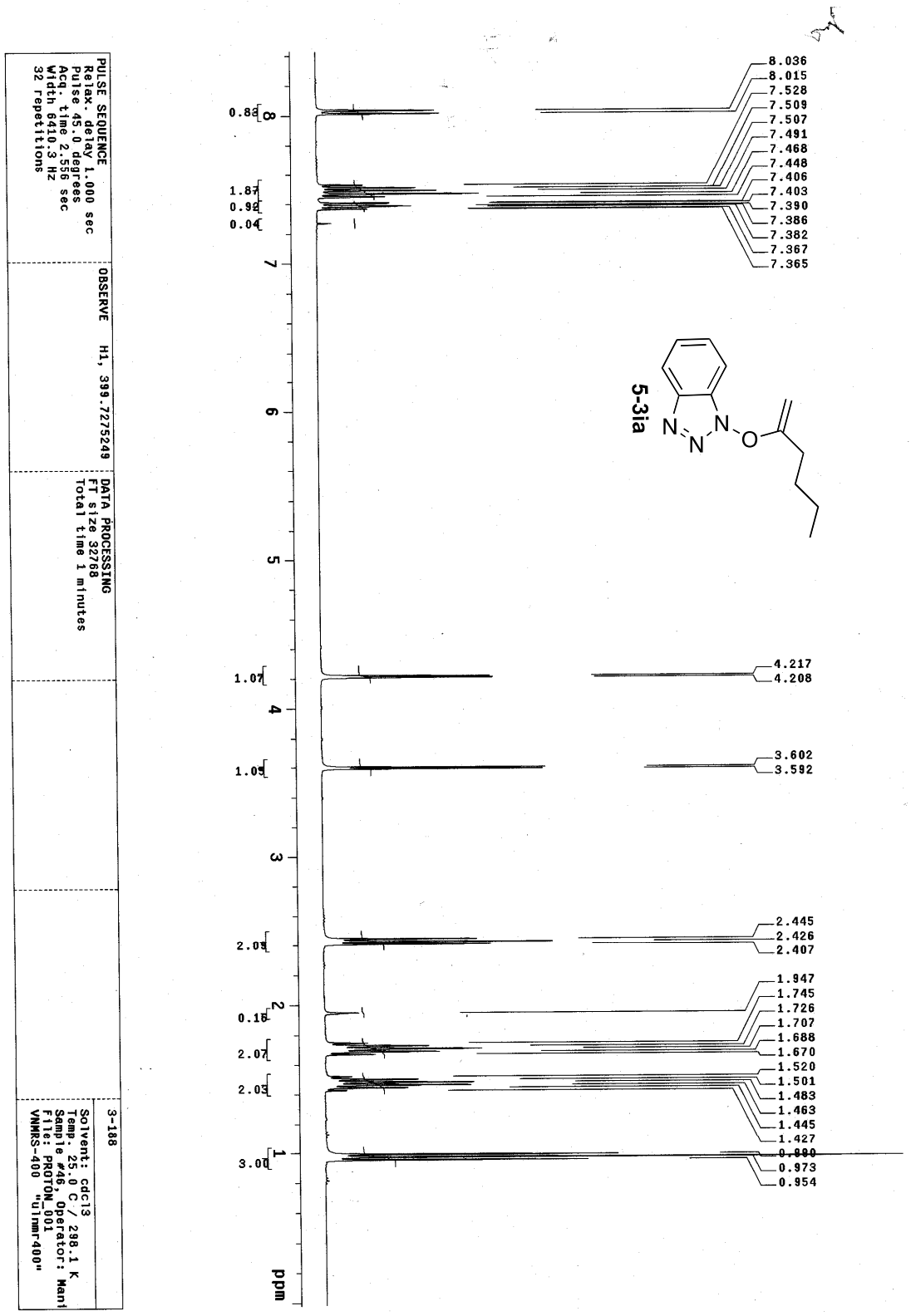
PULSE SEQUENCE
Relax. delay 1.000 sec
Pulse 45.0 degrees
Acq. time 2.556 sec
Width 6410.3 Hz
32 repetitions
OBSERVE H1, 399.7275249
DATA PROCESSING
FT size 32768
Total time 1 minutes
3-188
Solvent: cdcl3
Temp. 25.0 C / 298.1 K
Sample #46, Operator: Manl
File: PROTON_001
VNMRS-400 "ulnmr400"
8.036
8.015
7.528
7.509
7.507
7.491
7.468
7.448
7.406
7.403
7.390
7.386
7.382
7.367
7.365
4.217
4.208
3.602
3.592
2.445
2.426
2.407
1.947
1.745
1.726
1.707
1.688
1.670
1.520
1.501
1.483
1.463
1.445
1.427
0.880
0.973
0.954
5-3ia
ppm

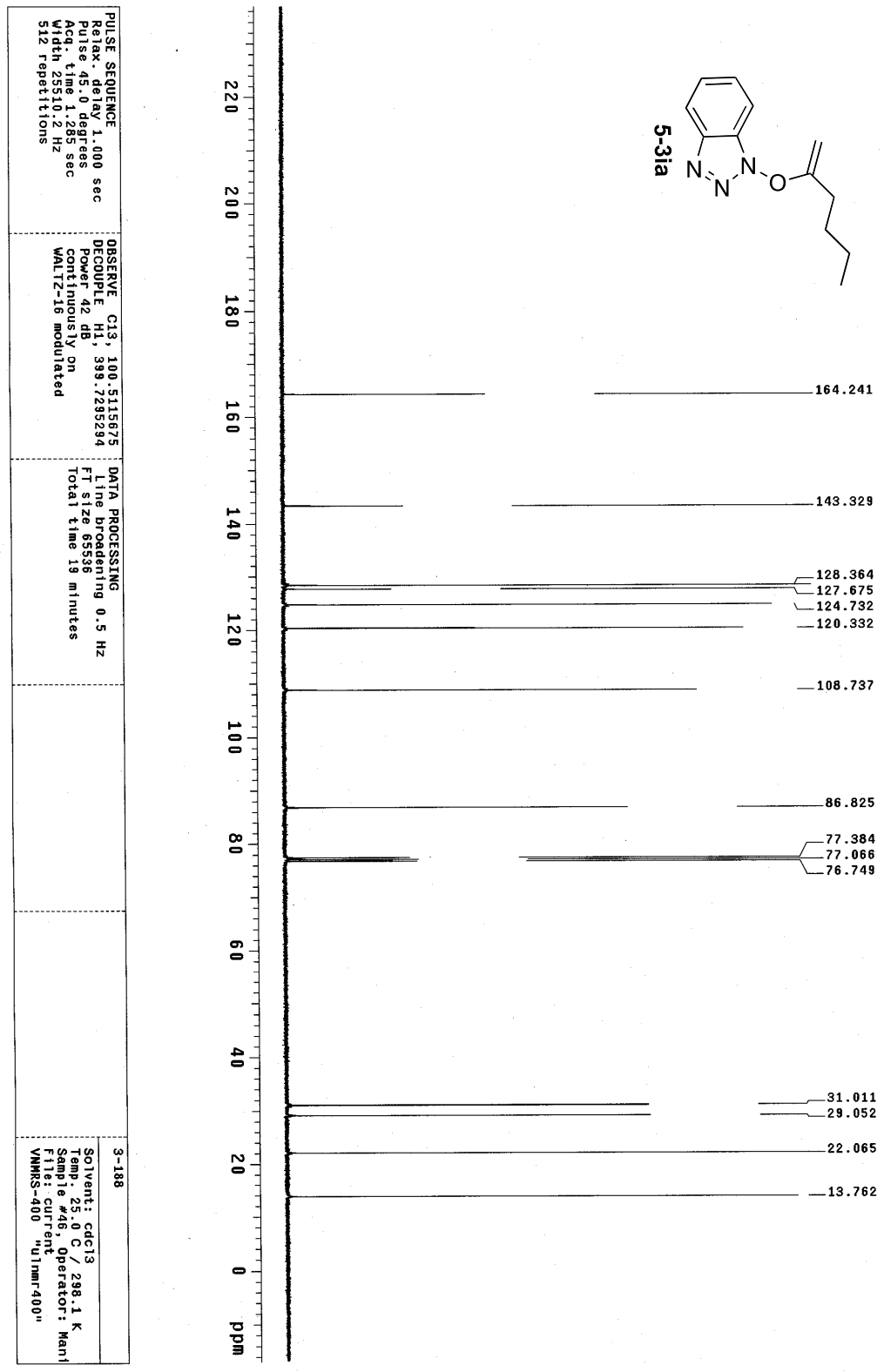
5-3ia
164.241
143.329
128.364
127.675
124.732
120.332
108.737
86.825
77.384
77.066
76.749
31.011
29.052
22.065
13.762
220
200
180
160
140
120
100
80
60
40
20
0
ppm
PULSE SEQUENCE
Relax. delay 1.000 sec
Pulse 45.0 degrees
Acq. time 1.285 sec
Width 25510.2 Hz
512 repetitions
OBSERVE C13, 100.5115675
DECOUPLE H1, 399.7295294
Power 42 dB
continuously on
WALTZ-16 modulated
DATA PROCESSING
Line broadening 0.5 Hz
FT size 65536
Total time 19 minutes
3-188
Solvent: cdcl3
Temp. 25.0 C / 298.1 K
Sample #46, Operator: Mani
File: current
VNMRS-400 "ulmnr400"

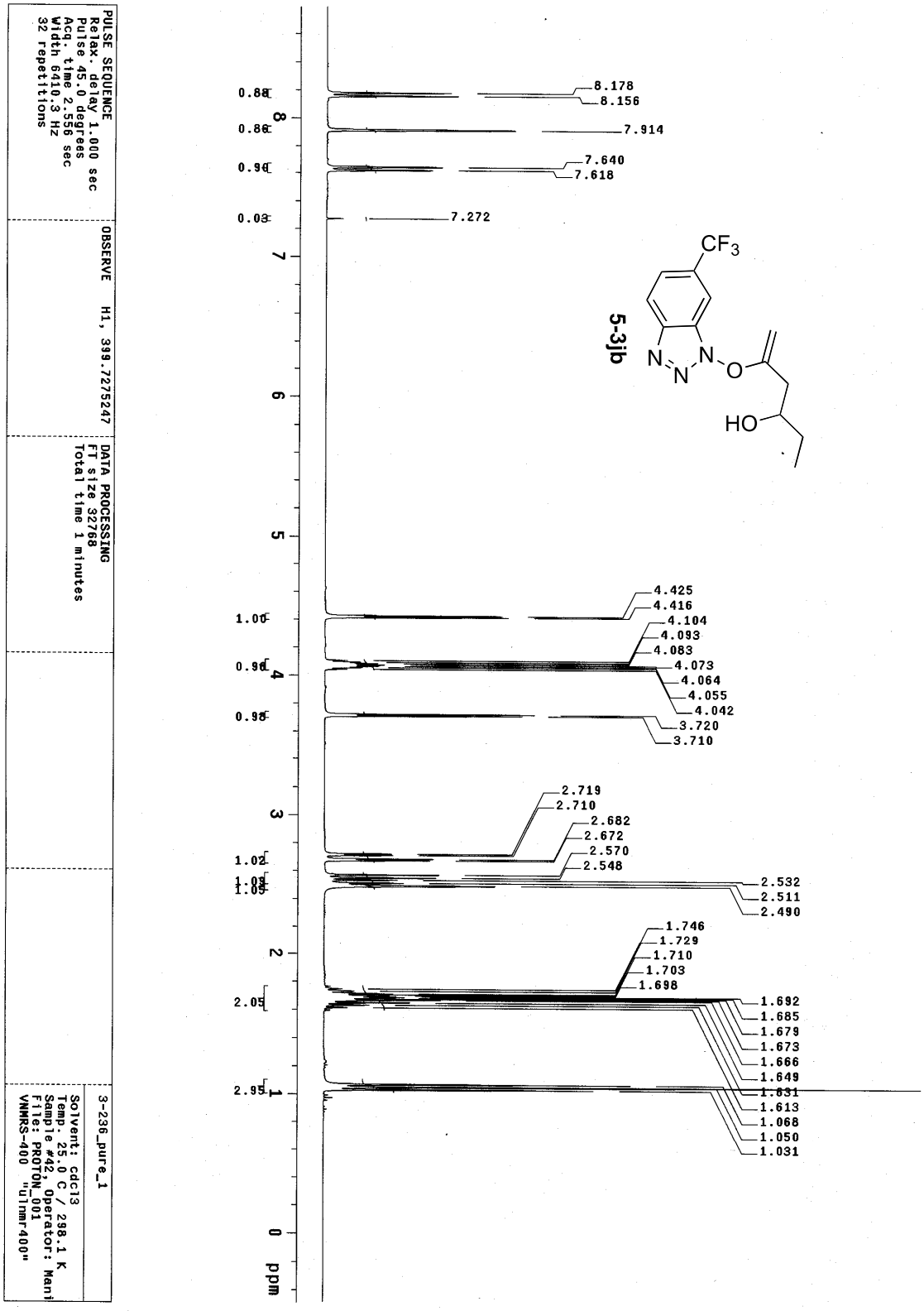
PULSE SEQUENCE
Relax. delay 1.000 sec
Pulse 45.0 degrees
Acq. time 2.556 sec
Width 6410.3 Hz
32 repetitions
OBSERVE H1, 399.7275247
DATA PROCESSING
FT size 32768
Total time 1 minutes
3-236_pure_1
Solvent: cdcl3
Temp. 25.0 C / 298.1 K
Sample #42, Operator: Manj
File: PROTON_001
VNMRS-400 "Ulmr400"
8.178
8.156
7.914
7.640
7.618
7.272
5-3jb
CF3
N
N
N
O
HO
4.425
4.416
4.104
4.093
4.083
4.073
4.064
4.055
4.042
3.720
3.710
2.719
2.710
2.682
2.672
2.570
2.548
2.532
2.511
2.490
1.746
1.729
1.710
1.703
1.698
1.692
1.685
1.679
1.673
1.666
1.649
1.631
1.613
1.068
1.050
1.031
ppm

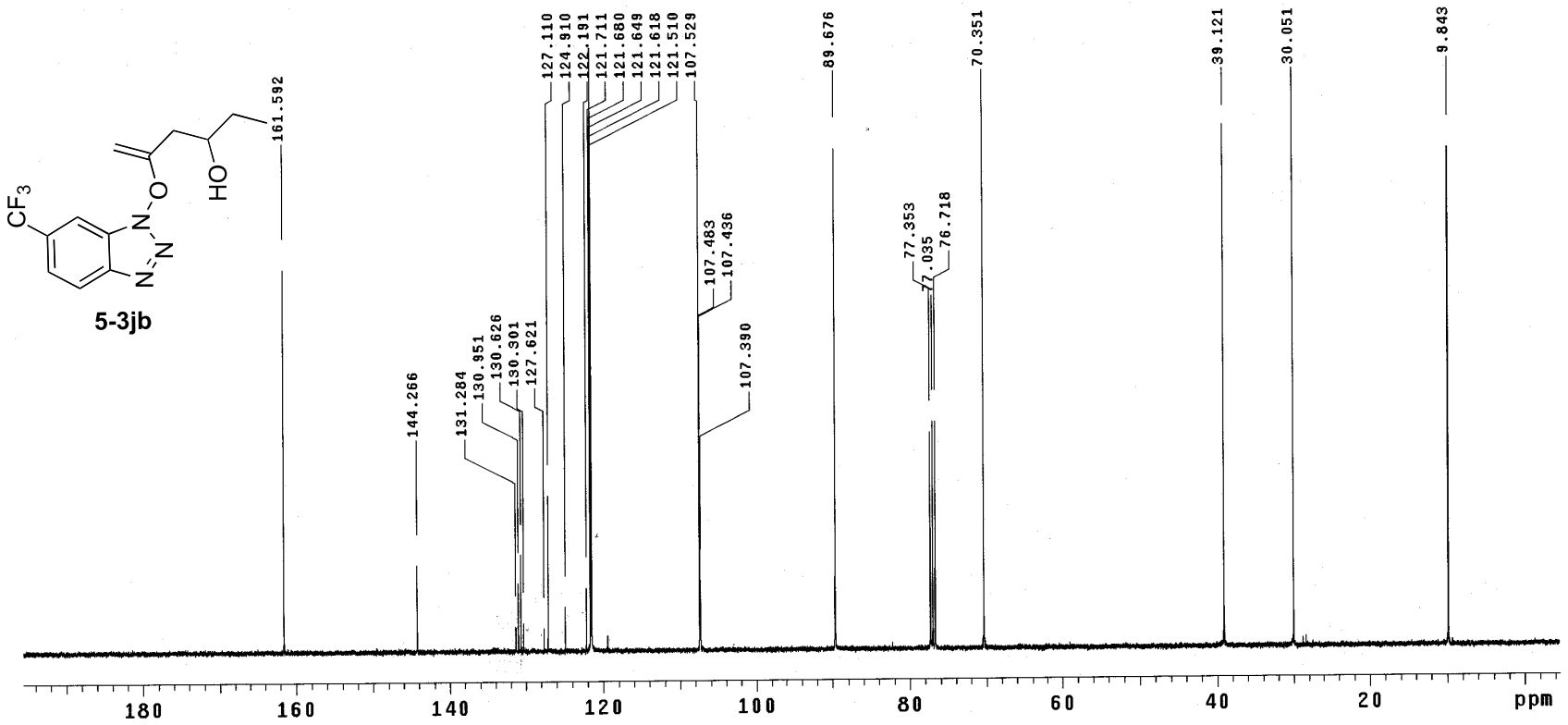

PULSE SEQUENCE Relax. delay 1.000 sec Pulse 45.0 degrees Acq. time 1.285 sec Width 25510.2 Hz 512 repetitions	OBSERVE C13, 100.5115675 DECOUPLE H1, 399.7295294 Power 42 dB continuously on WALTZ-16 modulated	DATA PROCESSING Line broadening 0.5 Hz FT size 65536 Total time 19 minutes			3-236_PURE Solvent: cdcl3 Temp. 25.0 C / 298.1 K Sample #42, Operator: Mani File: CARBON_001 VNMRS-400 "ulnmr400"

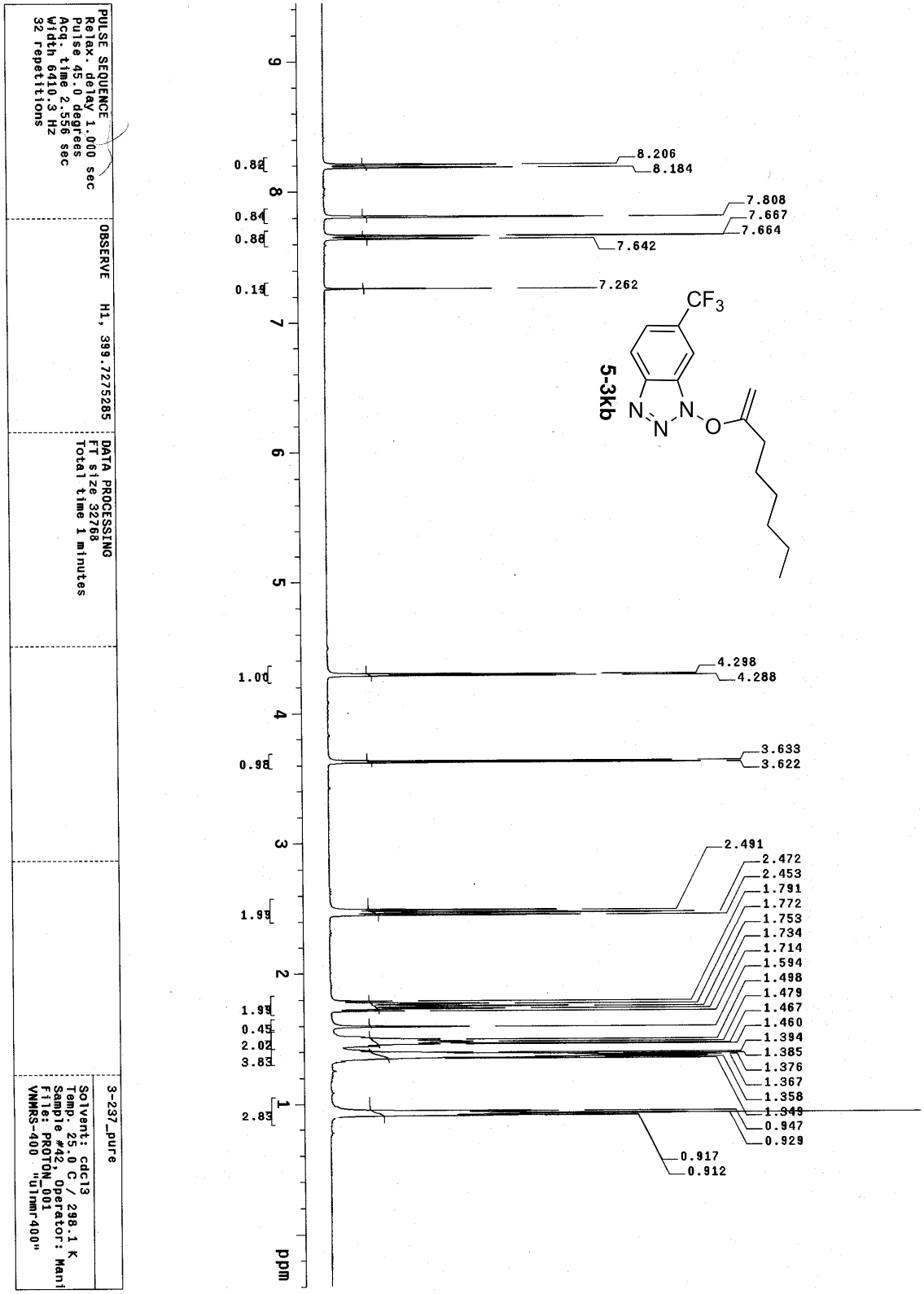
PULSE SEQUENCE
Relax. delay 1.000 sec
Pulse 45.0 degrees
Acq. time 2.556 sec
Width 6410.3 Hz
32 repetitions
OBSERVE H1, 399.7275285
DATA PROCESSING
FT size 32768
Total time 1 minutes
3-237_pure
Solvent: cdcl3
Temp. 25.0 C / 298.1 K
Sample #42, Operator: Mani
File: PROTON_001
VNMRS-400 "Ulmr400"
8.206
8.184
7.808
7.667
7.664
7.642
7.262
CF3
5-3kb
N
N
N
O
4.298
4.288
3.633
3.622
2.491
2.472
2.453
1.791
1.772
1.753
1.734
1.714
1.594
1.498
1.479
1.467
1.460
1.394
1.385
1.376
1.367
1.358
1.349
0.947
0.929
0.917
0.912
0.82
0.84
0.88
0.19
1.00
0.98
1.98
1.92
0.45
2.02
3.83
2.83
9
8
7
6
5
4
3
2
1
ppm

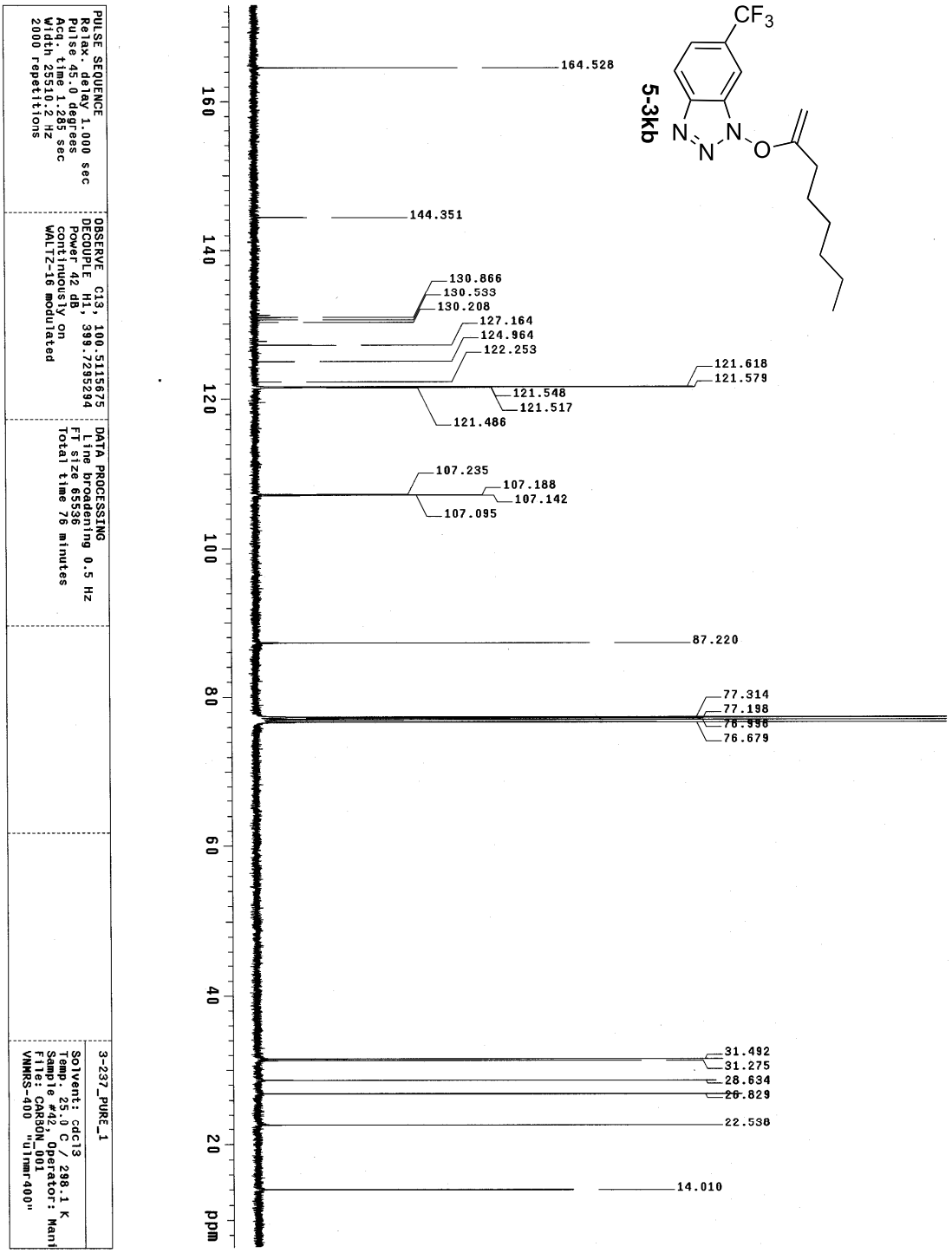
PULSE SEQUENCE
Relax. delay 1.000 sec
Pulse 45.0 degrees
Acq. time 1.285 sec
Width 25510.2 Hz
2000 repetitions
OBSERVE C13, 100.5115675
DECOUPLE H1, 399.7285284
Power 42 dB
continuously on
WALTZ-16 modulated
DATA PROCESSING
Line broadening 0.5 Hz
FT size 65536
Total time 76 minutes
3-237_PURE_1
Solvent: cdcl3
Temp. 25.0 C / 298.1 K
Sample #42 Operator: Mani
File: CARBON_001
VNMRS-400 "ujnmr400"
5-3kb
CF3
N
N
N
O
164.528
144.351
130.866
130.533
130.208
127.164
124.964
122.253
121.618
121.579
121.548
121.517
121.486
107.235
107.188
107.142
107.095
87.220
77.314
77.198
76.936
76.679
31.492
31.275
28.634
26.829
22.538
14.010
160
140
120
100
80
60
40
20
ppm

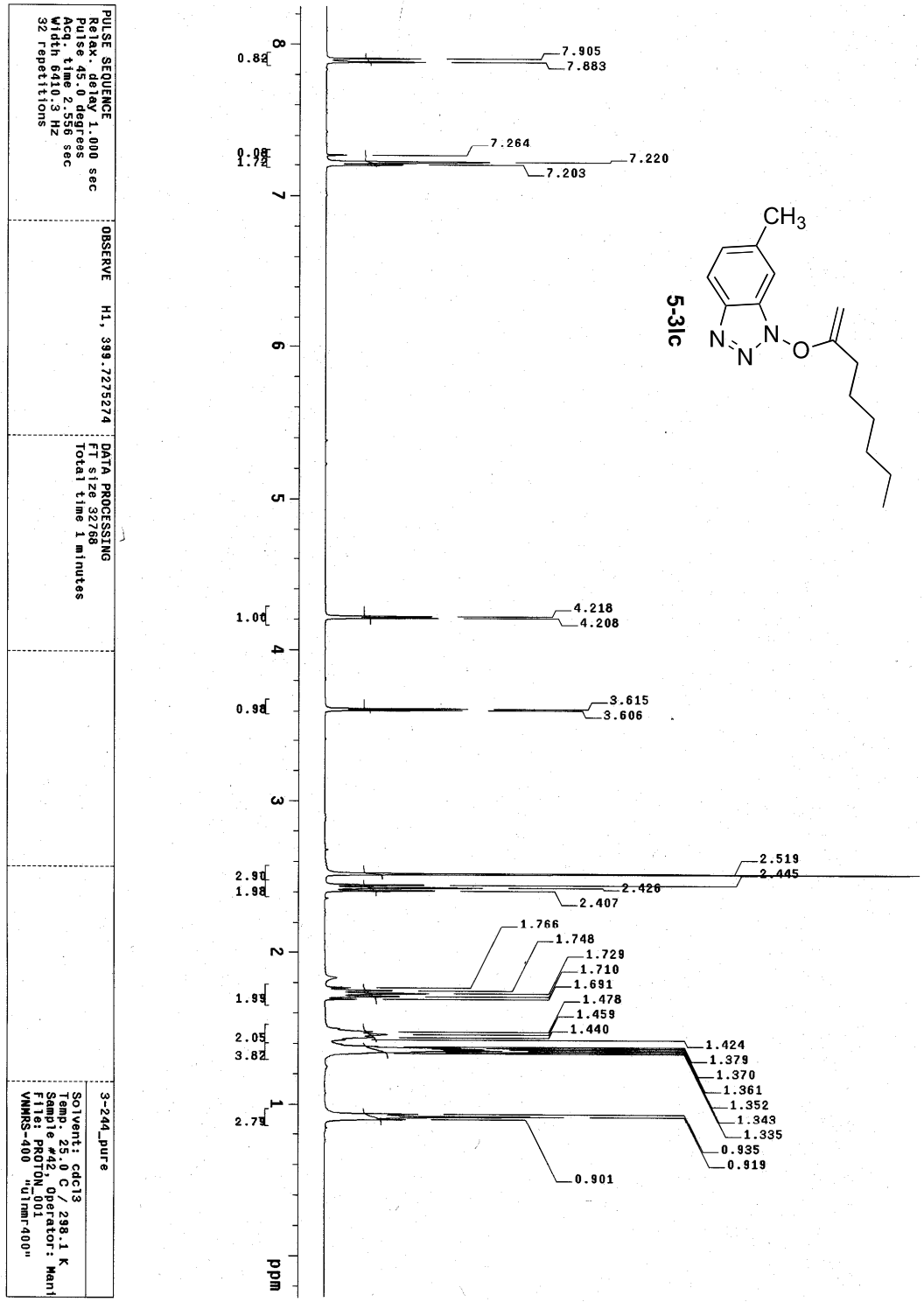
PULSE SEQUENCE
Relax. delay 1.000 sec
Pulse 45.0 degrees
Acq. time 2.556 sec
Width 6410.3 Hz
32 repetitions
OBSERVE H1, 399.7275274
DATA PROCESSING
FT size 32768
Total time 1 minutes
3-244_pure
Solvent: cdcl3
Temp. 25.0 C / 298.1 K
Sample #42, Operator: Man
File: PROTON_001
VNMRS-400 "u1nmr400"
7.905
7.883
7.264
7.220
7.203
4.218
4.208
3.615
3.606
2.519
2.445
2.426
2.407
1.766
1.748
1.729
1.710
1.691
1.478
1.459
1.440
1.424
1.379
1.370
1.361
1.352
1.343
1.335
0.935
0.919
0.901
0.82
0.08
1.72
1.00
0.98
2.90
1.98
1.99
2.05
3.82
2.75
ppm
5-3lc

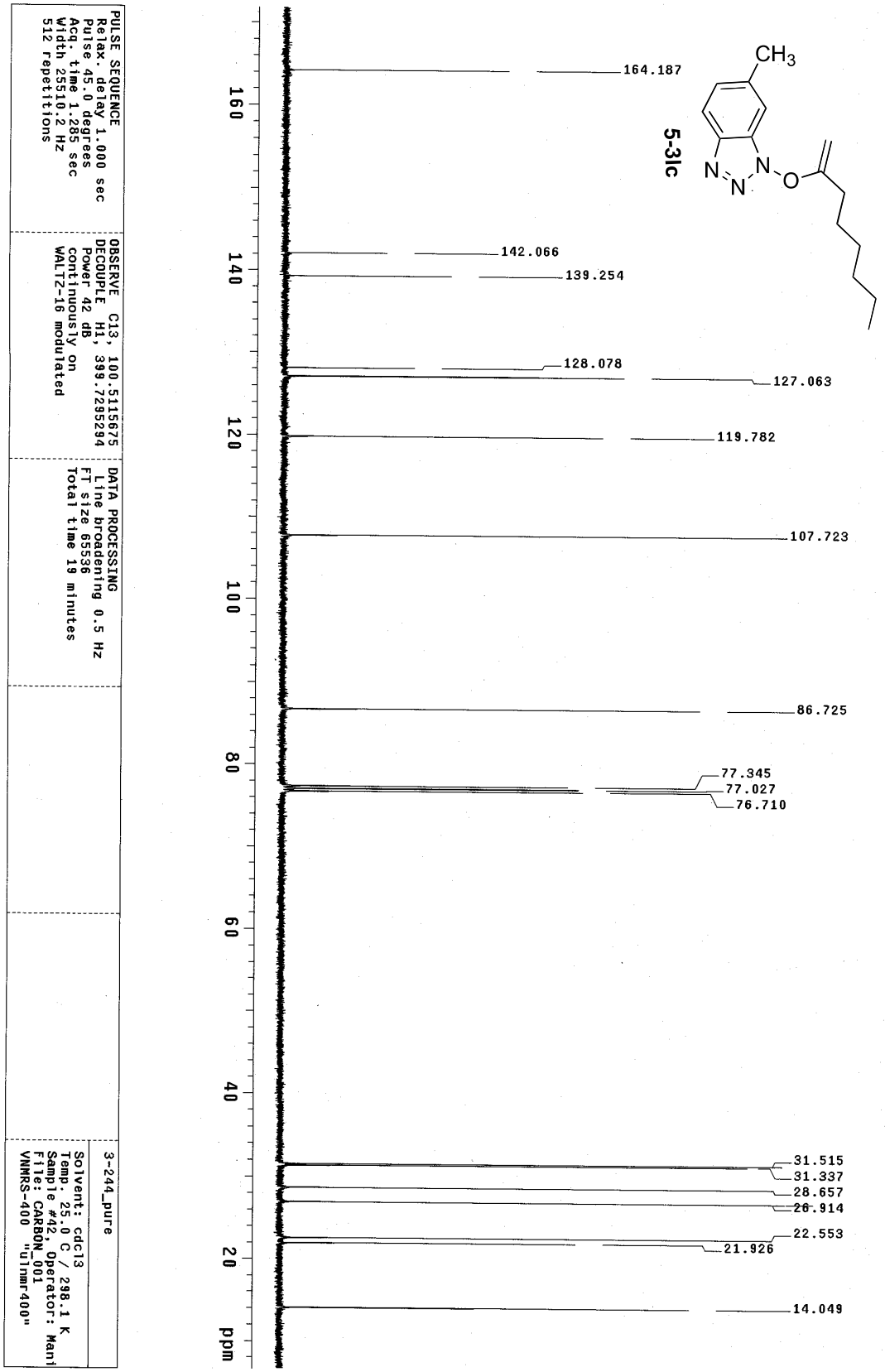
PULSE SEQUENCE
Relax. delay 1.000 sec
Pulse 45.0 degrees
Acq. time 1.285 sec
Width 25510.2 Hz
512 repetitions
OBSERVE C13, 100.5115675
DECOUPLE H1, 399.7295294
Power 42 dB
continuously on
WALTZ-16 modulated
DATA PROCESSING
Line broadening 0.5 Hz
FT size 65536
Total time 19 minutes
3-244_pure
Solvent: cdcl3
Temp. 25.0 C / 298.1 K
Sample #42, Operator: Mani
File: CARBON_001
VNMRS-400 "ulmr400"
5-3lc
CH3
N
N
N
O
164.187
142.066
139.254
128.078
127.063
119.782
107.723
86.725
77.345
77.027
76.710
31.515
31.337
28.657
26.914
22.553
21.926
14.049
160
140
120
100
80
60
40
20
ppm

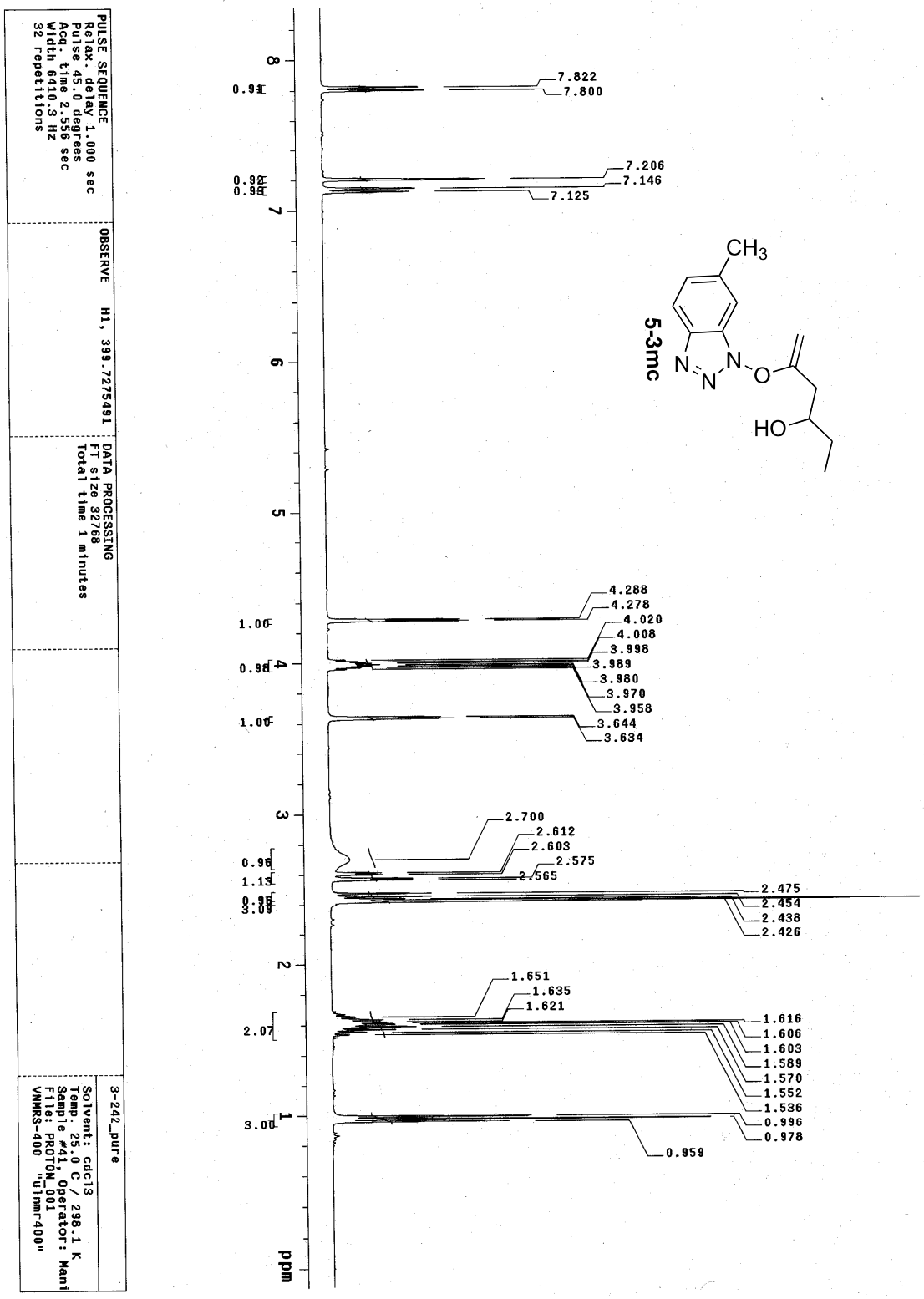
PULSE SEQUENCE
Relax. delay 1.000 sec
Pulse 45.0 degrees
Acq. time 2.556 sec
Width 6410.3 Hz
32 repetitions
OBSERVE H1, 399.7275491
DATA PROCESSING
FT size 32768
Total time 1 minutes
3-242_pure
Solvent: cdcl3
Temp. 25.0 C / 298.1 K
Sample #41, Operator: Mani
File: PROTON_001
VNMRS-400 "Ulmar400"
7.822
7.800
7.206
7.146
7.125
4.288
4.278
4.020
4.008
3.998
3.989
3.980
3.970
3.958
3.644
3.634
2.700
2.612
2.603
2.575
2.565
2.475
2.454
2.438
2.426
1.651
1.635
1.621
1.616
1.606
1.603
1.589
1.570
1.552
1.536
0.996
0.978
0.959
ppm
5-3mc
CH3
N
N
N
O
HO

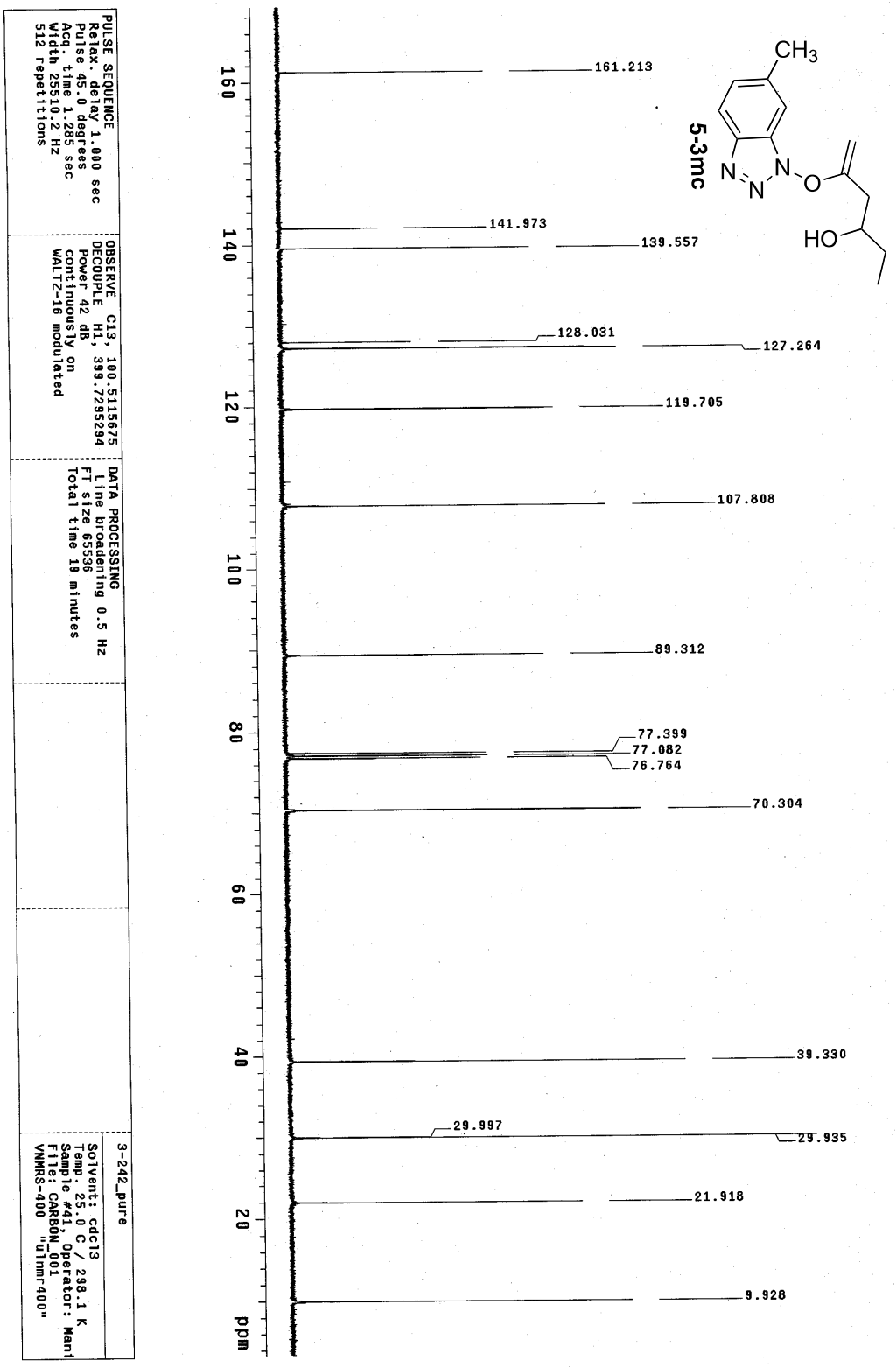
PULSE SEQUENCE
Relax. delay 1.000 sec
Pulse 45.0 degrees
Acq. time 1.285 sec
Width 25510.2 Hz
512 repetitions
OBSERVE C13, 100.5115675
DECOUPLE H1, 399.7295294
Power 42 dB
continuously on
WALTZ-16 modulated
DATA PROCESSING
Line broadening 0.5 Hz
FT size 65536
Total time 19 minutes
3-242_pure
Solvent: cdcl3
Temp. 25.0 C / 298.1 K
Sample #41, Operator: Mani
File: CARBON_001
VNMRS-400 "u1nmr400"
5-3mc
CH3
N
N
N
O
HO
161.213
141.973
139.557
128.031
127.264
119.705
107.808
89.312
77.399
77.082
76.764
70.304
39.330
29.997
29.935
21.918
9.928
160
140
120
100
80
60
40
20
ppm

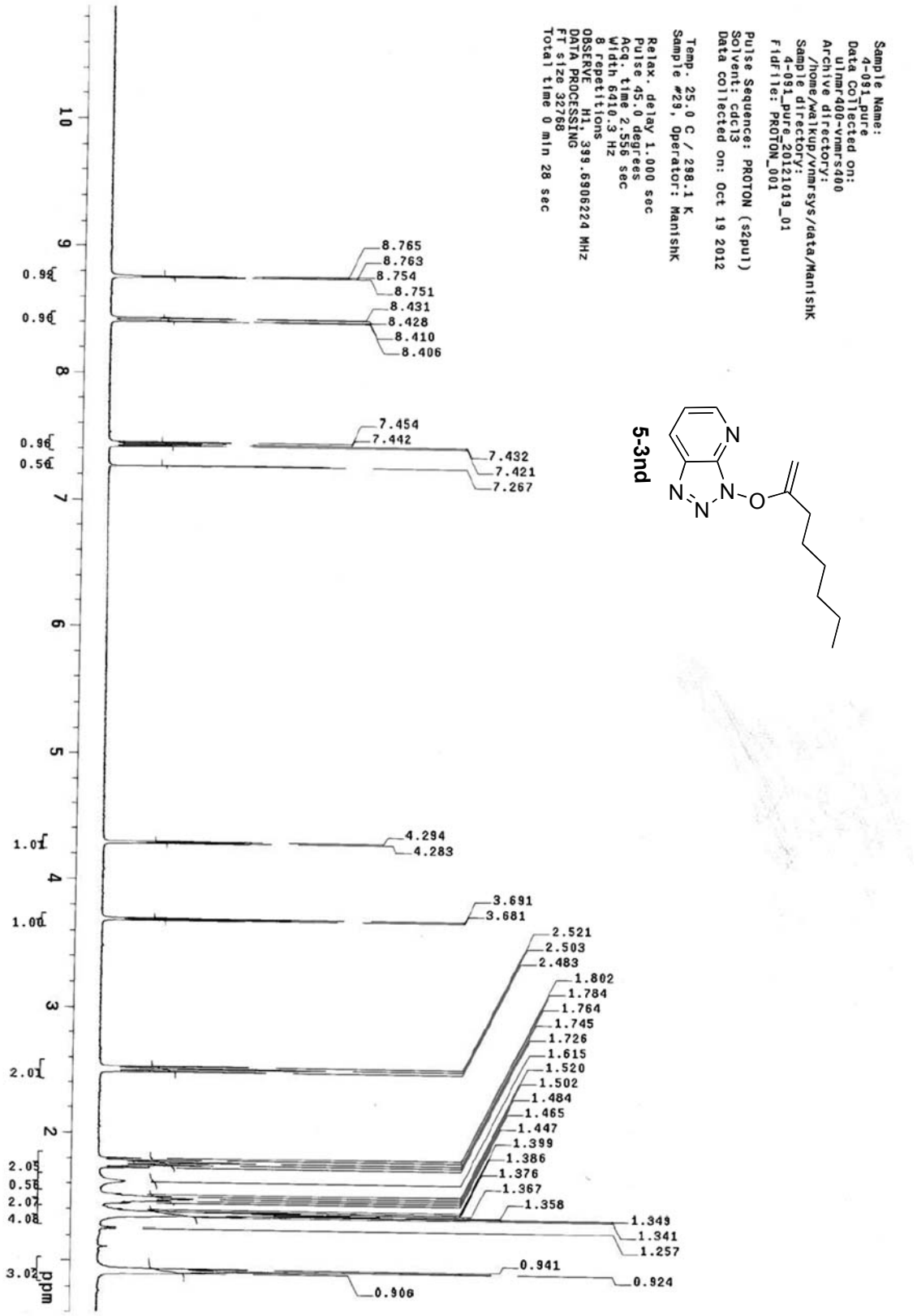
Sample Name:
4-091_pure
Data Collected on:
ulnmr400-vnmrs400
Archive directory:
/home/walkup/vnmrsys/data/ManishK
Sample directory:
4-091_pure_20121019_01
FidFile: PROTON_001
Pulse Sequence: PROTON (s2pul)
Solvent: cdcl3
Data collected on: Oct 19 2012
Temp. 25.0 C / 298.1 K
Sample #29, Operator: ManishK
Relax. delay 1.000 sec
Pulse 45.0 degrees
Acq. time 2.556 sec
Width 6410.3 Hz
8 repetitions
OBSERVE H1, 399.6906224 MHz
DATA PROCESSING
FT size 32768
Total time 0 min 28 sec
5-3nd
8.765
8.763
8.754
8.751
8.431
8.428
8.410
8.406
7.454
7.442
7.432
7.421
7.267
4.294
4.283
3.691
3.681
2.521
2.503
2.483
1.802
1.784
1.764
1.745
1.726
1.615
1.520
1.502
1.484
1.465
1.447
1.399
1.386
1.376
1.367
1.358
1.349
1.341
1.257
0.941
0.924
0.906
ppm

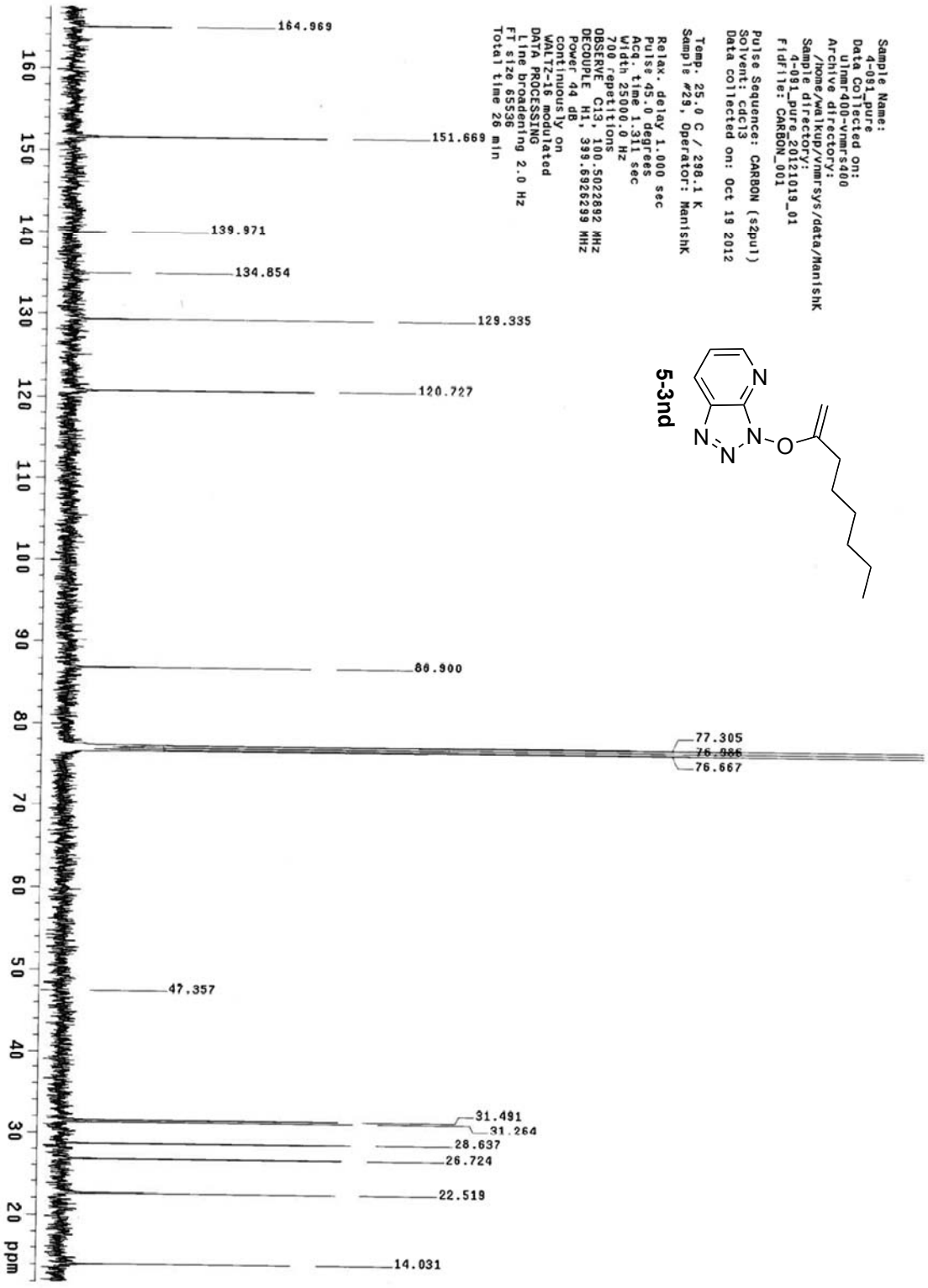
Sample Name:
4-091_pure
Data Collected on:
ulmar400-vmrs400
Archive directory:
/home/walkup/vmrsys/data/ManishK
Sample directory:
4-091_pure_20121019_01
Fidfile: CARBON_001
Pulse Sequence: CARBON (s2pul)
Solvent: cdcl3
Data collected on: Oct 19 2012
Temp. 25.0 C / 298.1 K
Sample #29, Operator: ManishK
Relax. delay 1.000 sec
Pulse 45.0 degrees
Acq. time 1.311 sec
Width 25000.0 Hz
700 repetitions
OBSERVE C13, 100.5022892 MHz
DECOUPLE H1, 399.6926299 MHz
Power 44 dB
continuously on
WALTZ-16 modulated
DATA PROCESSING
Line broadening 2.0 Hz
FT size 65536
Total time 26 min
5-3nd
164.969
151.669
139.971
134.854
129.335
120.727
86.900
77.305
76.986
76.667
47.357
31.491
31.264
28.637
26.724
22.519
14.031
160
150
140
130
120
110
100
90
80
70
60
50
40
30
20
ppm

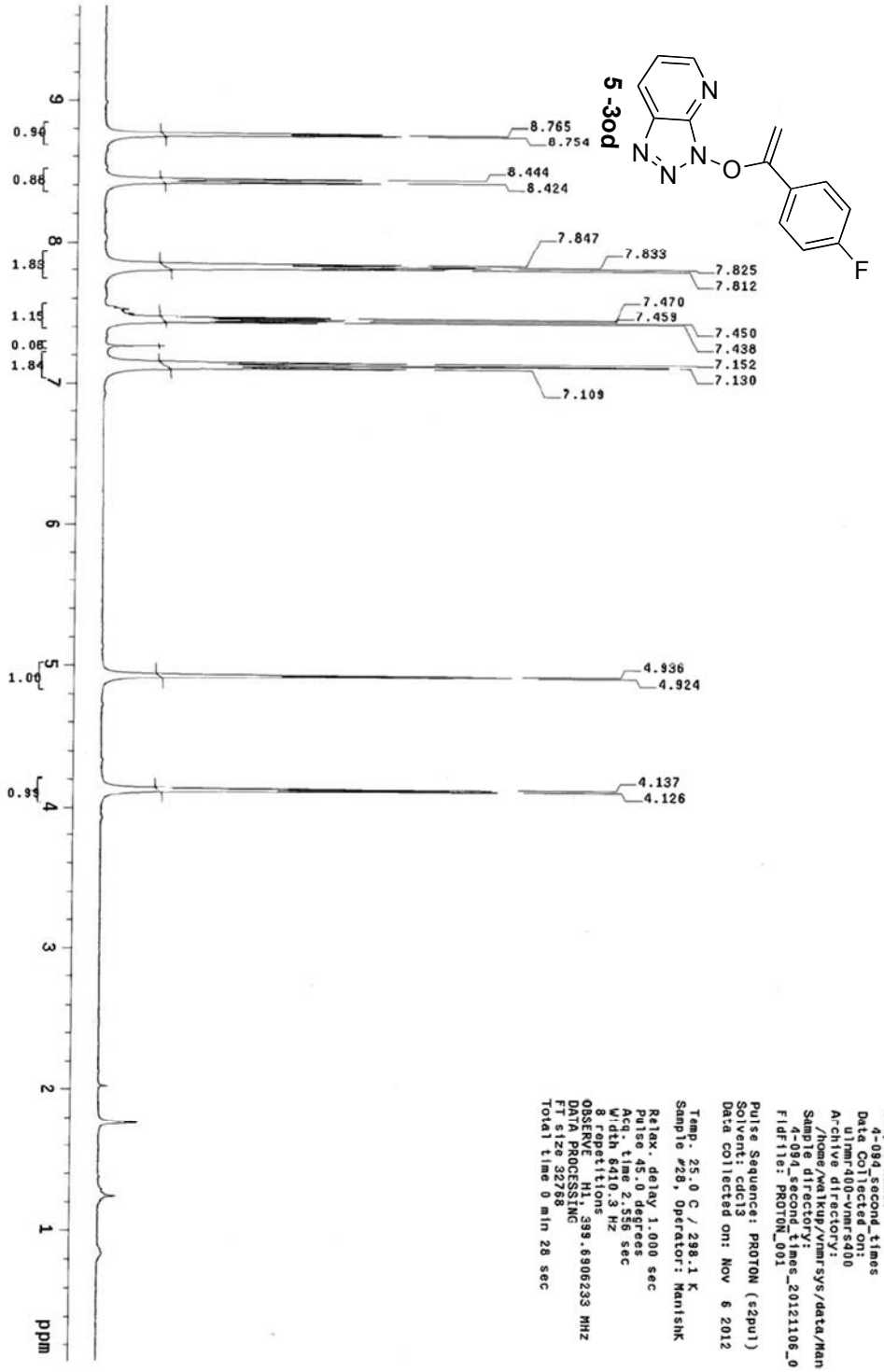
5-3od
F
8.765
8.754
8.444
8.424
7.847
7.833
7.825
7.812
7.470
7.459
7.450
7.438
7.152
7.130
7.109
4.936
4.924
4.137
4.126
0.94
0.88
1.89
1.19
0.06
1.84
1.00
0.93
ppm
Sample Name:
4-094_second_times
Data Collected on:
ulnmr400-vnmrs400
Archive directory:
/home/walkup/vnmrsys/data/Han
Sample directory:
4-094_second_times_20121106_0
FidFile: PROTON_001
Pulse Sequence: PROTON (s2pul)
Solvent: cdcl3
Data collected on: Nov 6 2012
Temp. 25.0 C / 298.1 K
Sample #28, Operator: ManishK
Relax. delay 1.000 sec
Pulse 45.0 degrees
Acq. time 2.556 sec
Width 6410.3 HZ
8 repetitions
OBSERVE H1, 399.6906233 MHz
DATA PROCESSING
FT size 32768
Total time 0 min 28 sec

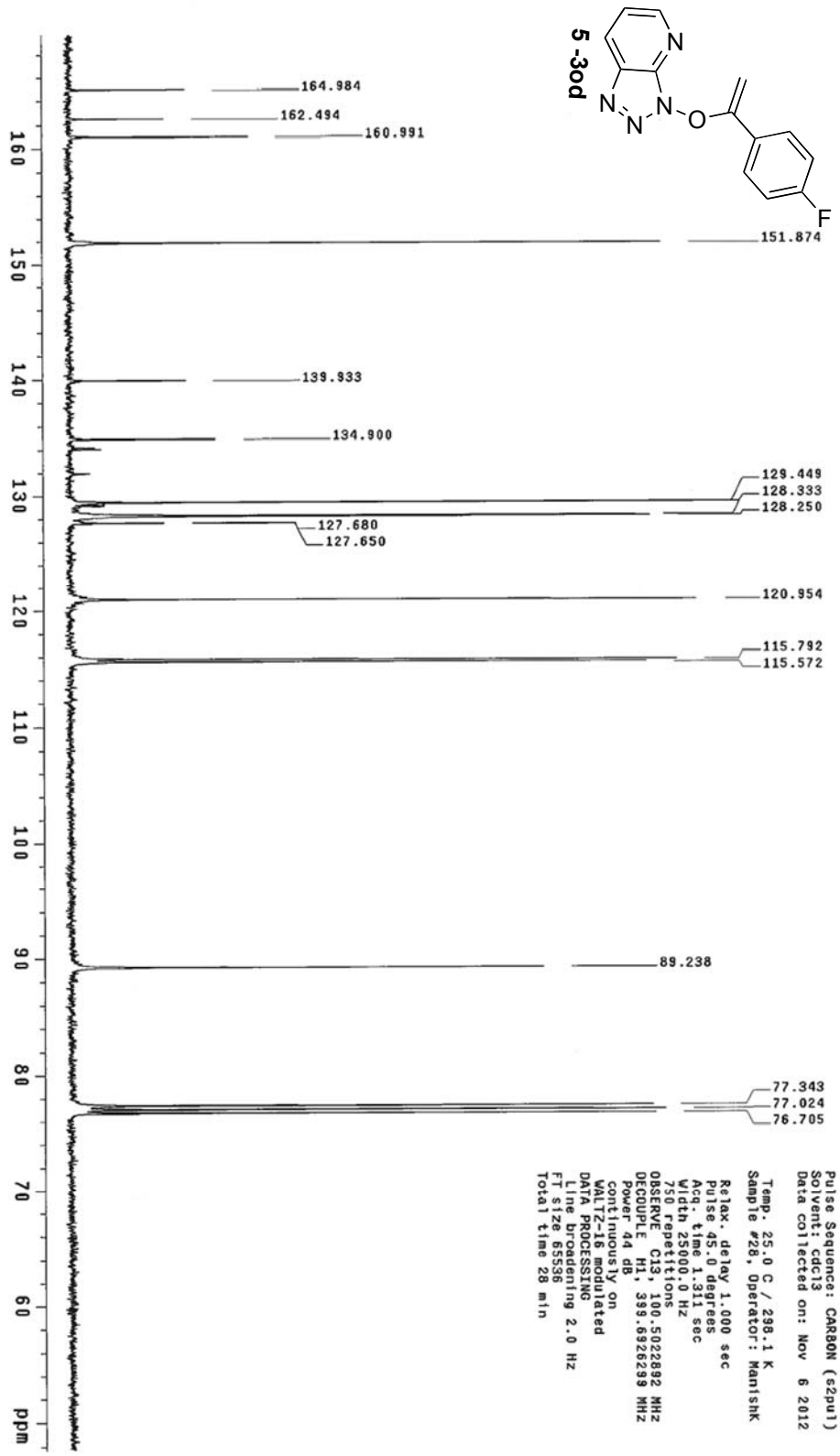
5 -3od
N
N
N
N
O
F
164.984
162.494
160.991
151.874
139.933
134.900
129.449
128.333
128.250
127.680
127.650
120.954
115.792
115.572
89.238
77.343
77.024
76.705
160
150
140
130
120
110
100
90
80
70
60
ppm
Sample Name:
4-094_carbon_second_time
Data Collected on:
Unmr400-vnmrs400
Archive directory:
/home/walkup/vnmrsys/data/Man
Sample directory:
4-094_carbon_second_time_2012
FidFile: CARBON_001
Pulse Sequence: CARBON (s2pul)
Solvent: cdcl3
Data collected on: Nov 6 2012
Temp. 25.0 C / 298.1 K
Sample #28, Operator: ManishK
Relax. delay 1.000 sec
Pulse 45.0 degrees
Acq. time 1.311 sec
Width 25000.0 Hz
750 repetitions
OBSERVE C13, 100.5022892 MHz
DECOUPLE H1, 399.6926299 MHz
Power 44 dB
continuously on
WALTZ-16 modulated
DATA PROCESSING
Line broadening 2.0 Hz
FT size 65536
Total time 28 min

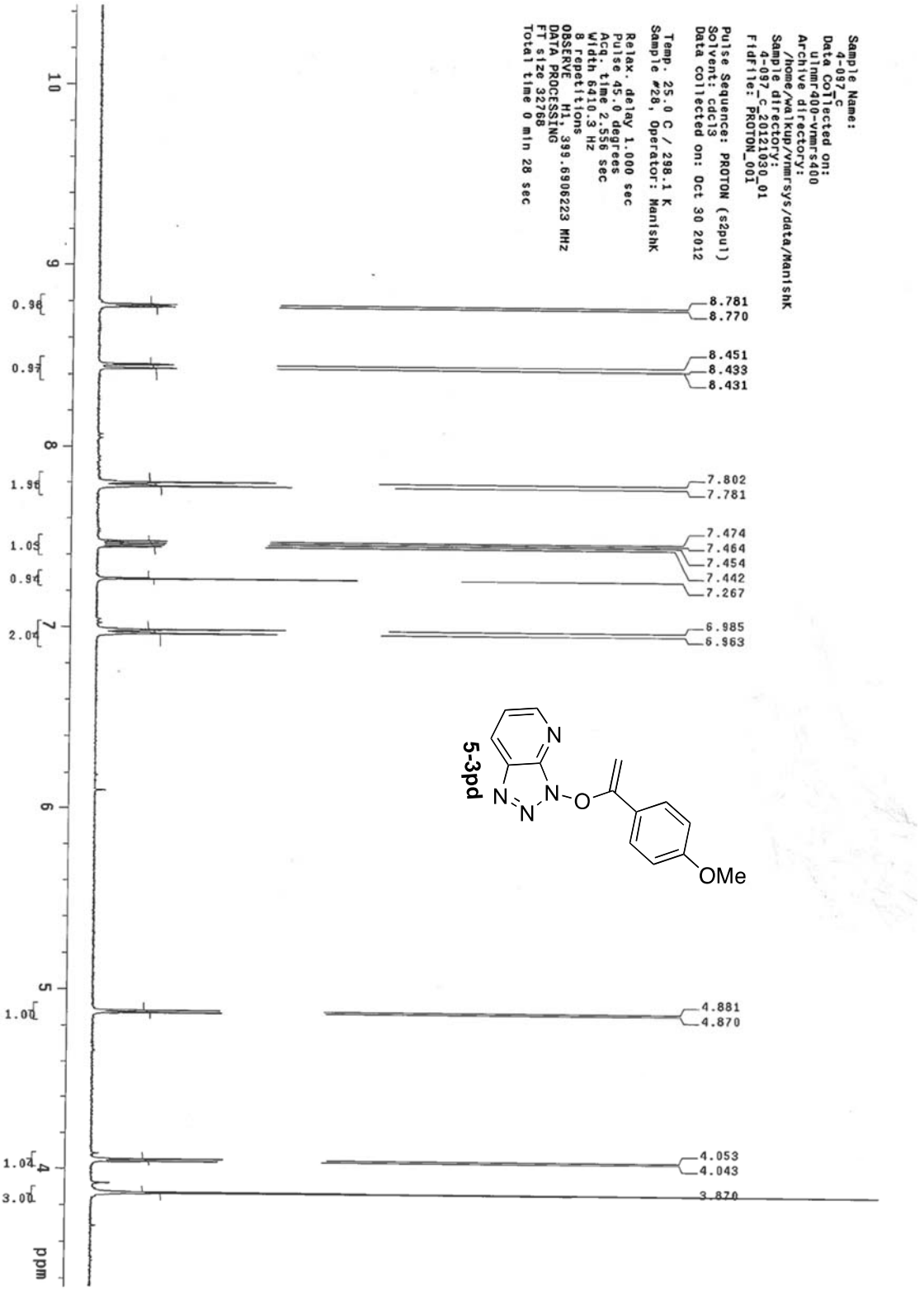
Sample Name:
4-097_c
Data Collected on:
ulnmr400-vnmrs400
Archive directory:
/home/walkup/vnmrsys/data/ManishK
Sample directory:
4-097_c_20121030_01
FidFile: PROTON_001
Pulse Sequence: PROTON (s2pul)
Solvent: cdcl3
Data collected on: Oct 30 2012
Temp. 25.0 C / 298.1 K
Sample #28, Operator: ManishK
Relax. delay 1.000 sec
Pulse 45.0 degrees
Acq. time 2.556 sec
Width 6410.3 Hz
8 repetitions
OBSERVE H1, 399.6906223 MHz
DATA PROCESSING
FT size 32768
Total time 0 min 28 sec
8.781
8.770
8.451
8.433
8.431
7.802
7.781
7.474
7.464
7.454
7.442
7.267
6.985
6.963
4.881
4.870
4.053
4.043
3.870
0.96
0.97
1.96
1.05
0.94
2.00
1.00
1.01
3.00
10
9
8
7
6
5
4
ppm
5-3pd
N
N
N
N
O
OMe

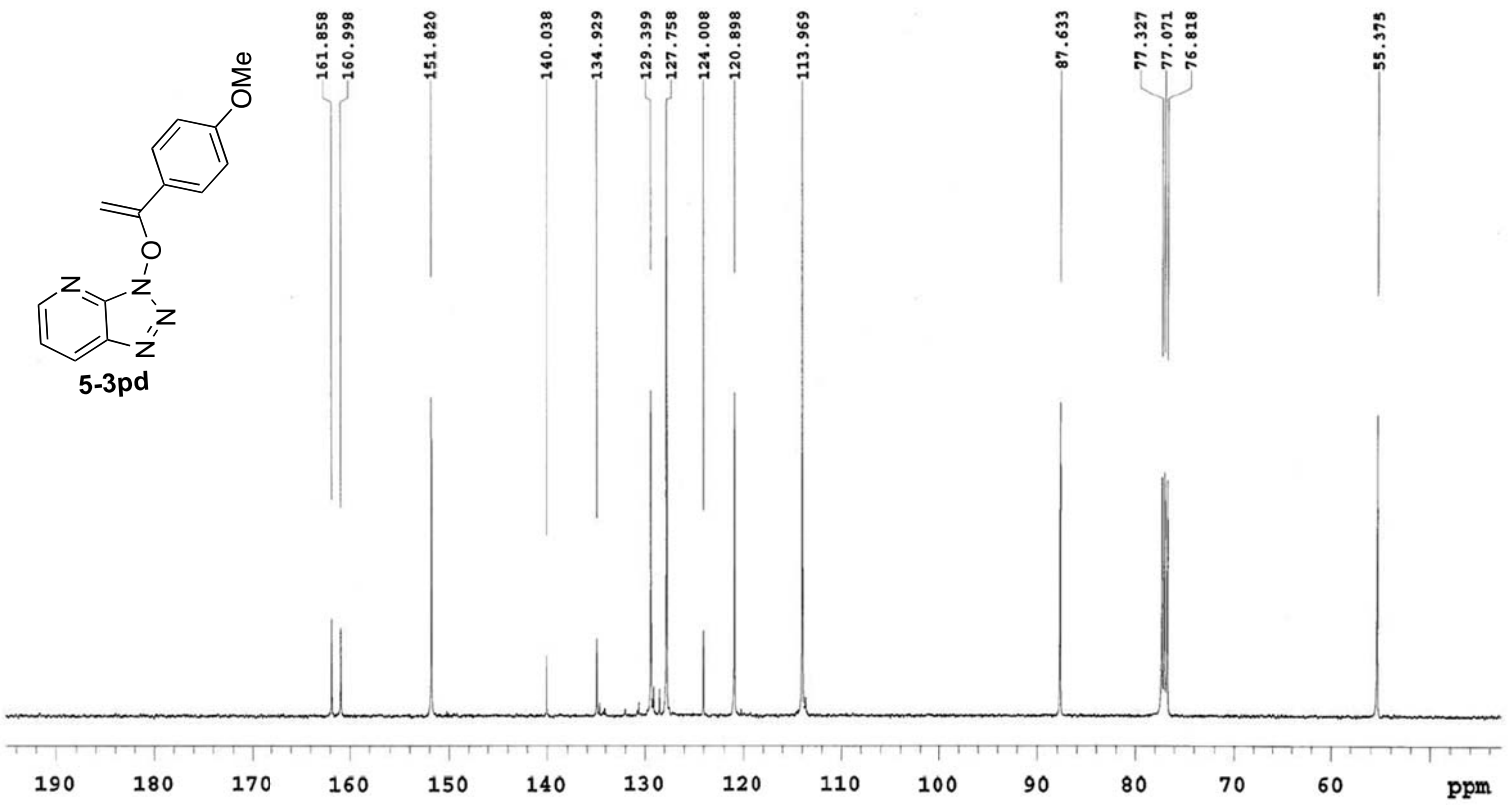

PULSE SEQUENCE Relax. delay 1.000 sec Pulse 45.0 degrees Acq. time 1.300 sec Width 30154.5 Hz 1000 repetitions	OBSERVE C13, 125.6346841 DECOUPLE H1, 499.6429206 Power 48 dB continuously on WALTZ-16 modulated	DATA PROCESSING Line broadening 3.0 Hz FT size 131072 Total time 38 minutes	Solvent: cdcl3 Temp. 25.0 C / 298.1 K Operator: ManishK File: Carbon_01 INOVA-500 "ulnmr500"	SAMPLE: 4-097 c Sample: 4-097 c Sample ID: ManishK_4-097_c_20121031_01 File: ManishK_4-097_c_20121031_01/data/
File: ManishK_4-097_c_20121031_01/data/Carbon_01.fid				Pulse Sequence: s2pul

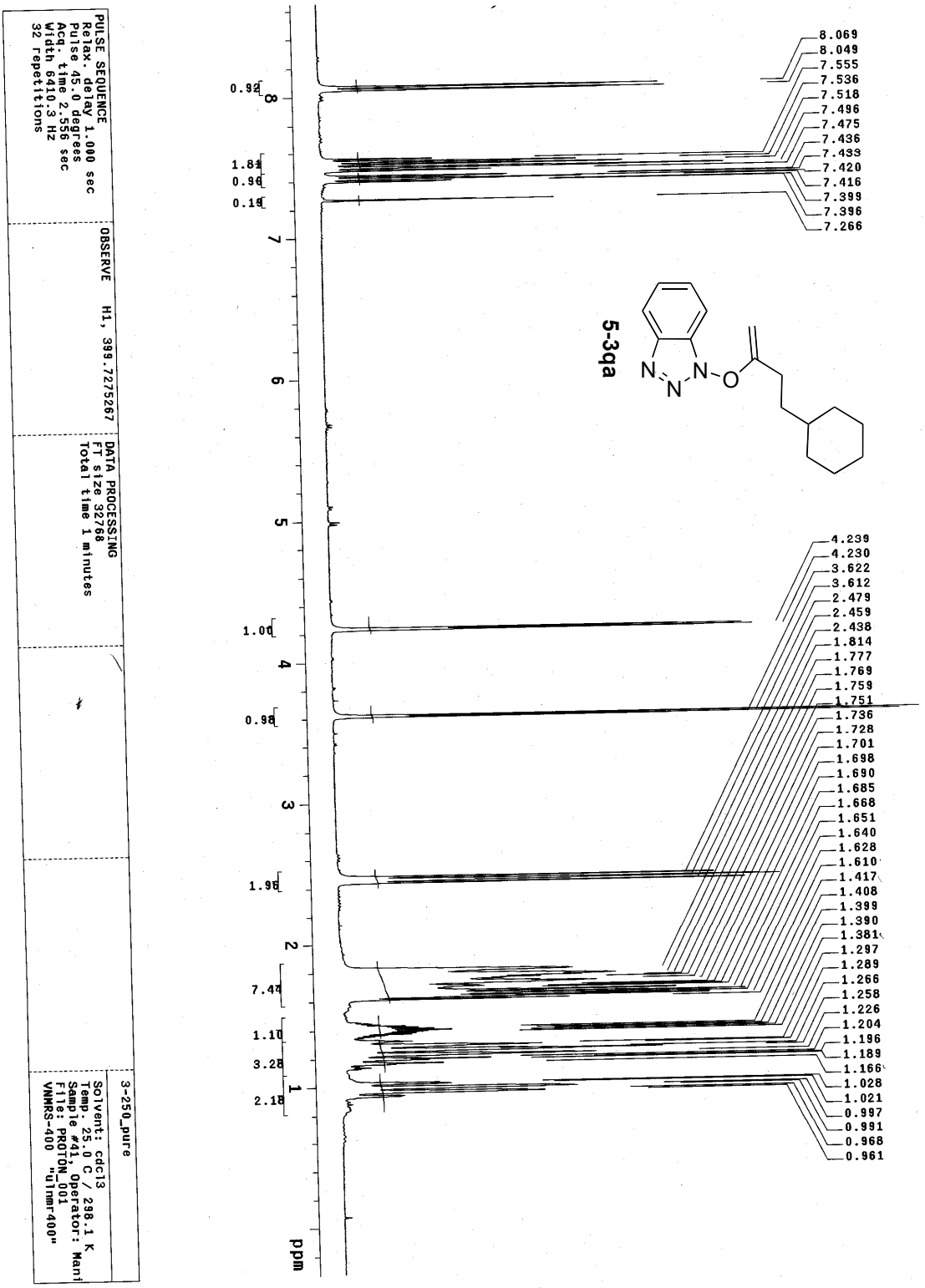
PULSE SEQUENCE
Relax. delay 1.000 sec
Pulse 45.0 degrees
Acq. time 2.556 sec
Width 6410.3 Hz
32 repetitions
OBSERVE H1, 399.7275267
DATA PROCESSING
FT size 32768
Total time 1 minutes
3-250_pure
Solvent: cdcl3
Temp. 25.0 C / 298.1 K
Sample #41, Operator: Mani
File: PROTON_001
VNMRS-400 "ulnmr400"
5-3qa
8.069
8.049
7.555
7.536
7.518
7.496
7.475
7.436
7.433
7.420
7.416
7.399
7.396
7.266
4.239
4.230
3.622
3.612
2.479
2.459
2.438
1.814
1.777
1.769
1.759
1.751
1.736
1.728
1.701
1.698
1.690
1.685
1.668
1.651
1.640
1.628
1.610
1.417
1.408
1.399
1.390
1.381
1.297
1.289
1.266
1.258
1.226
1.204
1.196
1.189
1.166
1.028
1.021
0.997
0.991
0.968
0.961
0.92
1.81
0.90
0.19
1.00
0.98
1.96
7.47
1.10
3.28
2.18
ppm

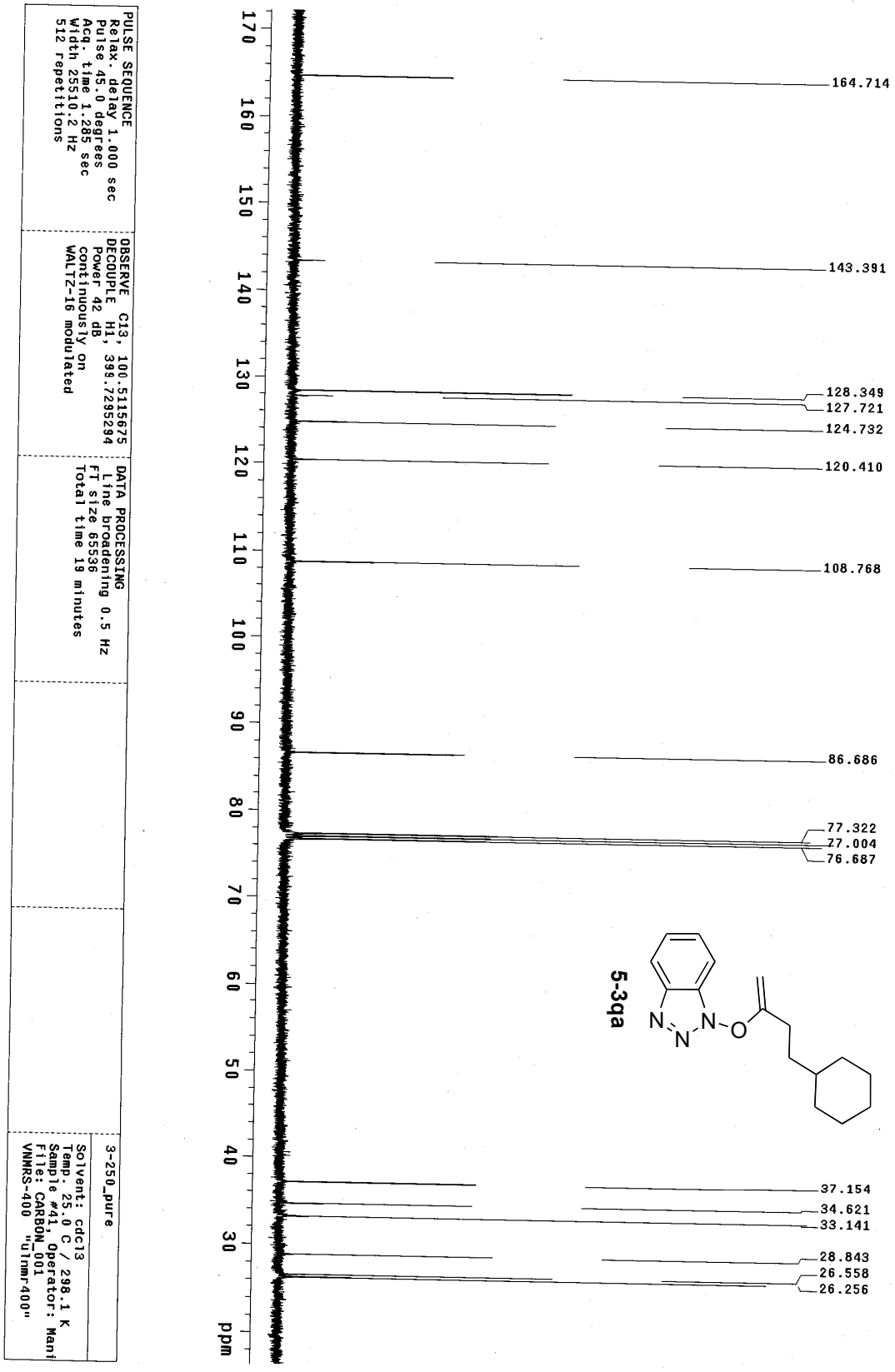
PULSE SEQUENCE
Relax. delay 1.000 sec
Pulse 45.0 degrees
Acq. time 1.285 sec
Width 25510.2 Hz
512 repetitions
OBSERVE C13, 100.5115675
DECOUPLE H1, 399.7295294
Power 42 dB
continuously on
WALTZ-16 modulated
DATA PROCESSING
Line broadening 0.5 Hz
FT size 65536
Total time 19 minutes
3-250_pure
Solvent: cdcl3
Temp. 25.0 C / 298.1 K
Sample #41, Operator: Mani
File: CARBON_001
VNMRS-400 "ulnmr400"
164.714
143.391
128.349
127.721
124.732
120.410
108.768
86.686
77.322
77.004
76.687
37.154
34.621
33.141
28.843
26.558
26.256
5-3qa
ppm

^{1}H and ^{13}C NMR spectra of compounds 5-4

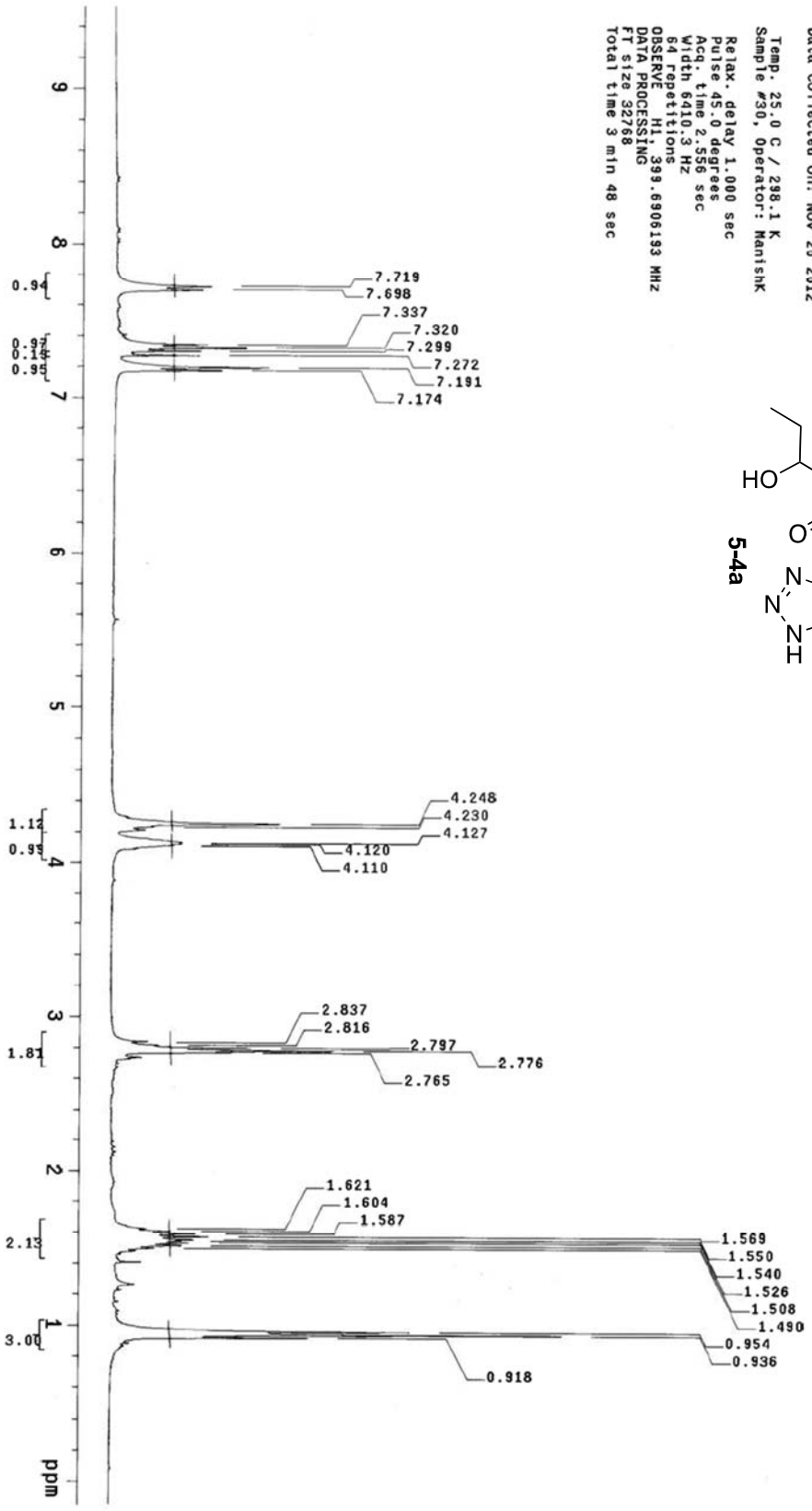
Sample Name:
4-106a_pure1
Data Collected on:
u1nmr400-vnmrs400
Archive directory:
/home/walkup/vnmrsys/data/ManishK
Sample directory:
4-106a_pure1_20121119_01
FidFile: PROTON_001
Pulse Sequence: PROTON (s2pul)
Solvent: cdcl3
Data collected on: Nov 20 2012
Temp. 25.0 C / 298.1 K
Sample #30, Operator: ManishK
Relax. delay 1.000 sec
Pulse 45.0 degrees
Acq. time 2.556 sec
Width 6410.3 Hz
64 repetitions
OBSERVE H1, 399.6906193 MHz
DATA PROCESSING
FT size 32768
Total time 3 min 48 sec
HO
O
N
N
NH
5-4a
7.719
7.698
7.337
7.320
7.299
7.272
7.191
7.174
4.248
4.230
4.127
4.120
4.110
2.837
2.816
2.797
2.776
2.765
1.621
1.604
1.587
1.569
1.550
1.540
1.526
1.508
1.490
0.954
0.936
0.918
ppm

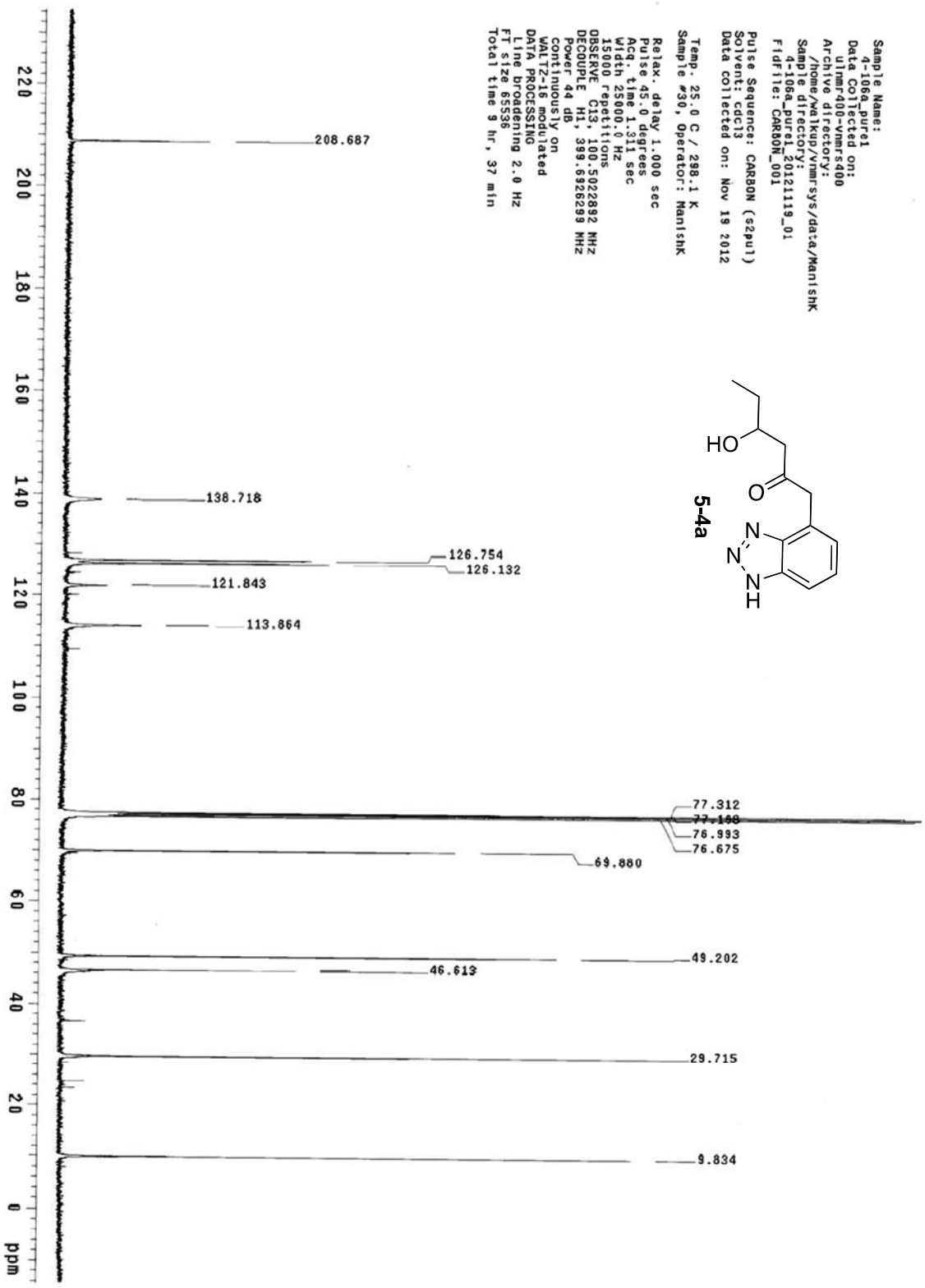
Sample Name:
4-106a_pure1
Data Collected on:
ulnmr400-vnmrs400
Archive directory:
/home/walkup/vnmrsys/data/ManishK
Sample directory:
4-106a_pure1_20121119_01
Fidfile: CARBON_001
Pulse Sequence: CARBON (s2pul)
Solvent: cdcl3
Data collected on: Nov 19 2012
Temp. 25.0 C / 298.1 K
Sample #30, Operator: ManishK
Relax. delay 1.000 sec
Pulse 45.0 degrees
Acq. time 1.311 sec
Width 25000.0 Hz
15000 repetitions
OBSERVE C13, 100.5022892 MHz
DECOUPLE H1, 399.6926299 MHz
Power 44 dB
continuously on
WALTZ-16 modulated
DATA PROCESSING
Line broadening 2.0 Hz
FT size 65536
Total time 9 hr, 37 min
208.687
138.718
126.754
126.132
121.843
113.864
77.312
77.188
76.993
76.675
69.880
49.202
46.613
29.715
9.834
220
200
180
160
140
120
100
80
60
40
20
0
ppm
HO
O
N
N
NH
5-4a

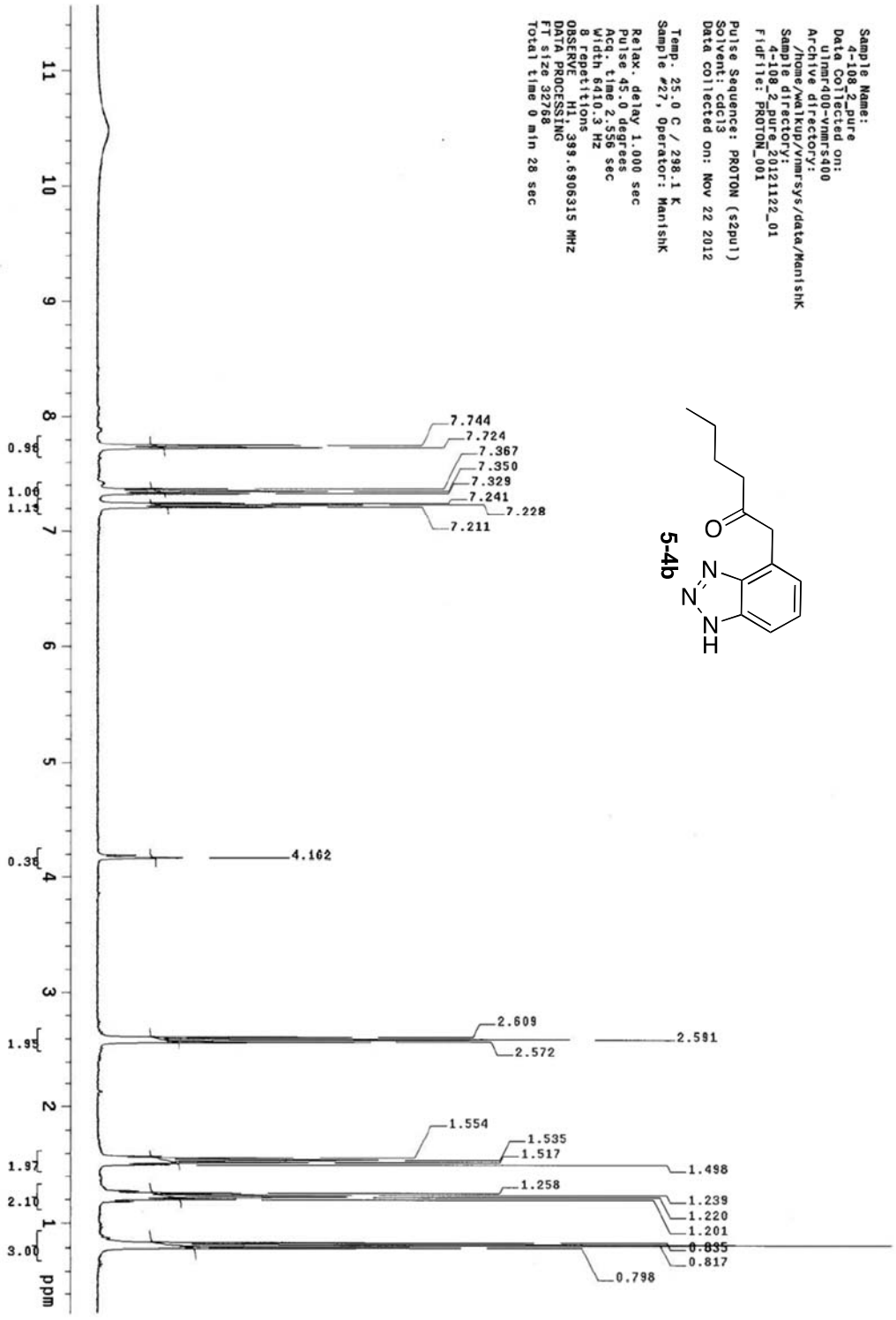
Sample Name:
4-108_2_pure
Data Collected on:
ulnmr400-vnmrs400
Archive directory:
/home/walkup/vnmrsys/data/ManishK
Sample directory:
4-108_2_pure_20121122_01
FidFile: PROTON_001
Pulse Sequence: PROTON (s2pul)
Solvent: cdcl3
Data collected on: Nov 22 2012
Temp. 25.0 C / 298.1 K
Sample #27, Operator: ManishK
Relax. delay 1.000 sec
Pulse 45.0 degrees
Acq. time 2.556 sec
Width 6410.3 Hz
8 repetitions
OBSERVE H1, 399.6906315 MHz
DATA PROCESSING
FT size 32768
Total time 0 min 28 sec
7.744
7.724
7.367
7.350
7.329
7.241
7.228
7.211
4.162
2.609
2.591
2.572
1.554
1.535
1.517
1.498
1.258
1.239
1.220
1.201
0.835
0.817
0.798
0.96
1.00
1.15
0.38
1.92
1.97
2.10
3.00
ppm
5-4b

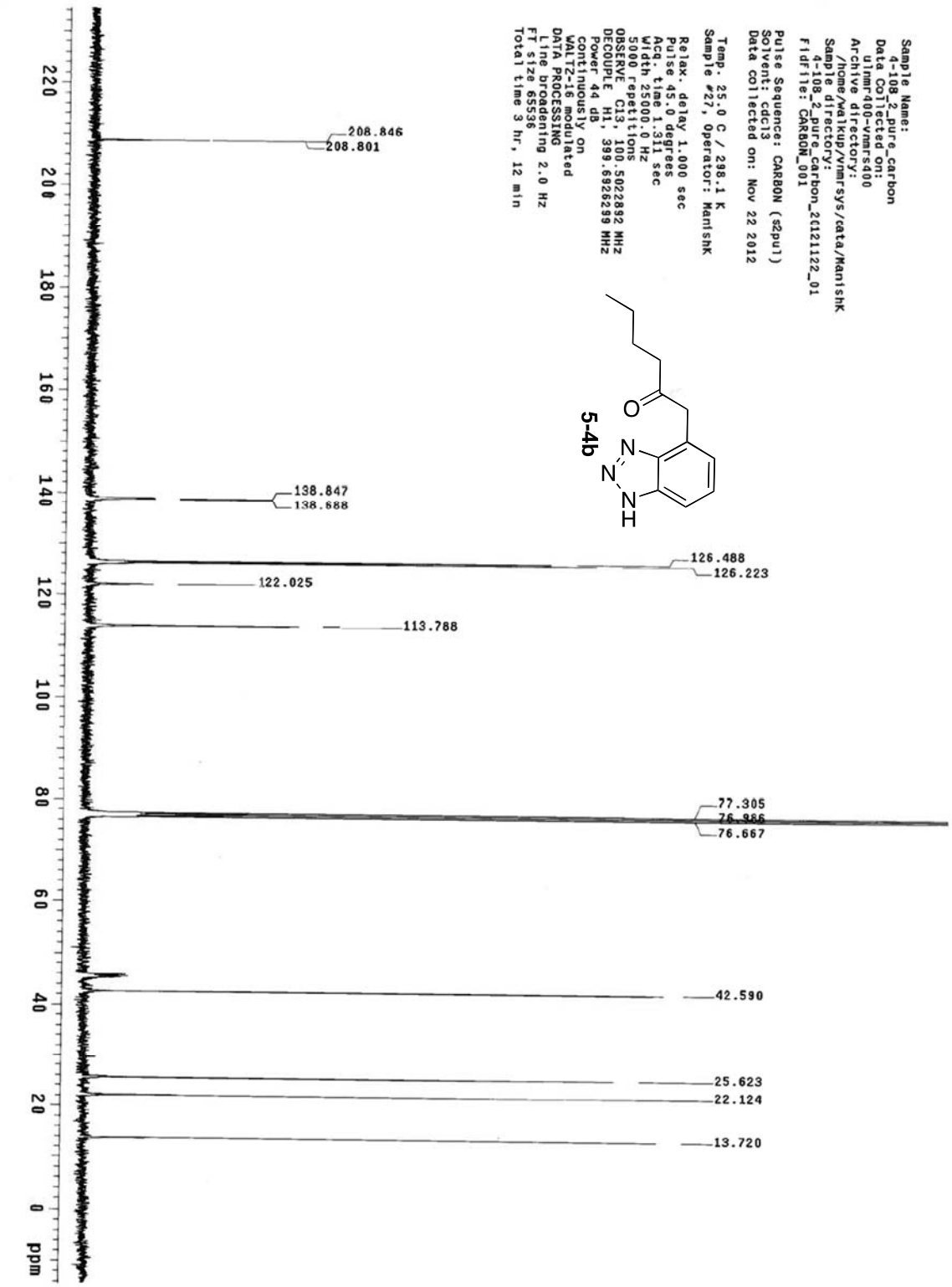
Sample Name:
4-108_2_pure_carbon
Data Collected on:
ulnmr400-vnmrs400
Archive directory:
/home/walkup/vnmrsys/data/ManishK
Sample directory:
4-108_2_pure_carbon_26121122_01
Fidfile: CARBON_001
Pulse Sequence: CARBON (s2pul)
Solvent: cdcl3
Data collected on: Nov 22 2012
Temp. 25.0 C / 298.1 K
Sample #27, Operator: ManishK
Relax. delay 1.000 sec
Pulse 45.0 degrees
Acq. time 1.311 sec
Width 25000.0 Hz
5000 repetitions
OBSERVE C13, 100.5022892 MHz
DECOUPLE H1, 399.6926299 MHz
Power 44 dB
continuously on
WALTZ-16 modulated
DATA PROCESSING
Line broadening 2.0 Hz
FT size 65536
Total time 3 hr, 12 min
5-4b
208.846
208.801
138.847
138.688
126.488
126.223
122.025
113.788
77.305
76.986
76.667
42.590
25.623
22.124
13.720
220
200
180
160
140
120
100
80
60
40
20
0
ppm

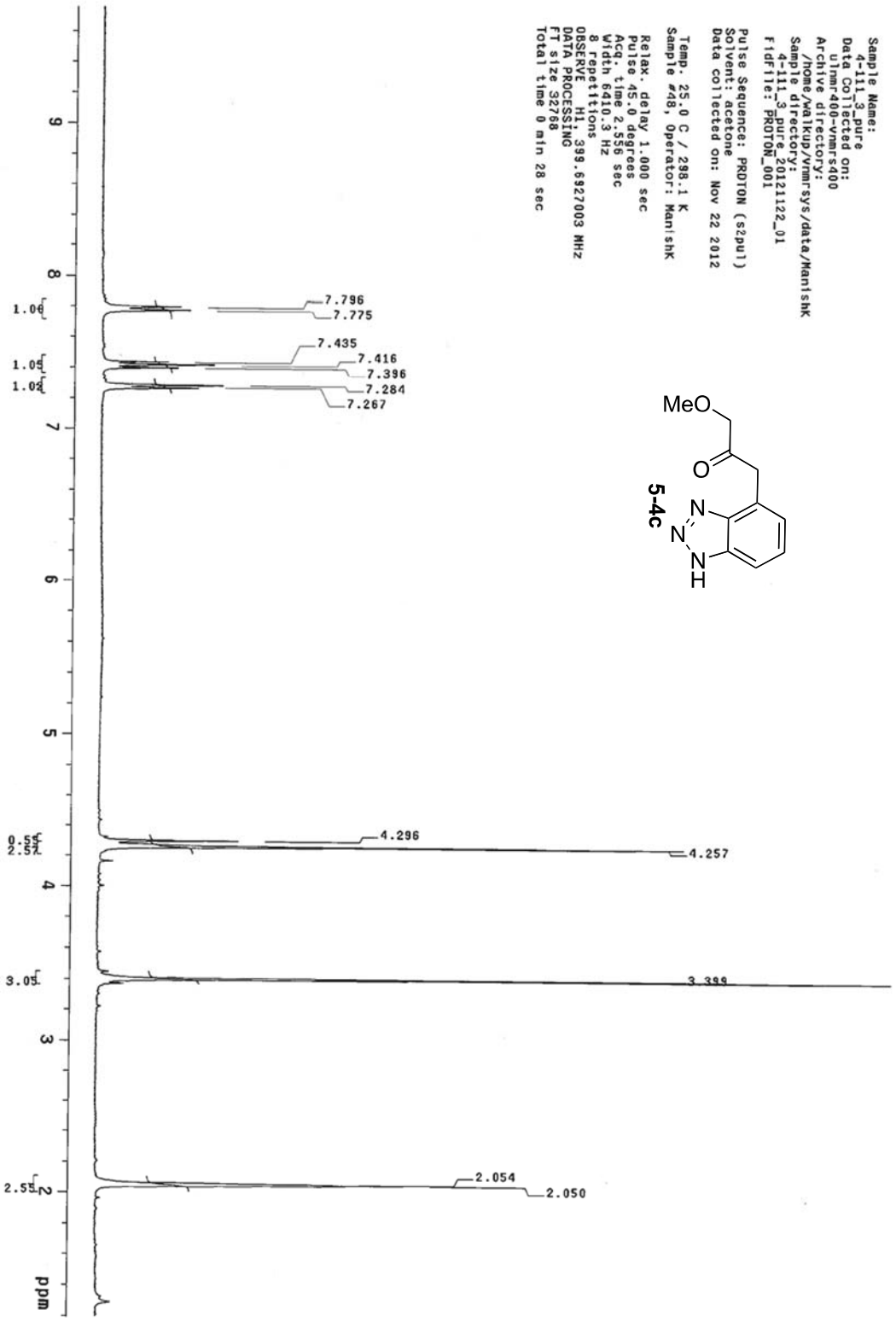
Sample Name:
4-111_3_pure
Data Collected on:
u1nmr400-vnmrs400
Archive directory:
/home/walkup/vnmrsys/data/ManishK
Sample directory:
4-111_3_pure_20121122_01
FidFile: PROTON_001
Pulse Sequence: PROTON (s2pul)
Solvent: acetone
Data collected on: Nov 22 2012
Temp. 25.0 C / 298.1 K
Sample #48, Operator: ManishK
Relax. delay 1.000 sec
Pulse 45.0 degrees
Acq. time 2.556 sec
Width 6410.3 Hz
8 repetitions
OBSERVE H1, 399.6927003 MHz
DATA PROCESSING
FT size 32768
Total time 0 min 28 sec
7.796
7.775
7.435
7.416
7.396
7.284
7.267
4.296
4.257
3.399
2.054
2.050
1.06
1.05
1.02
0.52
2.52
3.05
2.51
MeO
O
N
N
N
H
5-4c
ppm

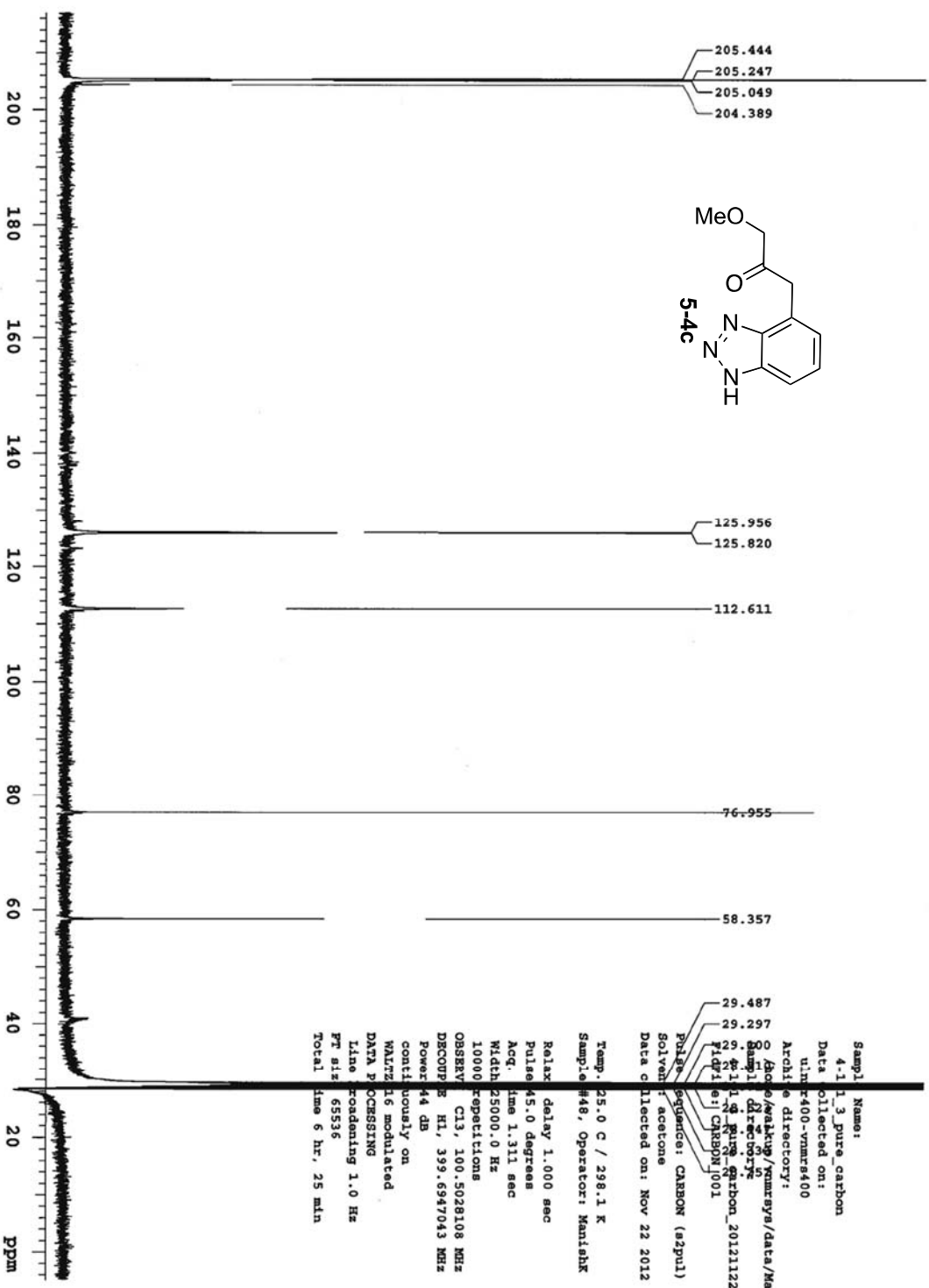
205.444
205.247
205.049
204.389
125.956
125.820
112.611
76.955
58.357
29.487
29.297
MeO
O
N
N
NH
5-4c
200
180
160
140
120
100
80
60
40
20
ppm

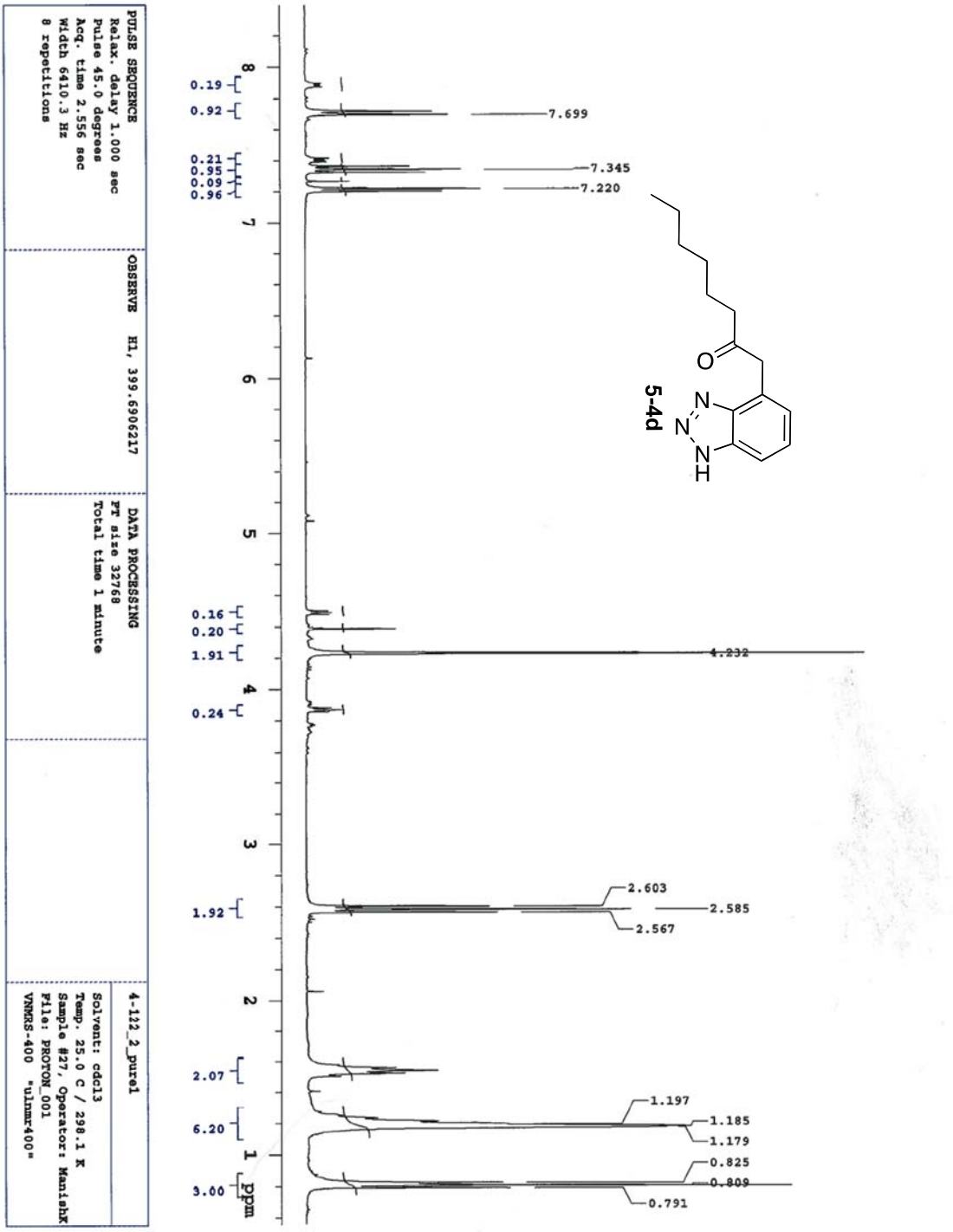
PULSE SEQUENCE
Relax. delay 1.000 sec
Pulse 45.0 degrees
Acq. time 2.556 sec
Width 6410.3 Hz
8 repetitions
OBSERVE H1, 399.6906217
DATA PROCESSING
FT size 32768
Total time 1 minute
4-122_2_pure1
Solvent: cdcl3
Temp. 25.0 C / 298.1 K
Sample #27, Operator: ManishK
File: PROTON_001
VNMRS-400 "ulnmr400"
5-4d
7.699
7.345
7.220
4.232
2.603
2.585
2.567
1.197
1.185
1.179
0.825
0.809
0.791
0.19
0.92
0.21
0.95
0.09
0.96
0.16
0.20
1.91
0.24
1.92
2.07
6.20
3.00
ppm

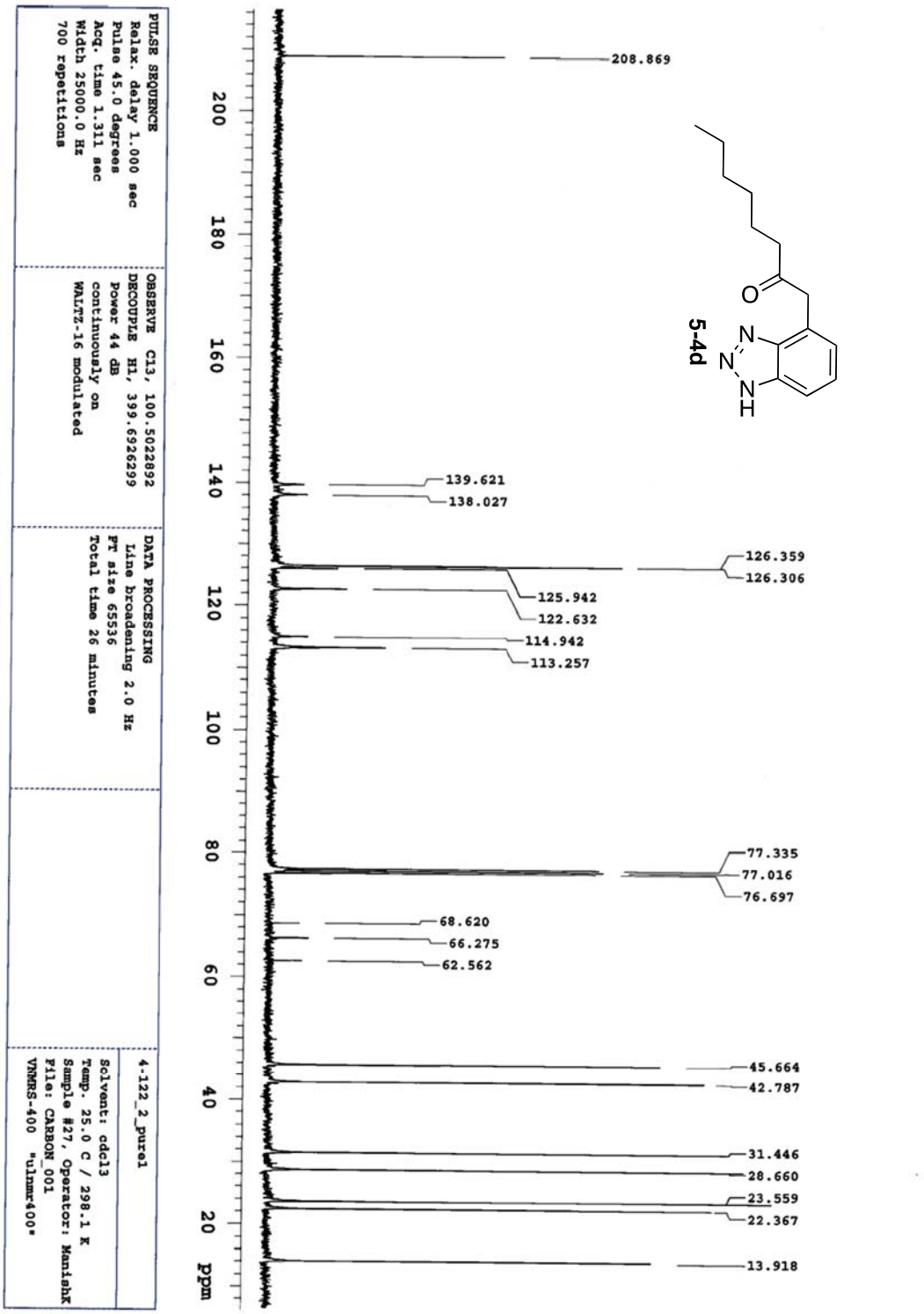
PULSE SEQUENCE
Relax. delay 1.000 sec
Pulse 45.0 degrees
Acq. time 1.311 sec
Width 25000.0 Hz
700 repetitions
OBSERVE C13, 100.5022892
DECOUPLE H1, 399.6926299
Power 44 dB
continuously on
WALTZ-16 modulated
DATA PROCESSING
Line broadening 2.0 Hz
FT size 65536
Total time 26 minutes
4-122_2_pure1
Solvent: cdcl3
Temp. 25.0 C / 298.1 K
Sample #27, Operator: Manish
File: CARBON_001
VNMRS-400 "ulnmr400"
208.869
139.621
138.027
126.359
126.306
125.942
122.632
114.942
113.257
77.335
77.016
76.697
68.620
66.275
62.562
45.664
42.787
31.446
28.660
23.559
22.367
13.918
200
180
160
140
120
100
80
60
40
20
ppm
O
N
N
NH
5-4d

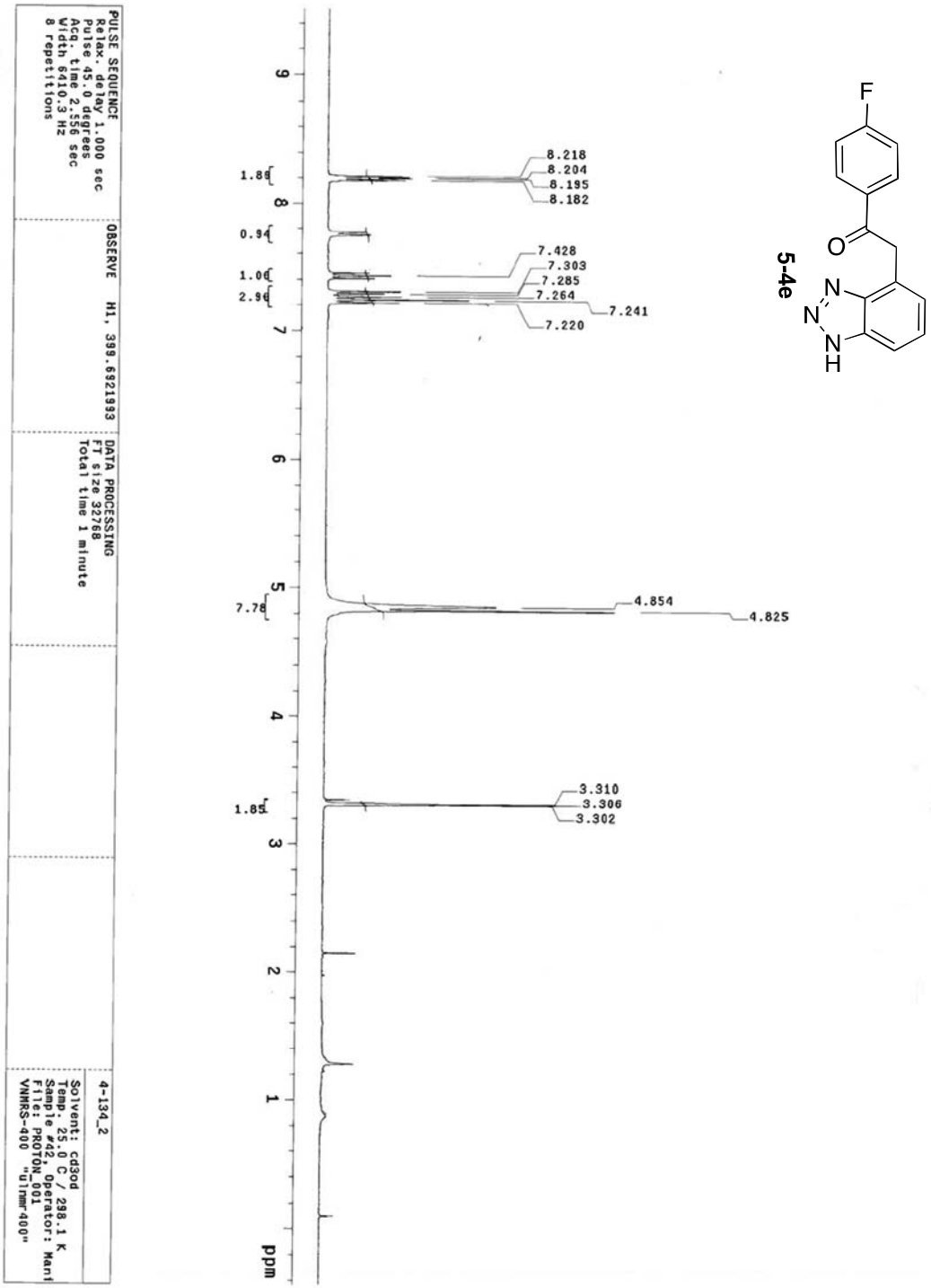
PULSE SEQUENCE
Relax. delay 1.000 sec
Pulse 45.0 degrees
Acq. time 2.556 sec
Width 6410.3 Hz
8 repetitions
OBSERVE H1, 399.6921993
DATA PROCESSING
FT size 32768
Total time 1 minute
4-134_2
Solvent: cd3od
Temp. 25.0 C / 298.1 K
Sample 242, Operator: Mani
File: PROTON_001
VNMRS-400 "Ulmmr400"
8.218
8.204
8.195
8.182
7.428
7.303
7.285
7.264
7.241
7.220
4.854
4.825
3.310
3.306
3.302
1.88
0.94
1.00
2.96
7.78
1.85
ppm
F
O
N
N
N
H
5-4e

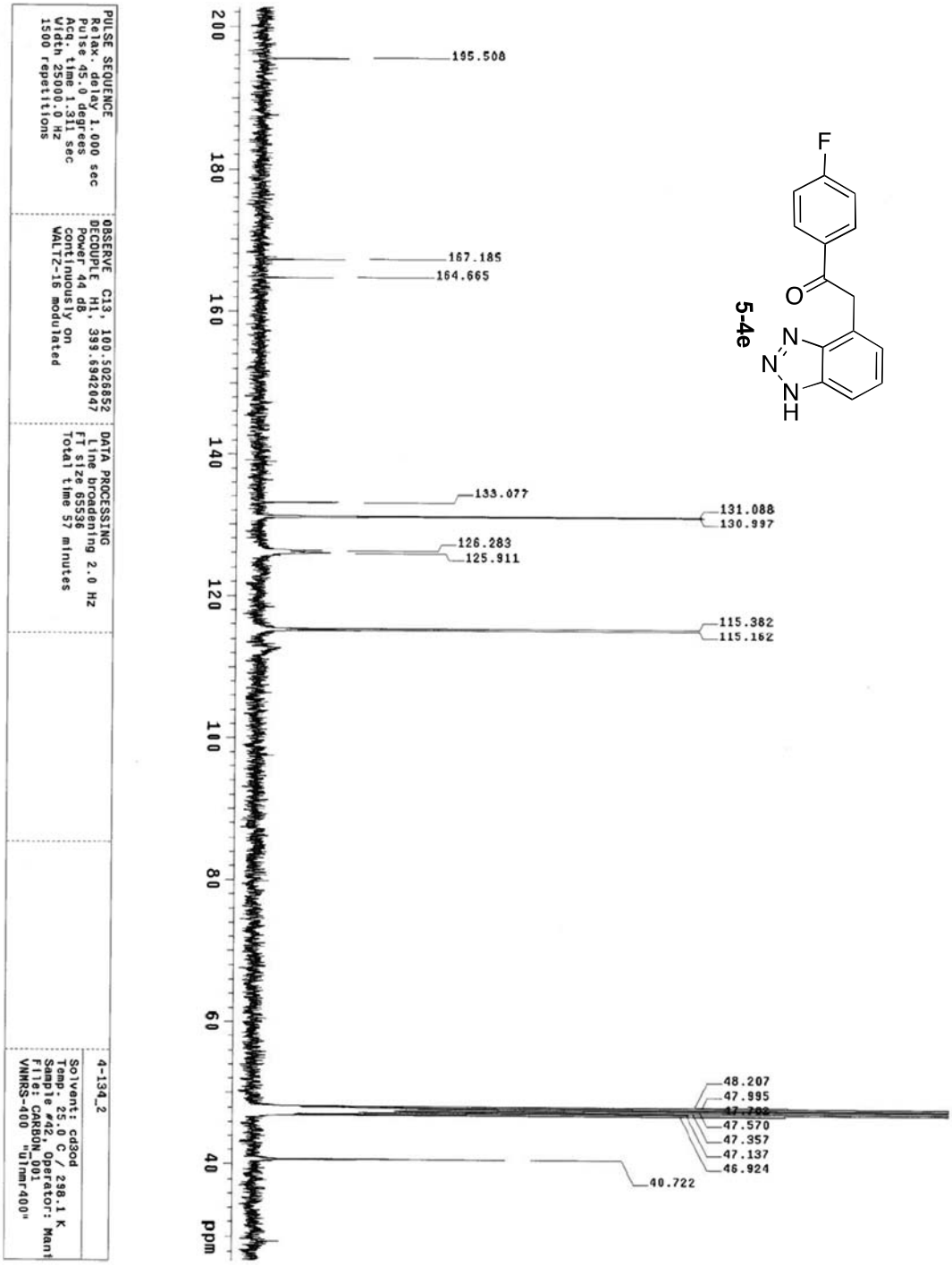
PULSE SEQUENCE
Relax. delay 1.000 sec
Pulse 45.0 degrees
Acq. time 1.311 sec
Width 25000.0 Hz
1500 repetitions
OBSERVE C13, 100.5026852
DECOUPLE H1, 399.6942047
Power 44 dB,
continuously on
WALTZ-16 modulated
DATA PROCESSING
Line broadening 2.0 Hz
FT size 65536
Total time 57 minutes
4-134_2
Solvent: cd3od
Temp. 25.0 C / 298.1 K
Sample #42, Operator: Mant
File: CARBON_001
VNMRS-400 "ujmr400"
5-4e
F
O
N
N
NH
195.508
167.185
164.665
133.077
131.088
130.997
126.283
125.911
115.382
115.162
48.207
47.995
47.782
47.570
47.357
47.137
46.924
40.722
200
180
160
140
120
100
80
60
40
ppm

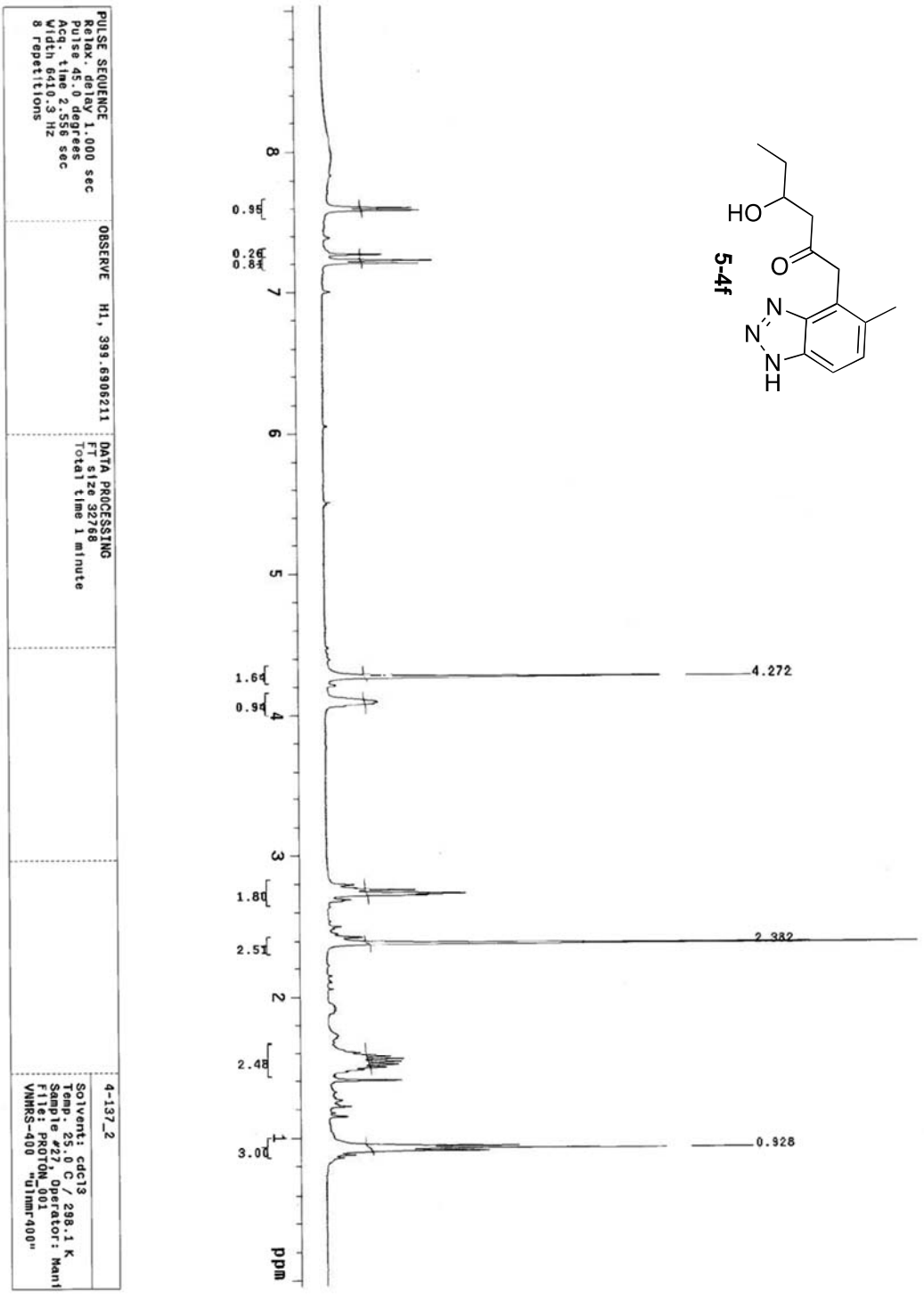
PULSE SEQUENCE
Relax. delay 1.000 sec
Pulse 45.0 degrees
Acq. time 2.556 sec
Width 6410.3 Hz
8 repetitions
OBSERVE H1, 399.6906211
DATA PROCESSING
FT size 32768
Total time 1 minute
4-137_2
Solvent: cdcl3
Temp. 25.0 C / 298.1 K
Sample #27, Operator: Mani
File: PROTON_001
VNMRS-400 "ulmnr400"
HO
O
N
N
H
5-4f
0.95
0.26
0.84
1.64
0.94
1.80
2.51
2.48
3.00
4.272
2.382
0.928
8
7
6
5
4
3
2
1
ppm

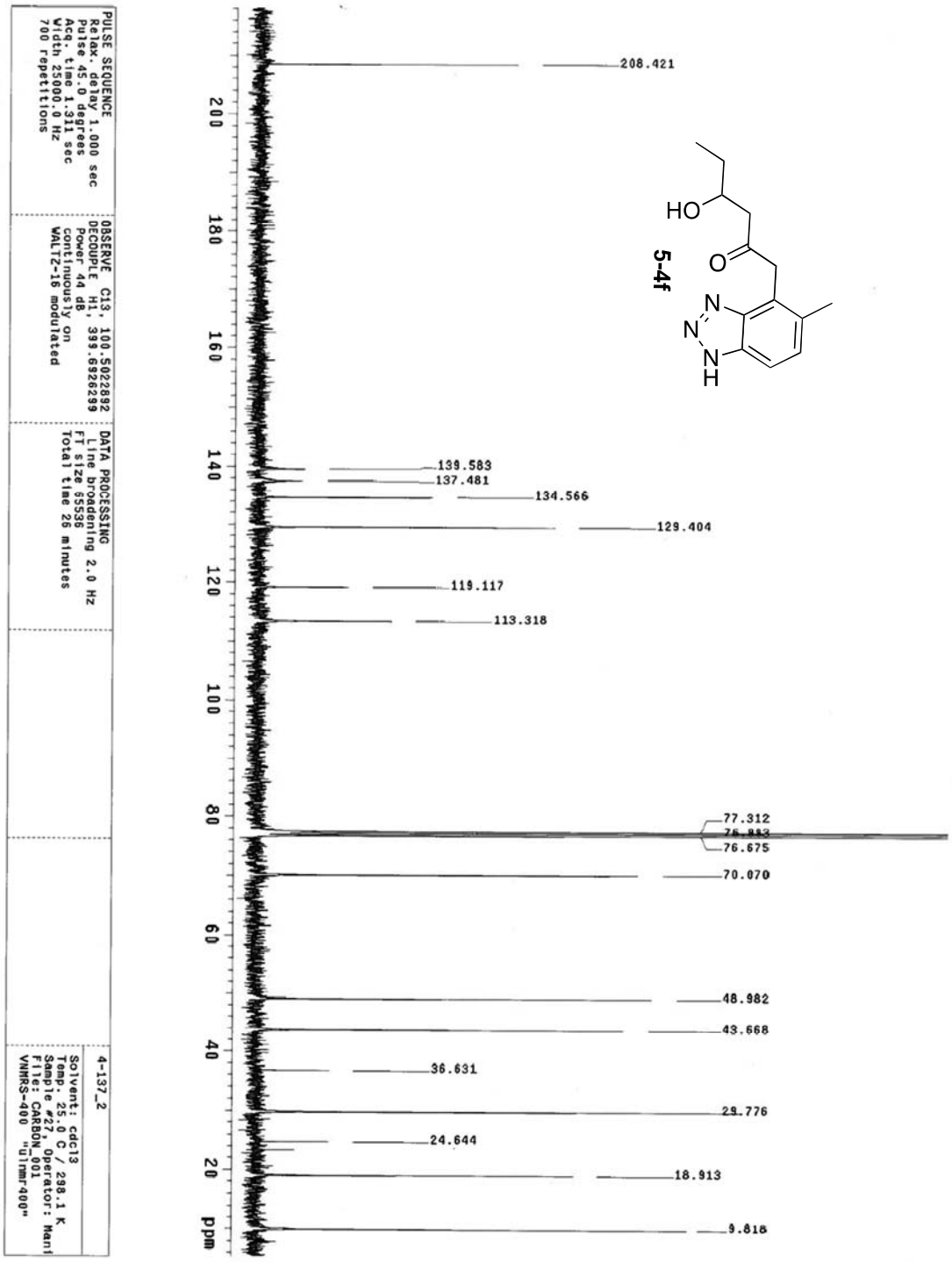
PULSE SEQUENCE
Relax. delay 1.000 sec
Pulse 45.0 degrees
Acq. time 1.311 sec
Width 25000.0 Hz
700 repetitions
OBSERVE C13, 100.5022882
DECOUPLE H1, 399.6926299
Power 44 dB
continuously on
WALTZ-16 modulated
DATA PROCESSING
FT size 65536
Total time 26 minutes
4-137_2
Solvent: cdcl3
Temp. 25.0 C / 298.1 K
Sample #27, Operator: Manf
File: CARBON_001
VNMRS-400 "ulnmr400"
208.421
139.583
137.481
134.566
129.404
119.117
113.318
77.312
76.675
70.070
48.982
43.668
36.631
29.776
24.644
18.913
9.818
HO
O
N
N
NH
5-4f
200
180
160
140
120
100
80
60
40
20
ppm

Crystallographic studies

Crystals of **5-3od** for X-ray diffraction studies were grown by evaporation from a 50:50 methanol/hexane solution. $C_{13}H_9FN_4O$: colorless plate, 0.33 x 0.24 x 0.07 mm^3, monoclinic, space group $P2_1/c$, a = 21.920(3) Å, b = 7.6412(7) Å, c = 7.0921(6) Å, $a = g = 90°$, b = 94.339(11)° V = 1184.5(2) $Å^3$, D_{calc} = 1.437 Mg/m^3, Z = 4. Data were collected on an Agilent Technologies/Oxford Diffraction Gemini CCD diffractometer at 100 K using MoKα radiation (0.71073 Å). For 3177 unique reflections I>2s(I) [R(int) 0.043] the final anisotropic full matrix least-squares refinement on F^2 for 208 variables converged at R1 = 0.060 and wR2 = 0.101 with a GOF of 1.06. Crystals of **5-4e,** $C_{14}H_{10}FN_3O$: colorless plate, 0.34 x 0.25 x 0.05 mm^3, monoclinic, space group $P2_1/n$, a = 13.6216(11) Å, b = 19.5088(9) Å, c = 15.1173(9) Å, $a = g$ = 90°, b = 116.200(9) °, V = 3604.6(4) $Å^3$, D_{calc} = 1.411 Mg/m^3, Z = 12. Data were collected on an Agilent Technologies/Oxford Diffraction Gemini CCD diffractometer at 100 K using MoKα radiation (0.71073 Å). For 7909 independent reflections I>2s(I) [R(int) 0.034] the final anisotropic full matrix least-squares refinement on F^2 for 634 variables converged at R1 = 0.045 and wR2 = 0.089 with a GOF of 1.07.

CONCLUSIONS

In the last decade there have been numerous reviews and publications on new gold catalyzed transformations. During the last few years our group has also developed new gold methodologies for the synthesis of interesting compounds and improved the efficiency of gold catalysis through ligand design. Specifically, some group members worked on ligand design and others focused on new reaction developments. Our experience with gold catalysis taught us that the major problem with this metal is the high catalyst loading (or low turnover number) required for most gold-catalyzed reactions. A major focus of this thesis is the investigation of basic mechanistic insights in gold-catalyzed reactions with the aim of reducing catalyst loading and improve overall efficiency.

We conducted detailed experimental studies to understand the mechanism of deactivation of gold active species. Based on the combination of experimental data, we proposed that disproportionation was preferred, as compared to reduction of active gold catalyst. We found that the substrate (alkyne/allene/alkene) may play a key role in the decay process. Moreover, we also found out that additives, coordinating counterions and solvents could play an important role in stopping the deactivation of the gold catalyst. To address the high resistance toward protodeauration in gold catalysis, we explored a new strategy to enhance the efficacy of gold-catalyzed reactions through hydrogen-bonding assisted

protodeauration using additives chosen for their pK_{BHX} (hydrogen-bond basicity) rather than for their pK_a. We found out that an ideal hydrogen bond acceptor additive should have (i) high hydrogen bonding basicity, (ii) low basicity, and (iii) low affinity toward cationic gold. Our studies suggested that additives with high hydrogen bonding basicity are often helpful when stage 2 in the target reaction is relatively slow as compared to stage 1. Additives with low basicity and low affinity toward cationic gold are useful when stage 1 in the target reaction is relatively slow as compared to stage 2. Hence, the overall effectiveness of a hydrogen bond acceptor will depend upon on the balance between the two effects. To address the threshold phenomenon in gold-catalyzed reactions, we examined what were the effects of impurities with high gold affinity impurities (halides, bases) in solvents, starting materials, filtration or drying agents on the reactivity of the gold catalyst. We found that these impurities had an adverse effect on gold catalyzed reactions, which may, in turn, significantly reduce the TON of cationic gold catalyzed reactions. We found that the use of a suitable acid activator (e.g. HOTf, $In(OTf)_3$) re-activates the gold catalyst and makes the reaction proceed smoothly at low gold catalyst loading. It should be noted that acid activators not only can re-activate the poisoned gold catalyst, but they can also positively influence the later stage in the gold catalytic cycle (e.g., protodeauration), acting as co-catalysts to speed-up the reaction.

To explore the reactivity of Au catalysts towards oxygen-atom transfer reactions, we investigated the gold-catalyzed addition of *O*-nucleophiles to alkynes to produce synthetically important vinyl ether products in excellent yields and

regioselectivities at room temperature. At higher temperatures, 3,3-sigmatropic rearrangement of vinyl ether products gives access to highly functionalized benzotriazoles. This two-step sequence represents an efficient oxygen transfer protocol of a nucleophilic oxygen atom to an alkyne group. Reaction of vinyl ether products with an electrophilic fluorinating reagent (Selectfluor) gives a fluorinated ketone in good yield and exclusive regioselectivity.

In the future, and as a corollary to our finding that additives play a very important role in catalysis, we would like to expand the use of additives, such as $LiNTf_2$, not only to other types of gold catalysis but also to other metal catalyzed reactions. Moreover, we would like to explore the application of the hydrogen bond basicity concept to other metal catalysis and organocatalysis. Finally, we would like to investigate whether acid activators only serve to re-activate a poisoned catalyst, or if they also can act as a co-catalysts in gold-catalyzed reactions.

REFERENCES

(1) Hashmi, A. S. K. *Gold-Catalyzed Organic Reactions. Chem. Rev.* **2007**, *107*, 3180-3211.

(2) Garcia, P.; Malacria, M.; Aubert, C.; Gandon, V.; Fensterbank, L. *Gold-Catalyzed Cross-Couplings: New Opportunities for C-bond-C Bond Formation. ChemCatChem* **2010**, *2*, 493-497.

(3) Arcadi, A. *Alternative Synthetic Methods through New Developments in Catalysis by Gold. Chem. Rev.* **2008**, *108*, 3266-3325.

(4) Gorin, D. J.; Sherry, B. D.; Toste, F. D. *Ligand Effects in Homogeneous Au Catalysis. Chem. Rev.* **2008**, *108*, 3351-3378.

(5) Jimenez-Nunez, E.; Echavarren, A. M. *Gold-Catalyzed Cycloisomerizations of Enynes: A Mechanistic Perspective. Chem. Rev.* **2008**, *108*, 3326-3350.

(6) Li, Z.; Brouwer, C.; He, C. *Gold-Catalyzed Organic Transformations. Chem. Rev.* **2008**, *108*, 3239-3265.

(7) Hashmi, A. S. K.; Rudolph, M. *Gold catalysis in total synthesis. Chem. Soc. Rev.* **2008**, *37*, 1766-1775.

(8) Widenhoefer, R. A. *Recent developments in enantioselective gold(I) catalysis. Chem. Eur. J.* **2008**, *14*, 5382-5391.

(9) Hashmi, A. S. K.; Schwarz, L.; Choi, J.-H.; Frost, T. M. *A New Gold-Catalyzed C−C Bond Formation. Angew. Chem., Int. Ed.* **2000**, *39*, 2285-2288.

(10) Leyva-Pérez, A.; Corma, A. *Similarities and Differences between the "Relativistic" Triad Gold, Platinum, and Mercury in Catalysis. Angew. Chem., Int. Ed.* **2012**, *51*, 614-635.

(11) Pernpointner, M.; Hashmi, A. S. K. *Fully relativistic, comparative investigation of gold and platinum alkyne complexes of relevance for the catalysis of nucleophilic additions to alkynes. J. Chem. Theory Comput.* **2009**, *5*, 2717-2725.

(12) Gorin, D. J.; Toste, F. D. *Relativistic effects in homogeneous gold catalysis. Nature* **2007**, *446*, 395-403.

(13) Pyykko, P.; Desclaux, J. P. *Relativity and the periodic system of elements. Acc. Chem. Res.* **1979**, *12*, 276-281.

(14) Bender, C. F.; Widenhoefer, R. A. *Room Temperature Hydroamination of N-Alkenyl Ureas Catalyzed by a Gold(I) N-Heterocyclic Carbene Complex. Org. Lett.* **2006**, *8*, 5303-5305.

(15) Jung, H. H.; Floreancig, P. E. *Gold-Catalyzed Heterocycle Synthesis Using Homopropargylic Ethers as Latent Electrophiles. Org. Lett.* **2006**, *8*, 1949-1951.

(16) Zhang, J.; Yang, C.-G.; He, C. *Gold(I)-Catalyzed Intra- and Intermolecular Hydroamination of Unactivated Olefins. J. Am. Chem. Soc.* **2006**, *128*, 1798-1799.

(17) Dombray, T.; Blanc, A. l.; Weibel, J.-M.; Pale, P. *Gold(I)-Catalyzed Cycloisomerization of β-Alkynylpropiolactones to Substituted α-Pyrones. Org. Lett.* **2010**, *12*, 5362-5365.

(18) Yao, X.; Li, C.-J. *Highly Efficient Addition of Activated Methylene Compounds to Alkenes Catalyzed by Gold and Silver. J. Am. Chem. Soc.* **2004**, *126*, 6884-6885.

(19) Hirano, K.; Inaba, Y.; Watanabe, T.; Oishi, S.; Fujii, N.; Ohno, H. *Gold-Catalyzed Intramolecular Alkyne Cycloisomerization Cascade: Direct Synthesis of Aryl-Annulated[a]carbazoles from Aniline-Substituted Diethynylarenes. Adv. Synth. Catal.* **2010**, *352*, 368-372.

(20) Widenhoefer, R. A.; Han, X. *Gold-Catalyzed Hydroamination of C–C Multiple Bonds. Eur. J. Org. Chem.* **2006**, *2006*, 4555-4563.

(21) Zeng, X.; Soleilhavoup, M.; Bertrand, G. *Gold-Catalyzed Intermolecular Markovnikov Hydroamination of Allenes with Secondary Amines. Org. Lett.* **2009**, *11*, 3166-3169.

(22) LaLonde, R. L.; Brenzovich, J. W. E.; Benitez, D.; Tkatchouk, E.; Kelley, K.; Goddard, I. I. I. W. A.; Toste, F. D. *Alkylgold complexes by the intramolecular aminoauration of unactivated alkenes. Chem. Sci.* **2010**, *1*, 226-233.

(23) Eisenstein, O.; Hoffmann, R. *Transition-metal complexed olefins: how their reactivity toward a nucleophile relates to their electronic structure. J. Am. Chem. Soc.* **1981**, *103*, 4308-4320.

(24) Brown, T. J.; Weber, D.; Gagné, M. R.; Widenhoefer, R. A. *Mechanistic Analysis of Gold(I)-Catalyzed Intramolecular Allene Hydroalkoxylation Reveals an Off-Cycle Bis(gold) Vinyl Species and Reversible C–O Bond Formation. J. Am. Chem. Soc.* **2012**, *134*, 9134-9137.

(25) Benitez, D.; Shapiro, N. D.; Tkatchouk, E.; Wang, Y.; Goddard, W. A.; Toste, F. D. *A bonding model for gold(I) carbene complexes. Nat. Chem.* **2009**, *1*, 482-486.

(26) Shen, Q.; Shekhar, S.; Stambuli, J. P.; Hartwig, J. F. *Highly Reactive, General, and Long-Lived Catalysts for Coupling Heteroaryl and Aryl Chlorides with Primary Nitrogen Nucleophiles. Angew. Chem., Int. Ed.* **2005**, *44*, 1371-1375.

(27) Zhang, G.; Huang, X.; Li, G.; Zhang, L. *Au-Containing All-Carbon 1,4-Dipoles: Generation and [4 + 2] Annulation in the Formation of Carbo-/Heterocycles. J. Am. Chem. Soc.* **2008**, *130*, 1814-1815.

(28) Hashmi, A. S. K. *Homogeneous Gold Catalysis Beyond Assumptions and Proposals—Characterized Intermediates. Angew. Chem. Int. Ed.* **2010**, *49*, 5232-5241.

(29) Wang, W.; Hammond, G. B.; Xu, B. *Ligand Effects and Ligand Design in Homogeneous Gold(I) Catalysis. J. Am. Chem. Soc.* **2012**, *134*, 5697-5705.

(30) Hardacre, C.; Katdare, S. P.; Milroy, D.; Nancarrow, P.; Rooney, D. W.; Thompson, J. M. *A catalytic and mechanistic study of the Friedel–Crafts benzoylation of anisole using zeolites in ionic liquids. J. Catal.* **2004**, *227*, 44-52.

(31) Mukherjee, A.; Sen, T. K.; Ghorai, P. K.; Mandal, S. K. *The Non-innocent Phenalenyl Unit: An Electronic Nest to Modulate the Catalytic Activity in Hydroamination Reaction. Sci. Rep.* **2013**, *3*.

(32) Wang, Z. J.; Benitez, D.; Tkatchouk, E.; Goddard Iii, W. A.; Toste, F. D. *Mechanistic Study of Gold(I)-Catalyzed Intermolecular Hydroamination of Allenes. J. Am. Chem. Soc.* **2010**, *132*, 13064-13071.

(33) Wang, W.; Kumar, M.; Hammond, G. B.; Xu, B. *Enhanced Reactivity in Homogeneous Gold Catalysis through Hydrogen Bonding. Org. Lett.* **2014**, *16*, 636-639.

(34) Malhotra, D.; Mashuta, M. S.; Hammond, G. B.; Xu, B. *A Highly Efficient and Broadly Applicable Cationic Gold Catalyst. Angew. Chem. Int. Ed.* **2014**, *53*, 4456-4459.

(35) Kumar, M.; Jasinski, J.; Hammond, G. B.; Xu, B. *Alkyne/Alkene/Allene-Induced Disproportionation of Cationic Gold(I) Catalyst. Chem. Eur. J.* **2014**, *20*, 3113-3119.

(36) Kumar, M.; Scobie, M.; Mashuta, M. S.; Hammond, G. B.; Xu, B. *Gold-Catalyzed Addition of N-Hydroxy Heterocycles to Alkynes and Subsequent 3,3-Sigmatropic Rearrangement. Org. Lett.* **2013**, *15*, 724-727.

(37) Zhang, C.; De, C. K.; Mal, R.; Seidel, D. *Alpha-amination of nitrogen heterocycles: ring-fused aminals. J. Am. Chem. Soc.* **2008**, *130*, 416-7.

(38) Trost, B. M.; Maulide, N.; Livingston, R. C. *A Ruthenium-Catalyzed, Atom-Economical Synthesis of Nitrogen Heterocycles. J. Am. Chem. Soc.* **2008**, 16502-16503.

(39) Fustero, S.; Moscardo, J.; Jimenez, D.; Perez-Carrion, M. D.; Sanchez-Rosello, M.; Del Pozo, C. *Organocatalytic approach to benzofused nitrogen-containing heterocycles: enantioselective total synthesis of (+)-angustureine. Chemistry* **2008**, *14*, 9868-72.

(40) Vicario, J. L.; Badia, D.; Carrillo, L. *New methods for the asymmetric synthesis of nitrogen heterocycles 2005*; Research Signpost: Kerala, India, 2005.

(41) El Ashry, E. S. H.; El-Nemr, A. *Synthesis of naturally occurring nitrogen heterocycles from carbohydrates*; Blackwell Pub.: Oxford, UK ; Ames, Iowa, 2005.

(42) Wu, W.; Su, W. *Mild and Selective Ru-Catalyzed Formylation and Fe-Catalyzed Acylation of Free (N–H) Indoles Using Anilines as the Carbonyl Source. J. Am. Chem. Soc.* **2011**, *133*, 11924-11927.

(43) Shen, L.; Zhang, M.; Wu, Y.; Qin, Y. *Efficient Assembly of an Indole Alkaloid Skeleton by Cyclopropanation: Concise Total Synthesis of (±)-Minfiensine. Angew. Chem., Int. Ed.* **2008**, *47*, 3618-3621.

(44) Gabriele, B.; Mancuso, R.; Salerno, G.; Lupinacci, E.; Ruffolo, G.; Costa, M. *Versatile Synthesis of Quinoline-3-Carboxylic Esters and Indol-2-Acetic Esters by Palladium-Catalyzed Carbonylation of 1-(2-Aminoaryl)-2-Yn-1-Ols. J. Org. Chem.* **2008**, *73*, 4971-4977.

(45) Nakamura, M.; Ilies, L.; Otsubo, S.; Nakamura, E. *2,3-Disubstituted Benzofuran and Indole by Copper-Mediated C−C Bond Extension Reaction of 3-Zinciobenzoheterole. Org. Lett.* **2006**, *8*, 2803-2805.

(46) Potavathri, S.; Pereira, K. C.; Gorelsky, S. I.; Pike, A.; LeBris, A. P.; DeBoef, B. *Regioselective Oxidative Arylation of Indoles Bearing N-Alkyl Protecting Groups: Dual C−H Functionalization via a Concerted Metalation−Deprotonation Mechanism. J. Am. Chem. Soc.* **2010**, *132*, 14676-14681.

(47) Newhouse, T.; Lewis, C. A.; Eastman, K. J.; Baran, P. S. *Scalable Total Syntheses of N-Linked Tryptamine Dimers by Direct Indole−Aniline Coupling: Psychotrimine and Kapakahines B and F. J. Am. Chem. Soc.* **2010**, *132*, 7119-7137.

(48) Nuss, J. M.; Harrison, S. D.; Ring, D. B.; Boyce, R. S.; johnson, K.; Pfister, K. B.; Ramurthy, S.; Seely, L.; Wagman, A. S.; Desai, M. C.; Levine, B. H., 2006; Vol. US 7,045,519 B2.

(49) Katritzky, A. R.; Rachwal, S. *Synthesis of Heterocycles Mediated by Benzotriazole. 1. Monocyclic Systems. Chem. Rev.* **2009**, *110*, 1564-1610.

(50) Katritzky, A. R.; Rachwal, S. *Synthesis of Heterocycles Mediated by Benzotriazole. 2. Bicyclic Systems. Chem. Rev.* **2011**, *111*, 7063-7120.

(51) Krause, N.; Winter, C. *Gold-Catalyzed Nucleophilic Cyclization of Functionalized Allenes: A Powerful Access to Carbo- and Heterocycles. Chem. Rev.* **2011**, *111*, 1994-2009.

(52) Widenhoefer, R. A. *Recent Developments in Enantioselective Gold(I) Catalysis. Chem. Eur. J.* **2008**, *14*, 5382-5391.

(53) Fürstner, A.; Davies, P. W. *Catalytic Carbophilic Activation: Catalysis by Platinum and Gold π Acids. Angew. Chem., Int. Ed.* **2007**, *46*, 3410-3449.

(54) Hashmi, A. S. K.; Hutchings, G. J. *Gold Catalysis. Angew. Chem., Int. Ed.* **2006**, *45*, 7896-7936.

(55) Hashmi, A. S. K. *The Catalysis Gold Rush: New Claims. Angew. Chem., Int. Ed.* **2005**, *44*, 6990-6993.

(56) Gorin, D. J.; Toste, F. D. *Nature* **2007**, *446*, 395-403.

(57) Jimenez-Nunez, E.; Echavarren, A. M. *Molecular diversity through gold catalysis with alkynes. Chem. Commun.* **2007**, 333-346.

(58) Marion, N.; Nolan, S. P. *Propargylic Esters in Gold Catalysis: Access to Diversity. Angew. Chem., Int. Ed.* **2007**, *46*, 2750-2752.

(59) Xiao, J.; Li, X. *Gold α-Oxo Carbenoids in Catalysis: Catalytic Oxygen-Atom Transfer to Alkynes. Angew. Chem., Int. Ed.* **2011**, *50*, 7226-7236.

(60) Ye, L.; Cui, L.; Zhang, G.; Zhang, L. *Alkynes as Equivalents of α-Diazo Ketones in Generating α-Oxo Metal Carbenes: A Gold-Catalyzed Expedient Synthesis of Dihydrofuran-3-ones. J. Am. Chem. Soc.* **2010**, *132*, 3258-3259.

(61) Ye, L.; He, W.; Zhang, L. *Gold-Catalyzed One-Step Practical Synthesis of Oxetan-3-ones from Readily Available Propargylic Alcohols. J. Am. Chem. Soc.* **2010**, *132*, 8550-8551.

(62) Lu, B.; Li, C.; Zhang, L. *Gold-Catalyzed Highly Regioselective Oxidation of C−C Triple Bonds without Acid Additives: Propargyl Moieties as Masked α,β-Unsaturated Carbonyls. J. Am. Chem. Soc.* **2010**, *132*, 14070-14072.

(63) He, W.; Li, C.; Zhang, L. *An Efficient [2 + 2 + 1] Synthesis of 2,5-Disubstituted Oxazoles via Gold-Catalyzed Intermolecular Alkyne Oxidation. J. Am. Chem. Soc.* **2011**, *133*, 8482-8485.

(64) Cui, L.; Zhang, G.; Peng, Y.; Zhang, L. *Gold or No Gold: One-Pot Synthesis of Tetrahydrobenz[b]azepin-4-ones from Tertiary N-(But-3-ynyl)anilines. Org. Lett.* **2009**, *11*, 1225-1228.

(65) Luo, Y.; Zhang, G.; Hwang, E. S.; Wilcoxon, T. A.; Zhang, L. *Beilstein J. Org. Chem.* **2011**, *7*, 596-600.

(66) Rudolph, M.; Hashmi, A. S. K. *Gold catalysis in total synthesis-an update. Chem. Soc. Rev.* **2012**, *41*, 2448-2462.

(67) Garcia, P.; Malacria, M.; Aubert, C.; Gandon, V.; Fensterbank, L. *Gold-Catalyzed Cross-Couplings: New Opportunities for C-C Bond Formation. ChemCatChem* **2010**, *2*, 493-497.

(68) Teles, J. H.; Brode, S.; Chabanas, M. *Cationic Gold(I) Complexes: Highly Efficient Catalysts for the Addition of Alcohols to Alkynes. Angew. Chem. Int. Ed.* **1998**, *37*, 1415-1418.

(69) Mizushima, E.; Sato, K.; Hayashi, T.; Tanaka, M. *Highly efficient AuI-catalyzed hydration of alkynes. Angew. Chem. Int. Ed.* **2002**, *41*, 4563-4565.

(70) Marion, N.; Ramon, R. S.; Nolan, S. P. *[(NHC)AuI]-Catalyzed Acid-Free Alkyne Hydration at Part-per-Million Catalyst Loadings. J. Am. Chem. Soc.* **2009**, *131*, 448-449.

(71) Blanco Jaimes, M. C.; Böhling, C. R. N.; Serrano-Becerra, J. M.; Hashmi, A. S. K. *Highly Active Mononuclear NAC–Gold(I) Catalysts. Angew. Chem. Int. Ed.* **2013**, *52*, 7963-7966.

(72) Oliver-Meseguer, J.; Cabrero-Antonino, J. R.; Domínguez, I.; Leyva-Pérez, A.; Corma, A. *Small Gold Clusters Formed in Solution Give Reaction Turnover Numbers of 107 at Room Temperature. Science* **2012**, *338*, 1452-1455.

(73) Hashmi, A. S. K. *Sub-Nanosized Gold Catalysts. Science* **2012**, *338*, 1434.

(74) Lavallo, V.; Wright, J. H.; Tham, F. S.; Quinlivan, S. *Perhalogenated Carba-closo-dodecaborate Anions as Ligand Substituents: Applications in Gold Catalysis. Angew. Chem., Int. Ed.* **2013**, *52*, 3172-3176.

(75) Duan, H.; Sengupta, S.; Petersen, J. L.; Akhmedov, N. G.; Shi, X. *Triazole−Au(I) Complexes: A New Class of Catalysts with Improved Thermal Stability and Reactivity for Intermolecular Alkyne Hydroamination. J. Am. Chem. Soc.* **2009**, *131*, 12100-12102.

(76) Brown, T. J.; Dickens, M. G.; Widenhoefer, R. A. *Syntheses, X-ray Crystal Structures, and Solution Behavior of Monomeric, Cationic, Two-Coordinate Gold(I) π-Alkene Complexes. J. Am. Chem. Soc.* **2009**, *131*, 6350-6351.

(77) Shapiro, N. D.; Toste, F. D. *Synthesis and structural characterization of isolable phosphine coinage metal π-complexes. Proc. Natl. Acad Sci.* **2008**, *105*, 2779-2782.

(78) Guérinot, A.; Fang, W.; Sircoglou, M.; Bour, C.; Bezzenine-Lafollée, S.; Gandon, V. *Copper Salts as Additives in Gold(I)-Catalyzed Reactions. Angew. Chem., Int. Ed.* **2013**, *52*, 5848-5852.

(79) Lemière, G.; Gandon, V.; Agenet, N.; Goddard, J.-P.; de Kozak, A.; Aubert, C.; Fensterbank, L.; Malacria, M. *Gold(I)- and Gold(III)-Catalyzed Cycloisomerization of Allenynes: A Remarkable Halide Effect. Angew. Chem., Int. Ed.* **2006**, *45*, 7596-7599.

(80) Bartholomew, C. H. *Mechanisms of catalyst deactivation. Appl. Catal., A* **2001**, *212*, 17-60.

(81) Hashmi, A. S. K. *Homogeneous gold catalysts and alkynes: A successful liaison. Gold Bull.* **2003**, *36*, 3-9.

(82) Hashmi, A. S. K.; Schuster, A. M.; Litters, S.; Rominger, F.; Pernpointner, M. *Gold Catalysis: 1,3-Oxazines by Cyclisation of Allene Amides. Chem. Eur. J.* **2011**, *17*, 5661-5667.

(83) Yang, C.-G.; He, C. *Gold(I)-Catalyzed Intermolecular Addition of Phenols and Carboxylic Acids to Olefins. J. Am. Chem. Soc.* **2005**, *127*, 6966-6967.

(84) Brenzovich, W. E.; Benitez, D.; Lackner, A. D.; Shunatona, H. P.; Tkatchouk, E.; Goddard, W. A.; Toste, F. D. *Gold-Catalyzed Intramolecular Aminoarylation of Alkenes: C-C Bond Formation through Bimolecular Reductive Elimination. Angew. Chem. Int. Ed.* **2010**, *49*, 5519-5522.

(85) Bardaji, M.; Uznanski, P.; Amiens, C.; Chaudret, B.; Laguna, A. *Aurophilic complexes as gold atom sources in organic media. Chem. Commun.* **2002**, 598-599.

(86) Attar, S.; Bearden, W. H.; Alcock, N. W.; Alyea, E. C.; Nelson, J. H. *Phosphole complexes of gold(I) halides: comparison of solution and solid-state structures by a combination of solution and CP/MAS phosphorus-31 NMR spectroscopy and x-ray crystallography. Inorg. Chem.* **1990**, *29*, 425-433.

(87) Mézailles, N.; Ricard, L.; Gagosz, F. *Phosphine Gold(I) Bis-(trifluoromethanesulfonyl)imidate Complexes as New Highly Efficient and Air-Stable Catalysts for the Cycloisomerization of Enynes. Org. Lett.* **2005**, *7*, 4133-4136.

(88) Bergamini, G.; Ceroni, P.; Balzani, V.; Gingras, M.; Raimundo, J.-M.; Morandi, V.; Merli, P. G. *Synthesis of small gold nanoparticles: Au(i) disproportionation catalyzed by a persulfurated coronene dendrimer. Chem. Commun.* **2007**, *0*, 4167-4169.

(89) Koelle, U.; Laguna, A. *Electrochemistry of Au-complexes. Inorg. Chim. Acta* **1999**, *290*, 44-50.

(90) Connelly, N. G.; Geiger, W. E. *Chemical Redox Agents for Organometallic Chemistry. Chem. Rev.* **1996**, *96*, 877-910.

(91) Au, L.; Lu, X.; Xia, Y. *A Comparative Study of Galvanic Replacement Reactions Involving Ag Nanocubes and $AuCl_2^-$ or $AuCl_4^-$. Adv. Mater.* **2008**, *20*, 2517-2522.

(92) Choy, J.-H.; Kim, Y.-I. *Gold Valence in $(AuI_3)0.25Bi_2Sr_2CaCu_2Oy$ by XPS and XANES Spectroscopy. J. Phys. Chem. B* **2003**, *107*, 3348-3350.

(93) Wang, W.; Jasinski, J.; Hammond, G. B.; Xu, B. *Fluorine-enabled cationic gold catalysis: Functionalized hydration of alkynes. Angew. Chem. Int. Ed.* **2010**, *49*, 7247-7252.

(94) Casaletto, M. P.; Longo, A.; Martorana, A.; Prestianni, A.; Venezia, A. M. *XPS study of supported gold catalysts: the role of Au^0 and $Au^{+\delta}$ species as active sites. Surf. Interface Anal.* **2006**, *38*, 215-218.

(95) de Almeida, M. P.; Martins, L. M. D. R. S.; Carabineiro, S. A. C.; Lauterbach, T.; Rominger, F.; Hashmi, A. S. K.; Pombeiro, A. J. L.; Figueiredo, J. L. *Homogeneous and heterogenised new gold C-scorpionate complexes as catalysts for cyclohexane oxidation. Catal. Sci. Technol.* **2013**, *3*, 3056-3069.

(96) Colton, R.; D'Agostino, A.; Traeger, J. C. *Electrospray mass spectrometry applied to inorganic and organometallic chemistry. Mass Spectrom. Rev.* **1995**, *14*, 79-106.

(97) Henderson, W.; Nickleson, B. K.; McCaffrey, L. J. *Polyhedron* **1998**, *17*, 4291-4313.

(98) Xu, B.; Wang, W.; Hammond, G. B. *Library-friendly synthesis of fluorinated ketones through functionalized hydration of alkynes and investigation of the reaction mechanism. J. Fluorine Chem.* **2011**, *132*, 804-810.

(99) Döpp, R.; Lothschütz, C.; Wurm, T.; Pernpointner, M.; Keller, S.; Rominger, F.; Hashmi, A. S. K. *Gold Catalysis: Hydrolysis of Di(alkoxy)carbenium Ion Intermediates as a Sensor for the Electronic Properties of Gold(I) Complexes. Organometallics* **2011**, *30*, 5894-5903.

(100) Cheeseman, T. P.; Odell, A. L.; Raethel, H. A. *trans-Effect order for alkene, alkyne, phosphine, arsine, stibine, and sulphide ligands from studies of diethylamine exchange reactions of L,PtCl$_2$,[14C]NHEt$_2$ in various solvents. Chem. Commun.* **1968**, *0*, 1496-1498.

(101) Christopher H. Gammons; Yunmei Yu; Williams-Jones, A. E. *Geochim. Cosmochim. Acta* **1997**, *61*, 1971-1983.

(102) Dias, H. V. R.; Fianchini, M.; Cundari, T. R.; Campana, C. F. *Synthesis and Characterization of the Gold(I) Tris(ethylene) Complex [Au(C2H4)3][SbF6]. Angew. Chem., Int. Ed.* **2008**, *47*, 556-559.

(103) Das, A.; Dash, C.; Yousufuddin, M.; Celik, M. A.; Frenking, G.; Dias, H. V. R. *Isolable Tris(alkyne) and Bis(alkyne) Complexes of Gold(I). Angew. Chem., Int. Ed.* **2012**, *51*, 3940-3943.

(104) Das, A.; Dash, C.; Celik, M. A.; Yousufuddin, M.; Frenking, G.; Dias, H. V. R. *Tris(alkyne) and Bis(alkyne) Complexes of Coinage Metals: Synthesis and Characterization of (cyclooctyne)3M+ (M = Cu, Ag) and (cyclooctyne)2Au+ and Coinage Metal (M = Cu, Ag, Au) Family Group Trends. Organometallics* **2013**, *32*, 3135-3144.

(105) Fianchini, M.; Dai, H.; Dias, H. V. R. *Organometallic wheels based on coinage metal ions and norbornene: syntheses and structural characterization of [M(norbornene)3][SbF6] (M = Au, Ag, Cu). Chem. Commun.* **2009**, *0*, 6373-6375.

(106) Braunstein, P.; Lehner, H.; Matt, D.; Burgess, K.; Ohlmeyer, M. J. In *Inorg. Synth.*; John Wiley & Sons, Inc., 2007.

(107) $Ph_3P(OTf)_2$ and even Ph_3PO are not detected in ^{31}P NMR in the decay solutions, possible reason is their ^{31}P NMR peaks are broad in reaction system.

(108) Hashmi, A. S. K.; Weyrauch, J. P.; Frey, W.; Bats, J. W. *Gold Catalysis: Mild Conditions for the Synthesis of Oxazoles from N-Propargylcarboxamides and Mechanistic Aspects. Org. Lett.* **2004**, *6*, 4391-4394.

(109) Doherty, S.; Smyth, C. H.; Knight, J. G.; Hashmi, S. A. K. *Synthesis of an electron-rich KITPHOS monophosphine, preparation of derived metal complexes and applications in catalysis. Nat. Protocols* **2012**, *7*, 1870-1883.

(110) Hashmi, A. S. K.; Loos, A.; Doherty, S.; Knight, J. G.; Robson, K. J.; Rominger, F. *Gold-Catalyzed Cyclizations: A Comparative Study of ortho,ortho'-Substituted KITPHOS Monophosphines with their Biaryl Monophosphine Counterpart SPHOS. Adv. Synth. Catal.* **2011**, *353*, 749-759.

(111) Hashmi, A. S. K.; Loos, A.; Littmann, A.; Braun, I.; Knight, J.; Doherty, S.; Rominger, F. *Gold(I) Complexes of KITPHOS Monophosphines: Efficient Cycloisomerisation Catalysts. Adv. Synth. Catal.* **2009**, *351*, 576-582.

(112) Hashmi, A. S. K.; Frost, T. M.; Bats, J. W. *Highly Selective Gold-Catalyzed Arene Synthesis. J. Am. Chem. Soc.* **2000**, *122*, 11553-11554.

(113) Mhamed Touil; Benjamin Bechem; A. Stephen K. Hashmi; Bernd Engels; Mohammad A. Omary; Rabaâ, H. *Journal of Molecular Structure: THEOCHEM* **2010**, *957*, 21-25.

(114) Leyva, A.; Corma, A. *Isolable Gold(I) Complexes Having One Low-Coordinating Ligand as Catalysts for the Selective Hydration of Substituted Alkynes at Room Temperature without Acidic Promoters. J. Org. Chem.* **2009**, *74*, 2067-2074.

(115) Canseco-Gonzalez, D.; Petronilho, A.; Mueller-Bunz, H.; Ohmatsu, K.; Ooi, T.; Albrecht, M. *Carbene Transfer from Triazolylidene Gold Complexes as a Potent Strategy for Inducing High Catalytic Activity. J. Am. Chem. Soc.* **2013**, *135*, 13193-13203.

(116) Nieto-Oberhuber, C.; López, S.; Echavarren, A. M. *Intramolecular [4 + 2] Cycloadditions of 1,3-Enynes or Arylalkynes with Alkenes with Highly Reactive Cationic Phosphine Au(I) Complexes. J. Am. Chem. Soc.* **2005**, *127*, 6178-6179.

(117) Choy, J.-H.; Kim, Y.-I. *Gold Valence in (AuI3)0.25Bi2Sr2CaCu2Oy by XPS and XANES Spectroscopy. J. Phys. Chem. B* **2003**, *107*, 3348-3350.

(118) Grapperhaus, C. A.; Poturovic, S. *Electrochemical Investigations of the [Tris(2-(diphenylphosphino)thiaphenolato)ruthenate(II)] Monoanion Reveal Metal- and Ligand-Centered Events: Radical, Reactivity, and Rate. Inorg. Chem.* **2004**, *43*, 3292-3298.

(119) Roth, K. E.; Blum, S. A. *Relative Kinetic Basicities of Organogold Compounds. Organometallics* **2010**, *29*, 1712-1716.

(120) Egorova, O. A.; Seo, H.; Kim, Y.; Moon, D.; Rhee, Y. M.; Ahn, K. H. *Characterization of Vinylgold Intermediates: Gold-Mediated Cyclization of Acetylenic Amides. Angew. Chem. Int. Ed.* **2011**, *50*, 11446-11450.

(121) Chen, Y.; Wang, D.; Petersen, J. L.; Akhmedov, N. G.; Shi, X. *Synthesis and characterization of organogold complexes containing an acid stable Au-C bond through triazole-yne 5-endo-dig cyclization. Chem. Commun.* **2010**, *46*, 6147-6149.

(122) Zeng, X.; Kinjo, R.; Donnadieu, B.; Bertrand, G. *Serendipitous Discovery of the Catalytic Hydroammoniumation and Methylamination of Alkynes. Angew. Chem. Int. Ed.* **2010**, *49*, 942-945.

(123) Laurence, C.; Brameld, K. A.; Graton, J. r. m.; Le Questel, J.-Y.; Renault, E. *The pK_{BHX} Database: Toward a Better Understanding of Hydrogen-Bond Basicity for Medicinal Chemists. J. Med. Chem.* **2009**, *52*, 4073-4086.

(124) Laurence, C.; Graton, J. r. m.; Berthelot, M.; Besseau, F. o.; Le Questel, J.-Y.; Luçon, M.; Ouvrard, C.; Planchat, A. l.; Renault, E. *An Enthalpic Scale of Hydrogen-Bond Basicity. 4. Carbon π Bases, Oxygen Bases, and Miscellaneous Second-Row, Third-Row, and Fourth-Row Bases and a Survey of the 4-Fluorophenol Affinity Scale. J. Org. Chem.* **2010**, *75*, 4105-4123.

(125) Reed, A. E.; Curtiss, L. A.; Weinhold, F. *Intermolecular interactions from a natural bond orbital, donor-acceptor viewpoint. Chem. Rev.* **1988**, *88*, 899-926.

(126) Ault, A. *General Acid and General Base Catalysis. J. Chem. Educ.* **2007**, *84*, 38.

(127) Kwan, E. E. *The Rate of Proton Transfer. J. Chem. Educ.* **2007**, *84*, 39.

(128) Wilson, T. J.; Li, N.-S.; Lu, J.; Frederiksen, J. K.; Piccirilli, J. A.; Lilley, D. M. J. *Nucleobase-mediated general acid-base catalysis in the Varkud satellite ribozyme. Proc. Natl. Acad. Sci. USA, Early Ed.* **2010**, 1-6, 6 pp.

(129) Kath-Schorr, S.; Wilson, T. J.; Li, N.-S.; Lu, J.; Piccirilli, J. A.; Lilley, D. M. J. *General Acid-Base Catalysis Mediated by Nucleobases in the Hairpin Ribozyme. J. Am. Chem. Soc.* **2012**, *134*, 16717-16724.

(130) Krauter, C. M.; Hashmi, A. S. K.; Pernpointner, M. *A New Insight into Gold(I)-Catalyzed Hydration of Alkynes: Proton Transfer. ChemCatChem* **2010**, *2*, 1226-1230.

(131) Weyrauch, J. P.; Hashmi, A. S. K.; Schuster, A.; Hengst, T.; Schetter, S.; Littmann, A.; Rudolph, M.; Hamzic, M.; Visus, J.; Rominger, F.; Frey, W.; Bats, J. W. *Cyclization of Propargylic Amides: Mild Access to Oxazole Derivatives. Chem. Eur. J.* **2010**, *16*, 956-963.

(132) Hashmi, A. S. K.; Schuster, A. M.; Rominger, F. *Gold Catalysis: Isolation of Vinylgold Complexes Derived from Alkynes. Angew. Chem. Int. Ed.* **2009**, *48*, 8247-8249.

(133) Hashmi, A. S. K.; Schuster, A. M.; Gaillard, S.; Cavallo, L.; Poater, A.; Nolan, S. P. *Selectivity Switch in the Synthesis of Vinylgold(I) Intermediates. Organometallics* **2011**, *30*, 6328-6337.

(134) ^{13}C NMR of good quality (**Au-4**) can't be obtained due to the broadening of peaks. According to report by Hashmi and coworkers, the vinyl carbon is not visible in the ^{13}C NMR spectrum even in isolated form of **Au-1**.

(135) Duan, H.; Sengupta, S.; Petersen, J. L.; Akhmedov, N. G.; Shi, X. *Triazole-Au(I) Complexes: A New Class of Catalysts with Improved Thermal Stability and Reactivity for Intermolecular Alkyne Hydroamination. J. Am. Chem. Soc.* **2009**, *131*, 12100-12102.

(136) Lein, M.; Rudolph, M.; Hashmi, S. K.; Schwerdtfeger, P. *Homogeneous Gold Catalysis: Mechanism and Relativistic Effects of the Addition of Water to Propyne. Organometallics* **2010**, *29*, 2206-2210.

(137) Hashmi, A. S. K.; Pernpointner, M.; Hansmann, M. M. *Theoretical insights into the superior activity of gold catalysts and reactions of organogold intermediates with electrophiles. Faraday Discuss.* **2011**, *152*, 179-184.

(138) Hashmi, A. S. K.; Braun, I.; Rudolph, M.; Rominger, F. *The Role of Gold Acetylides as a Selectivity Trigger and the Importance of gem-Diaurated Species in the Gold-Catalyzed Hydroarylating-Aromatization of Arene-Diynes. Organometallics* **2012**, *31*, 644-661.

(139) Liu, L.-P.; Xu, B.; Mashuta, M. S.; Hammond, G. B. *Synthesis and Structural Characterization of Stable Organogold(I) Compounds. Evidence for the Mechanism of Gold-Catalyzed Cyclizations. J. Am. Chem. Soc.* **2008**, *130*, 17642-17643.

(140) Not all additives are shown because lack of data about their pK_{BHX}; some pK_{BHX} data have been estimated from the pK_{BHX} of structural analogs.

(141) Brown, T. J.; Sugie, A.; Leed, M. G. D.; Widenhoefer, R. A. *Structures and Dynamic Solution Behavior of Cationic, Two-Coordinate Gold(I)–π-Allene Complexes. Chem. Eur. J.* **2012**, *18*, 6959-6971.

(142) Brown, T. J.; Dickens, M. G.; Widenhoefer, R. A. *Syntheses, X-ray Crystal Structures, and Solution Behavior of Monomeric, Cationic, Two-Coordinate Gold(I) pi-Alkene Complexes. J. Am. Chem. Soc.* **2009**, *131*, 6350-6351.

(143) Brown, T. J.; Dickens, M. G.; Widenhoefer, R. A. *Syntheses and X-ray crystal structures of cationic, two-coordinate gold(i) pi-alkene complexes that contain a sterically hindered o-biphenylphosphine ligand. Chem. Commun.* **2009**, 6451-6453.

(144) Brooner, R. E. M.; Widenhoefer, R. A. *Syntheses, X-ray Crystal Structures, and Solution Behavior of Cationic, Two-Coordinate Gold(I) η2-Diene Complexes. Organometallics* **2011**, *30*, 3182-3193.

(145) Brown, T. J.; Sugie, A.; Dickens, M. G.; Widenhoefer, R. A. *Solid-State and Dynamic Solution Behavior of a Cationic, Two-Coordinate Gold(I) π-Allene Complex. Organometallics* **2010**, *29*, 4207-4209.

(146) Brown, T. J.; Widenhoefer, R. A. *Cationic Gold(I) π-Complexes of Terminal Alkynes and Their Conversion to Dinuclear σ,π-Acetylide Complexes. Organometallics* **2011**, *30*, 6003-6009.

(147) Zhdanko, A.; Ströbele, M.; Maier, M. E. *Coordination Chemistry of Gold Catalysts in Solution: A Detailed NMR Study. Chem. Eur. J.* **2012**, *18*, 14732-14744.

(148) Zhu, Y.; Day, C. S.; Jones, A. C. *Synthesis and Structure of Cationic Phosphine Gold(I) Enol Ether Complexes. Organometallics* **2012**, *31*, 7332-7335.

(149) Hashmi, A. S. K.; Schwarz, L.; Choi, J.-H.; Frost, T. M. *A New Gold-Catalyzed C−C Bond Formation. Angew. Chem. Int. Ed.* **2000**, *39*, 2285-2288.

(150) Zhou, C.-Y.; Chan, P. W. H.; Che, C.-M. *Gold(III) Porphyrin-Catalyzed Cycloisomerization of Allenones. Org. Lett.* **2005**, *8*, 325-328.

(151) Tomás-Mendivil, E.; Toullec, P. Y.; Díez, J.; Conejero, S.; Michelet, V.; Cadierno, V. *Cycloisomerization versus Hydration Reactions in Aqueous Media: A Au(III)-NHC Catalyst That Makes the Difference. Org. Lett.* **2012**, *14*, 2520-2523.

(152) Luo, T.; Dai, M.; Zheng, S.-L.; Schreiber, S. L. *Syntheses of α-Pyrones Using Gold-Catalyzed Coupling Reactions. Org. Lett.* **2011**, *13*, 2834-2836.

(153) Cui, D.-M.; Meng, Q.; Zheng, J.-Z.; Zhang, C. *Gold-catalyzed addition of sulfonic acids to alkynes to form vinyl sulfonates. Chem. Commun.* **2009**, 1577-1579.

(154) Ye, L.; Wang, Y.; Aue, D. H.; Zhang, L. *Experimental and Computational Evidence for Gold Vinylidenes: Generation from Terminal Alkynes via a Bifurcation Pathway and Facile C–H Insertions. J. Am. Chem. Soc.* **2011**, *134*, 31-34.

(155) Chen, Y.; Yan, W.; Akhmedov, N. G.; Shi, X. *1,2,3-Triazole as a Special "X-Factor" in Promoting Hashmi Phenol Synthesis. Org. Lett.* **2010**, *12*, 344-347.

(156) Wang, D.; Gautam, L. N. S.; Bollinger, C.; Harris, A.; Li, M.; Shi, X. *1,2,3-Triazole Bound Au(I) (TA-Au) as Chemoselective Catalysts in Promoting Asymmetric Synthesis of Substituted Allenes. Org. Lett.* **2011**, *13*, 2618-2621.

(157) Wang, D.; Zhang, Y.; Cai, R.; Shi, X. *Triazole-Au(I) complex as chemoselective catalyst in promoting propargyl ester rearrangements. Beilstein J. Org. Chem.* **2011**, *7*, 1014-1020, No. 115.

(158) Wang, D.; Zhang, Y.; Harris, A.; Gautam, L. N. S.; Chen, Y.; Shi, X. *Triazole-gold-promoted, effective synthesis of enones from propargylic esters and alcohols: A catalyst offering chemoselectivity, acidity and ligand economy. Adv. Synth. Catal.* **2011**, *353*, 2584-2588.

(159) Zhou, C.-Y.; Chan, P. W. H.; Che, C.-M. *Gold(III) Porphyrin-Catalyzed Cycloisomerization of Allenones. Org. Lett.* **2005**, *8*, 325-328.

(160) Oxford, S. M.; Henao, J. D.; Yang, J. H.; Kung, M. C.; Kung, H. H. *Understanding the effect of halide poisoning in CO oxidation over Au/TiO2. Appl. Catal., A.* **2008**, *339*, 180-186.

(161) Chandler, B. D.; Kendell, S.; Doan, H.; Korkosz, R.; Grabow, L. C.; Pursell, C. J. *NaBr Poisoning of Au/TiO2 Catalysts: Effects on Kinetics, Poisoning Mechanism, and Estimation of the Number of Catalytic Active Sites. ACS Catal.* **2012**, *2*, 684-694.

(162) Bartholomew, C. H. *Mechanisms of catalyst deactivation. Appl. Catal., A.* **2001**, *212*, 17-60.

(163) O. Simone, D.; Kennelly, T.; l. brungard, n.; J. Farrauto*, R. *Reversible poisoning of palladium catalysts for methane oxidation. Appl. Catal.* **1991**, *70*, 87-100.

(164) Gaillard, S.; Bosson, J.; Ramón, R. S.; Nun, P.; Slawin, A. M. Z.; Nolan, S. P. *Development of Versatile and Silver-Free Protocols for Gold(I) Catalysis. Chem. Eur. J.* **2010**, *16*, 13729-13740.

(165) Gómez-Suárez, A.; Oonishi, Y.; Meiries, S.; Nolan, S. P. *[{Au(NHC)}2(μ-OH)][BF4]: Silver-Free and Acid-Free Catalysts for Water-Inclusive Gold-Mediated Organic Transformations. Organometallics* **2013**, *32*, 1106-1111.

(166) Nevado, C.; Echavarren, A. M. *Intramolecular Hydroarylation of Alkynes Catalyzed by Platinum or Gold: Mechanism and endo Selectivity. Chem. Eur. J.* **2005**, *11*, 3155-3164.

(167) Burfield, D. R.; Goh, E. H.; Ong, E. H.; Smithers, R. H. *Storage and decomposition of chloroform. Gazz. Chim. Ital.* **1983**, *113*, 841-3.

(168) Ghosh, N.; Nayak, S.; Sahoo, A. K. *Gold-Catalyzed Regioselective Hydration of Propargyl Acetates Assisted by a Neighboring Carbonyl Group: Access to α-Acyloxy Methyl Ketones and Synthesis of (±)-Actinopolymorphol B†. J. Org. Chem.* **2010**, *76*, 500-511.

(169) Wang, D.; Cai, R.; Sharma, S.; Jirak, J.; Thummanapelli, S. K.; Akhmedov, N. G.; Zhang, H.; Liu, X.; Petersen, J. L.; Shi, X. *"Silver Effect" in Gold(I) Catalysis: An Overlooked Important Factor. J. Am. Chem. Soc.* **2012**, *134*, 9012-9019.

(170) Nieto-Oberhuber, C.; Muñoz, M. P.; Buñuel, E.; Nevado, C.; Cárdenas, D. J.; Echavarren, A. M. *Cationic Gold(I) Complexes: Highly Alkynophilic Catalysts for the exo- and endo-Cyclization of Enynes. Angew. Chem. Int. Ed.* **2004**, *43*, 2402-2406.

(171) Bartolomé, C.; Ramiro, Z.; Pérez-Galán, P.; Bour, C.; Raducan, M.; Echavarren, A. M.; Espinet, P. *Gold(I) Complexes with Hydrogen-Bond Supported Heterocyclic Carbenes as Active Catalysts in Reactions of 1,6-Enynes. Inorg. Chem.* **2008**, *47*, 11391-11397.

(172) Bartolomé, C.; Ramiro, Z.; García-Cuadrado, D.; Pérez-Galán, P.; Raducan, M.; Bour, C.; Echavarren, A. M.; Espinet, P. *Nitrogen Acyclic Gold(I) Carbenes: Excellent and Easily Accessible Catalysts in Reactions of 1,6-Enynes. Organometallics* **2010**, *29*, 951-956.

(173) Toullec, P. Y.; Genin, E.; Antoniotti, S.; Genêt, J.-P.; Michelet, V. *Au2O3 as a Stable and Efficient Catalyst for the Selective Cycloisomerization of γ-Acetylenic Carboxylic Acids to γ-Alkylidene-γ-Butyrolactones. Synlett* **2008**, *2008*, 707-711.

(174) Tang, Y.; Yu, B. *Identification of (phosphine)gold(i) hydrates and their equilibria in wet solutions. RSC Adv.* **2012**, *2*, 12686-12689.

(175) Xi, Y.; Wang, D.; Ye, X.; Akhmedov, N. G.; Petersen, J. L.; Shi, X. *Synergistic Au/Ga Catalysis in Ambient Nakamura Reaction. Org. Lett.* **2013**, *16*, 306-309.

(176) Johansson, M. J.; Gorin, D. J.; Staben, S. T.; Toste, F. D. *Gold(I)-Catalyzed Stereoselective Olefin Cyclopropanation. J. Am. Chem. Soc.* **2005**, *127*, 18002-18003.

(177) Muzart, J. *Gold-catalysed reactions of alcohols: isomerisation, inter- and intramolecular reactions leading to C–C and C–heteroatom bonds. Tetrahedron* **2008**, *64*, 5815-5849.

(178) Shapiro, N. D.; Toste, F. D. *Rearrangement of Alkynyl Sulfoxides Catalyzed by Gold(I) Complexes. J. Am. Chem. Soc.* **2007**, *129*, 4160-4161.

(179) Li, G.; Zhang, L. *Gold-Catalyzed Intramolecular Redox Reaction of Sulfinyl Alkynes: Efficient Generation of α-Oxo Gold Carbenoids and Application in Insertion into R-CO Bonds. Angew. Chem., Int. Ed.* **2007**, *46*, 5156-5159.

(180) Fang, R.; Yang, L. *Mechanism of the Gold(I)-Catalyzed Rearrangement of Alkynyl Sulfoxides: A DFT Study. Organometallics* **2012**, *31*, 3043-3055.

(181) Cuenca, A. B.; Montserrat, S.; Hossain, K. M.; Mancha, G.; Lledós, A.; Medio-Simón, M.; Ujaque, G.; Asensio, G. *Gold(I)-Catalyzed Intermolecular Oxyarylation of Alkynes: Unexpected Regiochemistry in the Alkylation of Arenes. Org. Lett.* **2009**, *11*, 4906-4909.

(182) Wang, Y.; Ye, L.; Zhang, L. *Au-catalyzed synthesis of 2-alkylindoles from N-arylhydroxylamines and terminal alkynes. Chem. Commun.* **2011**, *47*, 7815-7817.

(183) Wang, Y.; Liu, L.; Zhang, L. *Combining Zn ion catalysis with homogeneous gold catalysis: an efficient annulation approach to N-protected indoles. Chem. Sci.* **2013**, *4*, 739-746.

(184) Lehmann, F.; Koolmeister, T.; Odell, L. R.; Scobie, M. *A Versatile New Synthetic Route to 1N-Hydroxyindazoles. Org. Lett.* **2009**, *11*, 5078-5081.

(185) Loudon, J. D.; Tennant, G. *Substituent interactions in ortho-substituted nitrobenzenes. Quarterly Rev., Chem. Soc.* **1964**, *18*, 389-413.

(186) Spence, T. W. M.; Tennant, G. *The chemistry of nitro-compounds. Part II. The scope and mechanism of the base-catalysed transformations of someNN-disubstituted o-nitrobenzamides. J. Chem. Soc., Perkin Trans. 1* **1972**, *0*, 97-102.

(187) Guo, Y.; Twamley, B.; Shreeve, J. n. M. *Pd-catalyzed arylation of silyl enol ethers of substituted alpha -fluoroketones. Org. Biomol. Chem.* **2009**, *7*, 1716-1722.

(188) Kim, K.-Y.; Kim, B. C.; Lee, H. B.; Shin, H. *Nucleophilic Fluorination of Triflates by Tetrabutylammonium Bifluoride. J. Org. Chem.* **2008**, *73*, 8106-8108.

(189) Prakash, G. K. S.; Beier, P. *Construction of Asymmetric Fluorinated Carbon Centers. Angew. Chem. Int. Ed.* **2006**, *45*, 2172-2174.

(190) de Haro, T.; Nevado, C. *Gold-Catalyzed Synthesis of α-Fluoro Acetals and α-Fluoro Ketones from Alkynes. Adv. Synth. Catal.* **2010**, *352*, 2767-2772.

APPENDIX- LIST OF ABBREVIATIONS

CV: Cyclic voltammetry

$CoCp^*_2$: Decamethylcobaltocene

DCM: Dichloromethane

DMSO: Dimethylsulfonyl Oxide

DCE: Dichloroethane

DMPU: 1,3-Dimethyl-3,4,5,6-tetrahydro-2(1H)-pyrimidinone

ESI-MS: Electrospray Ionization mass spectrometry

EtOAc: Ethyl Acetate

GC: Gas Liquid Chromatography

h: Hour

HOMO: Highest occupied molecular orbital

HRMS: High resolution mass spectroscopy

Hz: Hertz

HOBt: Hydroxybenzotriazole

HCl: Hydrochloric acid

HMPA: Hexamethylphosphoramide

LUMO: Lowest unoccupied molecular orbital

L: Ligand

MHz: Megahertz

M: Molar

mg: Milligram

min: Minute

mL: Milliliter

mmol: Millimole

mM: Millimolar

m/z: Mass to charge ratio

NHC: N-Heterocyclic carbene

Nu: Nucleophile

NMR: Nuclear magnetic resonance spectroscopy

NTf_2: Bis(trifluoromethanesulfonyl)imide

ppm: Parts per million

rt: Room temperature

AgOTf: Silver triflate

$AgSbF_6$: Silver hexafluoroantimonate

TBAHFP: Tetrabutylammonium hexafluorophosphate

TfOH: Trifluoromethanesulfonic acid

TLC: Thin layer chromatography

tert: Tertiary

THF: Tetrahydrofuran

TON: Turnover number

TfO: Triflate

THF: Tetrahydrofuran

Ph_3P: Triphenyl phosphine

PPN: Bis(triphenylphosphine)iminium

XPS: X-ray photoelectron spectroscopy

α: Alpha

β: Beta

δ: Delta

γ: Gamma

m: Meta

o: Ortho

p: Para

APPENDIX- COPYRIGHT PERMISSION

JOHN WILEY AND SONS LICENSE TERMS AND CONDITIONS

Apr 14, 2014

This is a License Agreement between Manish Kumar ("You") and John Wiley and Sons ("John Wiley and Sons") provided by Copyright Clearance Center ("CCC"). The license consists of your order details, the terms and conditions provided by John Wiley and Sons, and the payment terms and conditions.

All payments must be made in full to CCC. For payment instructions, please see information listed at the bottom of this form.

License Number	3367790648205
License date	Apr 14, 2014
Licensed content publisher	John Wiley and Sons
Licensed content publication	Chemistry - A European Journal
Licensed content title	Alkyne/Alkene/Allene-Induced Disproportionation of Cationic Gold(I) Catalyst
Licensed copyright line	© 2014 WILEY-VCH Verlag GmbH & Co. KGaA, Weinheim
Licensed content author	Manish Kumar,Jacek Jasinski,Gerald B. Hammond,Bo Xu
Licensed content date	Feb 12, 2014
Start page	3113
End page	3119
Type of use	Dissertation/Thesis
Requestor type	Author of this Wiley article
Format	Print and electronic
Portion	Full article
Will you be translating?	No
Title of your thesis / dissertation	Mechanistic Insights and Functionalization of Alkynes in Homogeneous Gold Catalysis
Expected completion date	Jun 2014
Expected size (number of pages)	170
Total	0.00 USD

Terms and Conditions

Terms and Conditions are not available at this time.

If you would like to pay for this license now, please remit this license along with your payment made payable to "COPYRIGHT CLEARANCE CENTER" otherwise you will be invoiced within 48 hours of the license date. Payment should be in the form of a check or money order referencing your account number and this invoice number RLNK501277852.

RightsLink®

Home | Create Account | Help

Title: Enhanced Reactivity in Homogeneous Gold Catalysis through Hydrogen Bonding

Author: Weibo Wang, Manish Kumar, Gerald B. Hammond, and Bo Xu

Publication: Organic Letters

Publisher: American Chemical Society

Date: Jan 1, 2014

User ID

Password

Enable Auto Login

LOGIN

Forgot Password/User ID?

If you're a copyright.com user, you can login to RightsLink using your copyright.com credentials. Already **a RightsLink user** or want to learn more?

PERMISSION/LICENSE IS GRANTED FOR YOUR ORDER AT NO CHARGE

This type of permission/license, instead of the standard Terms & Conditions, is sent to you because no fee is being charged for your order. Please note the following:

- Permission is granted for your request in both print and electronic formats, and translations.
- If figures and/or tables were requested, they may be adapted or used in part.
- Please print this page for your records and send a copy of it to your publisher/graduate school.
- Appropriate credit for the requested material should be given as follows: "Reprinted (adapted) with permission from (COMPLETE REFERENCE CITATION). Copyright (YEAR) American Chemical Society." Insert appropriate information in place of the capitalized words.
- One-time permission is granted only for the use specified in your request. No additional uses are granted (such as derivative works or other editions). For any other uses, please submit a new request.

BACK | CLOSE WINDOW

Title: Gold-Catalyzed Addition of N-Hydroxy Heterocycles to Alkynes and Subsequent 3,3-Sigmatropic Rearrangement

Author: Manish Kumar, Martin Scobie, Mark S. Mashuta, Gerald B. Hammond, and Bo Xu

Publication: Organic Letters

Publisher: American Chemical Society

Date: Feb 1, 2013

PERMISSION/LICENSE IS GRANTED FOR YOUR ORDER AT NO CHARGE

This type of permission/license, instead of the standard Terms & Conditions, is sent to you because no fee is being charged for your order. Please note the following:

- Permission is granted for your request in both print and electronic formats, and translations.
- If figures and/or tables were requested, they may be adapted or used in part.
- Please print this page for your records and send a copy of it to your publisher/graduate school.
- Appropriate credit for the requested material should be given as follows: "Reprinted (adapted) with permission from (COMPLETE REFERENCE CITATION). Copyright (YEAR) American Chemical Society." Insert appropriate information in place of the capitalized words.
- One-time permission is granted only for the use specified in your request. No additional uses are granted (such as derivative works or other editions). For any other uses, please submit a new request.

BACK CLOSE WINDOW

CURRICULUM VITAE

Manish Kumar

Department of Chemistry
University of Louisville
Louisville, KY- 40292
Mobile: (502)-526-2743

E-mail: manishchem53@gmail.com

EDUCATION

PhD, Organic Chemistry, University of Louisville, Louisville, KY, USA 2009-2014
Thesis title: "Mechanistic Insights and Functionalization of Alkynes in Homogeneous Gold Catalysis"

MS, Organic Chemistry, Panjab University, Chandigarh, India 2005-2007
Thesis title: "Synthesis of dithiocyanate, Thiocyanatin A, a nematocidal natural product isolated from marine sponge, *Oceanapia sp*"

BS, Chemistry, Botany & Zoology, GPG College, Bilaspur, Himachal Pradesh University, Shimla, India 2002-2005

RESEARCH EXPERIENCE

Graduate Teaching/Research Assistant, Department of Chemistry, University of Louisville, 08/2009-06/2014

Advisor: Prof. Gerald B. Hammond

- Synthesis of functionalized benzotriazoles using addition of nucleophile to alkyne and subsequently followed by sigmatropic rearrangement.
- Unraveled the intricate details of mechanism of gold catalyst deactivation and to overcome the reactivity-stability dilemma of gold catalysis through additives (neutral organic compounds, counter ions, solvents).
- Understanding of the mechanistic insights of gold catalyzed reactions using kinetics.

Research Project in Organic Chemistry, Department of Chemistry, Institute of Himalayan BioResource Technology (CSIR Lab) Palampur, India. 11/2008-07/2009

Advisor: Dr. Pralay Das

- Development of novel and new organic transformations on transition metal solid support catalyst.

MS Research Project, Panjab University, Chandigarh, India 08/2006-04/2007

Adviser: Prof. M. L. Sharma

- Synthesis of dithiocyanate, Thiocyanatin A, a nematocidal natural product isolated from marine sponge, *Oceanapia sp.*

RESEARCH/TECHNICAL SKILLS

- Handled several organic reagents and catalysts, Familiar with protecting groups, Microwave reactors, Metal catalysts such as Au Pd, Pt, solid supported.
- Experience in air sensitive reagents, Hand over heterocyclic synthesis, Multistep synthesis, Synthesized biologically active compounds, Skill in scale up of reaction.
- Spectroscopic analysis and data interpretation through ^{1}H NMR, ^{13}C NMR, ^{31}P, ^{19}F, two dimension NMR, and GCMS.
- Trained in using UV-Vis, FTIR, electrochemistry, NMR, GCMS, LCMS, FTMS, HRMS, and XPS.
- Microsoft office program suite, Endnote program, Gaussian, Molden, Chemdraw and ChemWindow, Fortran 90 language.
- Laboratory equipment maintenance including vacuum pumps, glove box, and schlenk line.
- Impurity profile study on the basis of spectra.
- Experience in the isolation of compounds by MDAP, Flash Master (CombiFlash).
- Familiar with safety assessment of chemicals Material safety database (MSDS) as well as lab safety.
- Proficient in using research database softwares such as SciFinder and Reaxys.
- Trained and mentored undergraduate and new graduate students.
- Presenting theoretical topics and scientific research at group meetings, chemistry department, regional and national meetings.
- Personal skills include collaboration, organization, good verbal and written communication skills.

TEACHING EXPERIENCE

- Summer-Spring Term, 2013-2014
  Teaching Assistant, Chem 344 Organic II Laboratory: Synthesis & characterization.

- Fall-Spring Term, 2010-2012
  Teaching Assistant, Chem 344 Organic II Laboratory: Synthesis & characterization.

- Summer Term, 2010
  Teaching Assistant, Chem 207 Analytical I Laboratory.

- Spring Term, 2010
  Teaching Assistant, Chem 344 Organic II Laboratory: Synthesis & characterization.

- Fall Term, 2009
  Teaching Assistant, Chem 343 Organic I Laboratory: Synthesis & characterization.

FELLOWSHIPS, HONORS AND AWARDS

- University of Louisville Graduate Student Council Travel Award for attending 247th ACS National Meeting, Dallas, Texas, 16th – 20th March 2014.
- Received prestigious IMD-3 Travel Award **(Institute of Molecular Diversity and Drug Design)** for ACS National meeting, Indianapolis, Indiana**,** 8th – 12th September 2013.
- University of Louisville Graduate Student Council Travel Award for attending 42nd ACS Regional Meeting, Indianapolis, Indiana, 7th – 9th June 2011.
- Selected with scholarship to pursue PhD from University of Louisville, Kentucky (USA) (2009).
- Qualified CSIR-UGC (NET) examination (June 2007) with CSIR ranking (SPM) conducted by University Grant Commission and CSIR for Junior Research Fellowship and Lecturer Ship eligibility.
- Qualified Graduate Aptitude Test in Engineering (GATE) with 409 (94%) score & 293 all India ranking (2007).
- Qualified Defence Research and Development Organization (DRDO) Scientist Entry Test (2007).
- Qualified State Level Eligibility Test (SLET), Himachal Pradesh (INDIA) (2006).
- Qualified "Bhabha Atomic Research Center" written test for admission to Ph.D (2007).
- Qualified "Indian Institute of Science, Bangalore" written test for admission to Ph.D (2007).
- First Rank holder in OCET conducted by Panjab University, Chandigarh for admission to MSc. (H.S.) (Chemistry) course (2005).
- Second Rank holder in M.Sc. entrance test conducted by Himachal Pradesh University for admission to M.Sc. (Chemistry) course (2005).
- Qualified College cadre Lecturer test conducted by Himachal Pradesh Public Service Commission (HPPSC) (2008).
- National Merit Scholarship, 1999.

PUBLICATIONS & PRESENTATIONS

Manuscripts (Published/ submitting/ in preparation):

- Cationic Gold Catalyst Poisoning and Re-activation, **Kumar, M.;** Hammond, G. B.; Xu, Bo. *Org. Lett.* **2014,** *16*, 3452-3455.

- Alkyne/Alkene/Allene Induced Disproportionation of Cationic Gold(I) Catalyst, **Kumar, M.;** Jacinski, J.; Hammond, G. B.; Xu, Bo. *Chem. Eur. J.* **2014**, *20*, 3113-3139.

- Enhanced Reactivity in Homogeneous Gold Catalysis through Hydrogen Bonding, Wang, W.; **Kumar, M.;** Hammond, G. B.; Xu, B. *Org. Lett.* **2014**, *16*, 636-639.

- Gold-catalyzed Addition of *N*-Hydroxy Heterocycles to Alkynes and Subsequent 3,3-Sigmatropic Rearrangement, **Kumar, M.;** Scobie, M.; Mashuta, M. S.; Hammond, G. B.; Xu, B. *Org. Lett.* **2013**, *15*, 724-727.

- Copper Promoted C-N and C-O Type Cross-Coupling Reactions, Das, P.; Sharma, D.; **Kumar, M**.; Singh, B. *Curr. Org. Chem.* **2010**, *14*, 753-783.

Conferences, Workshops:

- Organic Fluorine Chemistry: Basic Concepts and Application to Materials and Drug Sciences: Professor Kenji Uneyama, Okayama University, Japan: University of Louisville, October 2013.
- Introduction to new ab initio quantum chemistry program: Q-Chem, University of Louisville, March-2010.
- Attended and participated rigorously in the **First Chandigarh Science Congress** session held at **Chandigarh,** march, 2007.
- Attended and participated rigorously in the "**National Symposium and 3rd R.C.Paul Symposium** organized by Chemistry Department, Panjab University, Chandigarh, February, 2007.

Selected Conference Oral & Poster Presentations:

- **Kumar**, **M**.; Malhotra, D.; Hammond, G. B.; Xu, B. Kinetic Model in Homogeneous Gold Catalysis. 247th ACS National Meeting, Dallas (TX) on 19th March, 2014(Oral). Abstract#: ORGN-554

- **Kumar**, **M**.; Jasinski, J.; Hammond, G. B.; Xu, B. Understanding Gold Decay Mechanism and Improving Efficiency of Gold Catalysis through Rational Choice of Additives. IMD^3 Fall Fest meeting, Louisville (KY) on 8th November, 2013(Oral). Abstract#: 5

- **Kumar**, **M**.; Jasinski, J.; Hammond, G. B.; Xu, B. Understanding Gold Decay Mechanism and Improving Efficiency of Gold Catalysis through Rational Choice of Additives. 246th ACS National Meeting, Indianapolis (IN) on 9th September, 2013(Oral). Abstract#: ORGN-183

- **Kumar**, **M**.; Xu, B.; Hammond, G. B. An Efficient Synthesis of 5-Substituted Benzotriazole via Gold-catalyzed Intermolecular Alkyne Oxidation.The Fourth Annual Graduate Research Symposium, University of Louisville (KY), March – 2012 (Poster). Abstract#: 21

- **Kumar**, **M**.; Xu, B.; Hammond, G. B. An Efficient Synthesis of 5-Substituted Benzotriazole via Gold-catalyzed Intermolecular Alkyne Oxidation.The 14th Annual IMD3 Symposium, Hank Wagner Conference Center at Jewish Hospital & St. Mary's Healthcare Louisville (KY), March – 2012 (Poster). Abstract#: 17
- **Kumar**, **M**.; Xu, B.; Vaisberg, A. J.; Hammond, G. B. Synthesis of aromatic derivatives of benzothienopyrimidines showing anti-cancer activity. 42nd ACS Regional Meeting, Indianapolis (IN) on 9th June, 2011(Oral). Abstract#: CERM-171

PROFESSIONAL MEMBERSHIP

- American Chemical Society, March 2010 – Present.
- ACS Organic Division, May 2013- 2014.